

**CONTINUOUS FLOW SYNTHESIS OF SILICON COMPOUNDS AS  
FEEDSTOCK FOR SOLAR-GRADE SILICON PRODUCTION**

by

**FIDELIS CHIGONDO**

Submitted in fulfilment of the requirements for the degree

**DOCTOR TECHNOLOGIAE: CHEMISTRY**

in the

FACULTY OF SCIENCE

**NELSON MANDELA METROPOLITAN UNIVERSITY**

Promoter: Prof P Watts

Co-promoter: Prof B Zeelie

December 2016

## DECLARATION

I, *Fidelis Chigondo* hereby declare that the thesis submitted for the degree *Doctor Technologiae Chemistry*, at Nelson Mandela Metropolitan University, is my original work and has not previously been submitted for assessment to any other institution, or for any other qualification.

F. Chigondo



## **DEDICATION**

To my late wife, Justice Chokuda Chigondo  
I will always remember the joy, love and happiness we shared.

To my late sister, Shylet Chigondo Guvakuva  
Your legacy shall live forever.

To my daughter, Tanatswa Felistars Chigondo  
You are such a treasure from God.

To my parents and family  
Your love, support and encouragement is a blessing.

## ACKNOWLEDGEMENTS

I would like to express my profound gratitude and appreciation to the following people:

- ❖ My promoter, Prof P Watts for his guidance and academic support.
- ❖ My co-promoter Prof B Zeelie for advice and support.
- ❖ Dr G Dugmore and Mr L Mcingana for assistance with reactor technology.
- ❖ Mr C Bosma for statistical analysis consultation.
- ❖ NMMU InnoVenton: Institute of Chemical Technology research team and staff.
- ❖ The flow chemistry research group.
- ❖ My fellow postgraduate colleagues.
- ❖ My parents and family for their moral support.
- ❖ InnoVenton: Institute for Chemical Technology NRF Doctoral bursary and NMMU post-graduate bursary for the financial support.

## EXECUTIVE SUMMARY

This thesis describes the key steps in the production of high purity (solar-grade) silicon from metallurgical-grade silicon for use in the production of photovoltaic cells as alternative renewable, environmentally benign and cheap energy source. The initial part of the project involves the development and optimization of a small chemical production platform system capable of producing alkoxysilanes from metallurgical-grade silicon as green precursors to solar-grade silicon production.

Specifically, the main aim of the study was to synthesize trialkoxysilanes in continuous flow mode, although the synthesis on monosilane was also done in batch mode. The alkoxylation reaction was carried out in a traditional slurry phase batch reactor, packed bed flow tubular reactor and also attempted in a continuous flow falling film tubular reactor. The effect of key parameters which affect the silicon conversion and selectivity for the desired trialkoxysilane were investigated and optimized using ethanol as a reagent model. The synthesis was then extended to the other alcohols namely methanol, *n*-propanol and *n*-butanol.

Copper catalysts which were tested in the alkoxylation reaction included: CuCl, Cu(OH)<sub>2</sub>, CuO and CuSO<sub>4</sub>. CuCl and Cu(OH)<sub>2</sub> showed comparable activity in the batch mode but the former was more efficient in the packed bed flow tubular reactor. Cu(OH)<sub>2</sub> could be used as a non-halide catalyst but its activity is limited to short reaction cycles (<10 h). The uncatalysed reaction resulted in negligible reaction rates in both types of reactors. High temperature catalyst pre-heating (>500 °C) resulted in a lower rate of reaction and selectivity than when slightly lower temperatures are used (<350 °C) in both reactors, although much difference was noticed in the packed bed flow tubular reactor. Synthesis in the batch reactor needed longer silicon-catalyst activation time, higher pre-heating temperature and higher catalyst amounts as compare to the packed bed flow tubular reactor. Reaction temperature and alcohol flow rate influenced the reaction in both methods. The optimum reaction temperature range and alcohol flow rate was comparable in both reactors (230 to 240 °C) and 0.1 mL/min respectively. The effect of alcohol R-group

(C1 to C4) on the reaction revealed that conversion and selectivity generally decrease with an increase in carbon chain length in both methods. Ethanol showed highest selectivity (>95% in batch and >97% in flow) and conversion (about 88% in batch and about 64% in flow) as compared to all other alcohols studied showing that it could be the most efficient alkoxylation alcohol for this reaction. Overall, the packed bed flow tubular reactor resulted in higher selectivity to trialkoxysilanes than the batch system. Performing the reaction under pressure resulted in increased conversion but selectivity to the desired trialkoxysilane diminished. Synthesis in a continuous flow falling film tubular reactor was not successful as it resulted in very poor conversion and selectivity.

Monosilane was successfully synthesized from the disproportionation of triethoxysilane using homogeneous and heterogeneous catalysts in batch mode. The results obtained from homogeneous catalysis showed that the reaction can be conducted at room temperature. The heterogeneous catalysis method resulted in slow conversion at room temperature but mild heating up to 55 °C greatly improved the reaction. Conducting the reaction under neat conditions produced comparable results to reactions which were carried out using solvents. The disproportionation reaction was best described by the first order kinetic model.

The results obtained in this research indicate that the packed bed flow tubular reactor can be utilized with future modifications for continuous flow synthesis of alkoxylation alcohols as feedstock for the solar-grade silicon production.

**Key words:** *silicon, copper catalyst, trialkoxysilane, monosilane, batch reactor, packed bed flow tubular reactor*

## RESEARCH OUTPUT

### Conference proceedings

Fidelis Chigondo, Paul Watts and Ben Zeelie. Semi-continuous flow process for the selective direct synthesis of trialkoxysilanes. 5<sup>th</sup> IUPAC International Conference on Green Chemistry, Durban (South Africa), 17-21 August 2014. Oral presentation.

Fidelis Chigondo, Paul Watts and Ben Zeelie. Selective synthesis of trialkoxysilanes in a semi-continuous flow reactor. American Chemical Society, Green Chemistry Institute. 19<sup>th</sup> Green Chemistry & Engineering Conference, North Bethesda, Maryland (United States of America), 14-16 July 2015. Poster presentation.

### Patents

Chigondo F, Watts P. Method for the selective synthesis of trialkoxysilanes. PCT Patent application number PCT/IB2016/056255, 18 October 2016.

### Peer reviewed journals

Chigondo F, Zeelie B, Watts P. Selective direct synthesis of trialkoxysilanes in a packed bed flow tubular reactor. ACS Sustain Chem Eng. 2016; 4: 6237-6243.

Chigondo F, Watts P. Disproportionation of triethoxysilane over anion exchange resins. Catal Lett. 2016; 146: 1445-1448.

Chigondo F, Zeelie B, Watts P. Slurry phase selective synthesis of trialkoxysilanes. (*In preparation*).

# CONTENTS

|  |     |
|--|-----|
| DECLARATION.....   | ii  |
| DEDICATION.....  | iii |
| ACKNOWLEDGEMENTS.....  | iv  |
| EXECUTIVE SUMMARY.....   | v   |
| RESEARCH OUTPUT.....   | vii |
| LIST OF ABBREVIATIONS.....   | xii |
| CHAPTER 1.....   | 1   |
| 1.0 INTRODUCTION.....  | 1   |
| 1.1 Background to the research.....                                | 1   |
| 1.2 Literature review.....   | 3   |
| 1.2.1 Metallurgical methods.....                                   | 7   |
| 1.2.1.1 Slagging.....  | 8   |
| 1.2.1.2 Evacuation, gas blowing, oxidation and volatilization..... | 9   |
| 1.2.1.3 Electron beam melting and plasma purification.....         | 9   |
| 1.2.1.4 Alloying.....  | 10  |
| 1.2.1.5 Acid leaching.....   | 10  |
| 1.2.1.6 Directional solidification.....                            | 11  |
| 1.2.2 Chemical methods.....  | 11  |
| 1.2.2.1 The Siemens™ process.....                                  | 11  |
| 1.2.2.2 Union Carbide™ monosilane process.....                     | 13  |
| 1.2.2.3 The new silane process.....                                | 14  |
| 1.2.3 Reactors.....  | 16  |
| 1.2.3.1 Gas-liquid reactors.....                                   | 20  |
| 1.2.3.1.1 The bubble tower.....                                    | 20  |
| 1.2.3.1.2 Spray tower reactor.....                                 | 22  |
| 1.2.3.1.3 Packed columns.....                                      | 24  |
| 1.2.3.1.4 Continuous stirred tank reactor.....                     | 26  |
| 1.2.3.1.5 Tray columns.....  | 28  |



|  |    |
|--|----|
| 1.2.3.1.6 The falling liquid film reactor.....                                       | 31 |
| 1.2.3.2 Gas-solid reactors .....   | 33 |
| 1.2.3.2.1 Fluidized bed reactor.....   | 33 |
| 1.2.3.2.2 Packed bed reactors .....  | 35 |
| 1.2.4 Continuous flow synthesis .....  | 38 |
| 1.2.4.1 Advantages .....   | 38 |
| 1.2.4.2 Disadvantages .....  | 39 |
| 1.2.5 Synthesis of alkoxysilanes.....  | 40 |
| 1.2.6 Synthesis of monosilane .....  | 45 |
| 1.3 Research problem statement .....   | 49 |
| 1.4 Research hypothesis.....   | 50 |
| 1.5 Research objectives.....   | 50 |
| CHAPTER 2 .....  | 51 |
| 2.0 Experimental .....   | 51 |
| 2.1 Materials.....   | 51 |
| 2.2 Equipment setup .....  | 53 |
| 2.2.1 Glass batch reactor set-up.....  | 53 |
| 2.2.2 Falling film continuous flow reactor setup .....                               | 54 |
| 2.2.3 Packed bed flow tubular reactor set-up .....                                   | 55 |
| 2.3 Analytical procedures .....  | 58 |
| 2.3.1 Gas Chromatography (GC).....   | 58 |
| 2.3.2 Gas Chromatography-Mass Spectrometry (GC-MS) .....                             | 60 |
| 2.3.3 Nuclear Magnetic Resonance Spectroscopy .....                                  | 60 |
| 2.3.4 Fourier-Transform Infrared Spectroscopy (FT-IR) .....                          | 61 |
| 2.3.5 X-Ray Fluorescence (XRF).....  | 61 |
| 2.3.6 X-Ray Diffraction (XRD).....   | 61 |
| 2.3.7 Scanning Electron Microscopy-Energy Dispersive Spectroscopy (SEM-EDS) .        | 61 |
| 2.4 Synthesis procedures.....  | 64 |
| 2.4.1 Batch synthesis of trialkoxysilanes .....                                      | 64 |
| 2.4.1.1 Effect of various catalysts, catalyst amount, pre-heating time and pre-..... | 65 |
| heating temperature on the selectivity and rate of formation of.....                 | 65 |

|  |    |
|--|----|
| triethoxysilane .....  | 65 |
| 2.4.1.2 Effect of ethanol flow rate and reaction temperature on the conversion of silicon and the selectivity for triethoxysilane.....                   | 65 |
| 2.4.1.3 Effect of alcohol R-group on the conversion of silicon and selectivity towards trialkoxysilanes .....  | 66 |
| 2.4.2 Synthesis of trialkoxysilanes in a falling film continuous flow tubular reactor.....   | 66 |
| 2.4.3 Synthesis of trialkoxysilanes in a packed bed flow tubular reactor .....   | 67 |
| 2.4.4 Synthesis of monosilane .....  | 68 |
| 2.4.4.1 General procedure for the homogeneous catalysis.....   | 68 |
| 2.4.4.2 General procedure for heterogeneous catalysis.....   | 69 |
| CHAPTER 3 .....  | 70 |
| Slurry phase synthesis of trialkoxysilanes .....   | 70 |
| 3.1 Introduction .....   | 70 |
| 3.2 Characterization of silicon-catalyst mixtures .....  | 72 |
| 3.2.1 XRD analysis .....   | 72 |
| 3.2.2 SEM-EDS analysis .....   | 73 |
| 3.2.3 XRF analysis.....  | 75 |
| 3.3 Glass batch synthesis of trialkoxysilanes .....  | 76 |
| 3.3.1 Effect of catalyst type and loading on selectivity and rate of triethoxysilane formation.....  | 77 |
| 3.3.2 Effect of pre-heating temperature and activation time on the silicon-catalyst mixture on rate of formation and selectivity to triethoxysilane..... | 81 |
| 3.3.3 Selectivity and rate of formation of triethoxysilane with time .....   | 85 |
| 3.3.4 Effect of flow rate and temperature on trialkoxysilane selectivity and conversion of silicon .....   | 87 |
| 3.3.5 Effect of R-group on trialkoxysilane selectivity and conversion of silicon.....  | 92 |
| 3.4 Continuous flow synthesis of trialkoxysilanes in a falling film tubular reactor.....   | 93 |
| 3.5 Conclusion .....   | 96 |
| CHAPTER 4 .....  | 98 |
| Synthesis of trialkoxysilanes in a packed bed flow tubular reactor .....   | 98 |
| 4.1 Introduction .....   | 98 |

|  |     |
|--|-----|
| 4.2 Packed bed flow tubular reactor synthesis of trialkoxysilanes .....              | 98  |
| 4.2.1 Effect of copper catalyst type on the rate of triethoxysilane formation .....  | 98  |
| 4.2.2 The effect of catalyst loading on the rate of triethoxysilane formation .....  | 99  |
| 4.2.3 Effect of activation temperature and activation time on the rate of .....      | 100 |
| triethoxysilane formation.....   | 100 |
| 4.2.4 Effect of reaction temperature on silicon conversion and triethoxysilane.....  | 102 |
| selectivity .....  | 102 |
| 4.2.5 Effect of flow rate on triethoxysilane selectivity and silicon conversion..... | 103 |
| 4.2.6 Silicon conversion and triethoxysilane selectivity with time .....             | 105 |
| 4.2.7 Response surface modelling on silicon conversion .....                         | 106 |
| 4.2.8 Effect of pressure on silicon conversion and triethoxysilane selectivity ..... | 109 |
| 4.2.9 Effect of R-group on silicon conversion and triethoxysilane selectivity .....  | 111 |
| 4.3 Conclusion .....   | 112 |
| CHAPTER 5 .....  | 114 |
| Synthesis of monosilane .....  | 114 |
| 5.1 Introduction .....   | 114 |
| 5.2 Synthesis of monosilane by disproportionation of triethoxysilane .....           | 115 |
| 5.2.1 Homogeneous synthesis of monosilane .....                                      | 116 |
| 5.2.2 Heterogeneous synthesis of monosilane .....                                    | 120 |
| 5.3 Kinetics studies on the disproportionation reaction .....                        | 126 |
| 5.4 Conclusion .....   | 131 |
| CHAPTER 6 .....  | 133 |
| Conclusion and recommendations .....   | 133 |
| Conclusion.....  | 133 |
| Recommendations.....   | 136 |
| References.....  | 137 |
| Appendix .....   | 156 |
| Appendix A: Characterization data .....  | 156 |
| Appendix B: GC calibration curves for alkoxy silane quantification.....              | 175 |
| Appendix C: Response surface model validation graphs.....                            | 180 |

## LIST OF ABBREVIATIONS

|                     |   |
|---------------------|---|
| ACN                 | Acetonitrile                                      |
| AR                  | Analytical Reagent                                |
| AMB                 | Amberlite   |
| BuOH                | Butan-1-ol  |
| $^{13}\text{C}$ NMR | Carbon-13 Nuclear Magnetic Resonance Spectroscopy |
| $\text{CDCl}_3$     | Deuterated chloroform                             |
| Cp                  | Commercial Purpose                                |
| DMSO                | Dimethylsulfoxide                                 |
| Eq                  | Equivalent  |
| EtOH                | Ethanol   |
| FT-IR               | Fourier Transform-Infrared Spectroscopy           |
| GC                  | Gas Chromatography                                |
| GC-MS               | Gas Chromatography-Mass Spectrometry              |
| h                   | Hours   |
| $^1\text{H}$ NMR    | Proton Nuclear Magnetic Resonance Spectroscopy    |
| Hz                  | Hertz   |
| Kg                  | Kilograms   |
| kWh                 | Kilowatt hour                                     |
| MW                  | Megawatts   |
| MeOH                | Methanol  |
| MHz                 | Mega Hertz  |
| Min                 | Minutes   |
| MPa                 | Megapascal  |
| NaOEt               | Sodium ethoxide                                   |
| PrOH                | Propan-1-ol                                       |
| quint               | Quintet   |
| R &D                | Research and Development                          |
| rt                  | Room temperature                                  |
| THF                 | Tetrahydrofuran                                   |

|                 |  |
|-----------------|--|
| TES             | Triethoxysilane  |
| TEOS            | Tetraethoxysilane  |
| s <sup>-1</sup> | Per second   |
| sext            | Sextet   |
| s               | Singlet  |
| SEM-EDS         | Scanning Electron Microscopy-Energy Dispersive<br>Spectroscopy |
| XRD             | X-Ray Diffraction  |
| XRF             | X-Ray Fluorescence   |

# CHAPTER 1

## 1.0 INTRODUCTION

### 1.1 Background to the research

The non-renewable nature of fossil fuels as an energy source means its future availability and also its environmental impact are causes for concern. This has spurred interest in diversification of energy sources, with particular interest in renewable energy such as solar energy. This has resulted in a shortage of solar-grade silicon feedstock for the solar industry and hence more efficient methods for the manufacture of these materials are required.

Silicon is the second most abundant element in the earth's crust, after oxygen, and is usually found in nature as silicon dioxide and silicate.<sup>1</sup> It is used in approximately 90% of worldwide photovoltaic installations where it represents approximately half of the cost of silicon solar cells. The remaining 10% comprise of thin film solar cells of various types like cadmium telluride, gallium arsenide germanium and copper indium diselenide.<sup>2</sup> The advantages of using silicon for solar cells are due to its natural abundance, high energy conversion efficiency, stability and low toxicity. The annual growth (around 30%) of the cumulative capacity of installed photovoltaic systems over the past 20 years demonstrates significant industrial and government commitment to photovoltaics worldwide.<sup>3</sup> The cost of producing solar-grade feedstock represents around 20% of the total cost of the solar cell production.<sup>4</sup>

Silicon is also used as an alloying element in the aluminium industry and as a reducing element in the steel industry.<sup>5</sup> The purity of silicon used directly in the metal industry is 98% and is commonly called metallurgical-grade silicon. Another application of silicon is for solar photovoltaic panel wafers. For this application, silicon must be purified to 99.9999% (six nines or 6N) purity, and is usually called solar-grade silicon.<sup>6</sup> Due to the increased demand for solar energy over non-renewable fossil energy, the demand for

silicon feedstock for the photovoltaic industry has escalated tremendously.<sup>7</sup> The production of solar-grade silicon is therefore a key step in the solar industry.

In order to address the increased demand for silicon feedstock, many production routes have been developed.<sup>8</sup> Production of solar-grade silicon through the metallurgical approach combines a number of refining steps in addition to directional solidification.<sup>9-10</sup> This approach has been limited by its failure to reduce boron and phosphorous impurities to satisfactory levels, because of their high segregation coefficients.<sup>11</sup> The approach involves several batch-wise steps, which present difficulties in operation, process control, pollution control and energy cost minimization. Chemical methods for the production of solar-grade silicon have also evolved. These methods are able to produce solar-grade silicon of better purity than the metallurgical process.<sup>12</sup> The chemical methods basically involves the reaction of metallurgical-grade silicon with hydrochloric acid to form volatile trichlorosilanes and purifying them by fractional distillation. High purity silicon is then obtained by reduction or decomposition of these trichlorosilanes.<sup>6,13</sup> The major problem of the chemical route is that it is highly energy intensive and involves the production of chlorosilanes by reactions with hydrochloric acid.<sup>4-5,14</sup> These compounds are corrosive and toxic and therefore pose safety and environmental problems. Most chemical routes are basically batch and semi-continuous processes.<sup>9</sup>

Another route to optimize the process is to produce monosilane by preparing alkoxysilanes *via* the direct reaction between primary alcohols and metallurgical-grade silicon. The alkoxysilane technology is safer ecologically compared to the chlorosilane technology, since products of intermediate stages are not as toxic.<sup>15</sup>

The synthesis of these alkoxysilane feedstocks could be carried out using continuous flow reactors. This technology has the ability to play an integral role in revolutionizing the chemical sector, not only from an environmental standpoint but also from a quality, safety and economic perspective.<sup>16-17</sup> This leads to the identification of reaction conditions that are suitable for use at a production level.

## 1.2 Literature review

The market for high purity silicon, which has been traditionally dominated by microelectronics application, has changed due to the expansion of the photovoltaic industry. About 90% of the solar cells are silicon based, of which 60% is used in the photovoltaic industry and 30% is the electronic industry.<sup>18</sup>

The worldwide photovoltaic market is increasing and has been dominated by Europe for years, but the rest of the world clearly has the greatest potential for growth. Europe's share of the global market for photovoltaics reduced from 74% in 2011 to 55% in 2012 and it is projected to fall below 50% in the next 5 years as secondary markets emerge.<sup>19</sup> China is promising to be a major player, as it has already surpassed Japan and USA, which were pioneers in the photovoltaic industry. Figure 1.1 shows the global market share for the installed photovoltaics in 2012. It can be seen that Germany, Italy, China, USA and Japan were leading in the market at that time.

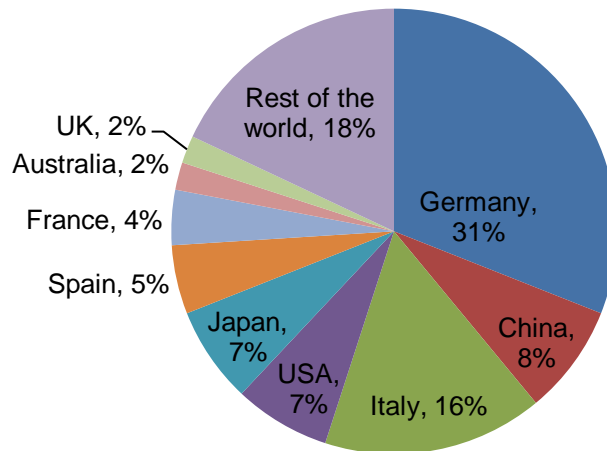


**Figure 1.1: Global market share of cumulative installed photovoltaics in 2012 (%MW)<sup>19</sup>**



The photovoltaic capacity outside Europe continues to grow, with new installations accounting for 13.9 GW in 2012, compared to 8 GW in 2011 and 3 GW in 2010. China is the major player followed by USA and Japan. Other countries and regions including Africa contributed only 8% in 2012.<sup>20</sup> With the emerging of new players like China in the industry and the need for alternative cheap energy, its partnership with African countries is likely to increase the global share. The market share of installed photovoltaics in 2012 is shown in Figure 1.2.

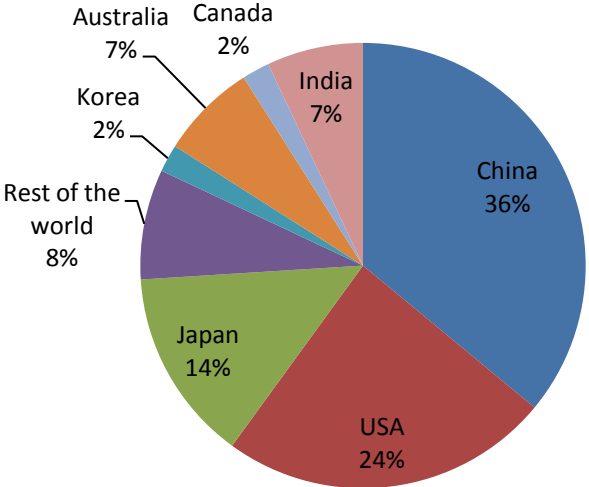


**Figure 1.2: Market share of cumulative installed photovoltaics outside Europe in 2012 (%MW)<sup>20</sup>**

There has been a tremendous growth in the photovoltaic industry from 2003 to present and the trend is projected to be maintained, as shown in Figure 1.3.<sup>19</sup> This growth has resulted in insufficient feedstock in the form of solar-grade silicon for the production of solar modules and the shortage is likely to worsen. The development of new cost effective and environmentally friendly production processes is therefore the new focus of researchers to address the problems encountered by current technologies.

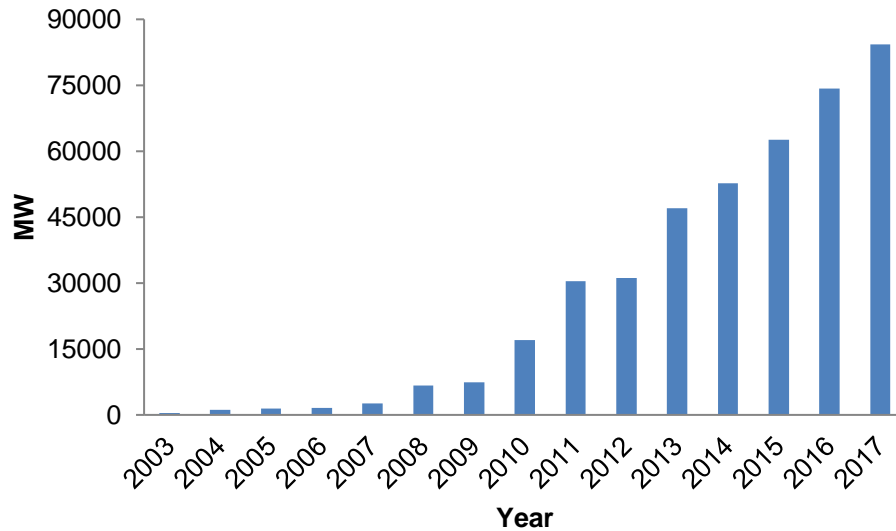
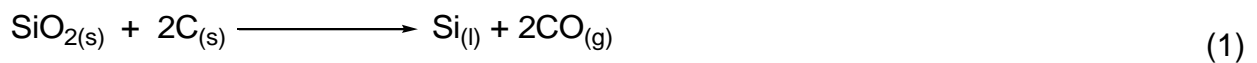


**Figure 1.3: Current and projected global annual photovoltaic power generation until 2017<sup>19</sup>**

Metallurgical-grade silicon is the initial material for the production of pure silicon for photovoltaic and electronic applications.<sup>21</sup> It is commercially produced in the smelting industry through the reduction of silicon oxide with carbon in submerged arc furnaces at high temperatures (>1900 °C)(Equation 1).<sup>12</sup> The raw materials preferred are lumpy quartz and carbon. Carbon raw material generally consists of metallurgical-grade coal, woodchips, charcoal and coke. The raw material mixture of quartz and carbon containing substances are charged from the top and heated by means of an intense electric arc sustained between the tips of three submerged electrodes and the electrical ground of the furnace. Liquid silicon metal is then tapped from the bottom of the furnace in 97-99% purity depending on the type and quality of raw material used.



It is used in alloying aluminium and steel and is unsuitable for solar applications since its purity is about 98wt% Si. Metallurgical-grade silicon costs US\$4/Kg<sup>22</sup> and more than one million metric tonnes are produced per year worldwide. In making metallurgical-grade silicon, approximately 12kWh/Kg of electrical energy is consumed. The impurities present

in metallurgical-grade silicon include Fe, Al, Ti, Mn, C, Ca, Mg, B and P.<sup>23</sup> The minimum required purity of silicon for photovoltaic applications is 99.9999wt% silicon referred to as solar-grade silicon. The cost of solar-grade silicon is in the range of US\$15-50/Kg<sup>22</sup> but its production cannot be quantified since there are currently no dedicated manufacturers for it throughout the world.<sup>6</sup> The purest form of silicon is termed electronic-grade silicon which costs more than US\$50/Kg<sup>22</sup> and its production is approximately 150 000 tonnes per year. This grade is marginally better in solar energy conversion but is very expensive and hence solar-grade silicon is preferred. Metallurgical-grade silicon therefore requires further purification methods for its applicability in the solar industry. Table 1.1 shows typical impurities of various grades of silicon.

**Table 1.1: Typical assay of various silicon grades**

| Element | Metallurgical-grade silicon (ppm) | Solar-grade silicon (ppm) | Electronic-grade silicon (ppm) |
|---------|-----------------------------------|---------------------------|--------------------------------|
| Si      | 98-99%                            | 99.9999% (6N)             | 99.9999999% (9N)               |
| Ca      | 2 000-3 000                       | <0.3                      | <0.01                          |
| Al      | 1 500-4 000                       | <0.1                      | <0.0008                        |
| Ca      | 500-600                           | <0.1                      | <0.003                         |
| B       | 40-80                             | <0.3                      | <0.0002                        |
| P       | 20-50                             | <0.1                      | <0.0008                        |
| C       | 600                               | <3                        | <0.5                           |
| O       | 3 000                             | <10                       | -                              |
| Ti      | 160-200                           | <0.01                     | <0.003                         |
| Cr      | 50-200                            | <0.1                      | -                              |

In general there are two principle methods for producing solar-grade silicon; namely metallurgical and chemical. The chemical methods are preferred because they lead to the production of much higher purity solar-grade silicon.

### 1.2.1 Metallurgical methods

In solar-grade silicon production through the metallurgical approach, metallurgical-grade silicon is purified by the combination of metallurgical techniques, as summarized in Figure 1.4. The techniques include slagging,<sup>23-24</sup> gas blowing,<sup>25</sup> evacuation,<sup>26</sup> formation of volatile species and oxidation of impurities,<sup>27</sup> zone refining,<sup>28</sup> electron beam melting,<sup>29</sup> acid leaching,<sup>30</sup> plasma,<sup>31</sup> alloying,<sup>32</sup> crystallization and directional solidification.<sup>33-34</sup> Directional solidification is the key process in this route as it removes most of the impurities with low segregation coefficients. The segregation coefficient is the ratio of an impurity in the solid phase to that in the liquid phase. Impurities with high segregation coefficients like P (0.35), B (0.8) As (0.3) and C (0.05) are removed by the other techniques. Electrochemical methods have also been used for the production of solar-grade silicon of higher purity than the metallurgical route, but they have also failed to remove B satisfactorily.<sup>35-36</sup>

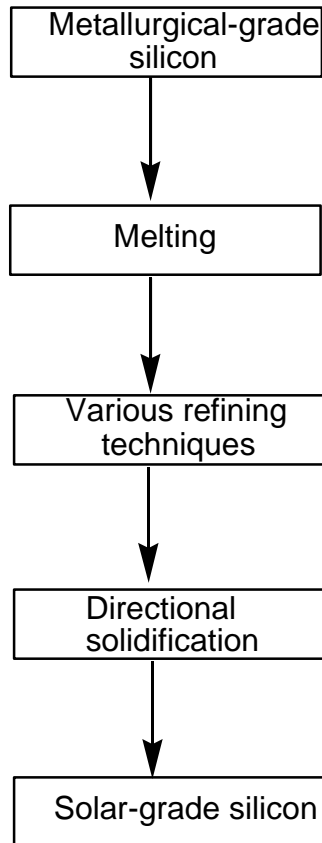


**Figure 1.4: Schematic diagram of the metallurgical process**

### 1.2.1.1 Slagging

Slagging is usually done by treating molten silicon with  $\text{CaO-SiO}_2\text{-Al}_2\text{O}_3\text{-MgO}$ ,  $\text{CaO-SiO}_2$ ,  $\text{CaOSiO}_2\text{-CaF}_2$  or  $\text{CaO-SiO}_2\text{-Al}_2\text{O}_3$  slags at high temperatures (about 1500 °C). The oxygen potential of the slag has a strong influence on impurity partitioning.<sup>37</sup> The impurities such as Al, S, P, Ga, Ca, B and Ge oxidise and dissolve in the slag.<sup>38</sup> Boron and phosphorus are the most difficult elements to remove from silicon and therefore a slag with strongly basic and oxidising characteristics is preferred.<sup>21</sup> It is important that the type of slag used in removing impurities has a higher solubility for impurities than molten silicon. The solubility of silicon in the slag must be low to minimize losses. In addition, the slag must be inert to molten silicon and must be able to be separated based on density differences. The slagging process depends on several factors like acidity and basicity, oxygen partial pressure, reaction kinetics, diffusion of impurities and partition coefficients

and therefore its optimization is still under research. The challenge of this method is the non-availability of boron free slag and the large amounts of slag to be used compared with silica refining process.

#### **1.2.1.2 Evacuation, gas blowing, oxidation and volatilization**

Evacuation involves heating molten silicon under vacuum so as to volatilize impurities with high vapour pressure, such as P.<sup>23</sup> This technique is also accompanied by the removal of other impurities like Mg, Na and Al. The reduction of boron and phosphorous from metallurgical-grade silica can be accomplished by purging moist gases through the molten silicon. The gases not only remove impurities but promote slagging and stirring of the melt to increase the rate of reactions.<sup>21</sup> The blowing of molten silicon with a moist gaseous mixture in argon is used to remove B as boron oxides, such as  $B_2O_3(g)$  at low temperatures. The phosphorus may be extracted as gaseous P above 1500 °C.<sup>24-25</sup> Oxidation and volatilization techniques can be used to convert impurities in molten silicon to other species, which can be removed as a slag. Oxidation is done by bubbling oxygen or oxygen containing species diluted with argon through molten silicon leading to the formation of oxides. Boron is removed by this technique as boron oxides such as HBO(g), which is stable in the vapour phase over a wide range of conditions.<sup>26</sup> The volatilization method involves the reaction of impurities such as B, P, Al, and Mg with species such as oxygen, hydrogen or chlorine and subsequently removing them in the vapour phase. The limitation of these techniques is that they are performed at high temperatures and hence making the process costly. Another disadvantage is that impurities with low vapour pressure are difficult to remove.

#### **1.2.1.3 Electron beam melting and plasma purification**

This process involves the acceleration of a beam of free electrons towards metallurgical-grade silicon granules resulting in the volatilization of impurities with higher vapour pressures than silicon.<sup>29</sup> Impurities which can be removed by this technique include C, Al and Ca, but B cannot be removed since its vapour pressure is much lower than that of silicon.<sup>9,31</sup> Plasma techniques are usually employed to remove B from silicon. The

procedure involves injecting hydrogen gas or steam with argon to effect the formation of boron compounds with high vapour pressure.<sup>27</sup> A plasma arc may also be run with argon and hydrogen gas mixed with oxygen to achieve the removal of B.<sup>31</sup> Other impurities like Al and Ti are also removed in the process. The disadvantage of plasma techniques is that they are highly energy intensive in terms of the amount of electricity used.

#### **1.2.1.4 Alloying**

In the alloying process metallurgical-grade silicon can be melted in the presence of a low melting solvent metal alloy such as Si-Al and the refining efficiency depends on the segregation behavior of impurities in solid silicon and the liquid phase.<sup>32</sup> Impurities such as B, Ni Fe, Al, Cu and P which have low solubility in solid silicon can be removed in the Si-Al phase during solidification.<sup>33</sup> The remaining impurities distributed at the grain boundaries can then be removed by electrochemical dissolution or acid leaching to obtain pure silicon crystals. Boron has also been extensively removed from silicon by the solidification refining technique using the Si-Al melt with Ti addition.<sup>34</sup> The alloying method has a disadvantage that an additional purification step for removal of residual aluminum in the silicon products is needed. In addition, the preparation of high purity Al alloying metal is expensive and has a significant impact on the cost of the final product.<sup>9</sup>

#### **1.2.1.5 Acid leaching**

The solidification of metallurgical-grade silicon during its production results in the distribution of metallic elements with low segregation coefficients in grain boundaries of solid silicon.<sup>33</sup> These metals include Al, Fe, Ca, Ti, Cu, Mn, Mg, Sn and Zn and these can be removed by acid leaching up to 90% as a primary purification process.<sup>30</sup> The process starts with the crushing of metallurgical-grade silicon and the breakage occurs mostly at grain boundaries due to their low strength, thereby exposing metallic impurities present at the surface. Inorganic acids like HNO<sub>3</sub>, H<sub>2</sub>SO<sub>4</sub>, HCl and HF, or a combination of these, have been used under different conditions to optimise this process.<sup>12,39-40</sup> The advantages of this purification method are that it is cheap, uses simple equipment and can handle large quantities of metallurgical-grade silicon at a time. The acid leaching methods is

however not effective in removing interstitial and substitution impurities such as boron, carbon and oxygen.

#### 1.2.1.6 Directional solidification

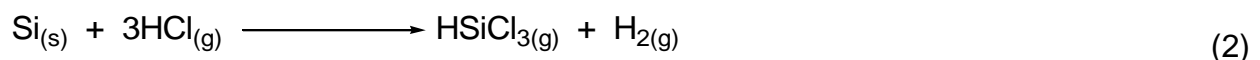
Directional solidification is the most important process in the purification of silicon using the metallurgical route. It is usually done as the last process after the removal of impurities with high segregation coefficients from metallurgical-grade silicon by other techniques discussed above. During solidification, many impurities with small segregation coefficients are segregated to the melt, resulting in more pure silicon solid.<sup>18</sup> This process is not suitable for the removal of B, P, Al, Ga, As, Sb because of their high segregation coefficients in the melt.<sup>37</sup> In practice, directional solidification is usually performed in heat exchanger furnaces for removal of most metallic impurities.<sup>27</sup>

#### 1.2.2 Chemical methods

In the chemical approach, the production of solar-grade silicon occurs through reduction and pyrolysis of volatile silicon compounds produced from metallurgical-grade silicon such as SiHCl<sub>3</sub>, SiH<sub>4</sub> and SiCl<sub>4</sub>. These methods include the Siemens™, the Union Carbide™ and the new silane processes.

##### 1.2.2.1 The Siemens™ process

The most commonly used chemical process, which contributes about 90% of high purity silicon production, is the Siemens™ batch-wise process (Figure 1.5).<sup>13,39</sup> In this process, metallurgical-grade silicon is hydrochlorinated without using a catalyst to form trichlorosilane at 300 °C and 1 bar (Equation 2).<sup>41-42</sup>



The trichlorosilane is subjected to purification by fractional distillation. High-purity SiHCl<sub>3</sub> is then vaporised, diluted with high-purity hydrogen at 1100 °C and introduced into the deposition reactors, where pure polycrystalline silicon is formed (Equation 3).



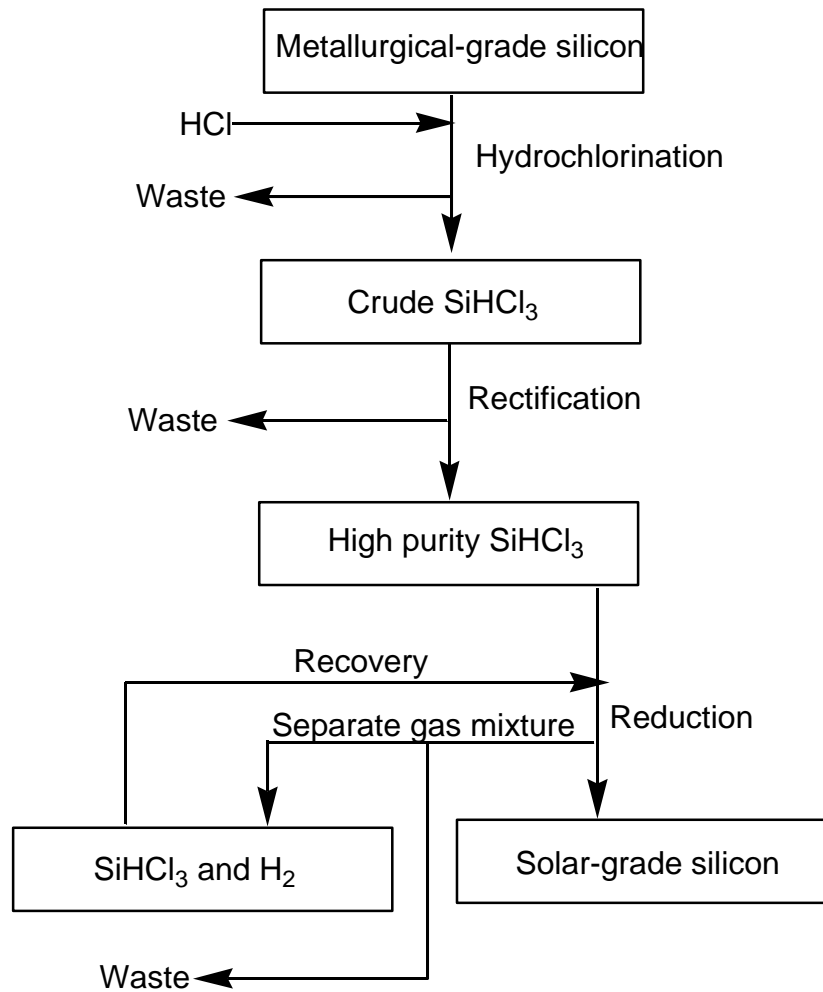
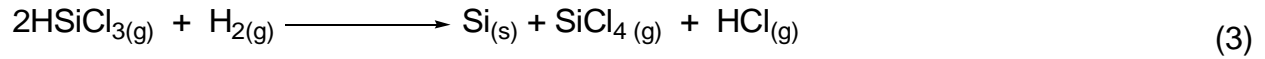
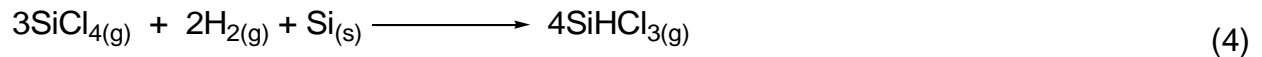


**Figure 1.5: Schematic diagram of the Siemens process**

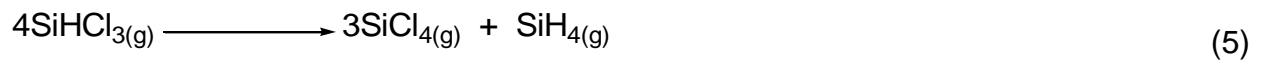
The disadvantage of the Siemens™ process is that it involves the production of chlorosilanes and reactions with hydrochloric acid at fairly high reaction temperatures. In addition to being toxic, these compounds are corrosive.<sup>9</sup> The process is also energy consuming, as it requires 200kWh/Kg of high purity silicon.

### 1.2.2.2 Union Carbide™ monosilane process

A modification of the Siemens™ process is the Union Carbide™ process (Figure 1.6),<sup>43</sup> which is less expensive in terms of energy consumption and more environmentally friendly since it recycles by-products.<sup>6</sup> In this process, metallurgical-grade silicon is reacted with silicon tetrachloride and hydrogen at 500 °C and 30 MPa to form trichlorosilane in a continuous fluidized bed reactor (Equation 4).



After purification and rectification, pure trichlorosilane undergoes disproportionation at 60 °C and 0.3 MPa to form silicon tetrachloride and silane (Equation 5). Silane is purified by fractional distillation and then decomposed at 800-850 °C to produce high purity silicon (Equation 6).<sup>12</sup> However, it is seen from the equation that for every mole of the product generated, three moles of tetrachlorosilane are regenerated; although this can be recycled it is clearly inefficient.



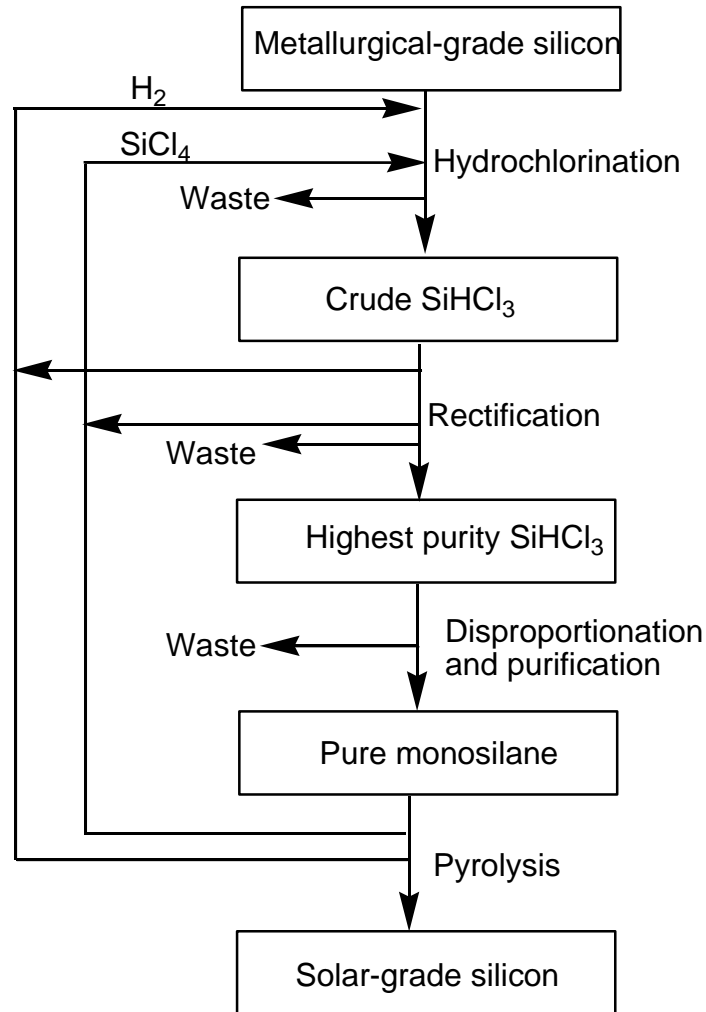


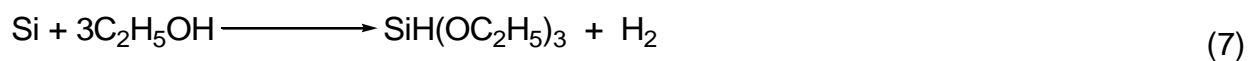
**Figure 1.6: Schematic diagram of the Union Carbide™ process**

The disadvantages of this method are that reactions are carried out at high pressure and temperature, which require costly equipment made from heat and pressure resistant and chemically inert materials.<sup>14</sup> The process also has more steps than the Siemens™ process and also produces toxic intermediates.

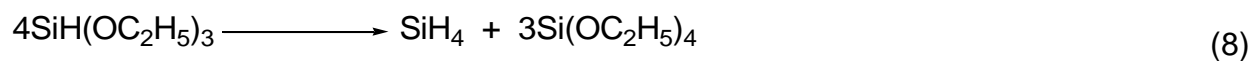
### 1.2.2.3 The new silane process

In order to improve on the costly, toxic and ecologically unfriendly Siemens™ and Union Carbide™ processes, a new method for the production of silane has emerged, although

no large scale production has been reported. A typical flow diagram for this process is shown in Figure 1.7.<sup>44-45</sup> Available literature indicate that this process is still under research and prototype stage and hence a lot of work still needs to be done to develop an integrated system for industrial application. At the first stage, powdered metallurgical-grade silicon and anhydrous ethanol are reacted at a temperature just above 180 °C at atmospheric pressure in the presence of a copper-based catalyst (Equation 7). At optimum conditions 85-90% of triethoxysilane is produced and the remainder could be tetraethoxysilane and diethoxysilane.<sup>45</sup>



The triethoxysilane is disproportionated at ambient or low temperature to form silane and tetraethoxysilane in the presence of a catalyst, which has not been disclosed in the literature (Equation 8).



The purified silane is then decomposed at about 800-850°C to produce high purity silicon.



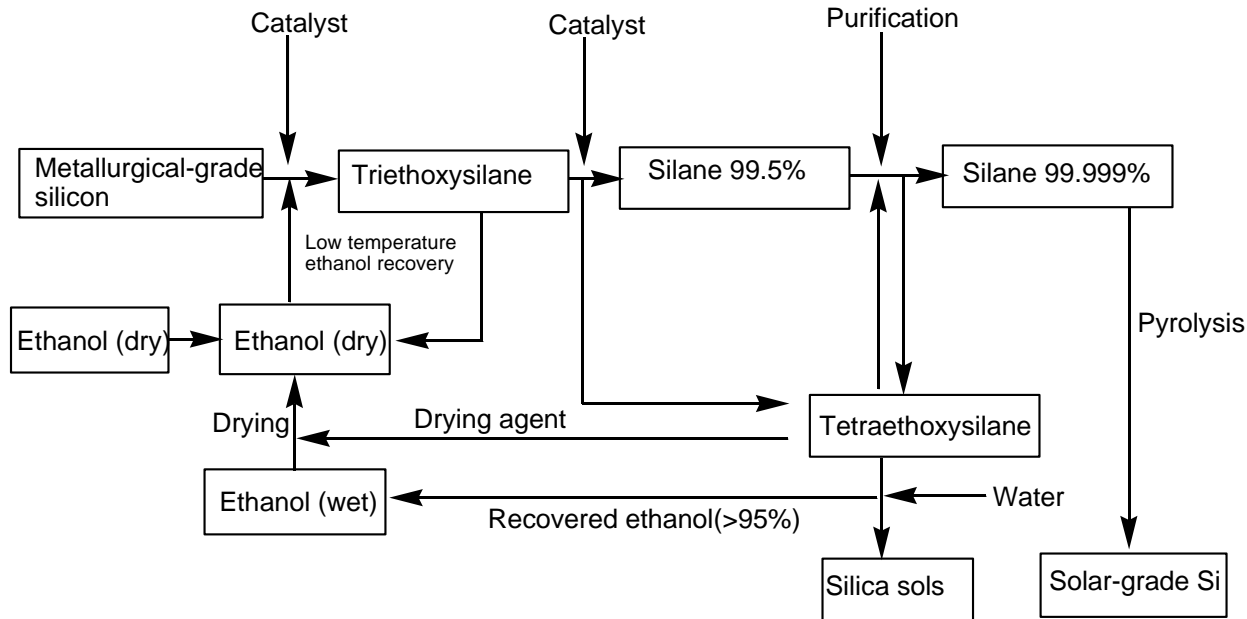


**Figure 1.7: Schematic diagram of the new silane process**

The major advantages of this method are that the reactions are carried out at lower temperatures and at atmospheric pressure, the by-products are converted into useful applications and ethanol may be recycled. The method is more energy efficient as it uses 30 kWh/kg of solar-grade silicon produced vs about 200 kWh/kg in the trichlorosilane method. The silicon yield is higher (80% to 95%) compared to the traditional trichlorosilane method (6% to 20%).<sup>46</sup> The method is also more environmentally friendly than the traditional methods since the reactions are conducted at lower temperature and there is no use of toxic and corrosive hydrochloric acid.<sup>47</sup>

### 1.2.3 Reactors

Reactors can be classified into batch type and continuous flow type on the basis of their kinetic behaviour. The batch reactor (Figure 1.8) is operated by feeding the raw material(s) into the reaction vessel and stirring to improve the contact of the reactants and the diffusion of the product in the case of heterogeneous reactions.<sup>48</sup> The product is recovered from the reactor after the reaction by several methods. The batch reactor can be in the form of a tank reactor. The batch type reactor is ideal for slow reaction rate liquid

phase reactions which take typically several hours. These type of reactors can be used for small scale production and are multi-purpose.

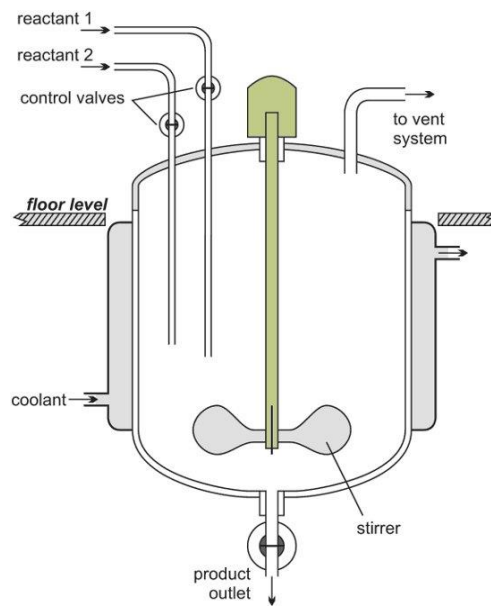


**Figure 1.8: An illustration of a batch reactor**

In the continuous flow reactor type, raw materials are fed continuously and products are continuously taken out. An example is a plug flow tubular reactor shown in Figure 1.9 equipped with a temperature gauge-controller (TC) and a flow recorder-controller (QRC). This type of reactor is ideal for large scale production plants, with high reaction rates and constant operation conditions.

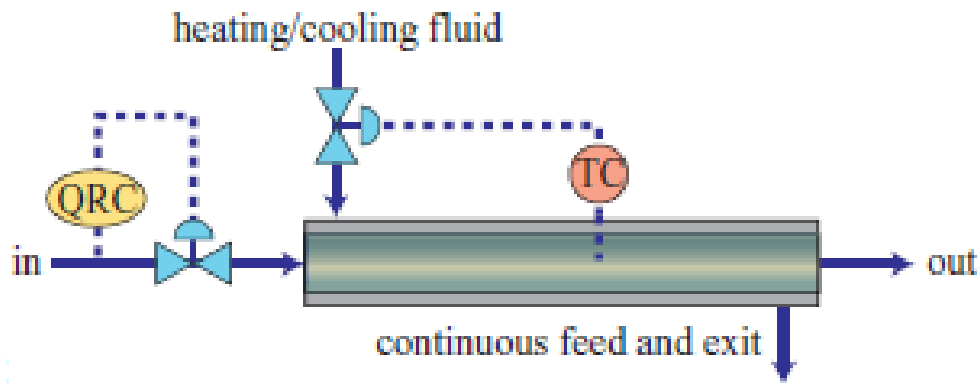


**Figure 1.9: A plug flow tubular reactor**

Continuous flow reactors can be divided into tubular reactors and continuous stirred tank reactors.<sup>49</sup> In a tubular reactor, the concentration of reactants is highest at the inlet and gradually decreases toward the outlet, while the concentration of the product gradually increases along the reactor. The residence times for all the reactant molecules passing through a tubular reactor are equal.<sup>50</sup> The continuous stirred tank reactor is equipped with a stirrer for vigorous agitation of the reaction mixture. Unlike the tubular reactor, the temperature and the chemical composition in the tank reactor is kept constant throughout the reaction and the residence time of the reacting molecules is not equal. The comparison between batch and continuous reactors is shown in Table 1.2.<sup>51</sup>

**Table 1.2: Comparison between batch and continuous reactors**

| <b>Attribute</b>   | <b>Batch reactor</b>                     | <b>Continuous flow tubular reactor</b>  | <b>Continuous stirred tank reactor</b>                                |
|--|--|---|---|
| <b>Temperature and concentration</b>                           | Unsteady state conditions                | Concentration changes in the direction of flow. No gradient of reaction rate and temperature in radial direction. | Composition in the reactor is uniform and equal to that at the outlet |
| <b>Mixing</b>  | Good mixing                              | No mixing and diffusion in axial position.  | Complete mixing   |
| <b>Required reactor volume</b>                                 | Relatively small                         | Relatively small  | Large   |
| <b>Distribution of products</b>                                | Large yield of intermediate product      | Large yield of intermediate product   | Small yield of intermediate product                                   |
| <b>Probability of reaction with specific composition ratio</b> | Impossible                               | Impossible  | Possible  |
| <b>Flexibility</b>   | Large                                    | Small   | Medium  |
| <b>Application</b>   | Multi-purpose and small scale production | Mass production   | Medium ideal where considerable heat transfer is needed               |



### **1.2.3.1 Gas-liquid reactors**

Gas-liquid reactors are widely used in industries for the purpose of gas purification and also for reactions such as halogenation, oxidation, hydrogenation and alkylation. There are at least three ways in which the reaction between a gas and a liquid may occur. The gas may either be dispersed as bubbles in the liquid, the liquid may be dispersed as droplets in the gas or the liquid and gas are brought together as films over a packing or wall. The choice of a gas-liquid reactor for a particular reaction depends on factors such as scale of operation, the power requirements and the magnitude and distribution of residence times. Examples of gas-liquid reactors include the bubble tower, spray tower, packed column, stirred tank and tray column and falling liquid film reactor.<sup>52</sup>

#### **1.2.3.1.1 The bubble tower**

A bubble tower column reactor (Figure 1.10) is basically a cylindrical vessel with a gas distributor at the bottom. The gas is sparged in the form of bubbles into either a continuous liquid phase or a liquid-solid suspension, and mixing is caused by the turbulent gas flow alone and usually additional energy input is required. The liquid or liquid-solid suspension can be in parallel or counter-current flow.

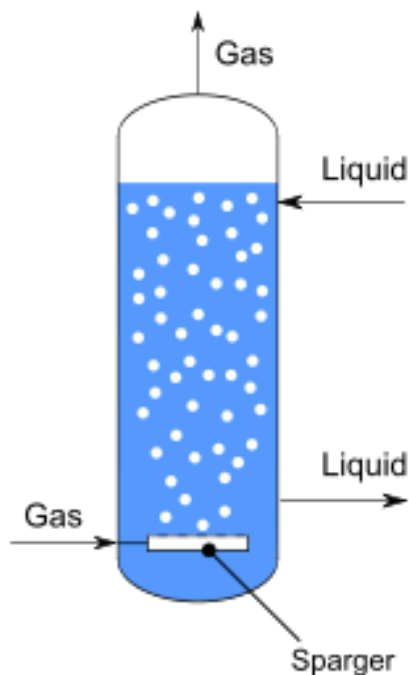
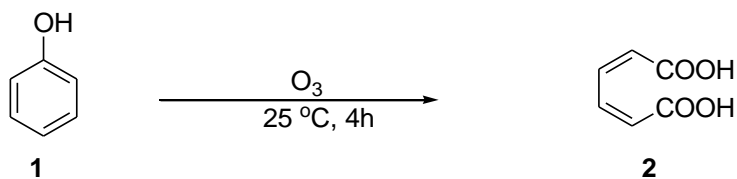


**Figure 1.10: An illustration of a bubble tower reactor**

Bubble tower reactors provide several advantages during operation and maintenance such as high heat and mass transfer rates, compactness and low operating and maintenance costs.<sup>53-54</sup> The bubble reactor is simple and energy saving since there are no moving parts involved. The reactor is suitable for slow reactions since liquid hold up is high. It is also characterized by moderate phase boundary surface.<sup>55</sup> Its disadvantage is the high pressure drop of the gas due to hydrostatic head of the liquid. Considerable backmixing and the relative difficulty in controlling axial and radial mixing of the liquid is also another disadvantage.<sup>56</sup>

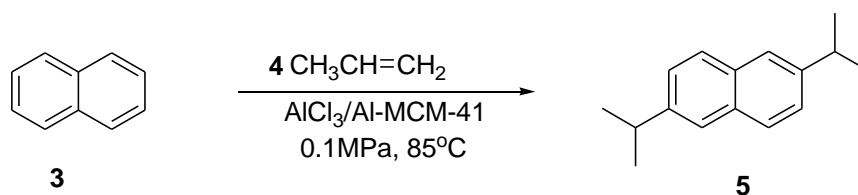
Reactions which have been performed in this kind of reactors include oxidation, alkylation and hydrogenation. Matheswaran and Moon<sup>57</sup> studied the ozonolysis of phenol **1** (Scheme 1) to hexa-2,4-dienedioic acid **2** in wastewater using a bubble tower column reactor. Their results showed that this type of reactor increases the rate of mass transfer of ozone and the rate of phenol oxidation. The effect of parameters such as ozone flow rate, initial phenol concentration and pH on the reaction was investigated to optimize the

process. The conversion of phenol ranged from 65 to 96% depending on the operating parameters used.



**Scheme 1: Ozonation of phenol**

The alkylation of naphthalene **3** with propylene **4** to 2,6-diisopropylnaphthalene **5** in the presence of immobilized aluminium chloride catalyst has been investigated in a slurry bubble column reactor (Scheme 2).<sup>58</sup> The conversion of naphthalene under optimized conditions was found to be 82%.



**Scheme 2: Alkylation of naphthalene to 2,6-diisopropylnaphthalene**

#### 1.2.3.1.2 Spray tower reactor

Spray towers consist of vacant cylindrical vessels containing nozzles that spray liquid in the form of droplets into the vessels. The inlet gas stream typically enters the bottom of the tower and moves upward, while liquid is sprayed downward counter-currently (Figure 1.11).

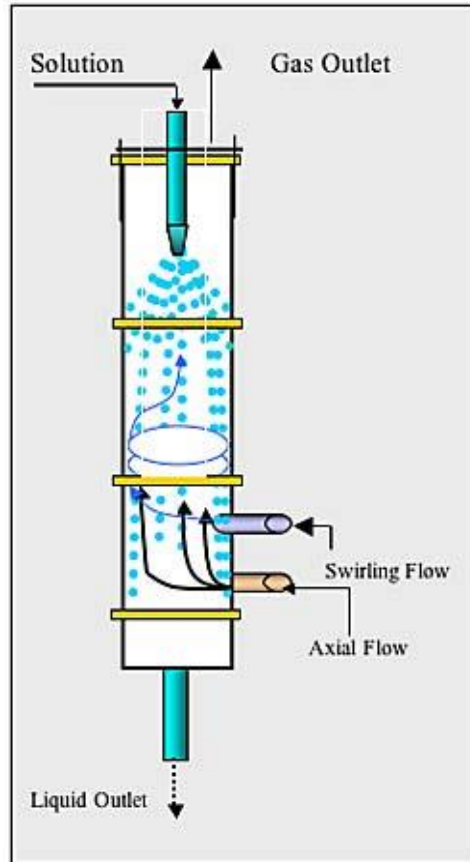
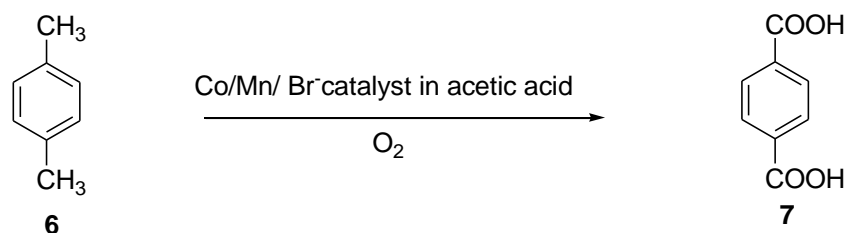


**Figure 1.11: Spray tower reactor**

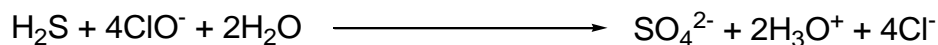
The gas-liquid interfacial area is relatively large but the contact time is small. These types of reactors are most useful for fast reactions due to the high velocity of gas particles.<sup>59</sup> They are also used when the product is formed suspended in a liquid or if the gas pressure must be minimised. The reactor is best suited for highly soluble gases. The main advantage of spray towers over other gas-liquid reactors is their completely open design since they have no internal parts except for the spray nozzles. This feature minimises scale build-up and plugging problems associated with other reactors.<sup>60</sup> The system has a limitation of low pressure drop for the gas phase. Furthermore, the process is characterised by low mass transfer efficiency due to bypassing and droplet coalescence and liquid entrainment in the gas phase.<sup>61</sup>

Spray towers are commonly used in the chemical and process industries for a number of applications including absorption, desorption, hydration and alkoxylation reactions. Li *et al.*<sup>62</sup> carried out the catalytic oxidation of *p*-xylene **6** to produce high-purity terephthalic acid **7** (Scheme 3) in a spray tower reactor. The reactor offered increased oxygen-liquid mass transfer area and reduced back mixing thereby facilitating oxidation. The terephthalic acid **7** was produced in high yield (95-98%) with less than 25 ppm of the by-product, 4-carboxybenzaldehyde.



**Scheme 3: Catalytic oxidation of *p*-xylene to terephthalic acid**

The removal of hydrogen sulphide has been investigated in a spray tower reactor using sodium hypochlorite as the liquid phase reactant (Scheme 4).<sup>63</sup> It was shown that the superficial gas velocity had a greater influence on the mass transfer parameters than the superficial liquid velocity. The optimized conditions managed to remove 99% of the hydrogen sulphide during the reaction.



**Scheme 4: Oxidation of hydrogen sulphide with sodium hypochlorite**

### 1.2.3.1.3 Packed columns

In packed column reactors, both the liquid and gas flow over a column filled with packings, with the flow usually in counter-current mode to enhance mass transfer of chemical reactions (Figure 1.12).

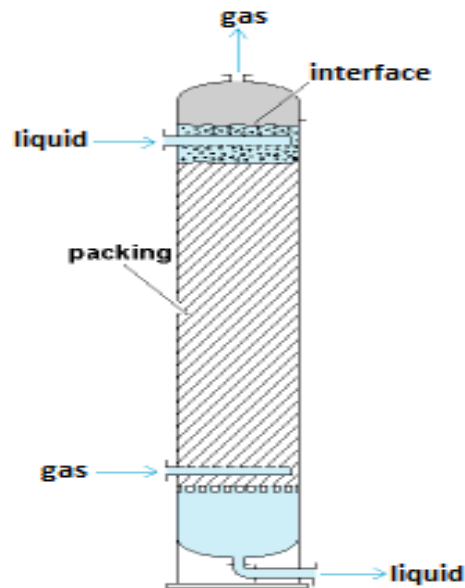
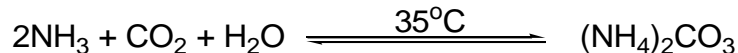


**Figure 1.12: Packed column reactor**

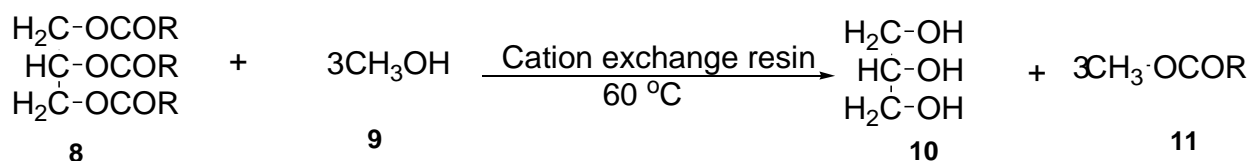
The packing can be solid shapes, such as ceramic rings or saddles to ensure appropriate flow and mixing of fluids. The liquid is distributed in the form of a film over the packing and the gas forms a continuous phase.<sup>64</sup> The gas-liquid interfacial area is enhanced by contact of gas rising through the void space between particles of the packing with a liquid film flowing down on the surface of the packing. These packings have a high specific surface, while the residence time is similar to the plug flow of an ideal tubular reactor.<sup>65</sup> Certain types of packings can be impregnated with catalysts as in the case with etherification, alkylation and esterification reactions.<sup>66</sup> The gas pressure drop is low and this type of reactor is suitable for reactions involving large volumes of gas. The design of these columns should take cognisance of flooding limits and mass transfer abilities.<sup>52</sup>

The application of a packed column reactor in the removal of carbon dioxide has been demonstrated.<sup>67</sup> In this study, aqueous ammonia was introduced from the top of the reactor as the liquid phase reactant to be in counter-current with carbon dioxide from the bottom (Scheme 5). The effect of operating variables on the absorption of carbon dioxide was studied and optimized to afford about 98% removal efficiency.



**Scheme 5: Reaction of aqueous ammonia with carbon dioxide**

Biodiesel production has been conducted in a column reactor packed with cation exchange resins.<sup>68</sup> In this research, the free fatty acids **8** were reacted with gaseous methanol **9** to form fatty acid methyl esters **11** and glycerol **10** as a by-product (Scheme 6). Under optimised condition, the reaction afforded 96% yield of the methyl ester.



**Scheme 6: Synthesis of biodiesel from free fatty acids**

**1.2.3.1.4 Continuous stirred tank reactor**

In this type of reactor, the liquid is agitated by an impeller to ensure good mixing so that there is a uniform composition throughout. An agitated tank generates small bubbles, which provide a high interfacial contact between gas and liquid phases in a reaction.<sup>69</sup> In a continuous stirred tank reactor (Figure 1.13), there is continuous feed of reactants and simultaneous extraction of products. There are no gradients of concentration and temperature with respect to location as perfect stirring is assumed. A fair approximation to perfect mixing is not difficult to attain in this type of reactor provided the phase is not too viscous. Therefore, the composition and the temperature of the streams leaving are equal to those existing inside the reactor.<sup>70</sup>

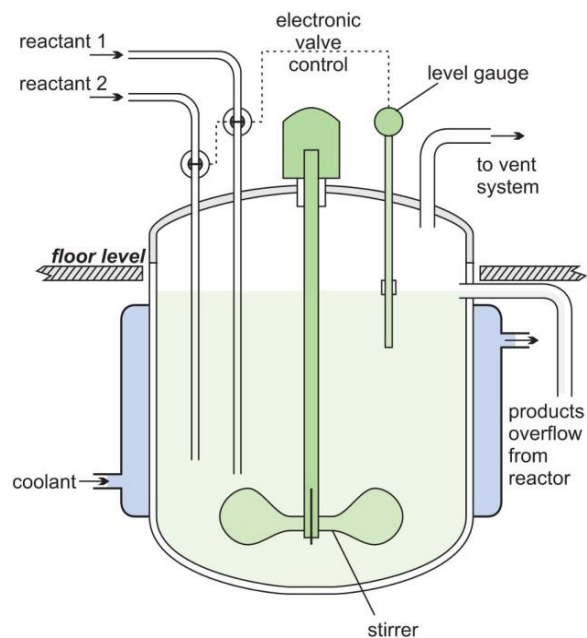


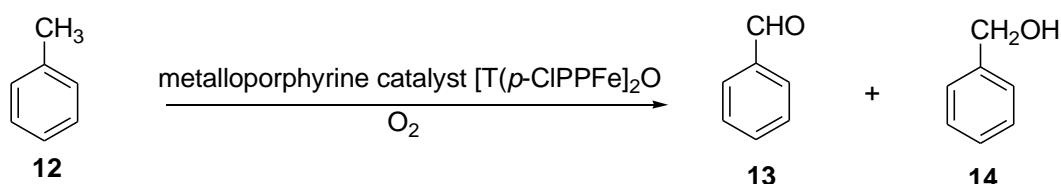
**Figure 1.13: An illustration of a continuous stirred tank reactor**

The continuous stirred tank reactor operates at the reactor outlet condition, which is at low substrate concentration and therefore low reaction rate. Such low concentrations can, however, be beneficial for the improvement of reaction selectivity, for autocatalytic type reactions and for the reduction of chemical hazard. Other advantages are that by-products can be removed in-between the reaction and that the reaction can be carried out in horizontal as well as vertical reactors. It is advantageous to have several continuous stirred tank reactors in series, as this reduces loss of unreacted starting materials. Temperature control is easy in this reactor because stirring minimizes hot spots and also the tanks offer a large surface area for cooling.<sup>71</sup> As compared to tubular reactors, the internal surface of stirred tank reactors is easy to clean and this is important in the case of reactions where there is possibility of solid deposition. The operation of continuous stirred tank reactors in series results in a stepwise change of composition between successive tanks. A usual consequence of the stepwise change in concentration is that the average reaction rate is lower than it would be in a tubular reactor. This type of reactor has a large liquid holdup, consumes considerable power and is more complex and expensive than tubular units. A steady state must be reached where the flow rate into the reactor equals the flow rate out, otherwise the tank would empty or overflow. Other



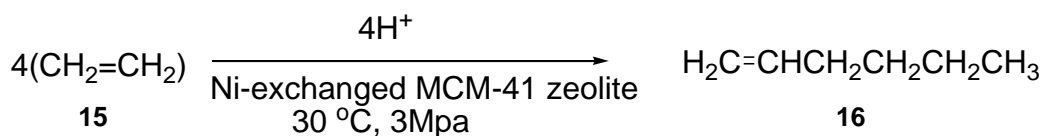
disadvantages of this system are that it cannot handle corrosive chemicals (if made of steel), high temperatures and high pressures.<sup>72</sup>

This reactor is ideal for chemical reactions such as polymerization, oxidation, esterification and saponification.<sup>73</sup> Luo *et al.*<sup>74</sup> investigated the aerobic oxidation of toluene **12** to benzaldehyde **13** and benzyl alcohol **14** (Scheme 7) in a series of three continuous stirred tank reactors. The conversion of toluene under optimized conditions was 8.7mol% whilst the total yield of benzaldehyde and benzyl alcohol was 4.2mol%.



#### Scheme 7: Selective oxidation of toluene

The oligomerization of ethylene **15** (Scheme 8) has been performed in continuous stirred tank reactors, resulting in the selective formation of C<sub>4</sub>, C<sub>6</sub> **16**, C<sub>8</sub> and C<sub>10</sub> olefins.<sup>75</sup> The reaction resulted in high conversion of ethylene (95%) when optimum conditions were employed.



#### Scheme 8: Oligomerization of ethylene to $\alpha$ -hexene

##### 1.2.3.1.5 Tray columns

A tray or plate column reactor contains sieve plates at intervals along its height as illustrated in Figure 1.14. The flow of gas and liquid is countercurrent, and liquid may be assumed to be distributed uniformly and radially on each plate. On each plate or tray, gas

is dispersed within the continuous liquid phase.<sup>76</sup> The gas-liquid interfacial area is relatively large, and the gas-liquid contact time is typically greater than that in a packed tower. The liquid content in the tray column reactor is relatively high, such that it can be used for reaction systems with low to moderate reaction rates. In contrast to continuously stirred tank reactors or bubble column reactors, the residence time in each tray is much more uniform. The tray columns are used where the operation required is stagewise and when large volumes of gases are used.<sup>77</sup> The shallow nature of the trays means the pressure drop of the gaseous phase and the liquid hold-up are relatively low.<sup>51</sup>

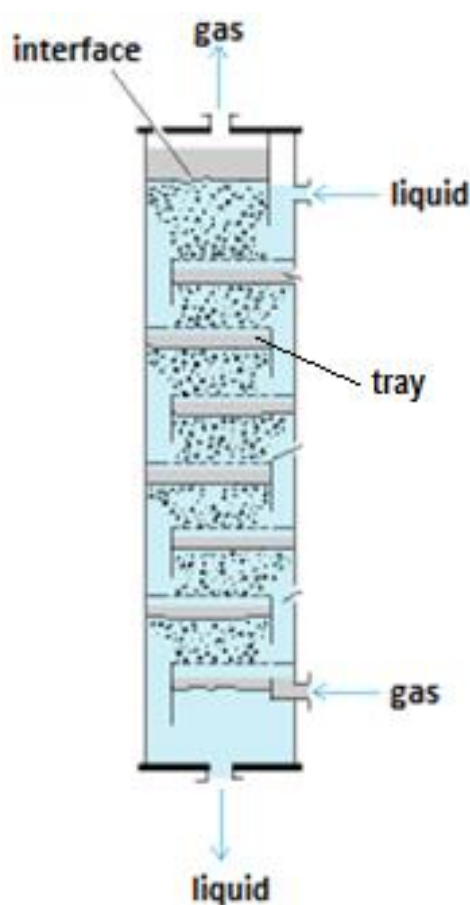


**Figure 1.14: Tray column reactor**

One important application of tray column reactors is their use in esterification reactions. von Harbou *et al.*<sup>78</sup> synthesized *n*-hexyl acetate from the reaction of *n*-hexanol and acetic acid in a tray column reactor. Acetic acid was introduced from the top of the reactor whilst the *n*-hexanol was introduced from the bottom in counter-current flow (Figure 1.15). A

strongly acidic and fully sulfonated ion-exchange resin (Amberlyst CSP2) was used as a heterogeneous catalyst. High conversion of acetic acid (94-96%) was realised under optimum conditions.

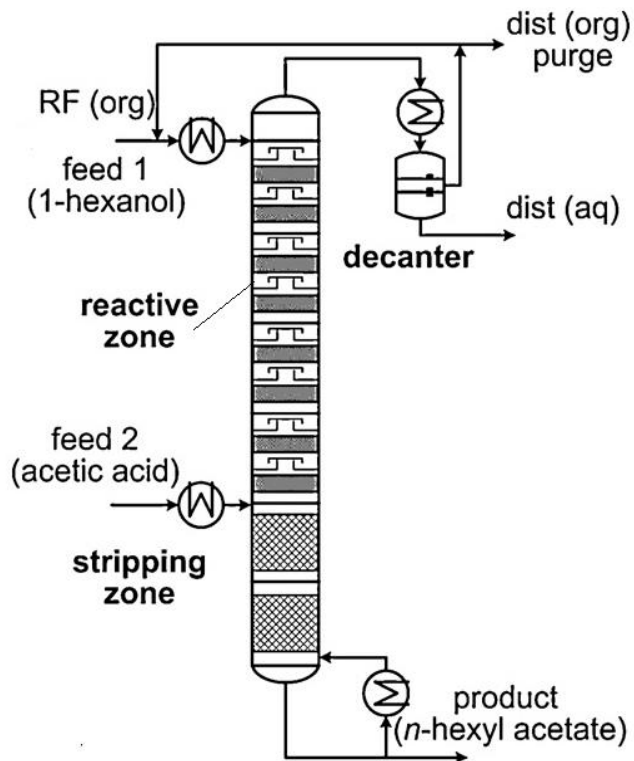


**Figure 1.15: Synthesis of *n*-hexyl acetate from the reaction of *n*-hexanol and acetic acid in a tray column reactor<sup>78</sup>**

Tray columns are also used in absorption of gases such as carbon dioxide and hydrogen sulphide. In one of the studies,<sup>79</sup> a sieve tray which has flat perforated plates was used. The flat perforated plates help to keep the liquid from flowing down through the holes and the CO<sub>2</sub> gas and methanol liquid are brought in contact in a counter-current flow. It was deduced that the maximum enhanced absorption rate of carbon dioxide was 9.7% when the methanol-based SiO<sub>2</sub> nanofluids were used.

### 1.2.3.1.6 The falling liquid film reactor

In the falling liquid film reactor, the liquid and gas are brought together as films over a packing or wall.<sup>80</sup> A continuous liquid film flows by gravity down a solid vertical tube having one free surface with counter-current gas flow as illustrated in Figure 1.16.

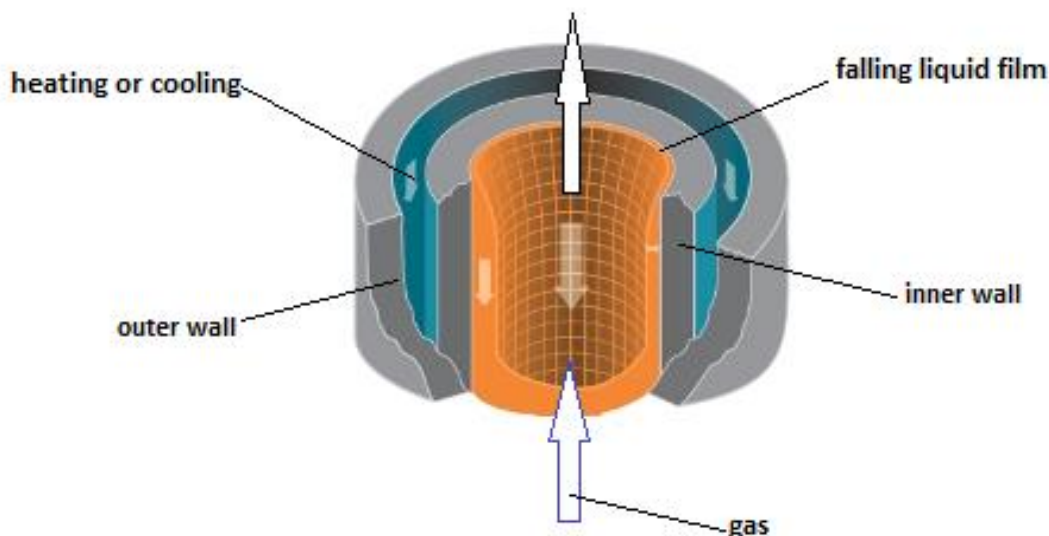
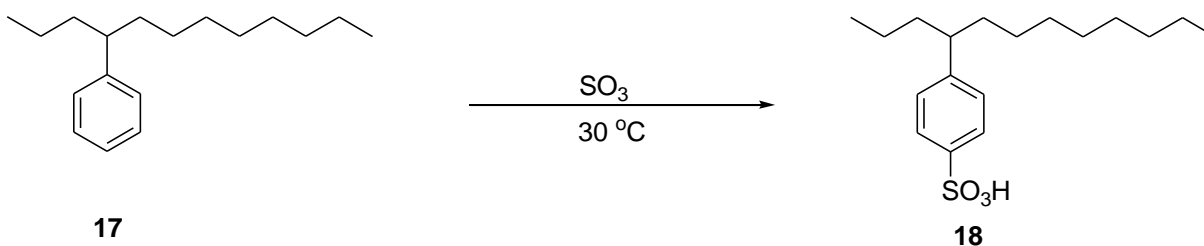


**Figure 1.16: A falling film reactor cross section**

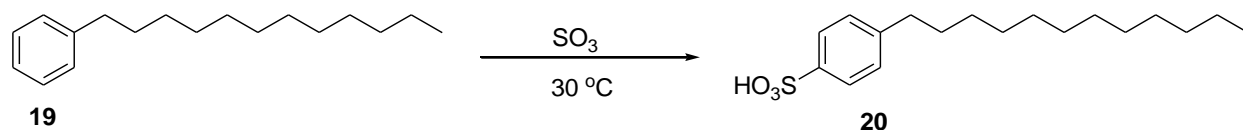
Its advantages are that liquid residence time is small, transfer rates are high for comparatively small pressure losses and it possesses a large interface of simple geometry.<sup>60</sup> The other advantage of falling film reactors is that they can be cooled externally and hence any heat released during a highly exothermic reaction can be dissipated *via* the reactor wall without forming hot spots in the reactor body. The system is however prone to flooding and poor wetting if not properly designed and operated.<sup>49</sup>

This reactor is preferred for very rapid exothermic gas-liquid reactions and has been widely used in sulphonation and chlorination reactions. Zaid *et al.*<sup>81</sup> investigated the sulphonation of low molecular weight linear alkyl benzene **17** (Scheme 9) in a corrugated wall falling film reactor. Their results showed that the sulphonated alkyl benzene **18** product obtained with the corrugated wall falling film reactor (91%) was greater than that obtained with the conventional smooth wall falling film reactor (76%).



### Scheme 9: Sulphonation of linear alkylbenzene

Mathematical modelling and simulations of falling film tubular reactors have been reported in the literature for sulphonation,<sup>82</sup> ethoxylation,<sup>83</sup> water treatment,<sup>84-85</sup> photocatalytic production of hydrogen<sup>86</sup> and sulphur dioxide adsorption.<sup>87</sup> In most cases factors such as film thickness and turbulence, chemical conversions, gas phase heat and mass transfer resistance and gas-liquid interfacial drag were considered and compared with other laboratory and industrial scale reactors. Some of these models have been recommended for design and operation of large scale industrial falling film reactors. Dabir *et al.*<sup>88</sup> modelled the sulphonation of dodecyl-benzene **19** (Scheme 10) and predicted the degree of chemical reaction conversion, liquid film thickness and longitudinal temperature along the reactor. The model conversion of dodecyl-benzene **19** was to dodecyl-benzenesulphonic acid **20** found to be about 93% conditions and comparable to the laboratory one of 94% under optimized.



### Scheme 10: Sulphonation of dodecyl-benzene

### 1.2.3.2 Gas-solid reactors

Gas-solid reactors are widely used in industry as they offer high heat and mass transfer rates. Specific examples of gas-solid reactions include combustion of solid fuels, manufacture of hydrogen by the reaction of steam with iron, chlorination of mineral ores and conversion of ferrous oxide to magnetic ferric oxide, dehydrogenation reactions and nitration reactions.<sup>89</sup> Gas-solid reactors can be basically classified into fluidized bed and packed bed reactors.

#### 1.2.3.2.1 Fluidized bed reactor

A fluidized bed reactor consists of a bed of granular solid material, supported over a fluid distributing plate (Fig 1.17) and is made to behave like a liquid by the passage of fluid which could be gas or liquid at a flow rate above a certain critical value.

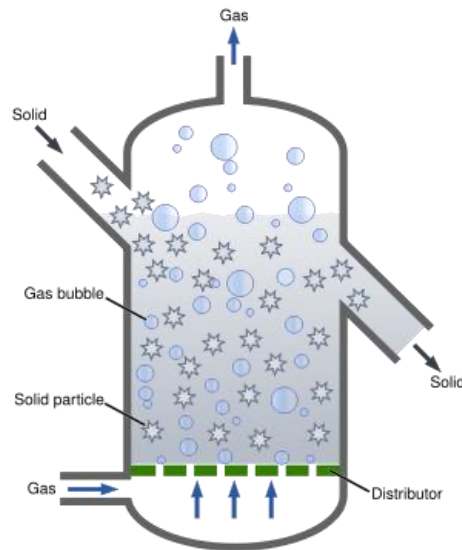


**Figure 1.17: Fluidized bed reactor**

This type of reactor is useful in carrying out several multiphase reactions.<sup>90</sup> Fluidized bed reactors are nowadays used in a vast number of industrial applications, which encompass the chemical, metallurgical, environmental and pharmaceutical sector. The most important advantage of fluidized reactors arise from the fact that the solid materials it contains are in a continuous motion and are normally well mixed. This leads to rapid

elimination of hot spots and the bed works essentially in an isothermal manner. Particle motion in this type of reactor makes temperature control easy because of the very high bed-to-surface heat.<sup>91</sup> The fluid-like properties of the gas-solid mixture enable the solid to be transferred without difficulty from one reaction vessel to another and this is a useful feature that allows continuous flow synthesis coupled with high throughput. Fluidized bed reactors have low maintenance costs since they have no moving parts and are not mechanically agitated.

The disadvantages of fluidized beds include the erosion of internal components caused by the fluid-like behaviour of fine solid particles within the bed and loss of fine particles through cyclone plugging, which can be costly if the catalyst or the starting material is expensive. There could also be the by-passing of the solid by gas bubbles which could severely limit conversion. Reactions that require a temperature gradient inside the reactor cannot be accomplished in a fluidized reactor.<sup>92</sup> Another disadvantage is that fine-sized particles need special techniques for fluidization. The fluidized reactor can result in undesirable products and complicated separation techniques as a result of generation of fines due to turbulent mixing, gas or liquid gas interaction at the distributor site and segregation due to agglomeration. The fact that the bed material in the reactor is expanded means that large vessels are needed for construction of fluidized reactors as compared to packed bed reactors. This is a disadvantage in terms of space and initial costs. This type of reactor can also be expensive in terms of energy needed for pumping in order to maintain fluidity. Pressure drops often occur and this leads to loss of bed surface area leading to low conversions.<sup>93</sup>

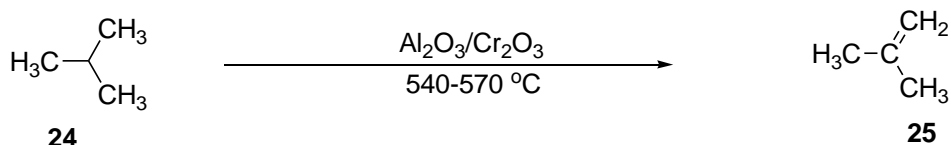
The application of fluidized beds in chemical processes include the production of gasoline, the polymerization of olefins as well as the production of synthetic natural gas *via* syngas methanation. The use of a fluidized reactor has been applied in the vapour phase ethylation of benzene (Scheme 11).<sup>94</sup> At optimized conditions, the maximum benzene **21** conversion of 17% was realized. The selectivity for ethylbenzene **22** and 1,2-diethylbenzene **23** was 60 and 37% respectively at 400 °C for 1:1 benzene to ethanol feed ratio. The products of this reaction afford monomers for styrene synthesis. The use

of a fluidized bed reactor in this case is seen as an environmentally friendly substitute for the conventional method that uses homogeneous catalysts.



**Scheme 11: Ethylation of benzene**

Fluidized bed reactors have also been used in dehydrogenation reactions for the production of pure olefins. Sanfilippo<sup>95</sup> demonstrated the dehydrogenation of isobutane **24** to isobutene **25** in the presence of aluminium and chromium oxide composites as catalyst (Scheme 12). The vapour phase reaction afforded 92-95% selectivity to isobutene. Isobutene is an important intermediate in the production of gasoline oxygenates and other fuel additives like isooctane.



**Scheme 12: Dehydrogenation of isobutane to isobutene**

### 1.2.3.2.2 Packed bed reactors

A packed bed reactor used in gas-solid reactions consists of a compact immobilized stack of a catalyst or reactant within a generally vertical vessel into which vaporized reagents are added for the reaction to occur on the bed and products are continuously removed (Fig. 1.18).



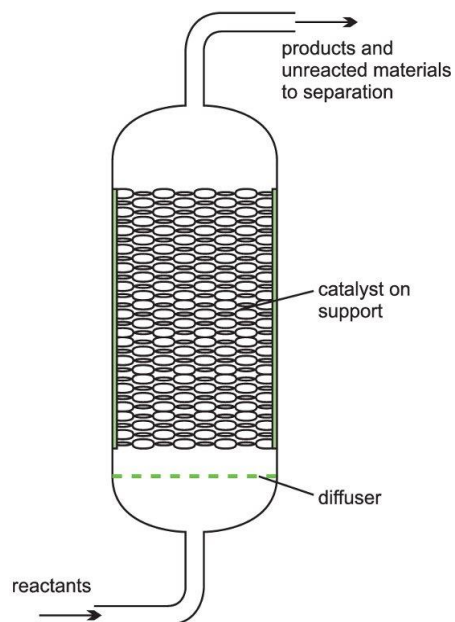


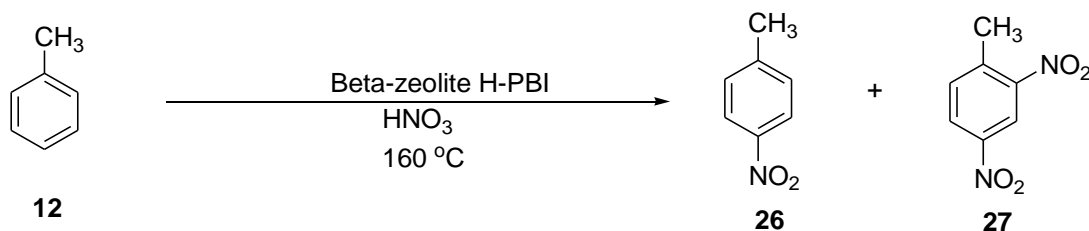
**Figure 1.18: Packed bed reactor**

In this reactor the solid can either be a reactant or a catalyst. The catalyst or the solid reactant is held in the reactor and does not need to be separated from products.<sup>96</sup> Industrial packed bed reactors range in size from small diameter to large diameter packed beds and are smaller than fluidized bed reactors.

Packed bed reactors offer advantages of ideal plug flow behaviour, lower maintenance, operation and construction costs and reduced loss due to attrition and wear. The other advantage is that there is more contact between reactant and catalyst than in other types of reactors and this lead to increased product formation and selectivity due to high conversion rate per weight of catalyst.<sup>56</sup> Packed bed reactors are continuously operated and are effective at high temperatures and pressures. The use of heterogeneous catalysts, which can be regenerated, means that the process is less costly and environmentally friendly. *In situ* activation of the catalyst ensures that the catalyst is freshly prepared before the reaction. Packed bed reactors also offer the advantage of continuous flow production and lead to high throughput.<sup>97</sup>

Large packed bed reactors are characterized with difficult temperature control and consequently poor heat transfer may also result in the generation of hot spots and thermal degradation of the catalyst. Channelling of the gas stream can occur, leading to ineffective regions in the reactor and side reactions are possible. The replacement of catalyst or solid reactant is also difficult in fixed-bed reactors and may require shutting down the process. Another major disadvantage of packed bed reactor is plugging of the bed, due to coke deposition which results in high pressure drop.<sup>59</sup>

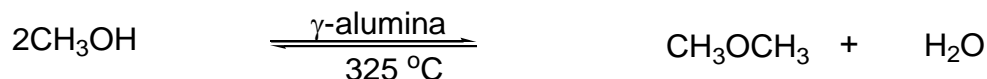
Packed bed reactors have been used to accomplish the gas phase continuous flow nitration reactions of benzene and its derivatives as an alternative to traditional mixed acid process which is not very eco-friendly.<sup>98</sup> In a typical reaction, vapourized toluene **12** was reacted with vapourized nitric acid on a beta-zeolite catalyst bed. The reaction produced 4-nitrotoluene **26** and 2,4-dinitrotoluene **27** as the nitrated products (Scheme 13). The selectivity and yield to the desired compound **26** were 60% and 55% respectively. The di-nitrated product was formed in 5% yield. The mononitrated compound **26** is useful in industry as a precursor for the synthesis of fine and bulk chemicals.



**Scheme 13: Vapour phase nitration of toluene**

Dimethylether is a promising alternative fuel with less sulphur and nitrogen oxides emissions and its synthesis is mainly done by the direct route, where hydrogen is reacted with carbon dioxide in the presence of a hybrid catalyst. The continuous flow synthesis of dimethylether in packed reactors was demonstrated by Ghavipour and Behbahani.<sup>99</sup> The reaction was accomplished through the indirect method where vaporized methanol was dehydrated to dimethylether over a  $\gamma$ -alumina catalyst (Scheme 14). In typical results, the

conversion of methanol was about 83% when the methanol flow rate of 12.7 mL/min and a catalyst bed of 40 g was used.



#### **Scheme 14: Dehydration of methanol to dimethylether**

### **1.2.4 Continuous flow synthesis**

In continuous flow synthesis, starting materials and reagents are fed at the inlets of the reactor by pumping mechanisms and at the same time products are continuously taken out. In homogeneous reactions, catalysts are fed at the inlets and in heterogeneous reactions solid catalysts are usually supported inside the reactor and the reaction occurs along the tube. The advent of continuous flow synthesis has brought many advantages over traditional batch processes. Some of the advantages and disadvantage of this process are outline below.<sup>100-105</sup>

#### **1.2.4.1 Advantages**

- Continuous mass production.
- Continuous reactors are generally able to cope with much higher reactant concentrations due to their superior heat transfer capacities as long as solubility is good. The ideal situation being to use solvent free conditions.
- Less space requirements as equipment used in continuous flow manufacturing is much smaller in size as compared to batch processing.
- Reduce required space.
- Improves quality.
- Reduce operator involvement.
- Constant reaction rate.
- Ease of balancing to determine kinetics due to steady state.
- Less down-time for cleaning and filling.
- Reaction temperature can be raised above the solvent's boiling point.

- Mixing can be achieved within seconds.
- Safety is increased because there is provision for recycling by-products and waste.
- Flow reactions can be easily automated with far less effort than batch reactions.
- Allows multi-step reactions to be arranged in a continuous sequence.
- Heat transfer is intensified as the area to volume ratio is large.
- Position along the flowing stream and reaction time point are directly related to one another.
- Purification of the product can be coupled with the reaction.
- Reactions which involve reagents containing dissolved gases are easily handled.
- Multi-phase liquid reactions can be performed.
- Scale up of a proven reaction can be achieved rapidly with little or no process development work.
- Better for indefinitely long production runs of one product or set of products.
- Operating cost relatively low.
- Process control and obtaining uniformity of product easier because of steady-state operation.
- Quality assurance testing can be improved as it is easier to monitor the process in continuous flow manufacturing as opposed to batch processing.
- Steady-state operation allows easy coupling with continuous down-stream operation.
- Operating cost relatively low.

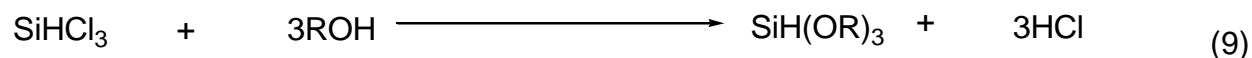
#### **1.2.4.2 Disadvantages**

- Capital cost may be relatively higher than batch process.
- Flexibility usually low.
- Dedicated equipment is needed for precise continuous dosing.
- Start up and shut down procedures have to be established.
- Costly shut down for cleaning very demanding.

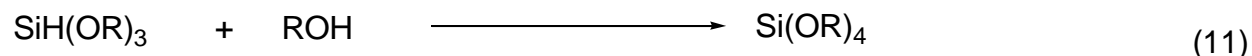
- Safety issues for the storage of reactive material still apply but the ideal scenario is to react intermediates *in situ* to avoid storage of highly dangerous materials.

### 1.2.5 Synthesis of alkoxysilanes

The widely used traditional method for the synthesis of alkoxysilanes involves the reaction of trichlorosilanes with alcohols (Equation 9, where R is alkyl) in the presence of copper-based catalyst.<sup>106</sup> Trichlorosilanes are produced by the reaction of silicon with hydrochloric acid (Equation 2). However, this approach is faced with challenges such as low selectivity and poor yield of the desired trialkoxysilane product, in addition to the toxic and corrosive hydrochloric acid by-product.



Various researchers have reported the direct synthesis of trialkoxysilane mostly in continuously stirred slurry phase tank reactors by reacting silicon metal with an alcohol (Equation 10) in the presence of copper-based catalyst and mostly using organic heat transfer fluids, such as diphenylalkanes. The challenge of this reaction is the selectivity towards the trialkoxysilanes over the undesired tetraalkoxysilane, which is also formed (Equation 11). In most cases, the trialkoxysilane produced was recovered from the products by distillation techniques.



Muraoka *et al.*<sup>107</sup> carried out the batch-wise synthesis of trialkoxysilane by reacting finely divided silicon with ethanol containing 0.17% hydrogen fluoride in the presence of copper

(I) chloride as a catalyst. Silicon and the catalyst were suspended in aromatic synthetic oil and heated to 250 °C, after which ethanol was introduced. The reaction afforded triethoxysilane (73.3%) and tetraethoxysilane (4.5%). The reaction resulted in the generation of hydrochloric acid, which was not ideal for the equipment used given its corrosive nature.

The use of finely divided copper (I) chloride catalyst with zinc or aluminium as promoters in the presence of hydrogen as a carrier gas in the alkoxylation reactions was investigated by Wit<sup>108</sup> in a fluidised-bed reactor. It was noted that if finely divided copper was used, the percentage of copper in the contact mass will remain practically the same, thereby increasing catalytic efficiency. The highest yield of triethoxysilane produced was 78%. This method however does not avoid the generation of toxic and corrosive hydrochloric acid, which results in the need for expensive corrosion resistant materials of construction for the reactor and related equipment. Furthermore, the use of copper (I) chloride catalyses the conversion of trialkoxysilane to tetraalkoxysilane, thereby decreasing the yield of the desired trialkoxysilane as a result of reduced selectivity.

Okamoto *et al.*<sup>109</sup> studied the reaction of hydrofluoric acid washed silicon with various primary, secondary and tertiary alcohols in a fixed-bed flow reactor. The reactions of silicon with ethanol, 1-propanol, and 1-butanol gave high silicon conversions of 95, 85, and 77% respectively, at 240 °C without heat treatment of the silicon-catalyst mixture. The selectivity of trialkoxysilanes was found to be greater than 99%. There were no noticeable reactions for secondary and tertiary alcohols. The high temperature pre-treatment of silicon-catalyst mixtures results in the formation of metallic copper which catalyses the dehydrogenation of alcohols to aldehydes and the reaction of trialkoxysilane with alcohol to give the undesired tetraalkoxysilane. Adding thiophene to the alcohol feed poisoned the metallic copper and improved yield of trialkoxysilanes.

Lewis, Cameron and Ritscher<sup>47</sup> reported the direct synthesis of trialkoxysilanes by reacting technical grade silicon with alcohols in batch and continuous processes in the presence of either  $\text{Cu}(\text{OH})_2$  or  $\text{Cu}_2\text{O}$  as catalysts. The same method was also reported

by Lewis and Yu.<sup>110</sup> In both studies, the reaction exhibited high selectivity to the trialkoxysilanes (80-95%), high overall silicon conversion (>70%) and high stable reaction rates. The use of cyanide and nitrile additives as promoters increased silicon conversion when ethanol, propanol and other higher alcohols were the reactants. The use of nanosize Cu<sub>2</sub>O also resulted in higher silicon conversion (70-80%). The disadvantage of this reaction is the use of toxic promoters, although corrosive chloride compounds are avoided. The use of catalytic amount of copper (II) hydroxide for the direct reaction of silicon metal with alcohol was also reported by Mendicino.<sup>111</sup> In this study high selectivity (>80%) and yield (>75%) of the trialkoxysilane was realised. The conversion rates of silicon were also high (>75%).

Anderson and Meyer<sup>112</sup> made use of halogen free copper catalyst in the form of cupric *bis*(diorganophosphate) in the direct synthesis of alkoxy silanes. The method eliminated the generation of toxic and corrosive chlorine compounds, but the selectivity of the desired triethoxysilane was low (<60%). The reaction was also characterised by low yields of triethoxysilane (<42%).

In recent research,<sup>113</sup> the use of aluminium as an additive has been seen to increase the rate of formation of trimethoxysilanes. In this research, methanol was reacted with silicon in a packed bed flow tubular reactor using copper (I) chloride as catalyst. It was also noted that the rate of trimethoxysilane formation increases by an increase in temperature from 250 °C to 350 °C and catalyst loading from 5 to 15%. The reaction however could only afford a yield of 28% for the desired trimethoxysilane. The use of copper (I) chloride as a catalyst results in the formation of corrosive hydrochloric acid, which can react with methanol to form methyl chloride and water. The produced trimethoxysilane can react with water to produce siloxanes.

Lei *et al.*<sup>114</sup> investigated the reaction of silicon with ethanol in a gas-solid stirred fluidized bed, with cuprous chloride prepared by a wet process as the catalyst. It was revealed that the use of hydrogen fluoride and ethyl chloride as promoters depressed the catalytic activity of metallic copper. This improved the yield (>75%) and selectivity (>80%) of

triethoxysilane. The use of a chloride in the form of methylchloride to promote high selectivity (78%) and stability of the trialkoxysilane was also observed by Ohta and Yoshizako.<sup>115</sup> The limitation of these methods is the production of hydrochloric acid, which is corrosive to the equipment used. Phosphate compounds have also been used as promoters in the production of trialkoxysilanes affording high yield (90%) and high silicon conversion (80-85%).<sup>116</sup>

A process in which surface-active additives are used in the slurry phase during the direct synthesis of trialkoxysilanes has also been disclosed.<sup>117</sup> The surface active additives shortened the period between the start of the reaction and the attainment of steady-state rates and selectivity. These additives also improved product yields (80-85%), silicon conversion (90-94%) and controlled or prevented foam formation. In this discovery, compositions comprising silicone antifoam compounds and fluorosilicone polymers were the preferred surface-active additives. The method afforded high selectivity (>85%) towards the desired triethoxysilane but failed to explain the fate of the surface active additives, which may interfere with the production process at high temperatures.

The effect of heat transfer solvents/fluids on the selectivity and yield of the desired trialkoxysilanes has been studied. A series of experiments were carried out using different heat transfer solvents. The use of diphenylalkanes resulted in high silicon conversion (80%) and high trialkoxysilane selectivity (96%).<sup>118</sup> It was concluded that diphenylalkanes are the most appropriate and also they are inert and cheaper than other conventional solvents normally employed.

Han *et al.*<sup>119</sup> studied the batch process for reaction of elemental silicon with methanol in the presence of copper using a small amount of cuprous chloride as an activator in dibenzyltoluene. The reaction worked well using a 0.5wt% copper chloride as an activator at a temperature of 240 °C. Trimethoxysilane was obtained with 81% selectivity from 85% conversion of elemental silicon. This reaction has an advantage of reducing the accumulation of hydrochloric acid since it uses catalytic amounts of copper chloride.



The alkoxylation reaction between ethanol and silicon in the presence of freshly prepared copper (I) chloride using dodecylbenzene as a solvent, in a stirred batch process, was reported by Harada and Yamada.<sup>120</sup> Their results showed high selectivity (>90%) for the triethoxysilane. The silicon metal conversion was almost 100%. These results are attributed to the use of freshly prepared catalyst and the addition of aluminium (0.36-0.37wt %) as a promoter. The yield of triethoxysilane was however low (<60%). A modification of this method by Brand<sup>121</sup> produced better results when freshly precipitated non-halogenated copper (II) oxide was used. In this reaction 72-80% of silicon was converted to alkoxysilanes affording high selectivity (90-92%) to the desired trialkoxysilane.

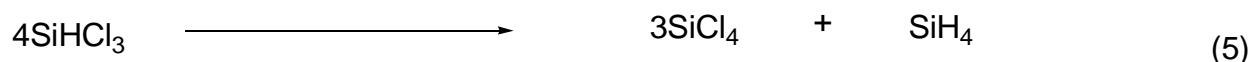
Microwave reactors have been found to accelerate the rate of trialkoxysilane production in high yields and high silicon conversion (95%).<sup>122</sup> The desired trialkoxysilanes were prepared with high selectivity (100%) and shorter reaction times and lower temperatures as compared to traditional approaches. The disadvantage of this method is that it is carried out batch-wise and presents problems in up-scaling.

The major challenge with the direct alkoxylation approach is the low selectivity and yield of the desired trialkoxysilane product and the slow conversion of metallic silicon. In most cases the reactions are carried out in batch or semi-continuous flow reactors and the production of hazardous compounds is not eliminated. These problems could be solved by the use of continuous flow synthesis. Continuous flow reactors offer several advantages over the traditional batch reactors, such as better mass and heat transfer, fewer transport limitations, more precise control of reaction variables, more safety and easier scaling-up for industrial applications.<sup>16-17,123</sup> This research therefore focuses on the development and optimization of a continuous flow process to increase the yield of trialkoxysilane, the conversion of silicon metal and to suppress the production of tetraalkoxysilane. The method should also minimise the use and production of toxic and corrosive compounds.

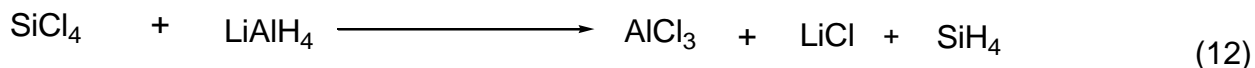
### 1.2.6 Synthesis of monosilane

The synthesis of monosilane is of great importance in industry, as it offers a precursor for the production of solar and electronic-grade silicon for application in the photovoltaic and semi-conductor industries respectively.

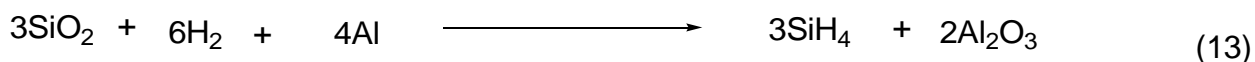
One of the developed industrial processes for the production of solar-grade silicon is the Union Carbide™ process, which produces the precursor monosilane through the disproportionation of silicon trichloride at 60 °C (Equation 5).<sup>12</sup> This invention is marred by the fact that it employs corrosive and toxic hydrochloric acid for the synthesis of trichlorosilane.



The other industrial route to monosilane involves the reduction of silicon tetrachloride with lithium aluminium hydride at room temperature (Equation 12).<sup>124</sup> This method has shortcomings in that the reducing agent used is air sensitive, expensive and the silicon tetrachloride starting material is corrosive. The production of lithium chloride and aluminium trichloride as by-products also requires more advanced separation techniques, apart from their toxicity.



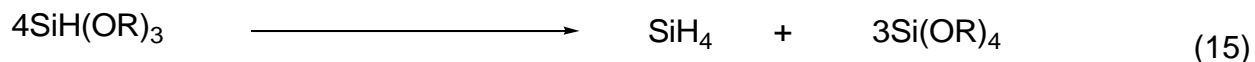
Monosilane can also be produced commercially by the reduction of silicon dioxide under Al and H<sub>2</sub> gas in a mixture of sodium chloride and aluminium chloride at temperature >1500 °C. The limitation of this method is that the reaction proceeds at very high temperature and pressure, apart from the low yield of monosilane realised (Equation 13).<sup>125</sup>



The small scale preparation of monosilane is done by first heating silicon dioxide with magnesium powder to form magnesium silicide at temperatures >800 °C. The magnesium silicide is then reacted with hydrochloric acid at room temperature to form monosilane gas (Equation 14).<sup>126</sup> This method has drawbacks in that a special compound magnesium silicide must be employed and its use results in the disposal of magnesium salts as sludge, thereby posing environmental problems. The method also results in low monosilane yield as other higher silanes are simultaneously formed. The use of corrosive hydrochloric acid is also another disadvantage.



The direct reaction of silicon with an alcohol to form trialkoxysilanes offers a promising environmentally friendly route to the commercial production of monosilane, which is a precursor to high purity silicon. Monosilane gas can be produced through the disproportionation of trialkoxysilanes in the presence of appropriate catalysts (Equation 15).



The liquid phase synthesis of monosilane has been studied by Tsuo *et al.*<sup>127</sup> In this study a 0.1% solution of sodium triethoxysilane in tetraethoxysilane was used as a catalyst for the disproportionation reaction. The reaction was carried out at 20 °C and the conversion of triethoxysilane was 98.5% after 20 h. The formed monosilane gas was purified by firstly passing it through cooled tetraethoxysilane in counter-current flow for the absorption of organoelemental compounds and lastly by adsorption onto activated carbon to remove the remaining impurities. The catalyst was recovered and concentrated to its original form by distilling off excess tetraethoxysilane for reuse. This method has an advantage because it is carried out at room temperature, but the long reaction time is of major concern for industrial application.

Muraoka and co-workers<sup>128</sup> demonstrated the use of a solution of sodium ethoxide (0.1wt%) in tetraethoxysilane as a catalyst in the formation of monosilane from triethoxysilane. The reaction was carried out in a stirred glass pressure reactor. The reactor had an inlet for triethoxysilane and the catalyst and an outlet for the products which could be drawn periodically for analysis. The yield of silane was found to be 90% under optimized conditions.

Imaki, Haji and Misu<sup>129</sup> used a stirred 100 mL pressure glass autoclave to prepare monosilane from trimethoxysilane in the presence of  $\gamma$ -aluminium oxide as a heterogeneous catalyst. The reaction afforded 90.9% conversion of trimethoxysilane in 2.5 h at 70 °C. The catalyst could easily be recovered from the liquid phase by filtration since it does not dissolve in the reaction mixture. The use of 2%-ruthenium supported on aluminium oxide and 5%-palladium supported on barium carbonate as catalysts resulted in conversions of 64.4 and 80.3% respectively. In the extension of their work, the use of a Pyrex glass tubular reactor packed with 0.5%-rhodium supported on aluminium oxide as a catalyst resulted in 45% conversion of trimethoxysilane after 1 h.

Wada, Haji and Yakotake<sup>130</sup> reported the use of a stirred autoclave in the liquid phase formation of monosilane by using sodium phenoxide or quaternary ammonium salts as catalysts at 40 °C. The reaction was also carried out in different solvents. The use of sodium phenoxide as a catalyst with *N*-methyl-2-pyrrolidone as solvent, resulted in 100% conversion of trimethoxysilane and evolution of 10 mmol of monosilane gas after 2 h.

The same results were obtained when quaternary ammonium salts, tetramethylammonium acetate and tetrabutylammonium acetate were applied as catalysts. When dimethylformamide was used as a solvent, in the presence of sodium phenoxide as a catalyst, the conversion of trimethoxysilane was 100% and 9.81 mmol of monosilane was produced.

Oligoethylene glycol ethers were evaluated as homogeneous catalysts for the production of monosilane from triethoxysilane.<sup>131</sup> It was postulated that, oxygen atoms in

oligoethylene glycol ethers coordinate readily with the silicon atom of triethoxysilane to form a hexacoordinated intermediate. This makes the Si-H bond weaker and thus more prone to dissociation. Typical results showed the triethoxysilane conversion of 69% after 110 days, when the reaction was conducted at room temperature using triethylene glycol dimethyl ether as a catalyst. Heating the reaction to 100 °C resulted in the reduction of reaction time to 11 h and the conversion of triethoxysilane was 75%. The drawbacks of the method are that it is very slow for industrial applications coupled also with the difficulty faced in separating the catalyst from by-products.

Inaba and Nagahama <sup>132</sup> carried out the gaseous phase synthesis of monosilane in the presence of aluminium oxide as catalyst. The reaction was carried out in a glass tube packed with a catalyst preheated at 250 °C. The conversion of trimethoxysilane and the corresponding monosilane yield were 63% each after 9 h. When triethoxysilane was used as a starting reagent under the similar conditions, its conversion and the corresponding monosilane yield were 26% each.

The use of a heterogeneous catalyst in the disproportionation reaction of trimethoxysilane to monosilane and tetramethoxysilane was also demonstrated by Ohno *et al.*<sup>133</sup> In this investigation, potassium fluoride and a catalyst activator (1,4-diazabicyclo[2.2.2]octane) supported on aluminium oxide was employed as a catalyst. The catalyst was packed in a Pyrex tube and activated by heating at 120 °C, after which preheated methanol vapour was introduced and the reaction was carried out at the same temperature. The conversion of trimethoxysilane was 94%. When the reaction was performed at the same conditions but using caesium chloride instead of potassium fluoride, the conversion of trimethoxysilane was 97%.

The use of heat treated calcium hydroxide in the disproportionation reaction was reported by Suzuki *et al.*<sup>134</sup> In this research, the catalyst was loaded into a tube and activated at 500 °C after which triethoxysilane was added at 120 °C. The reaction resulted in 70% conversion of triethoxysilane and 17% yield of monosilane. When potassium fluoride supported on aluminium oxide was used as a catalyst in this reaction<sup>135</sup>, the yield of

monosilane was 17-21% and 87% conversion of triethoxysilane was realised. Hydrotalcite thermally decomposed into aluminium and magnesium mixed oxides were also evaluated under the same conditions and the yield of monosilane and the conversion of triethoxysilane were 15-18% and 76% respectively.

Recently, the use of freshly prepared zirconium based catalysts for the production of monosilane from triethoxysilane has been reported.<sup>136</sup> The catalyst,  $\text{Zr}(\text{HPO}_4)_2 \cdot 0.3\text{H}_2\text{O}$  was preheated at 130 °C in a Pyrex tube before the addition of triethoxysilane. The conversion of triethoxysilane was found to be 83% at 130 °C. When trimethoxysilane was used as a starting material, the conversion was 95% at 130 °C.

The synthesis of monosilane from trialkoxysilanes is a promising and important step in the production of high purity silicon. Synthesis methods which are safe, economic and environmentally friendly are of great importance for large scale production.

### **1.3 Research problem statement**

The crystalline silicon photovoltaic industry continues to face a serious supply shortage of its raw material solar-grade silicon feedstock.<sup>3,6</sup> This is mainly due to the challenges in solar-grade silicon production and the growing demand for silicon feedstock.<sup>37-38</sup> Conventional batch and semi-continuous refining techniques for producing high-purity solar-grade silicon are highly energy intensive and not environmentally friendly.<sup>9,14</sup> The challenge therefore is to develop, optimize and demonstrate a more efficient continuous flow small production platform for the production of trialkoxysilanes to address economic and environmental challenges in the photovoltaic industry.

## 1.4 Research hypothesis

Silicon compounds, which are feedstocks for the photovoltaic industry, can be conveniently and directly synthesized from metallurgical-grade silicon and alcohols in a continuous flow reactor.

## 1.5 Research objectives

The overall objective of the broad project is to develop a small chemical production platform for the production of high purity (solar-grade) silicon. The current project involves the development and optimization of a continuous-flow chemical reactor system capable of producing silicon compounds from metallurgical-grade silicon.

The specific objectives of the present study are as follows:

- i. To design and construct a small production platform for the synthesis of trialkoxysilanes.
- ii. To synthesize (C1-C4) trialkoxysilanes so as to evaluate the effect of the R-group chain length on the conversion and selectivity of the reaction.
- iii. To study the effect of reaction conditions such as temperature, flow rate, residence time and reactants composition on the conversion, yield and selectivity to the trialkoxysilanes in both batch and continuous mode.
- iv. To synthesize monosilane from trialkoxysilanes.
- v. To characterize Si, Si-catalyst, Si-catalyst-alcohol mixtures by SEM-EDS, XRD and XRF so as to determine the morphology, phase compositions and the nature of interactions at surface interfaces.

## CHAPTER 2

### 2.0 Experimental

#### 2.1 Materials

Reagents used for synthesis and analysis are shown in Table 2.1. All reactions, unless specified, were carried out under a nitrogen atmosphere using glassware or reactor components dried overnight in an oven at 120 °C. Reagents used for reactions and analysis (methanol, ethanol, *n*-propanol and *n*-butanol) were purified by the usual methods<sup>137</sup> and others were used as received. All solvents were distilled from their respective suitable drying agents and stored under molecular sieves.



**Table 2.1: Reagents for synthesis and analysis**

| <b>Chemical name</b>  | <b>Formula</b>                                    | <b>Source</b>    | <b>Grade</b> |
|-----------------------|---|------------------|--------------|
| Silicon               | Si  | Sigma-Aldrich    | AR           |
| Dichloromethane       | CH <sub>2</sub> Cl <sub>2</sub>                   | Merck            | Cp           |
| Acetonitrile          | CH <sub>3</sub> CN                                | Merck            | HPLC         |
| Tetrahydrofuran       | C <sub>4</sub> H <sub>8</sub> O                   | Merck            | AR           |
| <i>n</i> -hexane      | C <sub>6</sub> H <sub>14</sub>                    | Sigma-Aldrich    | AR           |
| Dimethylsulfoxide     | (CH <sub>3</sub> ) <sub>2</sub> SO                | Sigma-Aldrich    | AR           |
| Methanol              | CH <sub>3</sub> OH                                | Merck            | AR           |
| Ethanol               | C <sub>2</sub> H <sub>5</sub> OH                  | Merck            | AR           |
| <i>n</i> -propanol    | C <sub>3</sub> H <sub>7</sub> OH                  | Merck            | AR           |
| <i>n</i> -butanol     | C <sub>4</sub> H <sub>9</sub> OH                  | Merck            | AR           |
| Trimethoxysilane      | SiH(OCH <sub>3</sub> ) <sub>3</sub>               | Sigma-Aldrich    | R & D        |
| Tetramethoxysilane    | Si(OCH <sub>3</sub> ) <sub>4</sub>                | Sigma-Aldrich    | R & D        |
| Triethoxysilane       | SiH(OC <sub>2</sub> H <sub>5</sub> ) <sub>3</sub> | Sigma-Aldrich    | R & D        |
| Tetraethoxysilane     | Si(OC <sub>2</sub> H <sub>5</sub> ) <sub>4</sub>  | Sigma-Aldrich    | R & D        |
| Tetrapropoxysilane    | Si(OC <sub>3</sub> H <sub>7</sub> ) <sub>4</sub>  | Sigma-Aldrich    | R & D        |
| Tetrabutoxysilane     | Si(OC <sub>4</sub> H <sub>9</sub> ) <sub>3</sub>  | Sigma-Aldrich    | R & D        |
| Marlotherm N          | Varied  | SASOL Germany    | Industrial   |
| Copper (II) Oxide     | CuO   | Fluka Analytical | R & D        |
| Copper (I) Chloride   | CuCl  | Fluka Analytical | R & D        |
| Copper (II) hydroxide | Cu(OH) <sub>2</sub>                               | Sigma-Aldrich    | R & D        |
| Copper (II) Sulphate  | CuSO <sub>4</sub>                                 | SAARCHEM         | AR           |
| Sodium ethoxide       | NaOC <sub>2</sub> H <sub>5</sub>                  | Alfa Aesar       | R & D        |
| Sodium hydroxide      | NaOH  | Merck            | AR           |
| Potassium hydroxide   | KOH   | Fluka            | AR           |
| γ-Aluminium oxide     | γ-Al <sub>2</sub> O <sub>3</sub>                  | Alfa Aesar       | AR           |
| Potassium fluoride    | KF  | UniLAB           | Cp           |
| Amberlite® IRA-93     | -   | BDH laboratory   | Nuclear      |
| Amberlite® IRA-904    | -   | Sigma-Aldrich    | Nuclear      |
| Amberlite® IRN-78     | -   | SUPELCO          | Nuclear      |

## 2.2 Equipment setup

### 2.2.1 Glass batch reactor set-up

Batch reactions were conducted in a 500 mL three-necked round bottom flask equipped with an overhead stirrer, thermometer and a flash distillation apparatus and placed in an oil bath on a hot plate, as shown in Figure 2.1. A peristaltic HPLC pump, GP1 (Knauer K-120, 10 mL head pump) with a flow rate range of 0.1-250 mL/min was used to pump liquid alcohol into the stirred silicon slurry in the round bottomed flask. A balance was used to measure the mass of alcohol pumped into the reaction mixture. The product mixture distilled out of the round bottomed flask and was condensed and collected in a 100 mL one neck round bottomed flask immersed in an ice bath.



**Figure 2.1: Glass batch reactor set up**

### 2.2.2 Falling film continuous flow reactor setup

The falling film tubular reactor consisted of a 20 mm (outer diameter) x 1000 mm (length) stainless steel tube. The feed lines for slurry, alcohol and nitrogen gas were made of  $\frac{1}{8}$  inch stainless steel tubing (Swagelok) which were expanded into  $\frac{1}{4}$  inch tubing (Swagelok) using reducers at the safety valves and expansion tanks inlets and outlets. The alcohol and nitrogen gas could be fed from both the bottom or the top of the reactor. The tubular reactor was fitted with a funnel which extended 150 mm from the top. The function of the funnel was to dispense the slurry onto the reactor walls and also to guide the reactor product stream to the condenser. The condenser used was a tube-in-tube type connected to chilled water. The falling film tubular reactor specifications are outlined in Table 2.2 and the reactor rig schematic flow diagram is shown in Figure 2.2.

**Table 2.2: Falling film reactor specifications**

| Item               | Specifications  |
|--------------------|---|
| Reactor type       | Falling film tubular reactor  |
| Reactor components | 20 mm (outer diameter) stainless steel tube with a $\frac{1}{8}$ inch alcohol inlets and a $\frac{1}{8}$ inch slurry outlet at the bottom |
| Dimensions         | 20 mm (outer diameter) x 1000 mm (length) stainless steel   |
| Reactor volume     | 176785.71 mm <sup>3</sup>   |
| Reactor area       | 47496.43 mm <sup>2</sup>  |
| Packing material   | Silicon carbide (100 mm from bottom)  |

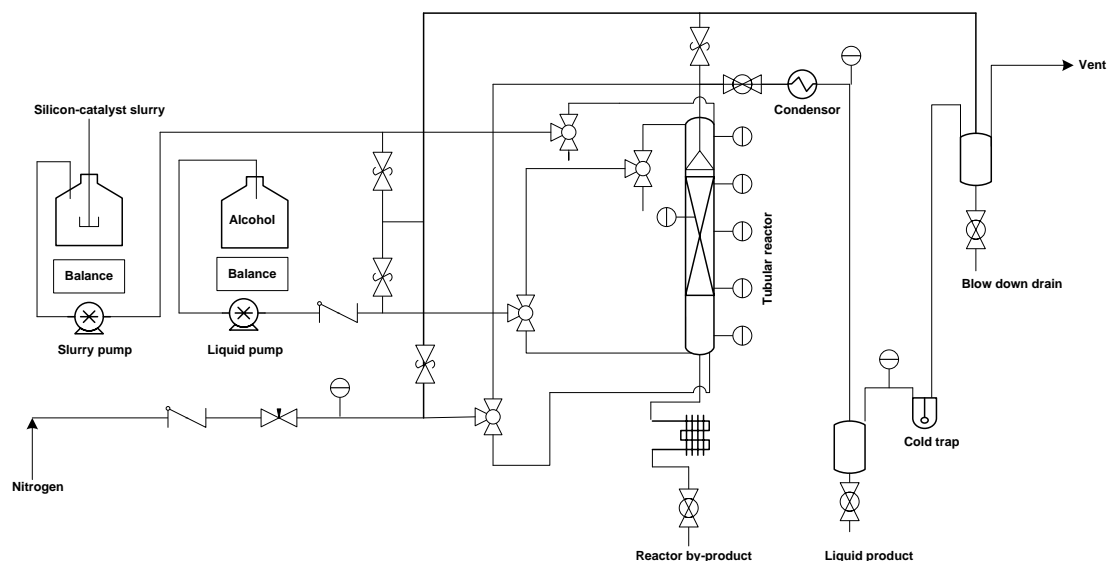


**Figure 2.2: Falling film continuous flow reactor schematic flow diagram**

### 2.2.3 Packed bed flow tubular reactor set-up

The packed bed flow tubular reactor was made from  $\frac{3}{8}$  and  $\frac{1}{8}$  inch stainless steel tubing (Swagelok). Powdered metallic silicon ( $<325\mu\text{m}$ ) and copper based catalyst were mixed thoroughly and packed into an already assembled tubular reactor. The reactor was plugged at both ends by use of glass wool to prevent catalyst or silicon carryover. The reactor was connected to the reactor rig and placed horizontally in the middle of a furnace (Eurotherm) which was plugged with glass wool at both ends to minimize heat loss. A pre-vaporization column packed with silicon carbide and molecular sieves was connected before the reactor. For some experiments, a back pressure regulator (0 to 34.4 bars) was connected after the reactor. The reactor specifications are as given in Table 2.3 and the reactor rig set up is as shown in Figures 2.3 and 2.4.

The reactor consisted of three components:

1. A pre-vapourization compartment which consisted of  $\frac{3}{8}$  inch x 150 mm stainless steel tube with 9.525 mm to 3.18 mm reducers packed with silicon carbide and molecular sieves.
2. A reactor compartment which was a  $\frac{3}{8}$  inch x 150 mm stainless steel tube with 9.525 mm to 3.18 mm reducers.
3. A tube-in-tube heat exchanger (3.18 mm to 6.35 mm) connected to a chiller at 0 °C, which was used for cooling the reactor product steam.

The key features of the reactor are summarized below:

**Table 2.3: Packed bed flow tubular reactor specifications**

| Item               | Specifications  |
|--------------------|---|
| Reactor type       | Tubular reactor   |
| Reactor components | 9.525 mm (outer diameter) with 9.525 to 3.18 mm reducers    |
| Dimensions         | 9.525 mm (outer diameter) x 150 mm (length) stainless steel |
| Reactor volume     | 7069.66 mm <sup>3</sup>                                     |
| Reactor area       | 3745.47 mm <sup>2</sup>                                     |
| Packing material   | Silicon powder and copper catalyst                          |

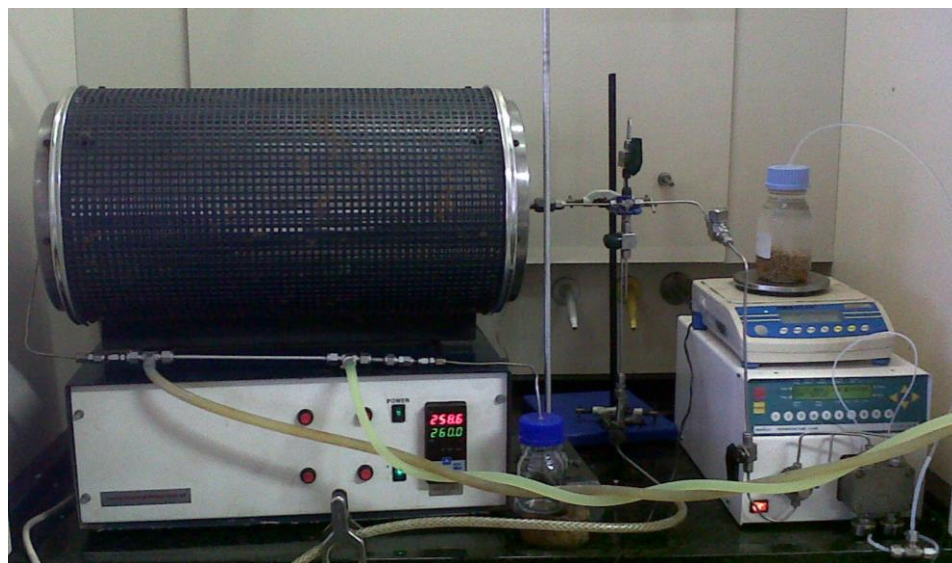


**Figure 2.3: Packed bed flow tubular reactor rig set up**

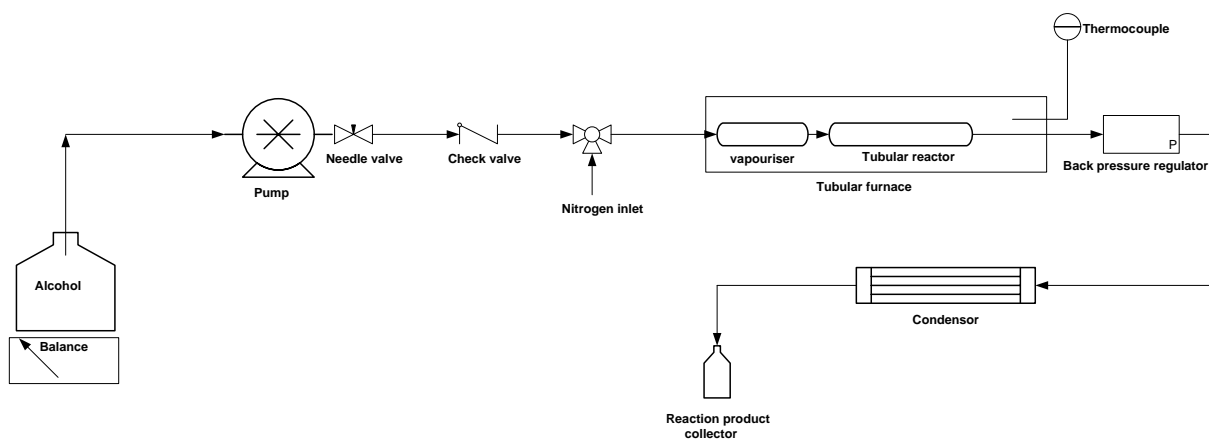


**Figure 2.4: Packed bed flow tubular reactor rig schematic flow diagram**

## 2.3 Analytical procedures

### 2.3.1 Gas Chromatography (GC)

Samples from the product mixture were quantified using the multiple point internal standard calibration curve method. The GC conditions were as follows:

|                            |                |
|----------------------------|----------------|
| GC model                   | Agilent 6850   |
| Column                     | DB-5           |
| FID temperature            | 300 °C         |
| Carrier gas                | N <sub>2</sub> |
| Injection volume           | 1 µL           |
| Carrier gas flow           | 3.2 mL/min     |
| Injector temperature       | 250 °C         |
| Initial column temperature | 70 °C          |
| Initial hold-up time       | 0 min          |
| Column ramp rate 1         | 3 °C/ min      |
| Final column temperature1  | 90 °C          |
| Hold-up time               | 0 min          |
| Column ramp rate 2         | 20 °C/ min     |
| Final column temp          | 220 °C         |
| Final hold-up time         | 3 min          |
| Split ratio                | 1:20           |
| Run time                   | 16.167 min     |

### Standard calibration methods

The multiple point internal standard calibration method for quantitative analysis was used. Trimethoxysilane, tetramethoxysilane, triethoxysilane, tetraethoxysilane, tetrapropoxysilane and tetrabutoxysilane standards were obtained from Sigma-Aldrich. Tripropoxysilane and tributoxysilane standards, which could not be sourced on the market, were synthesized in the lab, purified by low temperature vacuum distillation and characterised by GC-MS, FT-IR and NMR. Standards solutions for the respective product

mixtures were prepared in 10 mL volumetric flasks. Each standard was injected five times to determine repeatability of GC response to each analyte. A standard calibration curve with the ratio of the area of analytes over area of internal standard (nitrobenzene) in the Y-axis and the ratio of mass of analytes over the mass of internal standard in the X-axis was created for trialkoxysilane and tetraalkoxysilane respectively (Appendix B).

The following straight line equation is then obtained from the graph and used to calculate the mass of analytes in the sample:

$$\frac{A_x}{A_{is}} = m \frac{M_x}{M_{is}} + C \quad (16)$$

Where:  $A_x$  = Area of analyte  
 $A_{is}$  = Area of internal standard  
 $m$  = Gradient  
 $M_x$  = Mass of analyte  
 $M_{is}$  = Area of internal standard

Therefore to calculate the mass of analyte, the formula is rearranged as follows:

$$M_x = \left\{ \left( \frac{\frac{A_x}{A_{is}} - C}{m} \right) \right\} \times M_{is} \quad (17)$$

The obtained mass of the respective analyte was then multiplied by the respective dilution factors and then converted to g/L or moles.

In some cases, the multiple point external standard calibration method was used for quantification by plotting peak area (Y-axis) against sample amount (X-axis) and obtaining a linear equation which was used to calculate the amount of analyte in the collected samples.



### 2.3.2 Gas Chromatography-Mass Spectrometry (GC-MS)

Samples from the product mixture were characterized by GC-MS using the following conditions:

|                            |                 |
|----------------------------|-----------------|
| GC-MS model                | Thermo Finnigan |
| Column                     | DB-5            |
| FID temperature            | 300 °C          |
| Carrier gas                | He              |
| Carrier gas flow           | 1.0 mL/min      |
| Injector temperature       | 220 °C          |
| Injection volume           | 1 µL            |
| Initial column temperature | 70 °C           |
| Initial hold-up time       | 0 min           |
| Column ramp rate 1         | 3 °C/min        |
| Final column temperature1  | 90 °C           |
| Hold-up time               | 0 min           |
| Column ramp rate 2         | 20 °C/min       |
| Final column temp          | 220 °C          |
| Final hold-up time         | 3 min           |
| Split ratio                | 1:20            |
| Run time                   | 20 min          |

### 2.3.3 Nuclear Magnetic Resonance Spectroscopy

Proton ( $^1\text{H}$ ) and carbon ( $^{13}\text{C}$ ) NMR spectra of pure products were recorded at 400 MHz and 100 MHz respectively with a Bruker Ultrashield™ 400 Plus. The chemical shifts are given in parts per million (ppm) on a delta scale ( $\delta$ ) with reference to the residual solvent peak of  $\text{CDCl}_3$  at 7.26 ppm and 77 ppm for  $^1\text{H}$  and  $^{13}\text{C}$  respectively. Data for  $^1\text{H}$  NMR are reported as follows: Chemical shift (integration, multiplicity,  $J$  value).

### 2.3.4 Fourier-Transform Infrared Spectroscopy (FT-IR)

Infrared (IR) spectra ( $\nu_{\max}$ ) of purified products were recorded on Bruker Fourier-Transform Infrared Spectrophotometer by scanning 64 times per sample in the range 4000-400  $\text{cm}^{-1}$ . IR spectra were obtained without sample preparation.

### 2.3.5 X-Ray Fluorescence (XRF)

XRF analysis of silicon and silicon-catalyst mixture before and after the alkoxylation reaction was done using a P Analytical Epsilon 3 XRF.

### 2.3.6 X-Ray Diffraction (XRD)

Ambient temperature powder XRD measurements on silicon and silicon-catalyst mixtures before and after the reaction were performed on a Bruker D8 instrument with Cu radiation in standard Bragg-Brentano geometry using a Ni filter at the detector. The scan range was 10-70° 2 $\theta$ .

### 2.3.7 Scanning Electron Microscopy-Energy Dispersive Spectroscopy (SEM-EDS)

SEM-EDS analysis on silicon and silicon-catalyst mixtures before and after the reaction were done using a JEOL JSM-6380 model microscope. The powdered samples were mounted on the standard specimen stubs using an adhesive tape and coated with a thin layer of gold to prevent the sample from charging.

## Characterization of products

### Trimethoxysilane

$\nu_{\max}/\text{cm}^{-1}$  2947, 2844, 2199, 1460, 1192, 1073, 864, 786, 700 and 449

$\delta_{\text{H}}$  (400 MHz,  $\text{CDCl}_3$ ) 3.61 (9H, s) and 4.23 (1H, s)

$\delta_{\text{C}}$  (100 MHz,  $\text{CDCl}_3$ ) 50 (3C)

$m/z$  (EI) 123 ( $\text{M}^+$ , 7%), 122 (8), 121 (95), 91 (100), 61 (72) and 59 (72)

GC  $t_{\text{R}}$  = 2.29 min

GC-MS  $t_{\text{R}}$  = 1.01 min

### **Tetramethoxysilane**

$\nu_{\max}/\text{cm}^{-1}$  2947, 2844, 1461, 1192, 1072, 813 and 641

$\delta_{\text{H}}$  (400 MHz,  $\text{CDCl}_3$ ) 3.32 (12H, s)

$\delta_{\text{C}}$  (100 MHz,  $\text{CDCl}_3$ ) 50.4 (4C)

$m/z$  (EI) 154 ( $\text{M}^+ + 1$ , 8%), 153 ( $\text{M}^+$ , 38%), 152 (100), 151 (34), 121 (28), 91 (9) and 90 (5)

GC  $t_{\text{R}}$  = 3.09 min

GC-MS  $t_{\text{R}}$  = 1.35 min

### **Triethoxysilane**

$\nu_{\max}/\text{cm}^{-1}$  2976, 2928, 2886, 2184, 1484, 1443, 1391, 1295, 1167, 1100, 1072, 958, 853, 808, 767, 696 and 475

$\delta_{\text{H}}$  (400 MHz,  $\text{CDCl}_3$ ) 1.20 (9H, t,  $J = 7.1$ ), 3.80 (6H, q,  $J = 7.1$ ) and 4.23 (1H, s)

$\delta_{\text{C}}$  (100 MHz,  $\text{CDCl}_3$ ) 18.0 (3C) and 59.0 (3C)

$m/z$  (EI) 165 ( $\text{M}^+$ , 5%), 264 (10), 163 (74), 149 (92), 119 (100), 105 (92) and 91 (55)

GC  $t_{\text{R}}$  = 3.64 min

GC-MS  $t_{\text{R}}$  = 2.81 min

### **Tetraethoxysilane**

$\nu_{\max}/\text{cm}^{-1}$  2975, 2929, 2890, 1484, 1442, 1391, 1366, 1296, 1168, 1100, 1072, 957, 783, 654 and 470

$\delta_{\text{H}}$  (400 MHz,  $\text{CDCl}_3$ ) 1.19 (12H, t,  $J = 7.2$ ) and 3.79 (8H, q,  $J = 7.2$ )

$\delta_{\text{C}}$  (100 MHz,  $\text{CDCl}_3$ ) 18.0 (4C) and 58.2 (4C)

$m/z$  (EI) 209 ( $\text{M}^+$ , 10%), 194 (12), 193 (100), 163.1 (52), 149 (85) and 119 (37),

GC  $t_{\text{R}}$  = 6.63 min

GC-MS  $t_{\text{R}}$  = 5.27 min

### **Tripropoxysilane**

$\nu_{\max}/\text{cm}^{-1}$  2974, 2930, 2879, 2192, 1443, 1391, 1367, 1295, 1167, 1074, 1019, 910, 853, 767, 747, 696 and 475

$\delta_{\text{H}}$  (400 MHz,  $\text{CDCl}_3$ ) 0.91 (9H, t,  $J = 7.1$ ), 1.59 (6H, sext,  $J = 7.1$ ), 3.73 (6H, t,  $J = 7.1$ ) and 4.28 (1 H, s)

$\delta_C$  (100 MHz, CDCl<sub>3</sub>) 10.1 (3C), 25.5 (3C) and 65.0 (3C)

$m/z$  (EI) 207 (M<sup>+</sup>, 4%), 206 (11), 178 (12), 177 (100), 163 (12), 147 (30), 135 (86), 119 (34), 77 (17) and 63 (76)

GC  $t_R$  = 6.73

GC-MS  $t_R$  = 5.37

### **Tetrapropoxysilane**

$\nu_{max}/cm^{-1}$  2962, 2936, 2878, 1463, 1391, 1263, 1154, 1079, 1015, 901, 844, 745 and 498

$\delta_H$  (400 MHz, CDCl<sub>3</sub>) 0.78 (12H, t,  $J$  = 7.0), 1.45 (8H, sext,  $J$  = 7.0) and 3.59 (8H, t,  $J$  = 7.0)

$\delta_C$  (100 MHz, CDCl<sub>3</sub>) 9.8 (4C), 25.3 (4C) and 67.8 (4C)

$m/z$  (EI) 265 (M<sup>+</sup>, 2%), 264 (5), 237 (6), 236 (16), 235 (100), 193 (30), 151 (37), 121 (22) and 93 (12)

GC  $t_R$  = 11.55

GC-MS  $t_R$  = 13.15

### **Tributoxysilane**

$\nu_{max}/cm^{-1}$  2961, 2932, 2876, 2192, 1459, 1391, 1296, 1235, 1167, 1076, 1041, 1011, 959, 855, 802, 768, 733, 696, 474 and 430

$\delta_H$  (400 MHz, CDCl<sub>3</sub>) 0.91 (9H, t,  $J$  = 7.2), 1.37 (6H, sext,  $J$  = 7.2), 1.56 (6H, quint,  $J$  = 7.2), 3.77 (6H, t,  $J$  = 7.2) and 4.29 (1H, s)

$\delta_C$  (100 MHz, CDCl<sub>3</sub>) 13.7 (3C), 18.2 (3C), 34.5 (3C) and 63.2 (3C)

$m/z$  (EI) 249 (M<sup>+</sup>, 6%), 248(8), 247 (10), 233 (90), 205 (38), 191 (42), 175 (100), 161 (76), 147 (32) and 135 (37).

GC  $t_R$  = 11.09 min

GC-MS  $t_R$  = 6.80 min

### **Tetrabutoxysilane**

$\nu_{max}/cm^{-1}$  2958, 2933, 2874, 1463, 1387, 1301, 1265, 1235, 1151, 1084, 1040, 1010, 989, 902, 836, 800, 733, 522 and 413

$\delta_{\text{H}}$  (400 MHz,  $\text{CDCl}_3$ ) 0.84 (12H, t,  $J = 7.0$ ), 1.30 (8H, sext,  $J = 7.0$ ), 1.45-1.49 (8H, quint,  $J = 7.0$ ) and 3.68 (8H, t,  $J = 7.0$ )

$\delta_{\text{C}}$  (100 MHz,  $\text{CDCl}_3$ ) 13.5 (4C), 18.7 (4C), 34.3 (4C) and 62.9 (4C)

$m/z$  (EI) 321 ( $\text{M}^+$ , 1%), 320 (2), 219 (2), 279 (6), 278 (18), 277 (100), 263 (12), 221 (24), 205 (12), 165 (22), 123 (23) and 79 (33)

GC  $t_{\text{R}} = 14.17$  min

GC-MS  $t_{\text{R}} = 16.44$  min

## 2.4 Synthesis procedures

### 2.4.1 Batch synthesis of trialkoxysilanes

#### Typical procedure for slurry phase glass batch synthesis

Powdered metallic silicon (20.0124 g, 712.44 mmol), copper (I) chloride (1.1012 g, 5 wt%) and Marlotherm N (50 mL) were added to a 500 mL three-necked round bottom flask equipped with an overhead stirrer, thermometer and a flash distillation apparatus and placed in an oil bath on a hot plate. The temperature of the mixture was raised to 220 °C and maintained for 5 h while purging with nitrogen at 40 mL/min. Anhydrous alcohol was then added dropwise using an HPLC pump at 0.1 mL/min, while maintaining the temperature at 230 °C. Samples of distillate were collected at head temperature of 80 °C, weighed and analysed by GC using the multiple point internal standard calibration method over the course of the reaction at 1 h interval for a period of 6-24 h.

The stability and validity of this batch reactor was investigated by carrying out the alkoxylation reaction five times under the same conditions and determining the product composition by the same GC method. The relative standard deviation was found to be <5% (at 95% confidence limit) indicating low variations in the system. The GC analysis method was validated for reproducibility by analysing the same distillate product sample 5 times. The relative standard deviations obtained (<0.5%) show that the analysis has very low variations at 95% confidence limit.

In some cases, the collected mixtures after 6-24 h were combined and purified by vacuum distillation to obtain pure products which were characterised by IR, NMR and GC-MS.

The selectivity of the product and the silicon conversion were defined as follows:

$$\text{Selectivity (\%)} = \left[ \frac{\text{Amount of product (mol)}}{\text{Sum of amounts of silicon containing products (mol)}} \right] \times 100 \quad (18)$$

$$\text{Silicon conversion (\%)} = \left[ \frac{\text{Sum of amount of silicon containing products (mol)}}{\text{Amount of silicon charged into the reactor (mol)}} \right] \times 100 \quad (19)$$

#### **2.4.1.1 Effect of various catalysts, catalyst amount, pre-heating time and pre-heating temperature on the selectivity and rate of formation of triethoxysilane**

The catalysts evaluated were copper (I) chloride, copper (II) oxide, copper (II) sulphate and copper (II) hydroxide. A control experiment was performed without using a catalyst. The reaction was also investigated by varying copper (I) chloride catalyst loading (0, 2.5, 5, 10 and 15wt%), pre-heating temperature (220, 350, 500 and 700 °C) and pre-heating time (0, 5, 10, 15 and 20 h). The experiment was also done without any pre-heating conditions. All experiments were carried out in accordance with typical procedure for glass batch synthesis (2.4.1).

#### **2.4.1.2 Effect of ethanol flow rate and reaction temperature on the conversion of silicon and the selectivity for triethoxysilane**

A central composite design generated using Design Expert Version 5 software package (STAT-EASE INC.) was used to investigate the effect of reaction temperature and ethanol flow rate at on the conversion of silicon and selectivity for the triethoxysilane. The experimental domain was as given in Table 2.4 below and the reactions were carried out in accordance to the typical procedure for batch synthesis (2.4.1).

**Table 2.4: Experimental domain**

|         | Temperature °C | Flow rate (mL/min) |
|---------|----------------|--------------------|
| Minimum | 180            | 0.1                |
| Maximum | 240            | 1                  |

Multiple regression was done for both silicon conversion and triethoxysilane selectivity using STATISTICA Version 12 software package (StatSoft®) in order to come up with predictive models within the experimental domain. The models were validated by testing for outliers in the data and testing for normality of the data. Once the model was validated, three dimensional response surface graphs (STATISTICA) were used to draw conclusions and predictions.

#### **2.4.1.3 Effect of alcohol R-group on the conversion of silicon and selectivity towards trialkoxysilanes**

The direct alkoxylation of silicon was carried out in accordance to the typical procedure for glass batch synthesis using four primary alcohols of increasing carbon chain length at similar optimised experimental conditions. The alcohols tested were methanol, ethanol, *n*-propanol and *n*-butanol. The products were purified by vacuum distillation to obtain pure products which were characterised by IR, NMR and GC-MS.

#### **2.4.2 Synthesis of trialkoxysilanes in a falling film continuous flow tubular reactor**

##### **Typical procedure**

Powdered metallic silicon (50.1011 g, 1793.59 mmol), Copper (I) chloride (2.6550 g, 5wt%) and Marlotherm N (150 mL) were added to a 1000 mL three-necked round bottom flask placed in an oil bath. The stirred slurry was heated to 210-230 °C for 10 h while purging with nitrogen at 40 mL/min. The obtained Si/Cu slurry in marlotherm solvent was then transferred to a falling film continuous flow tubular (20 mm x 1000 mm) reactor after allowing it to cool. The tubular reactor was heated to 240 °C at five heating zones whilst purging with nitrogen (0.25 bar) from the bottom. A thermocouple was used to measure

the temperature at the middle of the reactor. The cooled slurry was pumped at varying flow rates (0.1 g/min to 1 g/min) into the tubular reactor from the top and it flowed down along the walls of the reactor as a thin film. Anhydrous ethanol was then metered into the reactor from the bottom using an HPLC pump at flow rates (0.1 to 1 mL/min). The column consisted of a 10 cm SiC packing at the bottom for pre-vapourization of ethanol. The vapourized ethanol flowed up the reactor in concurrent with the thin film of silicon slurry to maximise mass transfer. The unreacted silicon slurry was collected at the slurry outlet. The formed products and excess ethanol (distillates) entered through the funnel and eventually condensed and collected for GC analysis at 1 h intervals.

#### **2.4.3 Synthesis of trialkoxysilanes in a packed bed flow tubular reactor**

Powdered metallic silicon (5.2651 g, 187.44 mmol) copper (I) chloride (0.2652, 5wt%) g were mixed thoroughly and packed into an already assembled 9.925 mm x 150 mm stainless steel tubular reactor. The reactor was plugged at both ends by use of glass wool to prevent catalyst or silicon carry over. The reactor was then connected to the reactor rig and placed horizontally in the middle of a furnace which was plugged with glass wool at both outlets to minimise heat loss. A pre-vapourisation column (9.925 mm x 150 mm) packed with silicon carbide and a molecular sieve was connected before the reactor. For some of the reactions, a back pressure regulator (34.4 bars) was connected after the column. The chiller and the pump which pumped water to the heat exchanger were switched on. The mixture was heated to 220 °C for 2.5 h while purging with nitrogen at a flow rate of 40 mL/min. The temperature was then increased to 240 °C and anhydrous ethanol was delivered into the reactor using an HPLC pump at flow rate of 0.1 mL/min. The formed products and excess ethanol (distillates) condensed in the heat exchanger and were collected for GC analysis at 1 h intervals (about 6 mL) for a period of up to 24 h.

In further experiments, the effect of various catalysts (copper (I) chloride, copper (II) hydroxide, copper (II) oxide and copper (II) sulphate), catalyst amount (0-15wt%), pre-heating time (0-20 h) and pre-heating temperature (220-700 °C) on the selectivity and rate



of formation of triethoxysilane was investigated. The effect of reaction temperature (180-240 °C), reaction pressure (0-34.4 bars), alcohol flow rate (0.1-1mL/min) and alcohol R-group (C<sub>1</sub>-C<sub>4</sub>) on selectivity of trialkoxysilane and silicon conversion was also investigated. The effect of flow rate and temperature was specifically investigated by means of a central composite design. All experiments were carried out according to the typical procedure for synthesis in a packed bed flow tubular reactor (2.4.3).

## **2.4.4 Synthesis of monosilane**

### **2.4.4.1 General procedure for the homogeneous catalysis**

In a 50 mL three-necked round-bottom flask, triethoxysilane (1.78 g, 10.836 mmol) was added by means of a syringe through a septum and stirred in anhydrous acetonitrile (10 mL, 1.08 M). Sodium ethoxide (0.0147 g, 0.2167 mmol) was then added and the mixture stirred at room temperature. Samples were drawn from the reaction through the septum at 10 min interval to quantify the conversion of triethoxysilane over time by GC. The target product (monosilane gas) was evolved and a flame test and was conducted to characterize it, in addition to the silver nitrate solution test. The flame test was conducted by slowly discharging monosilane into the air through a glass pipet and observing the spontaneous ignition and the characteristic flame colour. The silver nitrate test was done by introducing monosilane into a 10 mL syringe containing a neutral solution of 0.3 M silver nitrate and shaking to observe the characteristic colour change. Monosilane is pyrophoric and hence the reaction was carried out under nitrogen. The monosilane gas was quenched by hydrolysing it to hydrated silicon dioxide by bubbling through a stirred 100 mL solution of 0.6 M potassium hydroxide. The by-product (tetraethoxysilane) was also quantified by GC and the result used to estimate the amount of monosilane formed. The experiment was repeated at 30, 40 and 60 °C. Further experiments were conducted under neat conditions (without using solvents) and also using hexane, dimethylsulfoxide and tetrahydrofuran as solvents. Sodium hydroxide was also evaluated as a catalyst using this general procedure.

#### 2.4.4.2 General procedure for heterogeneous catalysis

In a 50 mL three-necked round-bottomed flask, dry Amberlite® IRA-904 (0.251 g) and acetonitrile (10 mL, 1.08 M) were added. Triethoxysilane (1.78 g, 10.836 mmol) was then added and the mixture stirred at various temperatures (room temperature to 55 °C). The conversion of triethoxysilane and the formation of tetraethoxysilane by-product were monitored by GC by withdrawing samples at 15 min interval. The solid catalyst was recovered by filtration and dried for re-use. Other heterogeneous catalysts evaluated under this protocol are Amberlite® IRA-93, Amberlite® IRN-78 and potassium fluoride supported on  $\gamma$ -aluminium oxide. The potassium fluoride supported on a  $\gamma$ -aluminium oxide catalyst was prepared in accordance to a method available in literature.<sup>134</sup> This protocol was also further investigated under neat conditions (without using solvents).

The conversion of triethoxysilane was calculated in accordance to the following equation:

$$\text{Triethoxysilane conversion (\%)} = \left( \frac{M_o - M_e}{M_o} \right) \times 100 \quad (20)$$

Where  $M_o$  is the initial amount of triethoxysilane (mol),  $M_e$  is the amount of triethoxysilane (mol) after the reaction.

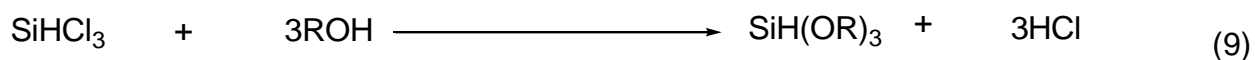
## CHAPTER 3

### Slurry phase synthesis of trialkoxysilanes

#### 3.1 Introduction

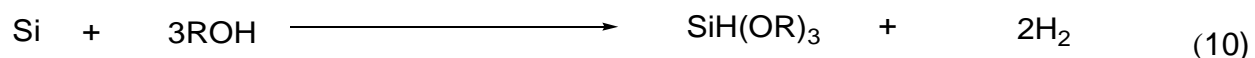
Trialkoxysilanes undergo various reactions such as addition, co-polymerization, co-polycondensation and disproportionation with other organic compounds to form organosilicon compounds. A variety of useful substances can be derived from these compounds, which can be utilized as raw materials for making silane coupling agents, coating agents, heat-resistant paints or silane gas.<sup>138-140</sup>

The disproportionation reaction leads to formation of silane, which is a precursor for solar-grade silicon production. The widely used method for the synthesis of alkoxy silanes involves the reaction of silicon with hydrochloric acid to form trichlorosilane (Equation 2) which is then reacted with primary alcohols in the presence of a copper catalyst (Equation 9).

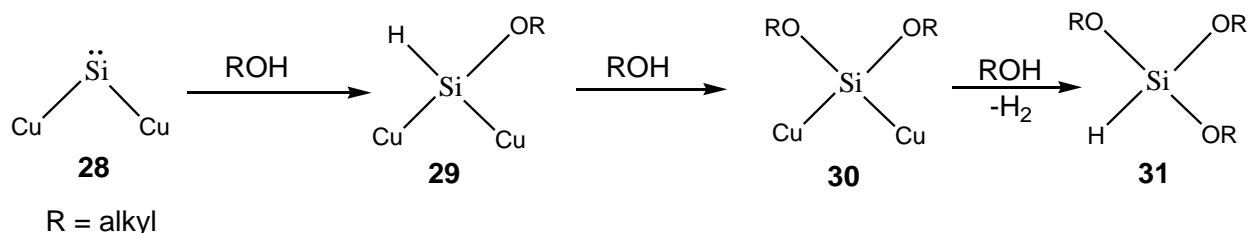


However, this approach is faced with challenges including the poor conversion of silicon, low selectivity and poor yield of the desired trialkoxysilane product, in addition to the toxic and corrosive hydrochloric acid by-product.

Therefore, much attention has been paid to the development of a direct synthesis method (Equation 10), and the improvement of selectivity for the trialkoxysilane.



There is a variety of opinions on the role of copper in the selective synthesis of trialkoxysilanes but the concept of copper-silicon phase formation during the activation stage is commonly accepted. The mechanism for the exclusive formation of trialkoxysilane has been proposed to pass through the silylene intermediate experimentally.<sup>141</sup> When copper catalyst and silicon are heated together, a Cu-Si alloy phase is formed. The migration of silicon to this region gives a surface silylene intermediate **28** which reacts with alcohol to form monoalkoxysilane **29**. The Si-H bond undergoes an attack by another alcohol molecule to form dialkoxysilane **30**, which undergoes further attack by alcohol with the simultaneous cleavage of two Si-Cu bonds to form trialkoxysilane **31** (Scheme 15).



**Scheme 15: Proposed reaction mechanism for the selective formation of trialkoxysilane<sup>141</sup>**

The direct synthesis method has to date been carried out in continuously stirred slurry phase tank reactors using heat transfer solvents/fluids, such as diphenylalkanes.<sup>107-122</sup> Continuously stirred slurry phase tank reactors are characterised by large liquid holdup, high energy consumption and are more complex and expensive than tubular units. These types of reactors are difficult for scale up for industrial mass production. Other disadvantages of this system are that it cannot handle corrosive chemicals, high temperatures and high pressures.<sup>72</sup> The selectivity towards trialkoxysilane and silicon conversion in this protocol depends on careful control of reaction conditions. Literature indicates that there is limited knowledge on a clear method for slurry phase synthesis of alkoxysilanes as seen from conflicting reaction conditions such as activation time, catalyst used and reaction time reported. Furthermore, the synthesis of these compounds in slurry the phase has been limited to lower order primary alcohols (C1 and C2).

In this chapter, the slurry phase method for the synthesis of (C1 to C4) trialkoxysilanes is discussed. The synthesis was done in a glass batch reactor and also attempted in a continuous flow falling film tubular reactor. Key parameters which influence the rate of silicon conversion and selectivity towards trialkoxysilane such as activation temperature and time, catalyst type and loading, reaction temperature and alcohol flow rate were investigated under batch conditions. Characterization of silicon and silicon-catalyst mixtures by SEM-EDS, XRD and XRF is also discussed.

### 3.2 Characterization of silicon-catalyst mixtures

Silicon-catalyst mixtures were characterised by SEM-EDS, XRD and XRF in order to determine the morphology, phase compositions, nature of interactions at surface interfaces.

#### 3.2.1 XRD analysis

The reaction of silicon with a primary alcohol to form trialkoxysilane is catalysed by copper containing compounds. The reaction is thought to proceed *via* the formation of a Cu-Si phase, which normally forms after activation at high temperatures.

XRD analysis samples were obtained by heating 5 g of silicon metal (<325 $\mu$ m particle size) with 5wt% copper (I) chloride as catalyst at 250 °C under a stream of nitrogen for 5 h and then reacting with ethanol (0.1 mL/min flow rate) for 2 h at 240 °C. A control experiment was done by using silicon metal without a catalyst under the same conditions. Figure 3.1 shows the XRD results for silicon and the activated Si-CuCl mixture before and after reaction with ethanol. It can be seen that a new diffraction peak between  $2\theta = 44.5$  and 46 appears when Si-Cu mixture is heated, and the intensity increases after 2 h of ethanol exposure assignable to  $\text{Cu}_3\text{Si}$  alloy.<sup>142-143</sup> This confirms the existence of the catalyst-silicon phase during the reaction. The  $\text{Cu}_3\text{Si}$  alloy in the activated Si-Cu mixture was in low concentration and could only be prominent after 2 h of reaction. This can be attributed to the size of the alloy ensemble compared to reactive silicon and as such the alloy could only be seen once most of the silicon had reacted with silicon.<sup>144</sup>

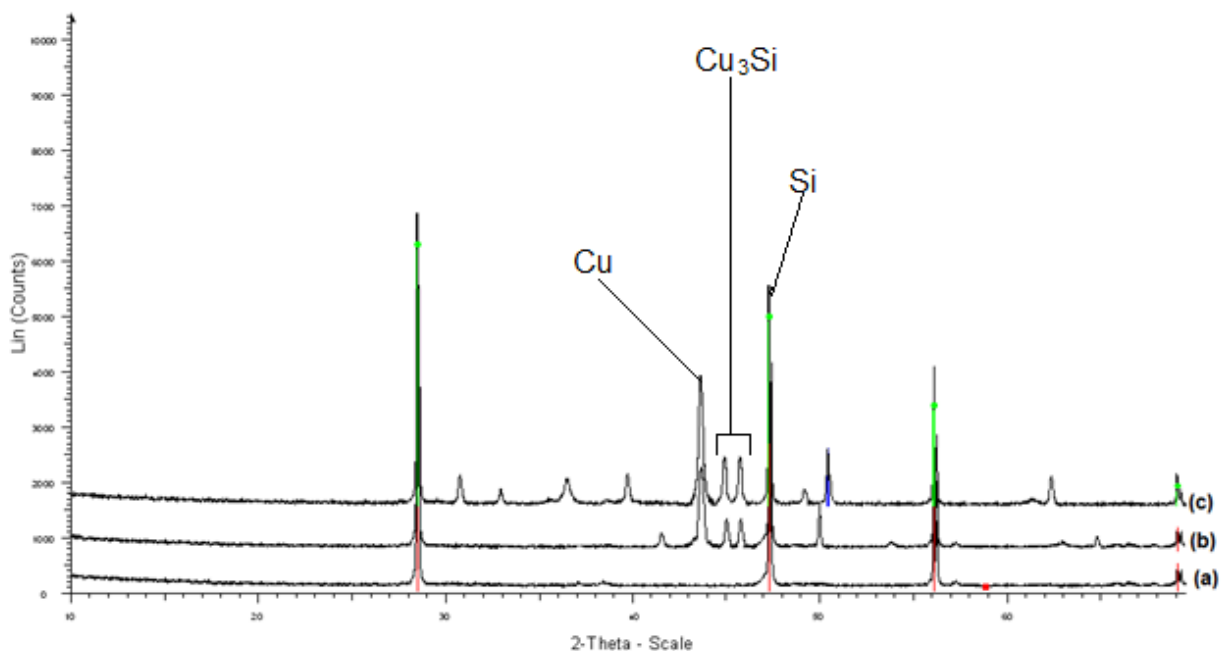


**Figure 3.1: XRD analysis for Si-Cu mixtures (a) pure silicon (b) heated Si-Cu(I)Cl (c) Si-Cu(I)Cl mixture after 2 h reaction**

### 3.2.2 SEM-EDS analysis

The same samples that were used for XRD analysis above were also subjected to SEM-EDS analysis. Figures 3.2 and 3.3 show backscattered SEM micrographs and EDS spectra for the activated Si-CuCl mixture before and after alkoxylation with ethanol respectively. It can be seen from the SEM images that two types of grain morphologies are present which, consist of the copper catalyst and silicon. The EDS spectrum of the activated Si-catalyst mixture after reaction with ethanol (Figure 3.3) shows signals assignable to C, Si, O, and Cu indicating that a chemical interaction exists between silicon and ethanol to form ethoxysilanes. The silicon intensity as shown in the EDS spectrum before reaction with ethanol (Figure 3.2) is higher than after reaction (Figure 3.3) further confirming that the silicon was consumed on exposure to ethanol.

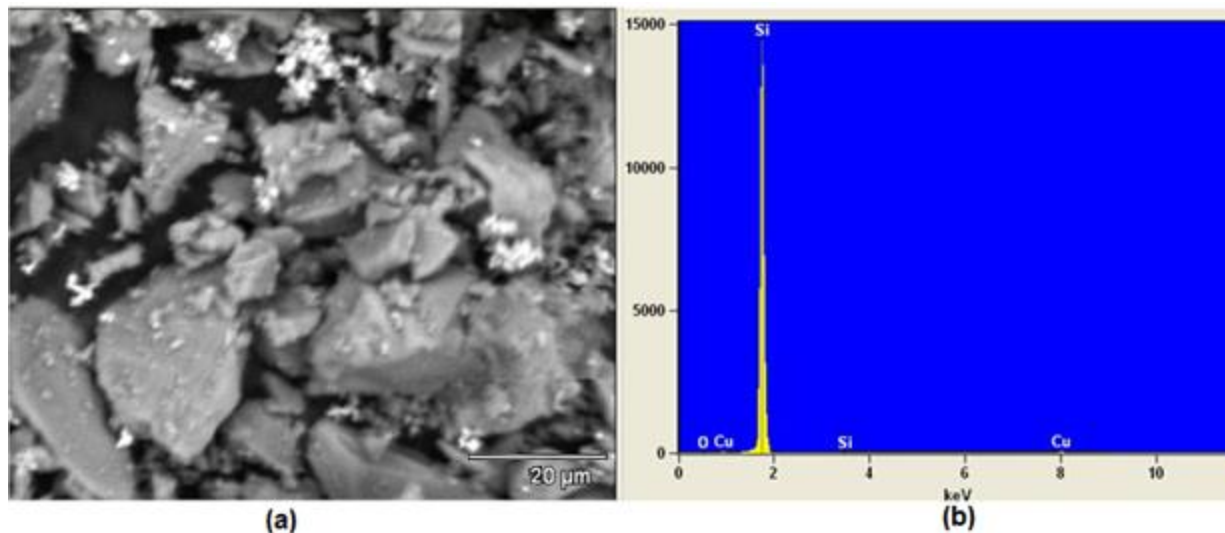


**Figure 3.2: SEM micrograph (a) and EDS spectrum (b) for heated Si-Cu(I)Cl mixture after 5 h at 250 °C**

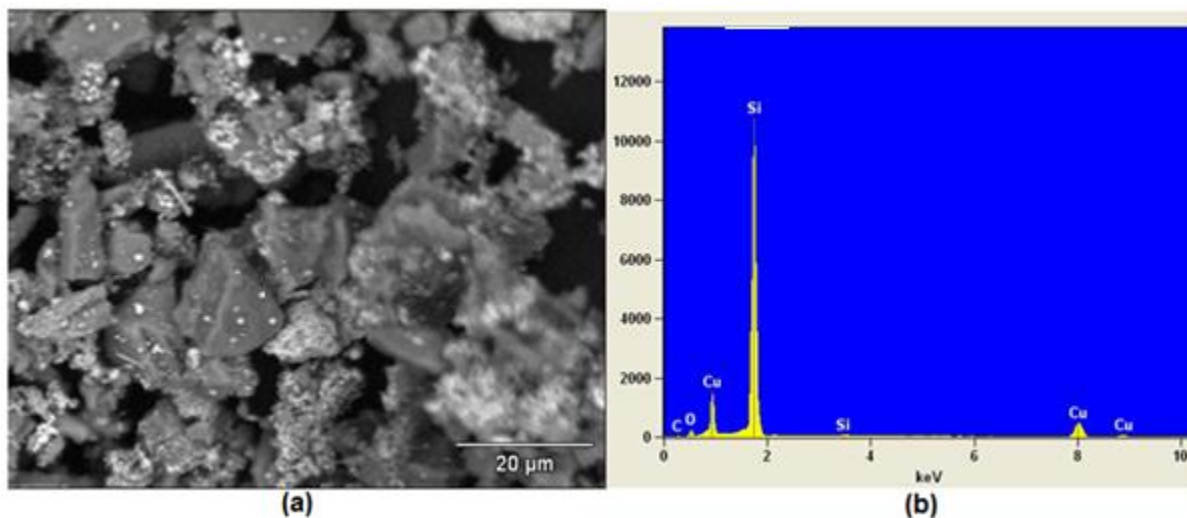


**Figure 3.3: SEM micrograph (a) and EDS spectrum (b) for Si-Cu(I)Cl mixture after the 2 h reaction with ethanol**

Further EDS analysis (Figure 3.4) of the Si-catalyst particles (same samples as above) after reaction with ethanol for 2 h revealed the presence of Cu (48%), Si (16%) and Cl (26%). The ratio of copper to silicon is 3:1 indicating the presence of the  $\text{Cu}_3\text{Si}$  intermediate, which becomes prominent after the reaction. This is in agreement with the mechanisms proposed in literature.<sup>141</sup>

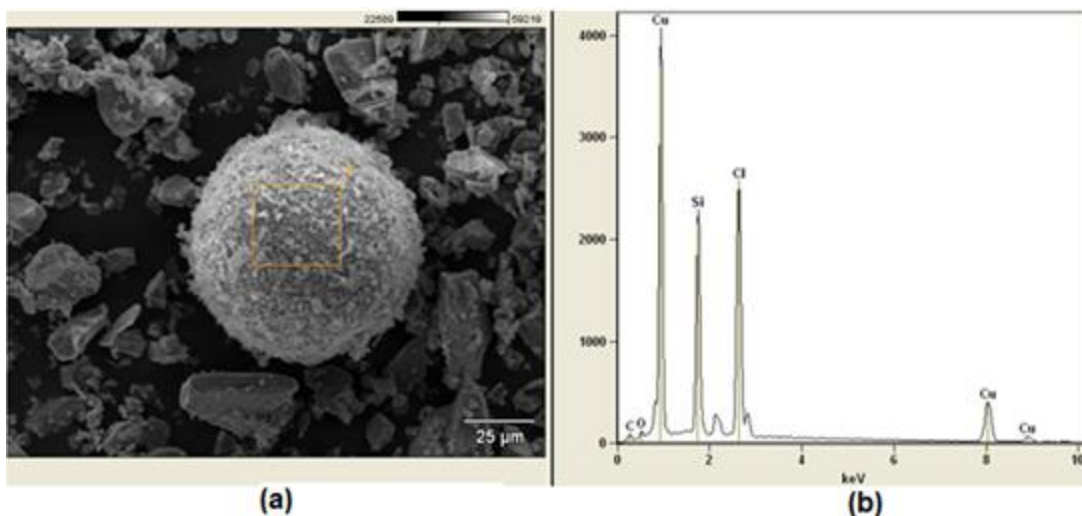


**Figure 3.4: SEM micrograph (a) and EDS spectrum (b) for Si-CuCl particle after reaction**

### **3.2.3 XRF analysis**

The same samples used for XRD and SEM-EDS analysis above were also analyzed by XRF. The XRF analysis (Table 3.1) of the silicon-catalyst mixtures after the reaction showed a decrease in the silicon content from 92.9% to 84.6% confirming the conversion of silicon to alkoxy silanes. The increase in copper content after the reaction also indicates the consumption of silicon and the exposure of the Si-Cu alloy intermediate.



**Table 3.1: XRF analysis of silicon, silicon-catalyst mixtures before and after 2 h reaction time with ethanol at 240 °C.**

| <b>Element</b> | <b>Silicon before activation (%)</b> | <b>Activated silicon-copper (I) chloride mixture (%)</b> | <b>Alkoxyated silicon copper (I) chloride mixture (%)</b> |
|----------------|--------------------------------------|--|---|
| Si             | 97.519                               | 92.948   | 84.587  |
| Cu             | 0.002                                | 5.681  | 14.674  |
| Al             | 0.00                                 | 0.000  | 0.000   |
| Fe             | 0.330                                | 0.173  | 0.187   |
| Na             | 1.597                                | 0.000  | 0.000   |
| Cl             | 0.338                                | 1.044  | 0.378   |
| Ca             | 0.158                                | 0.110  | 0.120   |
| P              | 0.000                                | 0.000  | 0.000   |
| Ti             | 0.034                                | 0.000  | 0.020   |
| V              | 0.002                                | 0.002  | 0.002   |
| Cr             | 0.002                                | 0.000  | 0.000   |
| Mn             | 0.012                                | 0.007  | 0.006   |
| Zr             | 0.003                                | 0.000  | 0.000   |
| Sn             | 0.000                                | 0.000  | 0.000   |
| Ba             | 0.000                                | 0.000  | 0.000   |
| Rh             | 0.000                                | 0.000  | 0.000   |
| Cd             | 0.000                                | 0.000  | 0.000   |
| Pb             | -                                    | 0.001  | 0.000   |
| Pd             | -                                    | 0.014  | 0.002   |
| Au             | -                                    | 0.001  | 0.002   |

### **3.3 Glass batch synthesis of trialkoxysilanes**

The synthesis of trialkoxysilanes was first carried out using ethanol as a model reagent before being applied to other alcohols. The synthesis was carried in accordance to the

general procedure outlined in section 2.4.1 and the experimental setup was as shown in Figure 2.1.

### **3.3.1 Effect of catalyst type and loading on selectivity and rate of triethoxysilane formation**

The reaction of alcohols with silicon is normally carried in the presence of copper compounds as catalysts. The most common soft Lewis acid used is copper (I) chloride but recently it has received criticism due to the production of the corrosive hydrochloric acid as a by-product.<sup>116</sup> The use of excessive amounts of catalysts is not only costly but poses an environmental problem. There is therefore the need to evaluate other more environmentally friendly catalysts for this reaction and also to minimize the amount of catalyst used. The direct reaction of silicon with ethanol in the presence of various catalysts namely copper (I) chloride (with varying amounts), copper (II) hydroxide, copper (II) oxide and copper (II) sulphate was investigated. The specific reaction conditions employed were: mass of silicon 20 g, volume of marlotherm N (heat transfer fluid) 150 mL, ethanol flow rate 0.1 mL/min, activation time 5 h, catalyst loading 5wt%, reaction temperature 240 °C and activation temperature 220 °C.

Figure 3.5 shows the effect of catalyst type on the rate of triethoxysilane formation when 5wt% of the various catalysts were evaluated. The reactivity of these catalysts can be explained in terms of whether they have big atomic radius, have low charge states and are strongly polarizable. There was rapid increase in the rate of triethoxysilane formation within the first 4 h generally for all catalysts and the rate reached a maxima after 5 h. Copper (I) chloride was the most effective catalyst with a maximum rate greater than 0.4 mol/h since it is the most soft Lewis acid which easily accepts electron pairs from silicon. Copper (II) hydroxide generally showed comparable results to copper (I) chloride. The least effective catalyst was copper (II) sulphate which only managed a maximum of less than 0.2 mol/h after 6 h. Thus, as compared to copper (II) oxide and copper (II) hydroxide, copper (II) sulphate is less selective because it is less polarizable and has a bulky group  $\text{SO}_4^{2-}$ . The rate of triethoxysilane formation was negligible when the reaction was uncatalysed. The use of a catalyst in the alkoxylation reaction is very important since its

absence results in very low selectivity and yield of the desired triethoxysilane. The results obtained indicate that copper (II) hydroxide can be employed in the direct synthesis of trialkoxysilane in place of the usually preferred copper (I) chloride, which generates corrosive hydrochloric acid.

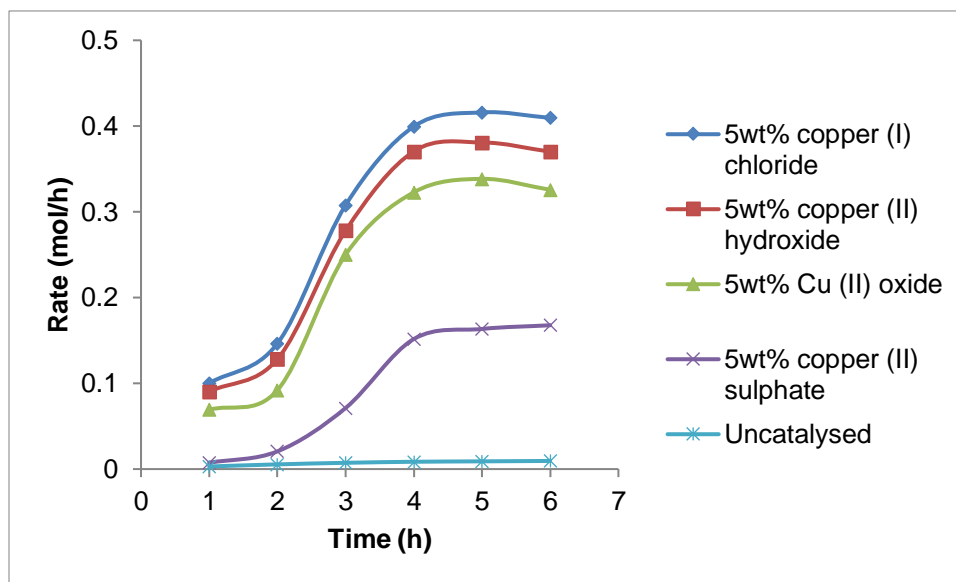


**Figure 3.5: Effect of catalyst type on the rate of triethoxysilane formation**

Under these conditions using 5wt% catalyst, Figure 3.6 shows the effect of catalyst type on the selectivity for the triethoxysilane. Copper (I) chloride, a soft Lewis acid showed the highest selectivity (>95%) whilst copper (II) hydroxide was generally comparable with selectivity greater than 93% after 6 h. The Cu (II) oxide catalysed reaction showed an increase in selectivity for the triethoxysilane over 6 h. Copper (II) sulphate showed the lowest selectivity for triethoxysilane in comparison to other catalysts. Its selectivity gradually increased from about 79 to 84% within 6 h.

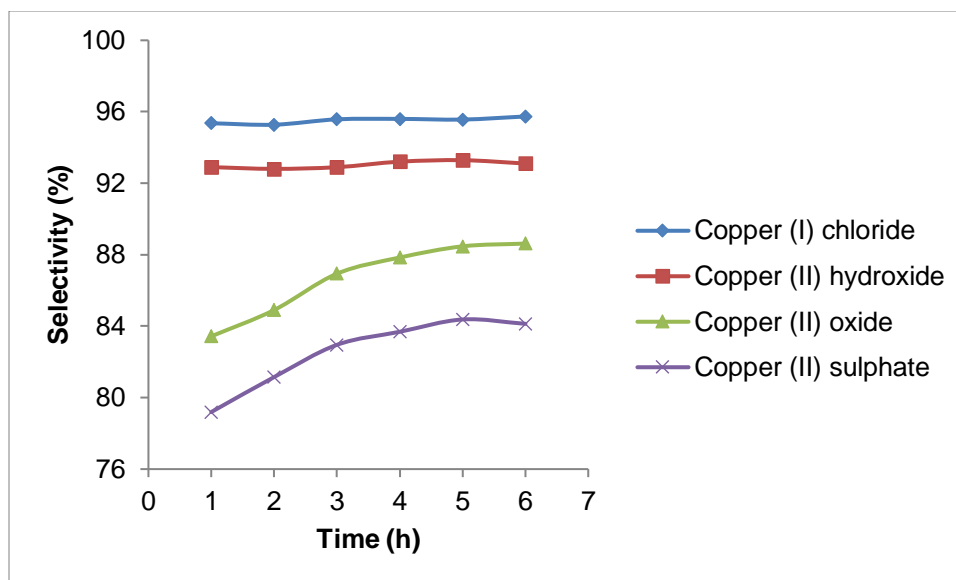


**Figure 3.6: Effect of catalyst type on triethoxysilane selectivity**

The effect of catalyst loading on the alkoxylation reaction was subsequently investigated at 2.5, 5, 10 and 15wt% copper (I) chloride catalyst amount based on silicon weight. The specific reaction conditions employed were: mass of silicon 20 g, volume of marlotherm N 150 mL, ethanol flow rate 0.1 mL/min, activation time 5 h, reaction temperature 240 °C and activation temperature 220 °C. The effect of catalyst loading on the rate of triethoxysilane formation (Figure 3.7) was comparable when 5, 10 and 15wt% catalyst loadings were used. Lower catalyst loading (2.5wt%) resulted in a slightly slower reaction. The possible explanation for this can be attributed to the fact that at lower amounts of copper catalyst the formation of the silicon-copper intermediate is limited, thereby slowing the reaction. The rate of triethoxysilane was negligible when the reaction was uncatalysed. Higher catalyst loading (>10%) does not make any significant difference on the rate of reaction and can also result in excessive accumulation of copper, which results in oxidation of the alcohol to an aldehyde as literature suggests.<sup>145</sup> The reaction can therefore be carried out using between 5 and 10% catalyst loading and as a result reduce the accumulation of copper catalyst which is a danger to the environment.

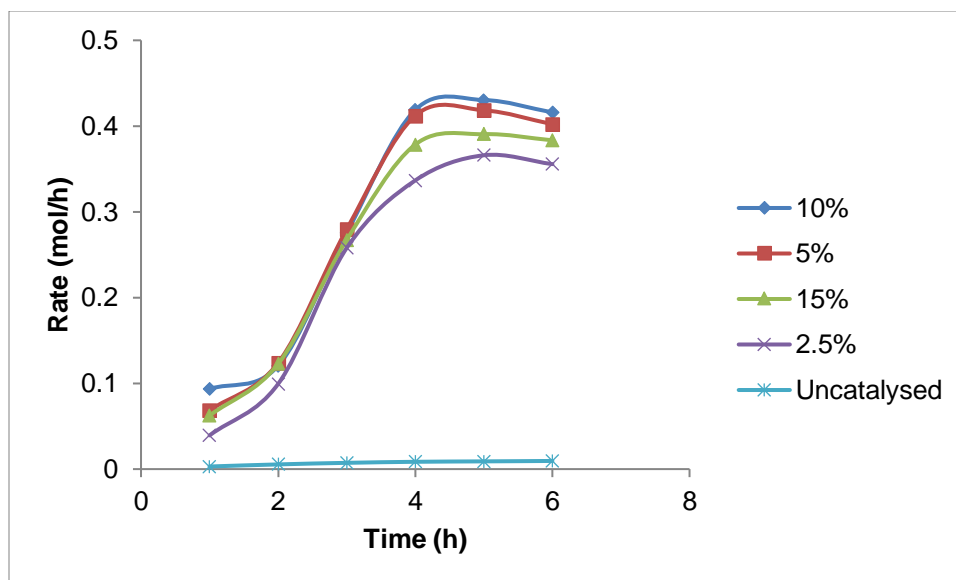


**Figure 3.7: Effect of catalyst loading on the rate of triethoxysilane formation**

The selectivity for the triethoxysilane over 6 h (under similar reaction conditions) was higher when between 5-10wt% of the catalyst was used as compared to other catalyst amounts (Figure 3.8). High catalyst amount of 15wt% resulted in lower selectivity due to excessive accumulation of copper, which results in the conversion of triethoxysilane to the undesired tetraethoxysilane and the formation silicon derivatives such as diethoxysilane.<sup>121</sup>

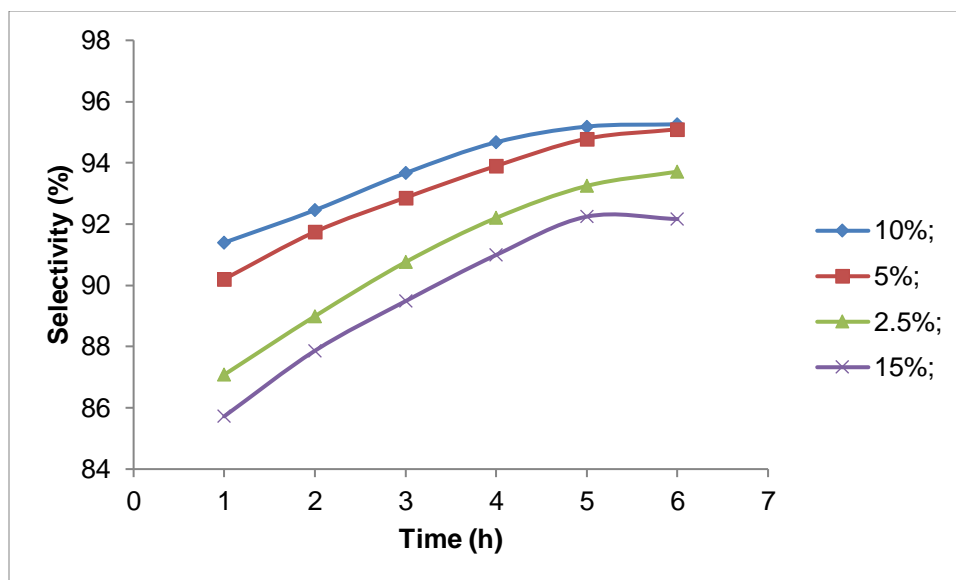


**Figure 3.8: Effective of catalyst amount on selectivity to triethoxysilane**

### **3.3.2 Effect of pre-heating temperature and activation time on the silicon-catalyst mixture on rate of formation and selectivity to triethoxysilane**

The direct synthesis of trialkoxysilane is postulated to proceed *via* the formation of a copper-silicon intermediate, which is formed during pre-heating. This intermediate alloy phase facilitates the formation and selectivity for the triethoxysilane. The pre-treatment also helps in removing the SiO<sub>2</sub> layers that are usually on the surface of silicon and thereby increasing its reactivity.

The effect of pre-heating temperature of the silicon-catalyst mixture on the rate of reaction and selectivity for triethoxysilane was studied at 220, 350, 500 and 700 °C using copper (I) chloride as catalyst. The specific reaction conditions employed were: mass of silicon 20 g, volume of marlotherm N 150 mL, flow rate 0.1 mL/min, activation time 5 h, catalyst loading 5wt% and reaction temperature 240 °C.

The effect of various pre-heating temperatures on the rate of formation and selectivity for the triethoxysilane is shown in Figure 3.9 and 3.10 respectively. The rate of triethoxysilane

formation for all pre-heating temperatures was rapid within the first 4 h and the maximum rate was achieved after 5 h. Pre-heating at lower temperatures of 220 and 350 °C favoured high rates of formation of the triethoxysilane (>0.4 mol/h) whilst high temperature activation resulted in lower reaction rates. The possible explanation for this is that high temperature pre-treatment tends to result in the accumulation of metallic copper, which catalyses the dehydrogenation of ethanol to an aldehyde and this inhibits the silicon-alcohol reaction as literature suggests.<sup>144</sup> When the reaction was carried out without the pre-heating stage, the rate of triethoxysilane formation was slower (maximum of <0.26 mol/h). This observation supports the fact that pre-activation of the silicon-catalyst mixture is an important step in removal of oxide layers and formation of the Cu-Si intermediate needed for the reaction.<sup>112</sup>

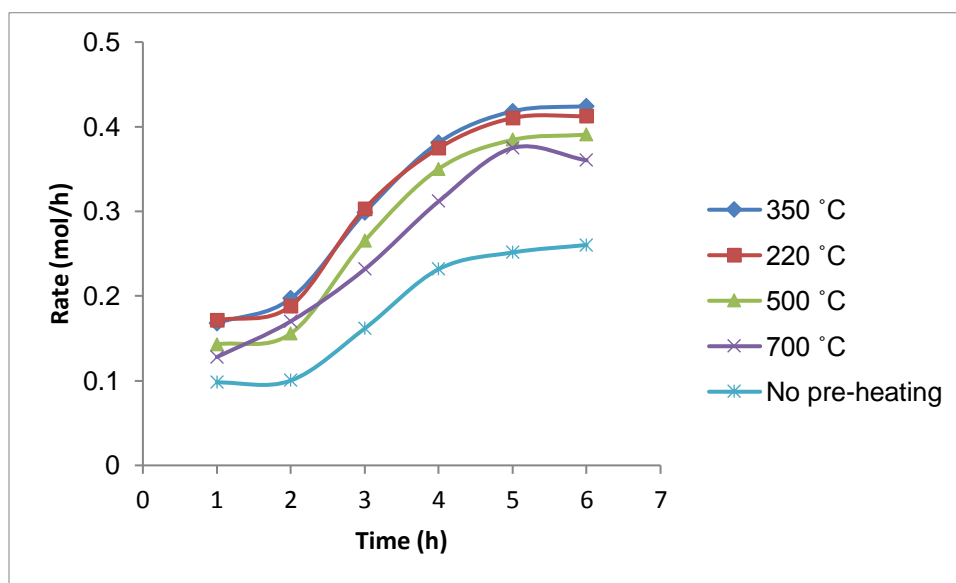


**Figure 3.9: Effect of pre-heating temperature on the rate of triethoxysilane formation**

The selectivity to triethoxysilane (under similar reaction conditions) was lower at a high pre-treatment temperature of 700 °C (<90%) than when the pre-treatment temperature was below 350 °C (>95%). High temperature lowers triethoxysilane selectivity because it

generates metallic copper, which catalyse the conversion of triethoxysilane to the undesired tetraethoxysilane.<sup>144</sup>

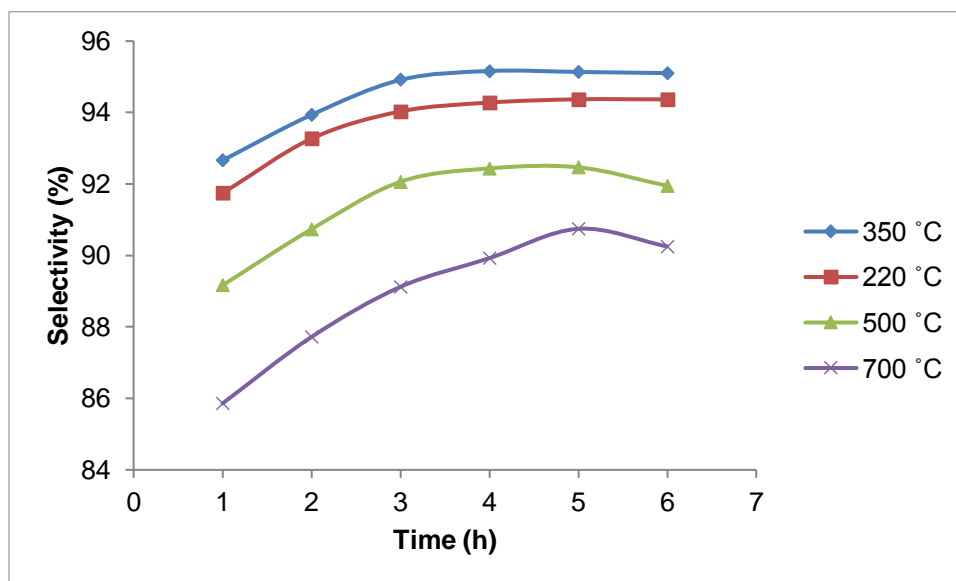


**Figure 3.10: Effective of pre-treatment temperature of the silicon-catalyst mixture on selectivity to triethoxysilane**

The effect of silicon-catalyst pre-heating time on the rate of triethoxysilane formation and selectivity was carried out by varying the time between 5 and 20 h using copper (I) chloride as the catalyst. The specific reaction conditions employed were: mass of silicon 20 g, volume of marlotherm N 150 mL, flow rate 0.1 mL/min, catalyst loading 5wt%, reaction temperature 240 °C and activation temperature 220 °C.

It was observed that there is no significant difference in the rate of triethoxysilane formation with varying pre-heating time (Figure 3.11) and thus lower activation temperatures can be employed to save time and energy. Information gathered from literature indicates pre-treatment temperatures of up to 24 h, which is a disadvantage for industrial application in terms of energy cost.



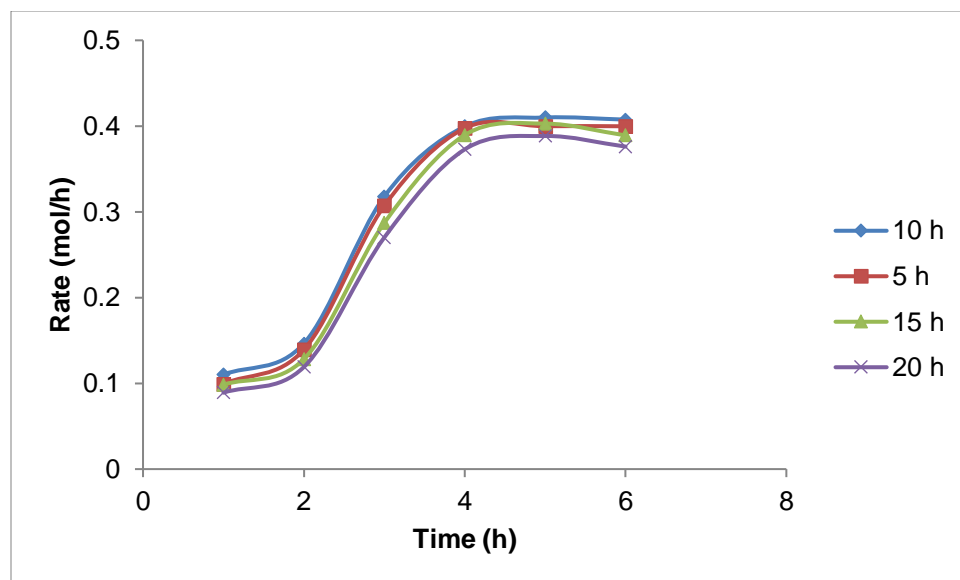


**Figure 3.11: Effect of activation time on the rate of triethoxysilane formation**

Figure 3.12 shows that shorter activation times (5 and 10 h) resulted in higher selectivity to the desired triethoxysilane (>94% at maximum) after 6 h (under similar reaction conditions). Longer activation times (20 h) resulted in slightly lower selectivity (<92% at maximum) which diminishes further with time. The possible explanation for the diminishing selectivity with increase in activation time could be that prolonged activation may lead to formation of the undesired side products as suggested in literature.<sup>109</sup>

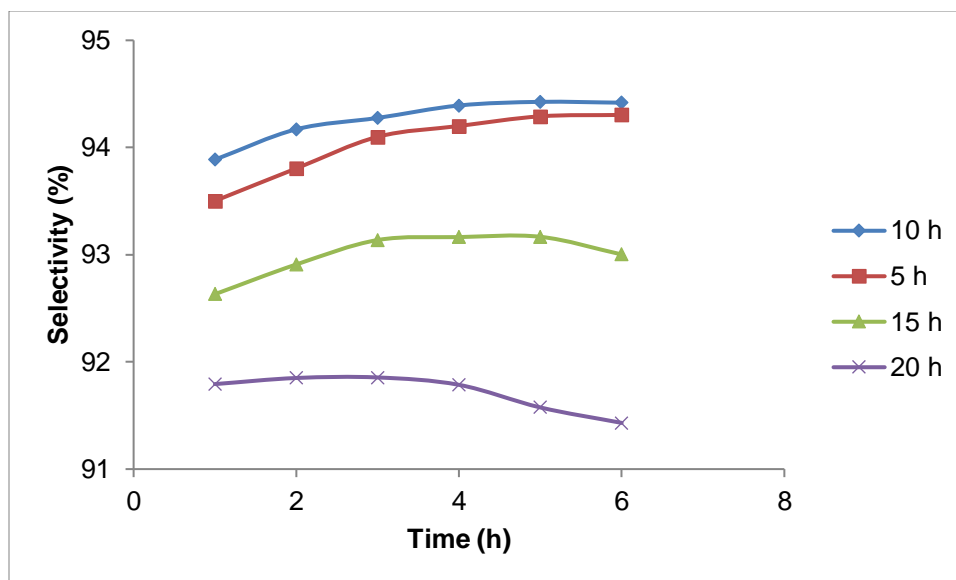


**Figure 3.12: Effect of activation time on the selectivity to the triethoxysilane**

### 3.3.3 Selectivity and rate of formation of triethoxysilane with time

The results obtained on the effect of catalyst type on the alkoxylation reaction above indicated that copper (I) chloride and copper (II) hydroxide have comparable effects over 6 h. The investigation was extended by monitoring the two catalysts over 28 h so as to compare their stabilities. The specific reaction conditions employed were: mass of silicon 20 g, volume of marlotherm N 150 mL, ethanol flow rate 0.1 mL/min, activation time 5 h, catalyst loading 5wt%, reaction temperature 240 °C, and activation temperature 220 °C.

The selectivity towards the triethoxysilane for both catalysts was comparable within the first 10 h (Figure 3.13). This trend is comparable with literature values. The selectivity due to copper (I) chloride remained almost constant between 12 and 28 h. When Cu (II) hydroxide is used as a catalyst the selectivity to triethoxysilane diminishes significantly after 10 h to less than 82% indicating that the catalyst loses effectiveness with time.

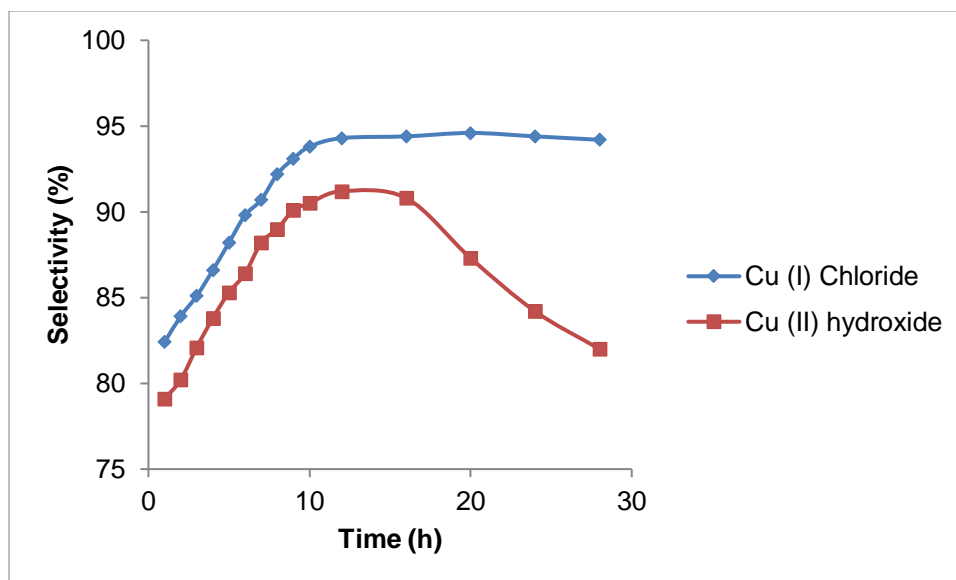


**Figure 3.13: Selectivity to triethoxysilane with time**

The rate of triethoxysilane formation increased rapidly within the first 4 h for both catalysts and reached maxima in about 6 h (Figure 3.14). When copper (II) hydroxide is used as catalyst, the rate of reaction diminishes at a rapid rate after 6 h to reach about 0.09 mol/h after 24 h. This phenomenon was also observed in literature.<sup>110</sup> The rapid rate of reaction within the first 6 h for both catalysts can be attributed to the availability of freshly activated silicon-catalyst mixture initially in large amounts. As the silicon is consumed during the later course of the reaction, the reaction slows down. The decrease in the rate of reaction can also be attributed to the loss of activity of the catalyst due to poisoning by by-products. The results indicate that copper (II) hydroxide may not be suitable for operating the reactor over a long time without catalyst replenishing.

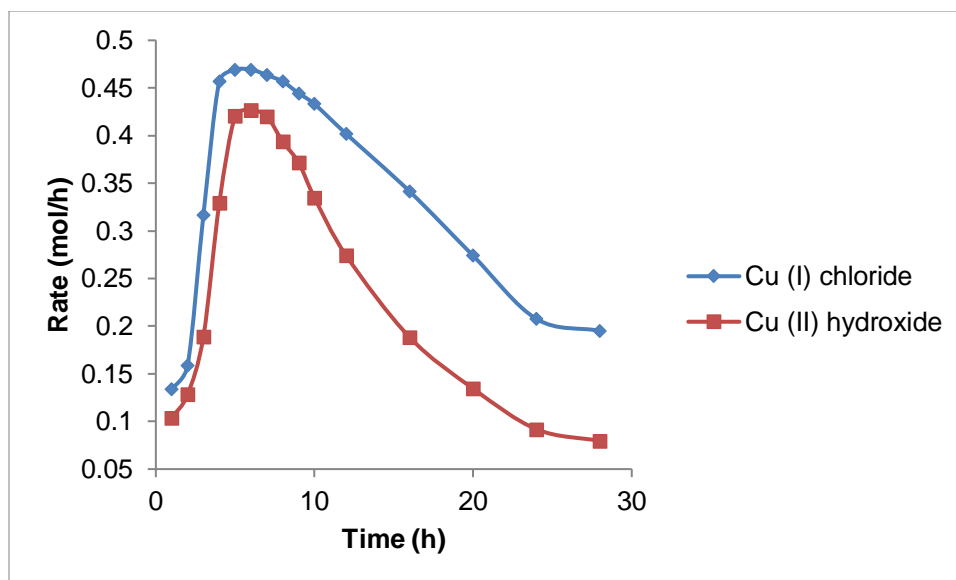


**Figure 3.14: Rate of triethoxysilane formation with time**

### **3.3.4 Effect of flow rate and temperature on trialkoxysilane selectivity and conversion of silicon**

A central composite design was used to investigate the effect of reaction temperature and ethanol flow rate on the conversion of silicon and selectivity for the triethoxysilane in the batch system using copper (I) chloride as a catalyst. The specific reaction conditions as deduced earlier employed were: mass of silicon 20 g in 150 mL marlothem N, activation time 5 h, catalyst loading 5wt% and activation temperature 220 °C. The varied experimental conditions were: reaction temperature (180 °C to 240 °C) and ethanol flow rate 0.1 to 1 mL/min. Temperatures below 180 °C were not included in the experimental domain as the reaction is not feasible at such temperatures. Very low flow rates were avoided since the alcohol is volatile and thus needed in excess. The experimental design together with the actual obtained results is shown in Table 3.2.

**Table 3.2: Experimental design and results for synthesis in semi-continuous batch mode**

| <b>Experiment number</b> | <b>Ethanol flow rate (mL/min)</b> | <b>Reaction temperature (°C)</b> | <b>Silicon conversion (%)</b> | <b>Triethoxysilane selectivity (%)</b> |
|--------------------------|-----------------------------------|----------------------------------|-------------------------------|--|
| 1                        | 0.6                               | 240                              | 84.4                          | 93.9                                   |
| 2                        | 0.9                               | 230                              | 80.3                          | 88.5                                   |
| 3                        | 0.2                               | 230                              | 87.9                          | 95.5                                   |
| 4                        | 0.6                               | 180                              | 77.4                          | 84.4                                   |
| 5                        | 0.6                               | 210                              | 82.3                          | 92.2                                   |
| 6                        | 1.0                               | 210                              | 79.4                          | 87.1                                   |
| 7                        | 0.2                               | 190                              | 82.7                          | 92.8                                   |
| 8                        | 0.1                               | 210                              | 85.0                          | 94.5                                   |
| 9                        | 0.6                               | 210                              | 82.4                          | 92.1                                   |
| 10                       | 0.6                               | 210                              | 82.3                          | 92.4                                   |
| 11                       | 0.6                               | 210                              | 82.4                          | 92.2                                   |
| 12                       | 0.9                               | 190                              | 76.5                          | 82.6                                   |
| 13                       | 0.6                               | 210                              | 82.3                          | 92.3                                   |

### **Response surface modelling**

In order to establish whether ethanol flow rate (effectively the reaction time) and reaction temperature have any statistically significant influence on conversion of silicon and triethoxysilane selectivity, response surface models were derived by means of multiple linear regression. In order to eliminate insignificant terms, backward regression (elimination of coefficient with the largest *p*-value, followed by recalculation of model coefficients and statistics) was used to determine the final model. The final results for the multiple linear regression for silicon conversion and triethoxysilane selectivity are shown in Table 3.3 and table 3.4 respectively.

It can be observed that the  $p$ -values for the coefficients for temperature ( $\beta_1$ ), flow rate ( $\beta_2$ ) and the squared term for temperature ( $\beta_4$ ) for both silicon conversion and triethoxysilane selectivity regression data are all smaller than 0.05. This suggests that these terms are statistically significant and that they influence the silicon conversion and triethoxysilane selectivity response significantly.

**Table 3.3: Final least squares regression data for silicon conversion ( $R^2 = 0.96$ )**

| <b>Coefficient symbol</b> | <b>Factor</b>          | <b>Estimated Coefficient</b> | <b>Standard error</b> | <b>T-stat</b> | <b>P-value</b> |
|---------------------------|------------------------|------------------------------|-----------------------|---------------|----------------|
| $\beta_0$                 | Intercept              | -2.592                       | 27.880                | -0.0930       | 0.928          |
| $\beta_1$                 | $X_1$ (Flow rate)      | -8.532                       | 0.823                 | -10.263       | <0.0001        |
| $\beta_2$                 | $X_2$<br>(Temperature) | 0.739                        | 0.266                 | 2.776         | 0.0215         |
| $\beta_4$                 | $X_2^2$                | -0.00149                     | 0.00633               | -2.348        | 0.0435         |

**Table 3.4: Final least squares regression data for triethoxysilane selectivity ( $R^2 = 0.92$ )**

| <b>Coefficient symbol</b> | <b>Factor</b>          | <b>Estimated coefficient</b> | <b>Standard error</b> | <b>T-stat</b> | <b>P-value</b> |
|---------------------------|------------------------|------------------------------|-----------------------|---------------|----------------|
| $\beta_0$                 | Intercept              | -75.872                      | 48.592                | -1.561        | 0.153          |
| $\beta_1$                 | $X_1$ (Flow rate)      | -10.868                      | 1.435                 | -7.573        | <0.0001        |
| $\beta_2$                 | $X_2$<br>(Temperature) | 1.518                        | 0.464                 | 3.273         | 0.00964        |
| $\beta_4$                 | $X_2^2$                | -0.0033                      | 0.00110               | -2.987        | 0.0153         |

The final surface response models fitted to both silicon conversion and triethoxysilane selectivity were:

$$\% \text{ Silicon conversion} = -2.592 - 8.532X_1 + 0.739X_2 - 0.00149X_2^2 \quad (21)$$

$$\% \text{ Triethoxysilane selectivity} = -75.872 - 10.868 X_1 + 1.518X_2 - 0.0033X_2^2 \quad (22)$$

Where,  $X_1$  = Ethanol flow rate and  $X_2$  = Reaction temperature.

The models were deemed valid for analysing the observed data after testing for outliers and normality of the data using STATISTICA (Appendix C).

### **Models interpretation**

The response surface models were used to interpret the data using 3-dimensional response surface plots generated from STATISTICA. Figure 3.15 shows the 3-dimensional response surface plot for predicted silicon conversion as a function of ethanol flow rate and reaction temperature. It can be observed that an increase in temperature resulted in an increase in silicon conversion and the graph levelled off at a temperature of 240 °C and flow rate of 0.1 mL/min where a maximum of about 88% conversion was predicted. When the reaction was carried out at these optimized conditions, the conversion was about 89% which is comparable with the predicted value. High reaction temperature tends to result in the accumulation of metallic copper, which catalyses the conversion of ethanol to ethanal and this limits the silicon-alcohol reaction as suggested in literature.<sup>109</sup> The graph also shows that a decrease in flow rate results in a linear increase in silicon conversion due to increase in residence time.

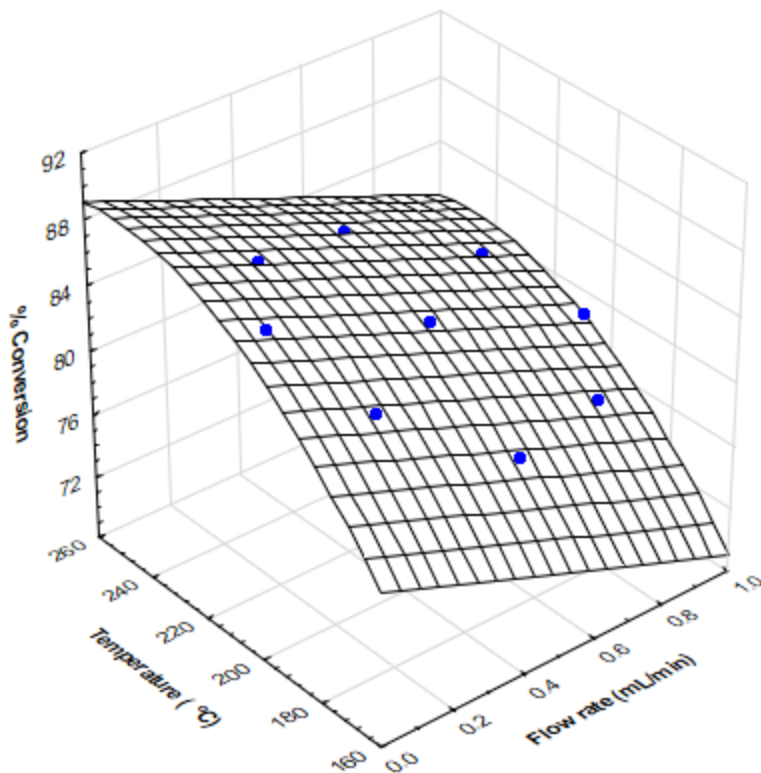


**Figure 3.15: 3-dimensional response surface plot for silicon conversion**

The 3-dimensional response surface plot for triethoxysilane selectivity as a function of ethanol flow rate and reaction temperature (Figure 3.16) showed related trends as was observed with silicon conversion. An increase in temperature resulted in an increase in selectivity up to a temperature of 230 °C corresponding to a maximum selectivity of 98% at 0.1mL/min. The observed selectivity under these optimized conditions was about 96%, which is comparable to the predicted one. The reason for the slight drop in selectivity after 230 °C can be attributed to the possible conversion of triethoxysilane to tetraethoxysilane by metallic copper at these high temperatures.<sup>112</sup>



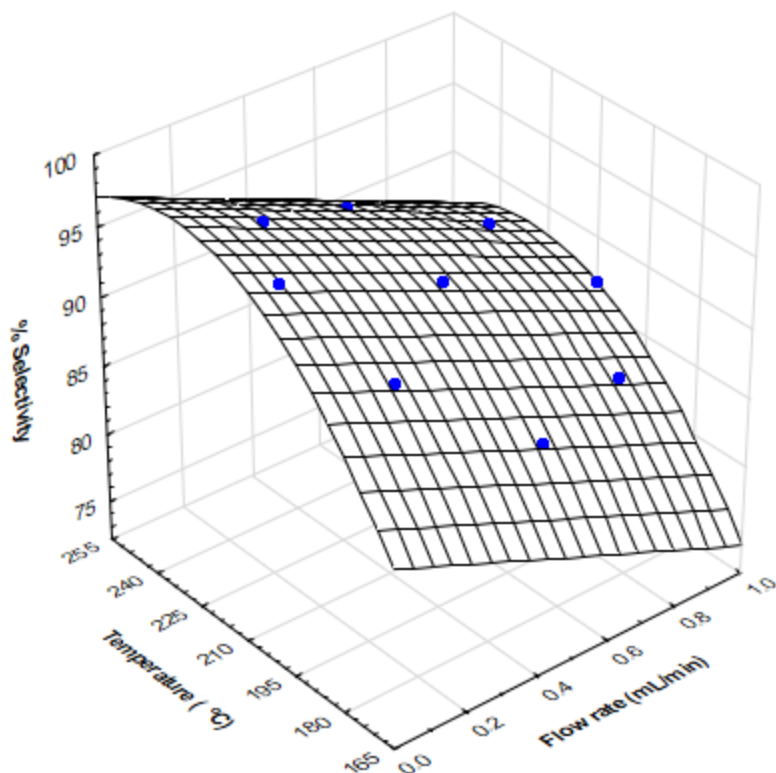


**Figure 3.16: 3-dimensional response surface plot for triethoxysilane selectivity**

### 3.3.5 Effect of R-group on trialkoxysilane selectivity and conversion of silicon

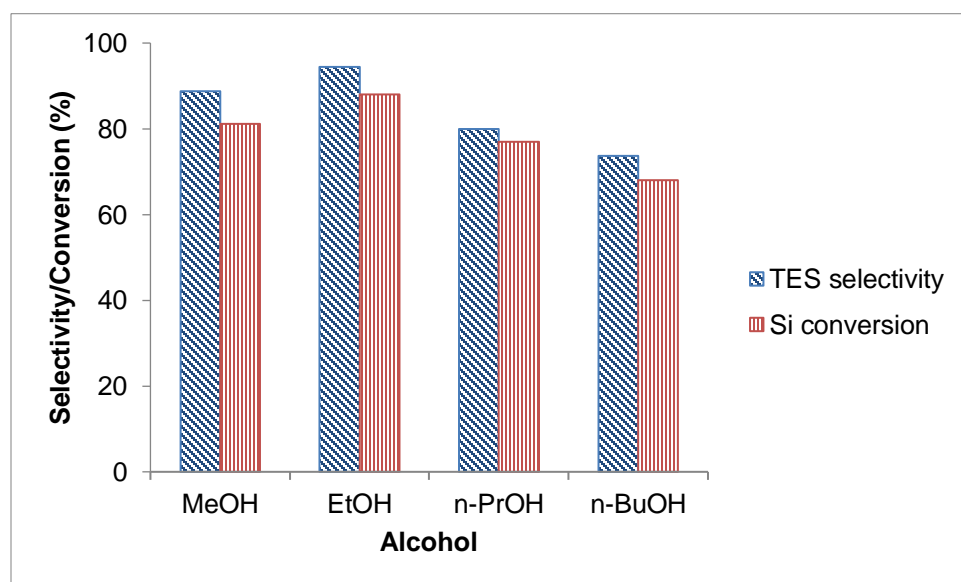
The work on the reaction of silicon with higher alcohols has been very limited to the best of our knowledge and as such it was worth investigating how other alcohols would perform. The direct alkoxylation of silicon was carried out using four primary alcohols of increasing carbon chain length at similar experimental conditions. The specific reaction conditions used were: mass of silicon 20 g in 150 mL marlotherm N, alcohol flow rate 0.1 mL/min, activation time 5 h, catalyst loading 5wt%, reaction time of 24 h, reaction temperature 240 °C and activation temperature 220 °C.

Figure 3.17 shows the effect of R-group (C1 to C4) on the conversion of silicon and selectivity towards trialkoxysilanes. Ethanol (C2) effected the highest silicon conversion of about 88% after 24 h whilst the use of butanol (C4) resulted in the lowest silicon conversion of 68%. The conversion of silicon generally decreased as we move from lower alcohols to higher alcohols due to decrease in reactivity with increasing chain length.<sup>146</sup>

Methanol (C1) effected lower conversion than ethanol and this could be attributed to the fact that the former is too volatile and hence less interaction with silicon slurry in the reactor.

The effect of R-group on the selectivity towards trialkoxysilanes showed an increase in selectivity from C1 (88.7%) to C2 (94.4%) alcohols. This trend can be attributed to the volatility of methanol. When propanol was used, the selectivity to the trialkoxysilane was less than that of ethanol and this can be attributed to the decrease in reactivity as the carbon chain increases.<sup>147</sup>

The lower selectivity and conversion observed on methanol as compared to ethanol can also be attributed to the fact that hydrochloric acid, which forms when copper (I) chloride is used as a catalyst reacts with methanol to form methyl chloride and water. This result in the loss of methanol starting material and water can react with trialkoxysilane to produce siloxanes, thus lowering selectivity. The presence of water in the reaction can also reduce the conversion of silicon metal.<sup>121-122</sup>



**Figure 3.17: Effect of R-group on trialkoxysilane selectivity and conversion**

### 3.4 Continuous flow synthesis of trialkoxysilanes in a falling film tubular reactor

After successful synthesis of trialkoxysilanes in semi-continuous batch mode, it was necessary to apply the method in continuous mode as a pilot small production platform for possible industrial application and up-scaling. The synthesis was carried out in a continuous flow falling film tubular reactor according to the experimental procedure outlined in section 2.4.2 and the reactor setup is as shown in Figure 2.2. Silicon (50 g) mixed with copper (I) chloride (5wt%) was first activated at 220 °C for 5 h in 150 mL marlotherm N (heat transfer fluid) prior to the reaction. The reaction conditions varied were: ethanol flow rate flow rate 0.1 to 1 mL/min, silicon slurry flow rate 0.1 to 1 g/min and reaction temperature 180 to 240 °C.

The reaction between silicon slurry and ethanol was characterised by very low silicon conversion, yield and selectivity for the desired trialkoxysilane. Attempted optimization of the ethanol flow rate, slurry flow rate and temperature did not improve formation of the triethoxysilane as only trace amounts of product were formed. The distillates contained triethoxysilane (3.5%) tetraalkoxysilane (4%) and other compounds contributed about 92.5% under optimized reaction conditions. Compounds which contributed 92.5% comprised of marlotherm volatiles, trace ethanal and trace diethoxysilane (see GC-MS spectra in Appendix A). The dehydrogenation of ethanol to ethanal which we noted was also observed in literature.<sup>109,134</sup> All three silanes could not be accurately quantified as they were in trace amounts. Typical results for the effect of reaction temperature (at constant ethanol flow rate of 0.1 mL/min and constant silicon slurry flow rate of 0.1 g/min) and ethanol flow rate (at constant temperature of 240 °C and constant silicon slurry flow rate of 0.1 g/min) are as depicted in Figure 3.18 and 3.19 respectively. It can be seen that product formation is better at lower ethanol flow rates 0.1-0.2 mL/min and reaction temperature of between 235 and 240 °C although in trace amounts.

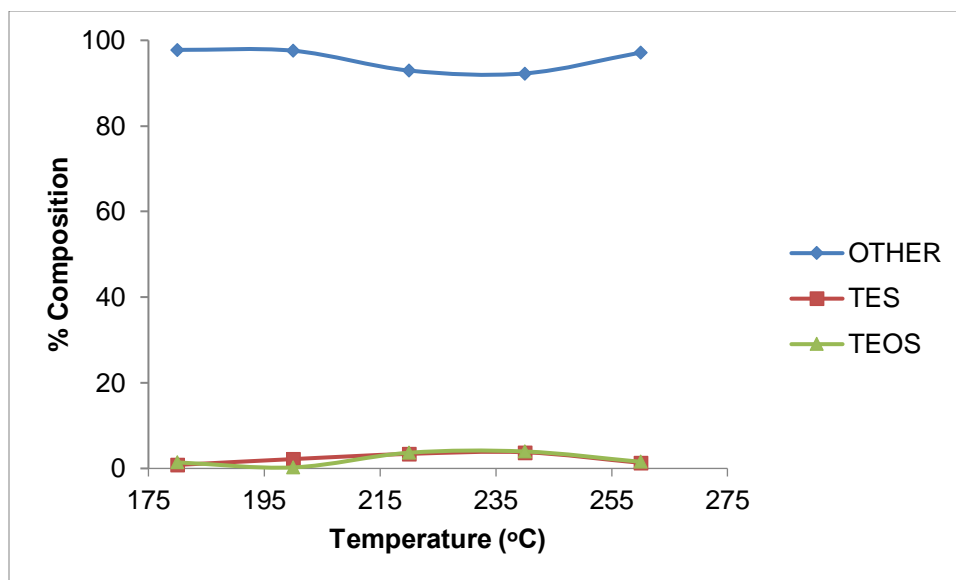


**Figure 3.18: Effect of temperature on the reaction**

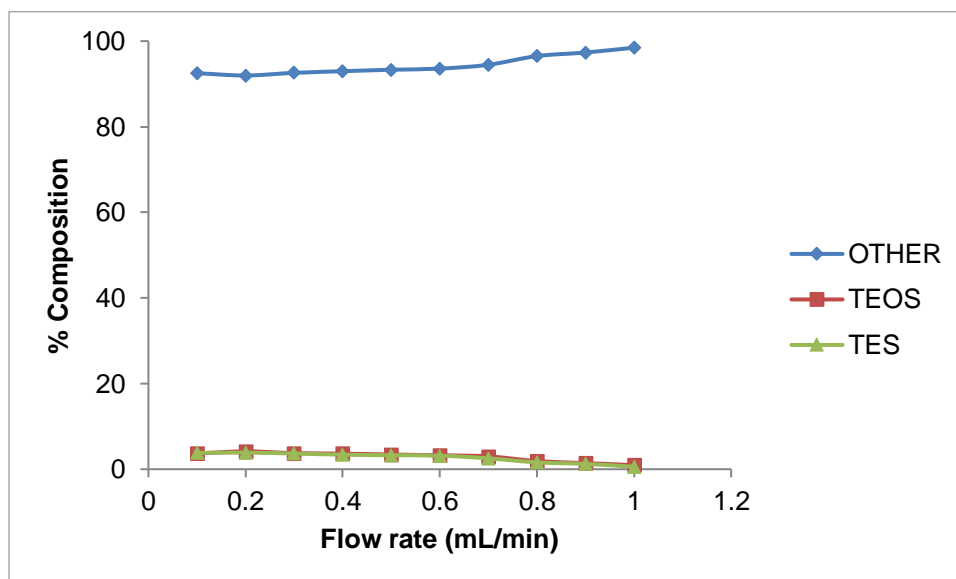


**Figure 3.19: Effect of ethanol flow rate on the reaction**

The possible reason for the poor reactivity of silicon slurry and alcohol in this system can be attributed to poor mass transfer in the reactor (gas vs liquid/solid) unlike in the semi-continuous batch reactor (liquid vs liquid/solid). The poor mass transfer means that the

substrate catalyst interactions are also limited. This observation was also observed by Beenackers and Van Swaij<sup>148</sup> in their review of mass transfer in gas-liquid slurry reactors. Steric hindrance due to bulky alkoxy groups formed on the observed diethoxysilane may have also contributed to the poor reactivity of silicon and alcohol under these conditions.

### 3.5 Conclusion

The synthesis of trialkoxysilanes in a glass batch reactor and in a falling film continuous flow tubular reactor has been studied. The Si-catalyst mixtures were analysed by SEM-EDS, XRD and XRF. The results confirmed the existence of a  $\text{Cu}_3\text{Si}$  phase after activation which is thought to act as an intermediate to aid the exclusive formation of trialkoxysilane.

The results obtained from investigations in the batch synthesis indicated that copper (I) chloride and copper (II) hydroxide are the most preferred catalysts and show comparable effects on the rate of reaction and selectivity to triethoxysilane. This means that copper (II) hydroxide can be used as a non-halide environmentally friendly copper catalyst substitute for shorter reaction cycles as it was however observed that it loses catalytic activity rapidly after 10 h. The selectivity for triethoxysilane and rate of reaction was higher at lower temperature (<350 °C) Si-catalyst pre-heating conditions than at high temperature pre-heating conditions (>500 °C). The amount of formed triethoxysilane was high at catalyst loading between 5 and 10wt%, indicating that higher catalyst loadings (>10%) do not improve selectivity and the rate of reaction but rather result in the accumulation of copper catalyst which is a danger to the environment. There was no significant difference in the effect of Si-catalyst pre-heating time on the rate of reaction and thus shorter activation times (5-10 h) can be employed. The effect of flow rate and temperature on the alkoxylation reaction was also investigated. The optimum conditions were found to be a temperature of 230 °C and flow rate of 0.1mL/min for triethoxysilane selectivity and 240 °C and 0.1mL/min for silicon conversion. The effect of R-group (C1 to C4) on the reaction revealed that silicon conversion and selectivity for trialkoxysilane decrease with an increase in carbon chain length. Ethanol showed higher selectivity

(>95%) and reactivity than other alcohols, indicating that it could be the most preferred alkoxylation alcohol for this reaction.

The results obtained from the synthesis of trialkoxysilanes in continuous mode in a falling film tubular reactor showed very poor conversion of silicon and selectivity to trialkoxysilane. The observation indicates poor mass transfer between silicon slurry and alcohol. It was also noted that the solvent used for forming the slurry (Marlotherm) contaminates the products and thus complicates the purification process. The reaction of silicon with alcohol in the absence of a heat transfer solvent (non-slurry) could be worthwhile to explore.

## CHAPTER 4

### Synthesis of trialkoxysilanes in a packed bed flow tubular reactor

#### 4.1 Introduction

The poor results obtained from the synthesis of trialkoxysilanes in a slurry phase continuous flow falling film tubular reactor in Chapter 3 were attributed to the poor mass transfer between alcohol and silicon slurry. It was decided to investigate the same reaction in a packed bed flow tubular reactor, where mass transfer is better and it is also easier to scale up in continuous production unlike the batch process.<sup>149</sup> Packed bed flow tubular reactors offer advantages of ideal plug flow behaviour, lower maintenance, operation and construction costs and are effective at high temperature and pressure.<sup>150-152</sup> The use of solid catalysts which are activated *in situ* ensures that the catalyst are freshly prepared before the reaction and the catalysts can be reused and thus promoting green manufacturing processes.<sup>153-154</sup>

Herein, the semi-continuous flow method for the synthesis of (C1 to C4) trialkoxysilanes in a packed bed flow tubular reactor is discussed. Similar reaction parameters which were investigated under the batch system namely, silicon-catalyst activation temperature and time, catalyst type and loading, reaction temperature and alcohol flow rate were tested under this protocol. Furthermore, effect of pressure on the reaction was also investigated.

#### 4.2 Packed bed flow tubular reactor synthesis of trialkoxysilanes

The synthesis of alkoxy silanes under this system was carried in accordance to the general procedure outlined in section 2.4.3 and the experimental setup and schematic flow diagram are as shown in Figure 2.3 and 2.4 respectively.

##### 4.2.1 Effect of copper catalyst type on the rate of triethoxysilane formation

The effect of copper catalyst type on the rate of triethoxysilane formation was investigated for copper (I) chloride, copper (II) hydroxide, copper (II) oxide and copper (II) sulphate. A control experiment was conducted with no catalyst present. The specific reaction

conditions used were: mass of silicon 5 g, flow rate 0.1 mL/min, catalyst loading 5wt%, activation time 2.5 h, reaction temperature 240 °C and activation temperature 220 °C.

The reaction profiles observed are similar to that in the batch system (Chapter 3). As can be seen from Figure 4.1, copper (I) chloride, copper (II) hydroxide, copper (II) oxide shows similar reaction rate profiles, with copper (I) chloride being preferred over copper (II) hydroxide and copper (II) oxide. Although the copper (II) sulphate catalysed reaction did yield triethoxysilane, the rate of the reaction is not ideal. The rate of triethoxysilane formation was negligible for the uncatalysed reaction. Copper (II) hydroxide and copper (I) chloride showed comparable rates of reaction in the batch system but the latter was more reactive in the packed bed flow tubular reactor.

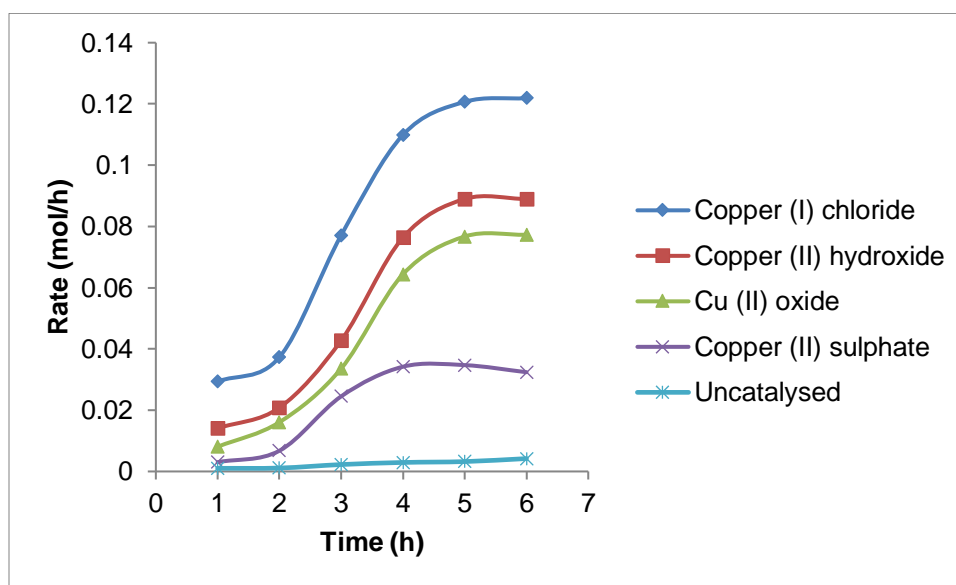


**Figure 4.1: Effect of copper catalyst type on the rate of triethoxysilane formation**

#### **4.2.2 The effect of catalyst loading on the rate of triethoxysilane formation**

The effect of catalyst loading concentration on the rate of triethoxysilane formation was investigated for catalyst loading concentrations of 2.5, 5, 10 and 15wt% of copper (I) chloride. A control experiment was conducted with no catalyst present. The specific



reaction conditions used were: mass of silicon 5 g, flow rate 0.1 mL/min, reaction temperature 240 °C, activation time 2.5 h and activation temperature 220 °C.

As can be seen from Figure 4.2, comparable reaction rates were obtained for all the selected catalyst loading amounts. The rate of triethoxysilane formation was negligible for the uncatalysed reaction. The results obtained in this experiment confirms that a catalyst loading concentration of 2.5wt% or less by weight of the catalyst-silicon mixture is equally as effective compared to higher loadings under this protocol. In the batch process a catalyst loading of 2.5wt% showed slightly lower rates of formation.

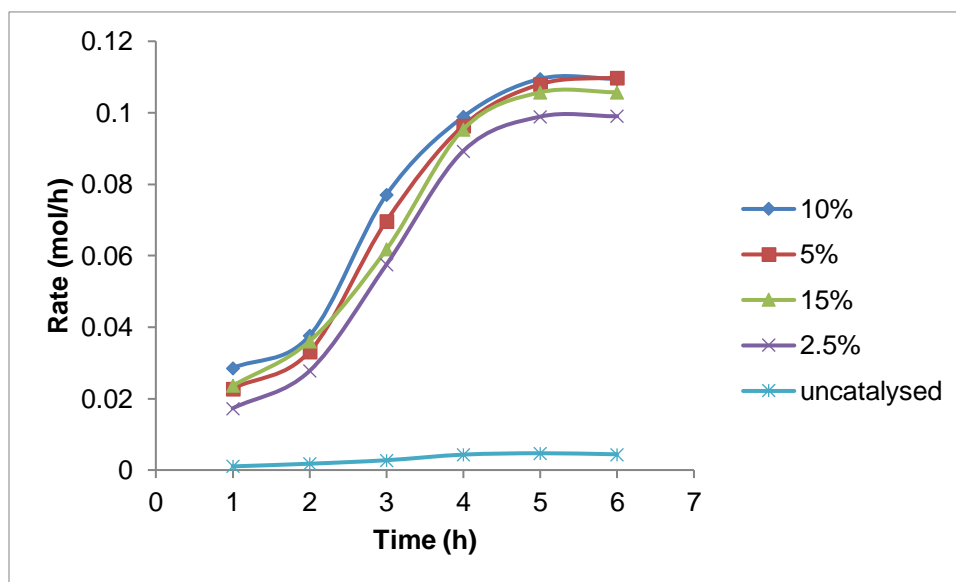


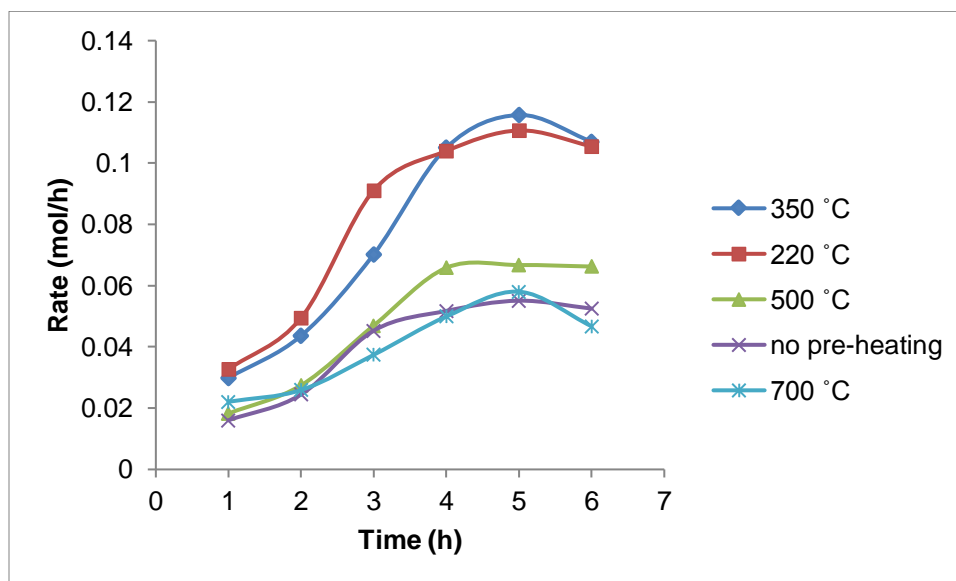
**Figure 4.2: Effect of catalyst loading on the rate of triethoxysilane formation**

#### **4.2.3 Effect of activation temperature and activation time on the rate of triethoxysilane formation**

The effect of activation temperature on the rate of triethoxysilane formation was investigated for 220 °C, 350 °C, 500 °C, and 700 °C. A control experiment was conducted with no catalyst present. Further, the effect of the duration of the activation cycle on the rate of triethoxysilane formation was investigated for 2.5, 5, 15 and 20 h. The reaction

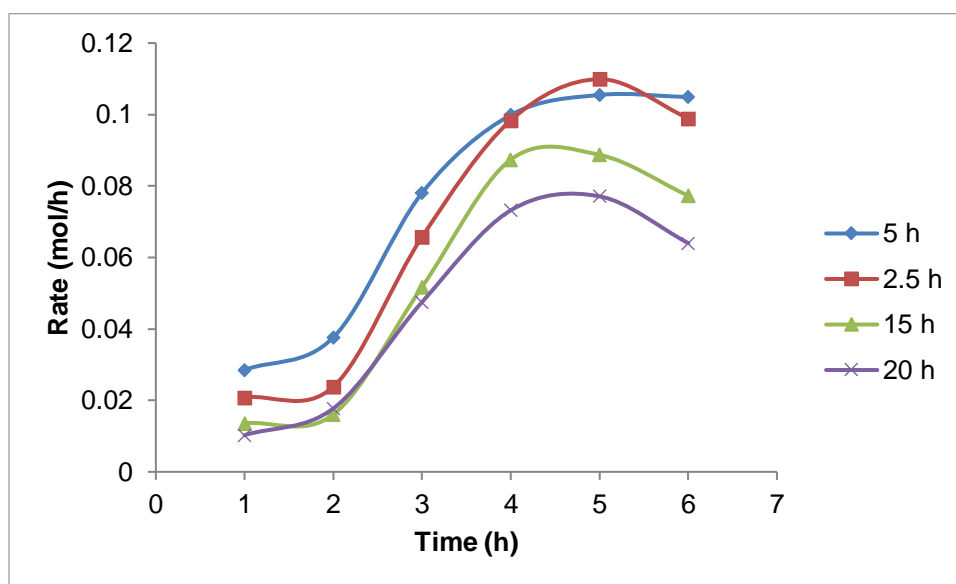
conditions used for the activation temperature experiments were: mass of silicon 5 g, flow rate 0.1 mL/min, activation time 2.5 h, catalyst loading 5wt% CuCl and reaction temperature 240 °C. The reaction conditions employed for the activation time experiments were: mass of silicon 5 g, flow rate 0.1 mL/min, catalyst loading 5wt% CuCl, reaction temperature 240 °C and activation temperature 220 °C.

Figure 4.3 shows a graphical representation of the results obtained for the activation temperature experiments. As can be seen from the graph, an activation temperature of 220 °C proved to be just as effective as an activation temperature of 350 °C. It appears that the catalyst deactivated to an extent when the activation temperature was over 500 °C, as the rate of triethoxysilane formation for the 500 °C and 700 °C experiments were similar compared to the rate of formation where no activation cycle was used. This is in contrast to the batch system where there wasn't much difference in reaction profiles for the temperatures investigated. It is clear from the results that an activation temperature of 220 °C may be employed in this method and thus save on energy costs.



**Figure 4.3: Effect of activation temperature on the rate of triethoxysilane formation**

The results obtained for activation time experiments (Figure 4.4) indicate that an optimal activation cycle may be one that is in the region of 2.5 to 5 h. Where the activation cycle is too long, that is greater than 15 h, the rate of triethoxysilane formation goes down. The possible reason for this trend is as explained earlier in the batch system. The results are in contrast with the batch method where there was no significant difference in the rate of triethoxysilane formation with varying pre-heating time. It can be noted that the packed bed flow tubular reactor system offers an advantage of shorter activation times compare to the batch system.



**Figure 4.4: Effect of activation time on the rate of triethoxysilane formation**

#### **4.2.4 Effect of reaction temperature on silicon conversion and triethoxysilane selectivity**

The effect of reaction temperature on triethoxysilane selectivity and silicon conversion was investigated at constant operation time of 24 h, ethanol flow rate of 0.1mL/min, activation time of 2.5 h, catalyst loading of 5wt% Cu(I)Cl and activation temperature 220 °C.

As can be seen from the results presented in Figure 4.5, reaction temperatures of between 220 °C and 240 °C were more effective in terms of both selectivity and conversion when compared to reaction temperatures below 220 °C. However, it was noted that both selectivity and conversion rates decreases when the temperature was higher than 240 °C indicating that the catalyst lost activity due to the same reasons as discussed earlier under the batch system.

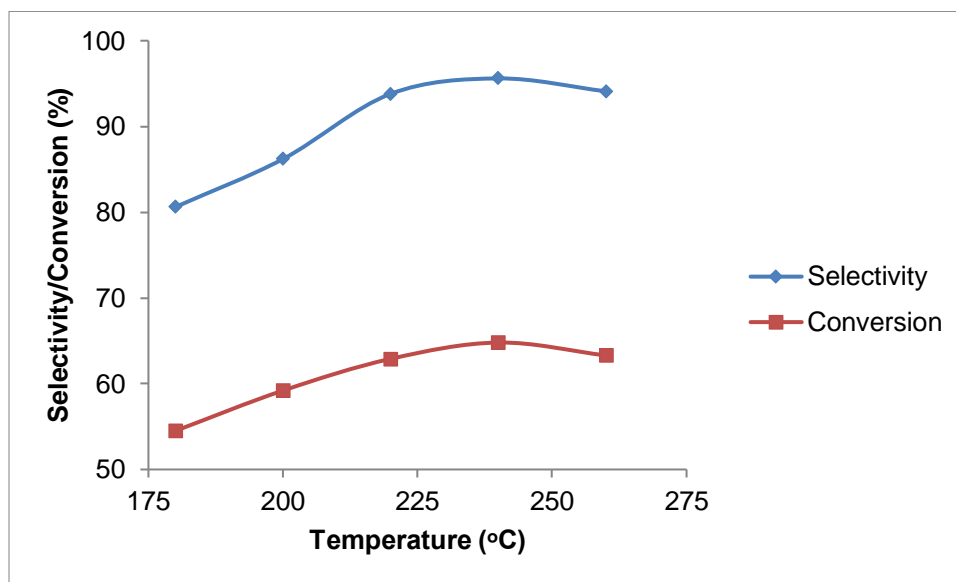


**Figure 4.5: Effect of temperature on conversion and selectivity**

#### **4.2.5 Effect of flow rate on triethoxysilane selectivity and silicon conversion**

The effect of flow rate on triethoxysilane selectivity and silicon conversion was investigated at similar reaction conditions as above at a reaction temperature of 240 °C by varying ethanol flow rate from 0.05 to 0.8 mL/min. This translates to 141 to 9 min residence time. As depicted in Figure 4.6, both selectivity and conversion decreased with an increase in flow rate. Maximum selectivity and conversion was achieved at 0.05 mL/min (about 95%) and 0.1 mL/min (about 64%) respectively.

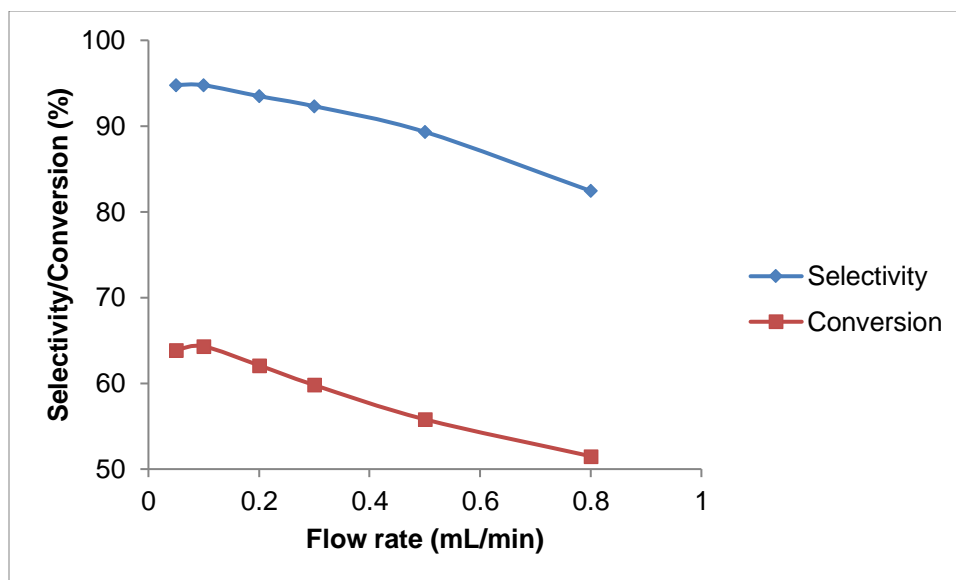


**Figure 4.6: Effect of flow rate on conversion and selectivity**

Figure 4.7 shows that silicon conversion increased rapidly with an increase residence time from 9 min (51%) to 35 min (62%) and gradually to 71 min (64%). It was also noted that conversion then decreased slightly from 64.3% (71 min residence time) to 63.9% (141 min residence time). This can be due to the fact that at very low flow rates, the concentration of absolute ethanol molecules in the reactor available to react with packed silicon is low. This is because the equation of reaction stoichiometrically requires three molecules of ethanol for each molecule of silicon. Generally a similar trend was observed for triethoxysilane selectivity where it increased from about 82% (9 min residence time) to about 95% (141 min residence time). It can be concluded that very low residence times promote high selectivity but may not be sufficiently enough to effectively deplete silicon starting material at an economical rate.

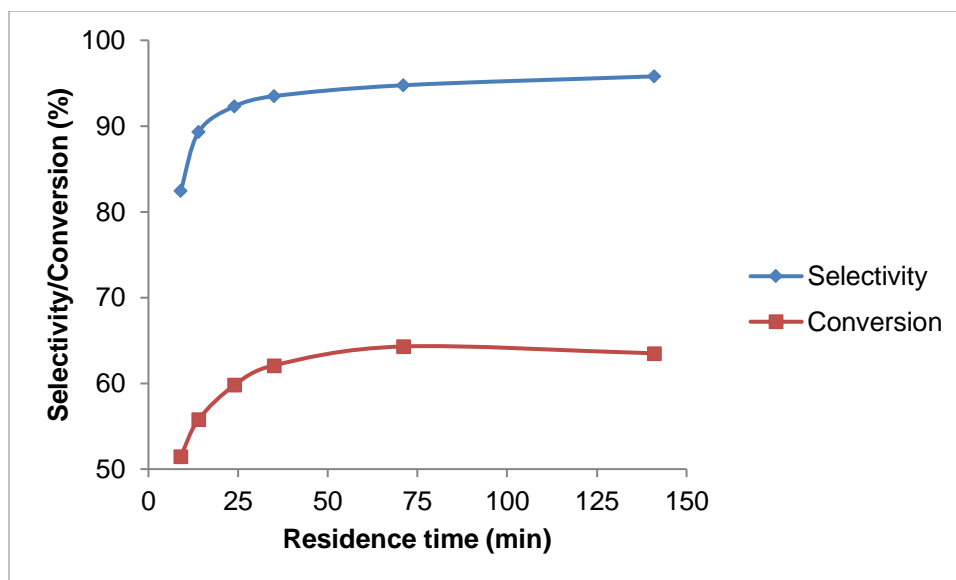


**Figure 4.7: Effect of residence time on conversion and selectivity**

#### 4.2.6 Silicon conversion and triethoxysilane selectivity with time

The selectivity to triethoxysilane and silicon conversion was monitored for a period of 30 h in order to access the stability of Cu(I)Cl catalyst with time. The reaction conditions used were: mass of silicon 5 g, flow rate 0.1 mL/min, activation time 2.5 h, catalyst loading 5wt% CuCl and reaction temperature 240 °C. It was observed that the conversion increased rapidly within the first 12 h (5% to 49%) after which it became almost constant between 24 and 30 h (Figure 4.8). This trend could be a result of the decreasing silicon amount with time in the reactor. The selectivity was extremely good for the entire period (about 95-98%) unlike in the batch system where it increased with time (82-95%). The excellent selectivity observed in the tubular reactor can be attributed to the efficient *in situ* catalyst activation, which is carried out in this method.

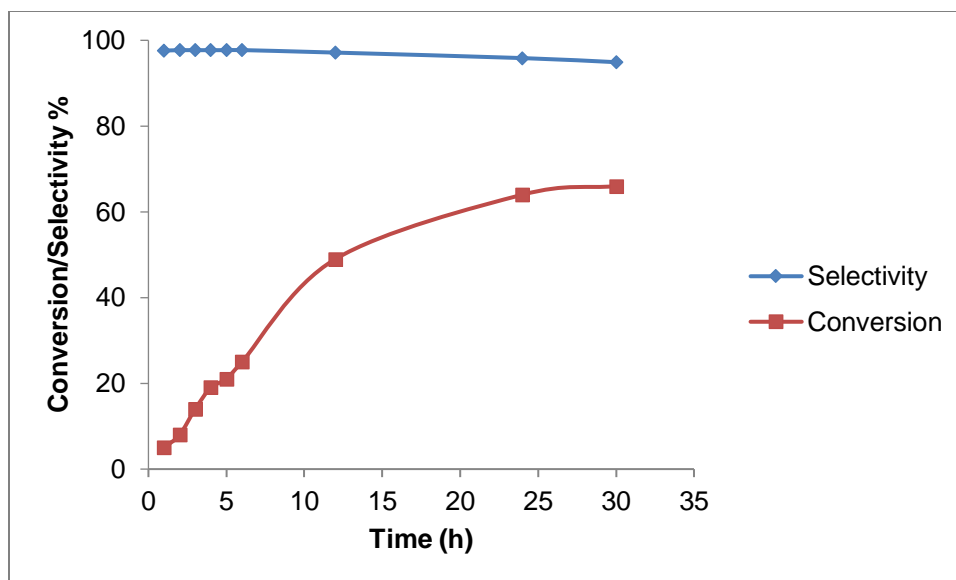


**Figure 4.8: Silicon conversion and triethoxysilane selectivity over 30 h**

#### 4.2.7 Response surface modelling on silicon conversion

The results obtained above showed that selectivity for triethoxysilane was extremely good (>97%) indicating that the condition used were optimum. However, the conversion of silicon was only moderate at about 64% and thus it was decided to investigate whether ethanol flow rate or residence time and reaction temperature have any statistically significant influence on conversion of silicon and also to optimize the reaction. A central composite design (Table 4.1) was applied in this investigation using copper (I) chloride as a catalyst at activation time 2.5 h, reaction period 24 h, catalyst loading 5wt% and activation temperature 220 °C for all experiments. Multiple regression was performed on observed data and the final data is shown in Table 4.2.

**Table 4.1: Experimental design and results for synthesis in packed bed flow tubular reactor**

| Experiment number | Ethanol flow rate (mL/min) | Reaction temperature (°C) | Silicon conversion (%) |
|-------------------|----------------------------|---------------------------|------------------------|
| 1                 | 0.6                        | 240                       | 60.8                   |
| 2                 | 0.9                        | 230                       | 57.3                   |
| 3                 | 0.2                        | 230                       | 63.1                   |
| 4                 | 0.6                        | 180                       | 54.9                   |
| 5                 | 0.6                        | 210                       | 58.8                   |
| 6                 | 1.0                        | 210                       | 54.0                   |
| 7                 | 0.2                        | 190                       | 58.8                   |
| 8                 | 0.1                        | 210                       | 62.6                   |
| 9                 | 0.6                        | 210                       | 58.6                   |
| 10                | 0.6                        | 210                       | 58.7                   |
| 11                | 0.6                        | 210                       | 58.6                   |
| 12                | 0.9                        | 190                       | 53.1                   |
| 13                | 0.6                        | 210                       | 58.5                   |

**Table 4.2: Final multiple regression data for silicon conversion ( $R^2 = 0.99$ )**

| Coefficient symbol | Factor              | Estimated coefficient | Standard error | T-stat  | P-value |
|--------------------|---------------------|-----------------------|----------------|---------|---------|
| $\beta_0$          | Intercept           | 2.111                 | 5.517          | 0.383   | 0.712   |
| $\beta_1$          | $X_1$ (Flow rate)   | -7.328                | 0.617          | -11.863 | <0.0001 |
| $\beta_2$          | $X_2$ (Temperature) | 0.480                 | 0.0524         | 9.146   | <0.0001 |
| $\beta_3$          | $X_1^2$             | -1.788                | 0.542          | -3.295  | <0.0109 |
| $\beta_4$          | $X_2^2$             | -0.0009               | 0.000125       | -7.209  | <0.0001 |

The final surface response models fitted to silicon conversion was:



$$\% \text{ Silicon conversion} = 2.111 - 7.328X_1 + 0.480X_2 - 1.788X_1^2 - 0.0009X_2^2 \quad (23)$$

Where,  $X_1$  = Flow rate and  $X_2$  = Reaction temperature.

The models were validated by testing for outliers and normality of the data using STATISTICA (Appendix C).

Figure 4.9 shows the 3-dimensional response surface plots for silicon conversion as a function of flow rate and temperature. As can be seen from the graph, an increase in temperature resulted in increase in conversion, after which it levelled off and reached a maximum at 240 °C. The same trend was observed for flow rate where a maximum was reached at 0.1 mL/min. The predicted conversion at these optimum conditions was deduced to be about 65%. When the reaction was carried out at these optimised conditions, the observed conversion was about 64%, which is comparable to the predicted value.

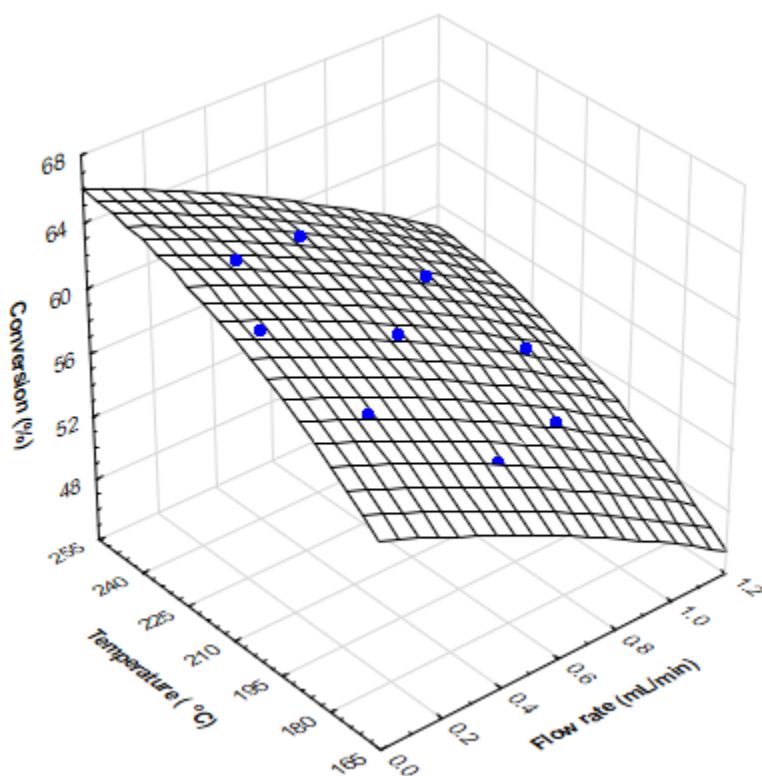


**Figure 4.9: 3-dimensional response surface plot for silicon conversion**

#### 4.2.8 Effect of pressure on silicon conversion and triethoxysilane selectivity

The results obtained earlier above (Figure 4.8) showed excellent selectivity (>97%) to triethoxysilane and silicon conversion of about 25% after 6 h at atmospheric pressure. In order to investigate whether increasing pressure would increase conversion, the pressure was varied from 1-34.4 bars at varied flow rates (0.02-0.8 mL/min) so as to keep ethanol in the liquid state. The constant reaction conditions used were: activation time 2.5 h, reaction period 6 h, catalyst loading 5wt% CuCl and reaction temperature 240 °C. As can be seen from figure 4.9, increase in pressure resulted in increase in conversion for all flow rates investigated. Major improvements in conversion were observed for lower flow rates, for example 25.6% at 1 bar to 38.9% at 34.4 bars for a flow rate of 0.02 mL/min after 6 h.

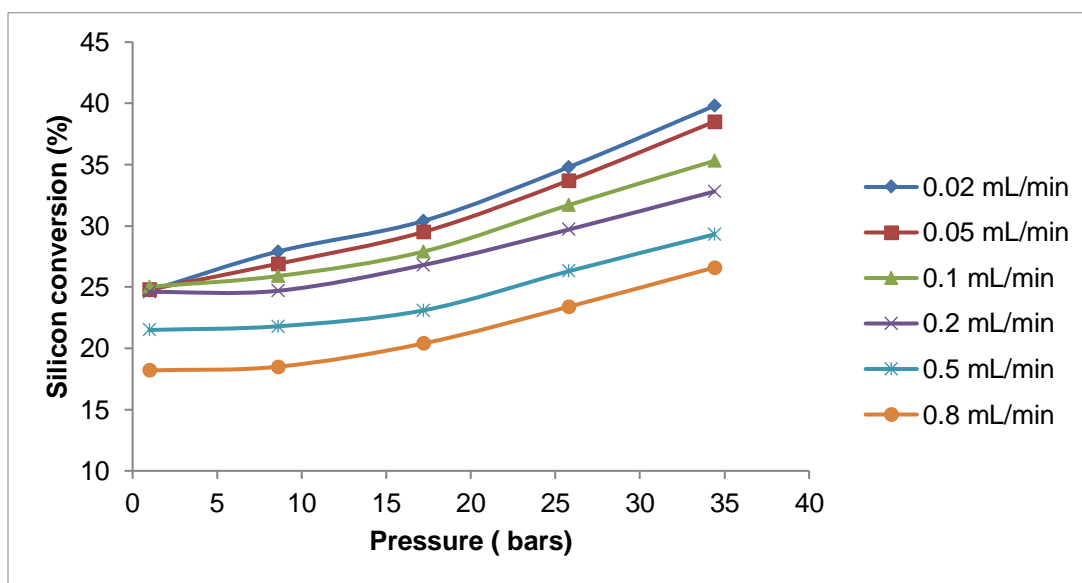


**Figure 4.9: Effect of pressure on silicon conversion at different flow rates**

Although conducting the reaction under pressure did help to increase silicon conversion, the selectivity to the desired triethoxysilane was lost to almost 0% after at about 25 bars at low flow rates (0.05 mL/min) (Figure 4.10) and at about 9 bars at higher flow rates (0.2 mL/min) (Figure 4.11). The desired trialkoxysilane product is converted to tetraalkoxysilane when pressure is raised above atmospheric pressure (Equation 24).

The results indicated that the reaction is best done at atmospheric pressure and it is a cost saving advantage at industrial level.

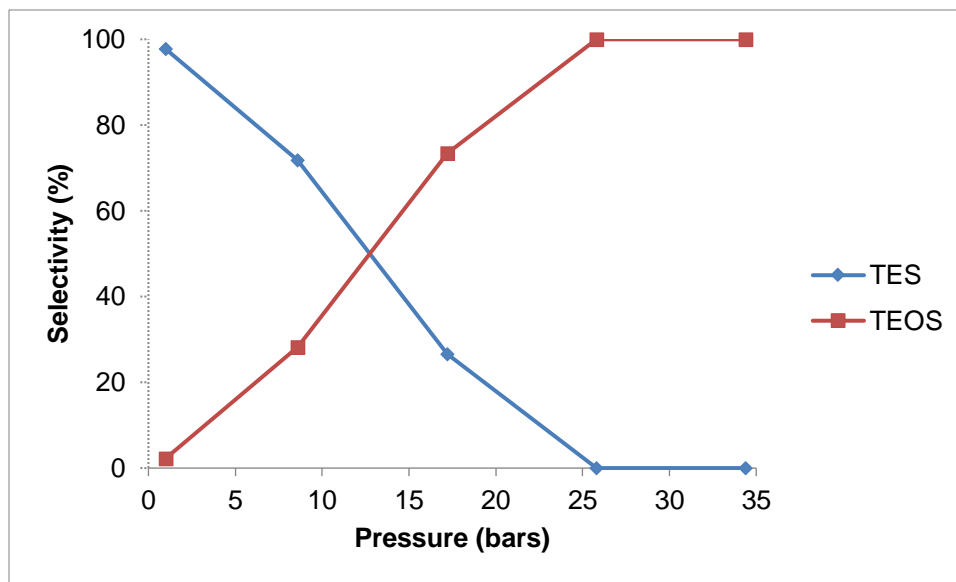
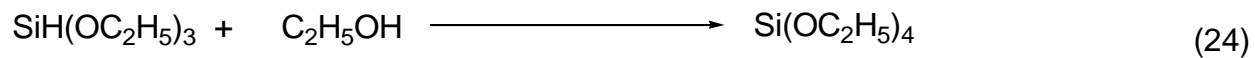


**Figure 4.10: Effect of pressure on triethoxysilane selectivity at 0.05 mL/min flow rate**

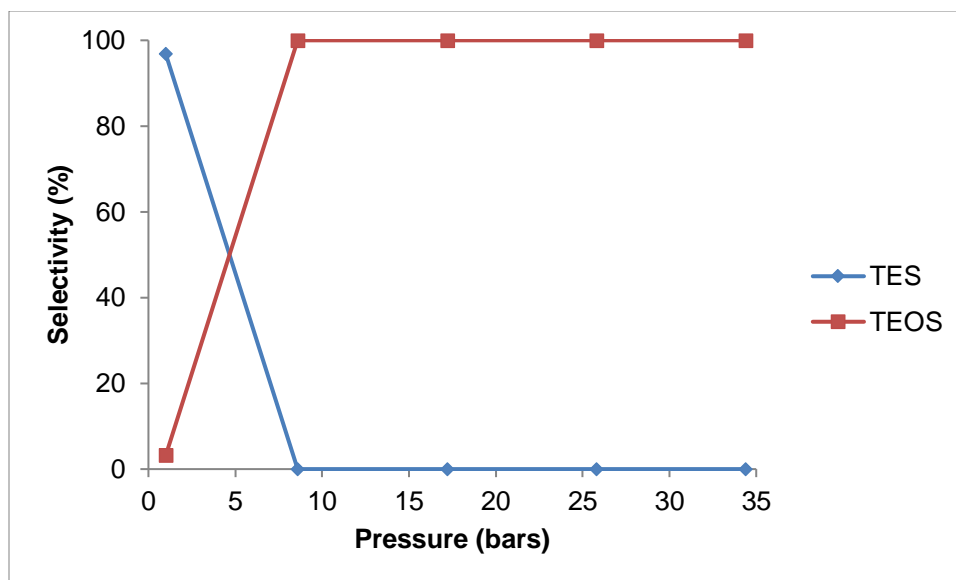


**Figure 4.11: Effect of pressure on triethoxysilane selectivity at 0.1 mL/min flow rate**

#### 4.2.9 Effect of R-group on silicon conversion and triethoxysilane selectivity

The effect of the R-group of the primary alcohol on silicon conversion and trialkoxysilane selectivity was investigated and compared for methanol, ethanol, *n*-propanol, and *n*-butanol. The reaction conditions used were: mass of silicon 5 g, flow rate 0.1 mL/min, activation time 2.5 h, activation temperature 220 °C, reaction period 24 h, catalyst loading 5wt% CuCl and reaction temperature 240 °C.

Silicon conversion was above 60% for both methanol and ethanol, while the conversion results for propanol and butanol were about 54 and 48% respectively (Figure 4.12). The general decrease in selectivity and conversion with increase in R-group is attributed to the decrease in reactivity with increasing carbon chain length. Similar reactivity trends were observed in the batch method although the conversions are lower using this system. The selectivity was about 93% for methanol and 95% for ethanol, while the selectivity results for propanol and butanol were also extremely good at above 90%. In contrast, the batch system generally showed lower selectivity than this method especially with higher order alcohols (C3-C4).

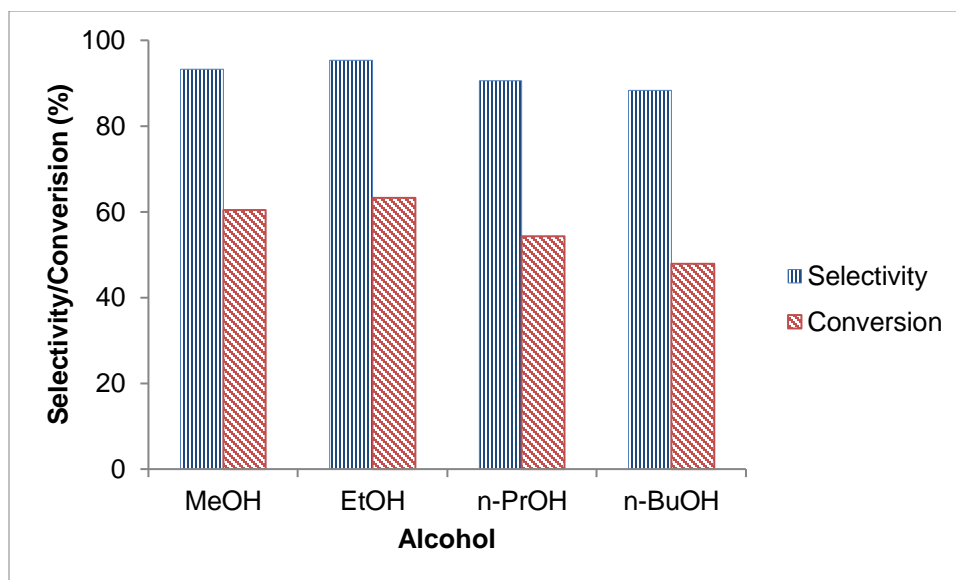


**Figure 4.12: Effect of R-group on silicon conversion and triethoxysilane selectivity**

### 4.3 Conclusion

The synthesis of trialkoxysilanes in a packed bed flow tubular reactor was achieved with higher trialkoxysilane selectivity (about 97% under optimised conditions) than previously realised in batch mode. Silicon conversion was fairly good at about 64% when ethanol was used as an alkoxylation alcohol. Although the conversion was lower than in the batch mode, the continuous operation of the tubular reactor ensures high throughput in industrial application. Copper (I) chloride catalyst was found to be the best catalyst for this reaction and it showed stability over 24 h. Copper (II) hydroxide may be used as an alternative environmentally benign non-halide containing catalyst for shorter production cycles although it's not as effective as copper (I) chloride. It was deduced that catalyst loading of 2.5 to 5wt%, activation temperature of 220 °C, activation time of 2.5 to 5 h was sufficient for the reaction unlike the batch system which required harsher conditions. Low activation temperatures and shorter activation times are an advantage for commercial application of the method in terms of costs. Silicon conversion and triethoxysilane selectivity increased with an increased in alcohol residence time or a decrease in flow

rate. The optimum temperature range and flow rate for the reaction were 220 °C to 240 °C and 0.1mL/min respectively. Performing the reaction under pressure resulted in improvement in conversion, but it drastically reduced selectivity to the desired compound. Ethanol gave the highest conversion and selectivity which generally decreased with an increase in alkyl group carbon chain.

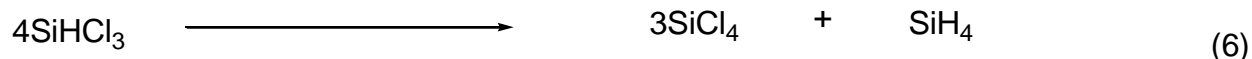
The packed bed flow tubular reactor exhibited better mass transfer between silicon and alcohol as indicated by higher conversion and selectivity than the previously used falling film tubular reactor. The method does not use heat transfer solvents unlike the batch and the falling film tubular reactor systems and as such there are no complications in purification. The method does not involve the usually practised concentrated hydrofluoric acid washing step for silicon before the reaction.<sup>155-156</sup> The acid washing step is corrosive and a danger to the environment and humans if included on large scale manufacturing process. The packed bed flow tubular reactor in the present study can easily be scale up and operated continuously for large scale industrial production.

## CHAPTER 5

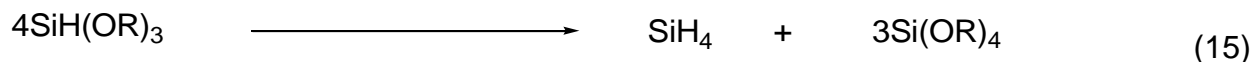
### Synthesis of monosilane

#### 5.1 Introduction

Monosilane is widely used as a highly pure silicon material for the production of amorphous and microcrystalline high purity silicon. This highly pure silicon is used for the production of solar cells, semiconductors, photosensitive materials and ceramic materials.<sup>157-159</sup> The conventional methods for the large scale synthesis of monosilane include the reduction of tetrachlorosilane and the disproportionation of trichlorosilane (Equation 6)<sup>160-162</sup> These methods have drawbacks in that the chlorosilane compounds employed as starting materials are corrosive and thus making the process costly since corrosion resistance reactors have to be used.<sup>163-164</sup> Another disadvantage is that the process is also carried out under pressure and the yield of monosilane is low.<sup>165</sup>

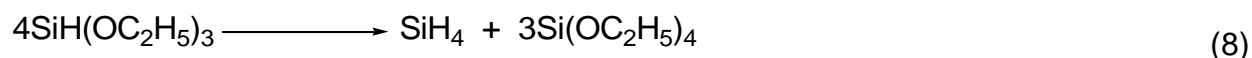


In this chapter, monosilane was synthesized by the disproportionation of trialkoxysilane (Equation 15) which was synthesized in Chapter 4 using the continuous flow packed bed reactor. The reaction was carried out at room temperature to mild heating and at atmospheric pressure and thus promises to be more cost effective than previous methods mentioned literature. The effect of reaction temperature, catalyst type and solvent used in the reaction was investigated.

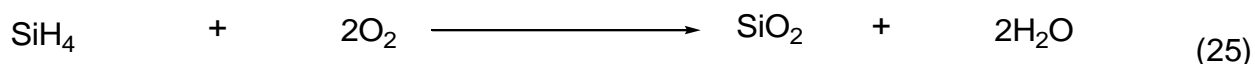


## 5.2 Synthesis of monosilane by disproportionation of triethoxysilane

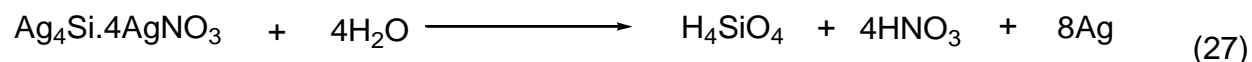
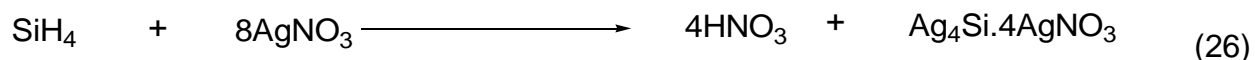
Synthesis of monosilane under homogeneous and heterogeneous catalysis was carried out according to the typical procedures outlined in 2.4.4.1 and 2.4.4.2. Triethoxysilane was used as a starting material to yield monosilane and the by-product tetraethoxysilane (Equation 8). The reaction was monitored by quantifying the conversion of triethoxysilane over time using GC. The by-product (tetraethoxysilane) was also quantified by GC and the result used to estimate the amount of monosilane formed.



The monosilane gas was characterised by the flame test<sup>166</sup> and also the silver nitrate solution test<sup>167</sup> as there was no immediately available appropriate gas sampling and GC instrumental method to characterise it. The gas formed spontaneously burnt upon contact with air with a characteristic bright yellow light confirming that monosilane was formed (Equation 25).

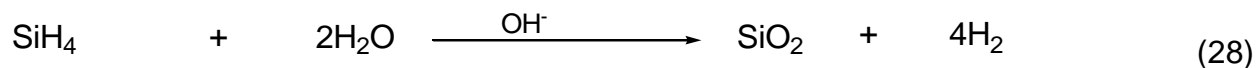


Monosilane reacted with a neutral solution of 0.3 M silver nitrate to form a yellowish-brown precipitate (Equation 26) which soon turned black (Equation 27), further confirming its presence.



The monosilane formed throughout the experiments was quenched by hydrolysing it to silicon dioxide and hydrogen by bubbling through a stirred solution of 0.6 M potassium hydroxide solution (Equation 28)<sup>168</sup> to avoid hazards of explosions if exposed to air.

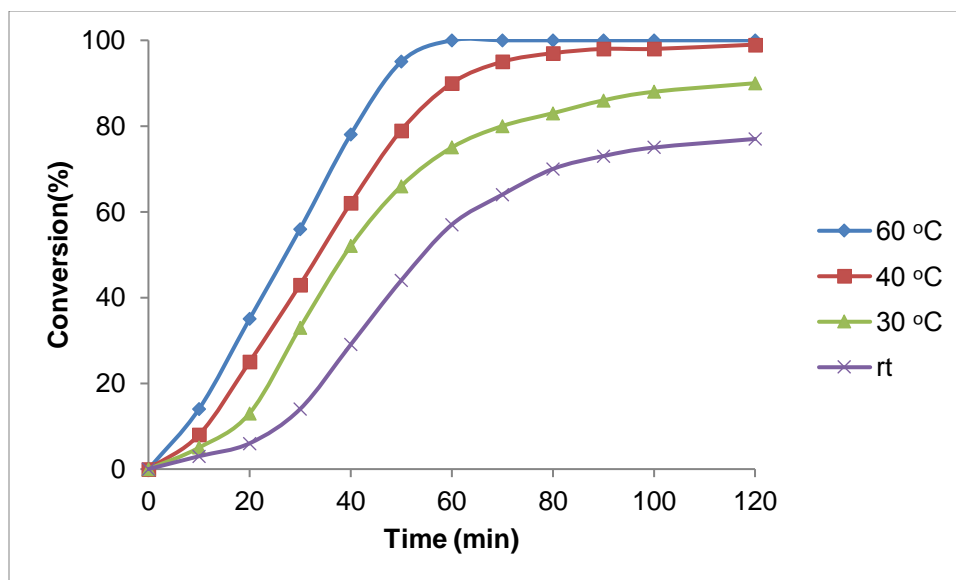




### 5.2.1 Homogeneous synthesis of monosilane

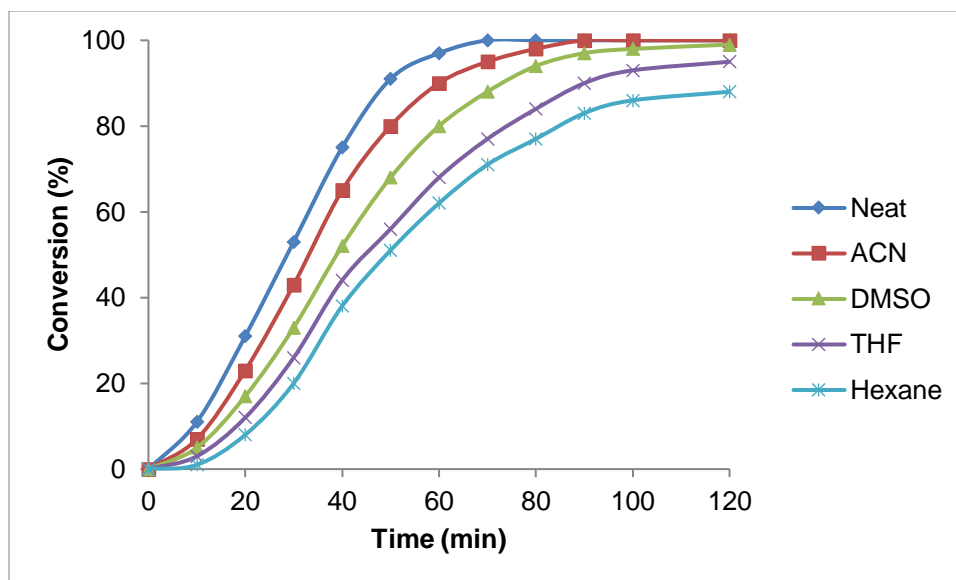
The synthesis of monosilane under homogeneous catalysis has been attempted in literature with the reaction carried out mostly in autoclaves under pressure, in the presence of alkali metal ethoxides<sup>128-130</sup> The starting material was mainly trimethoxysilane and limited work is reported on the more stable triethoxysilane which is discussed in this section.

The effect of temperature on the disproportionation of triethoxysilane (10.836 mmol) was investigated in the presence of sodium ethoxide (0.02 eq) as a catalyst at various temperatures (room temperature to 60 °C) using acetonitrile (10 mL) as a solvent. The results in Figure 5.1 indicate that conversion increased with an increase in temperature. At 60 °C, 100% conversion was achieved after 1 h whilst at room temperature the reaction was slower resulting in a maximum conversion of 77% after 2 h. The results reveal that the temperature employed may range from room temperature to moderate heating, thus saving on energy costs. The reaction could not be carried out above 60 °C, as raising the temperature may reduce the yield of monosilane due to formation of hydrogen as indicated in literature.<sup>169</sup>



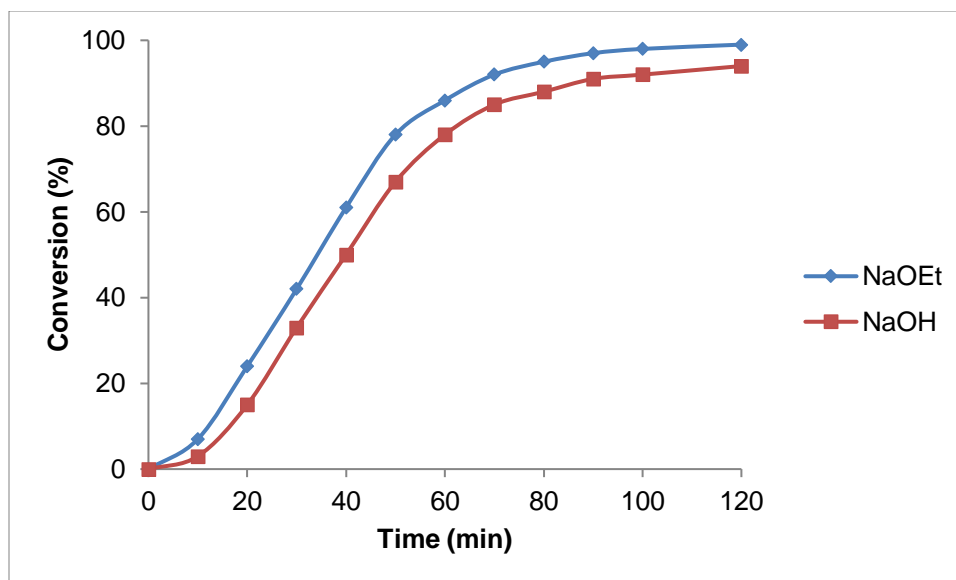
**Figure 5.1: Temperature dependence for the homogeneous reaction**

The effect of solvent type of the reaction was studied at 40 °C using sodium ethoxide (0.02 eq) as a catalyst in 10 mL mixtures with various solvents. The results obtained show that the reaction is more efficient in polar aprotic solvents (dimethylsulfoxide and acetonitrile) (Figure 5.2). The use of aprotic polar solvents increases the solubility of the catalyst and its catalytic activity, thus contributing to the efficiency of the reaction. The use of sulfur-containing aprotic polar solvents like dimethylsulfoxide was found to prevent oligomerization of the tetraalkoxysilane by-product by other workers in literature.<sup>130</sup> The reaction was also conducted without using a solvent at similar reaction conditions. The reaction proceeded faster under neat conditions (97% conversion after 1 h) as compared to cases where the best solvent acetonitrile was used (90% conversion after 1 h). The neat conditions offer advantages of reducing costs and green synthesis.



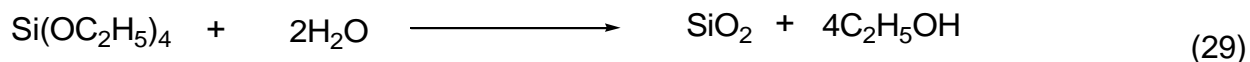
**Figure 5.2: Effect of solvent type on the reaction**

The disproportionation reaction under homogeneous conditions was also tested using sodium hydroxide (0.02 eq) as a catalyst at similar reaction conditions used for sodium ethoxide to compare catalytic activity. As can be seen from the results (Figure 5.3), sodium ethoxide gave slightly higher conversion (99%) than sodium hydroxide (94%) after 2 h indicating that either of them can be used. The advantage of these catalysts is that they are cheap, effective and recoverable in contrast to organic catalysts reported in literature.<sup>131</sup>



**Figure 5.3: Effect of homogeneous catalyst type on the reaction**

A plot of relative amount of reaction components as a function of time for the reaction carried out using sodium ethoxide (0.02 eq) as catalyst at 40 °C in acetonitrile revealed that the products, monosilane and tetraethoxysilane formed in the ratio 1:3 in accordance to the stoichiometric equation. The tetraethoxysilane by-product is useful at industrial level as it can be easily hydrolysed to ethanol and high purity silicon dioxide (Equation 29).<sup>170-171</sup>



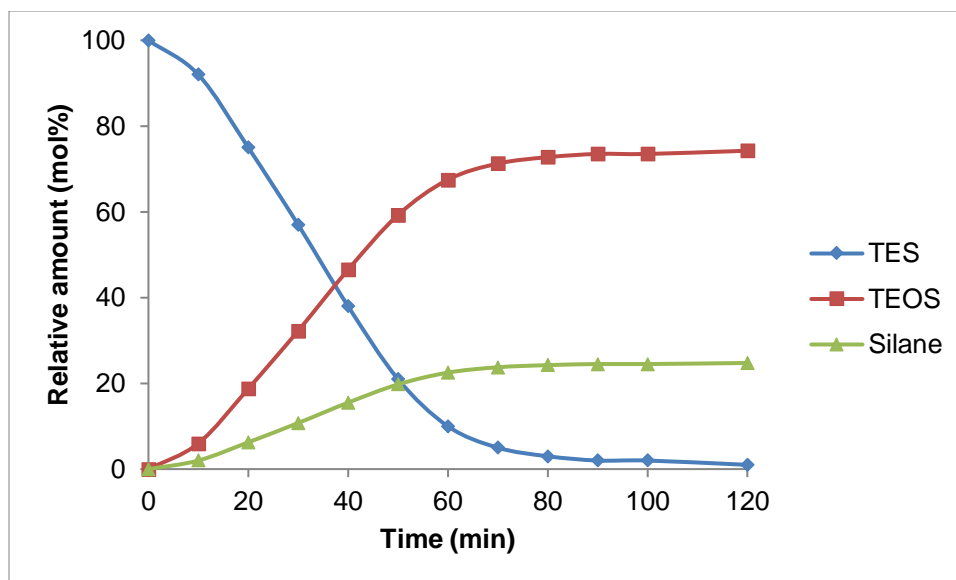


**Figure 5.4: Relative amounts of homogeneous reaction components with time**

### 5.2.2 Heterogeneous synthesis of monosilane

The disproportionation of trialkoxysilanes in the presence of heterogeneous catalyst has been reported with mainly metal oxides as the preferred catalysts at temperatures greater than 120 °C.<sup>132-136</sup> The use of anion exchange resins has also been attempted on trimethoxysilane at moderate temperatures but limited work is reported on triethoxysilane which the preferred precursor to high purity silicon.

The effect of temperature on the triethoxysilane (10.836 mmol) disproportionation reaction under this method was carried out at atmospheric pressure using dry Amberlite® IRA-78 (0.25 g) as a quaternary ammonium anion exchange catalyst in 10 mL acetonitrile. The reaction was much slower as compared to the homogeneous catalysed one above as complete conversion was achieved after 3 h at 55 °C (Figure 5.5). The temperature could not be increased further as the maximum temperature at which the anion exchange resins are active is limited to 60 °C. The conversion at room temperature was 63% after 3 h as compared to 77% after 2 h under homogeneous catalysis.

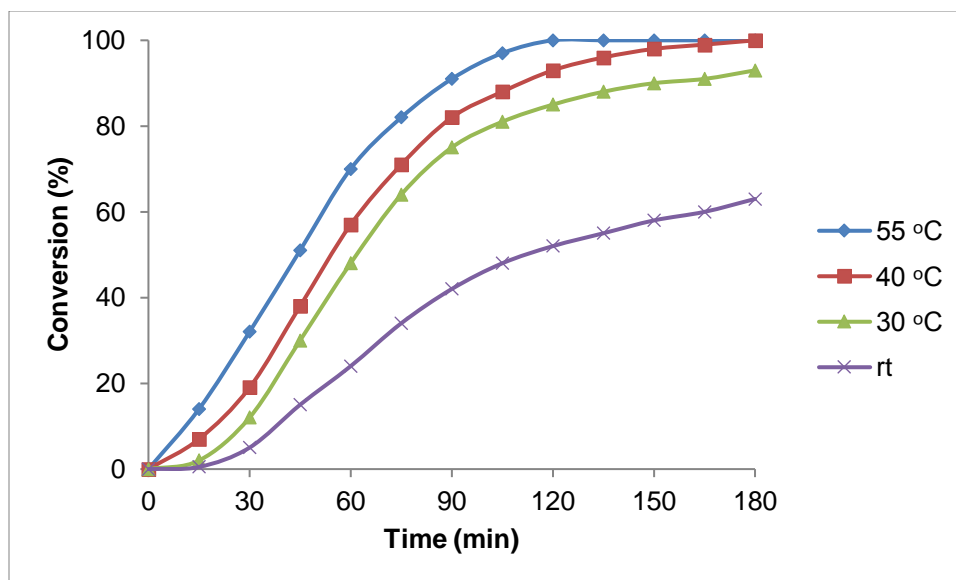


**Figure 5.5: Temperature dependence for the heterogeneous reaction**

The effect of various solvents (10 mL) on the reaction under this protocol was studied at 40 °C using Amberlite® IRA-78 (0.25 g) as a catalyst. Similar reaction profiles to the homogeneous catalysed reaction were observed although the reaction was slower (Figure 5.6). The neat reaction was comparable to a reaction where the best solvent was used. This means that the reaction can be efficiently done without using solvents and thus making the process environmentally friendly and cheap.

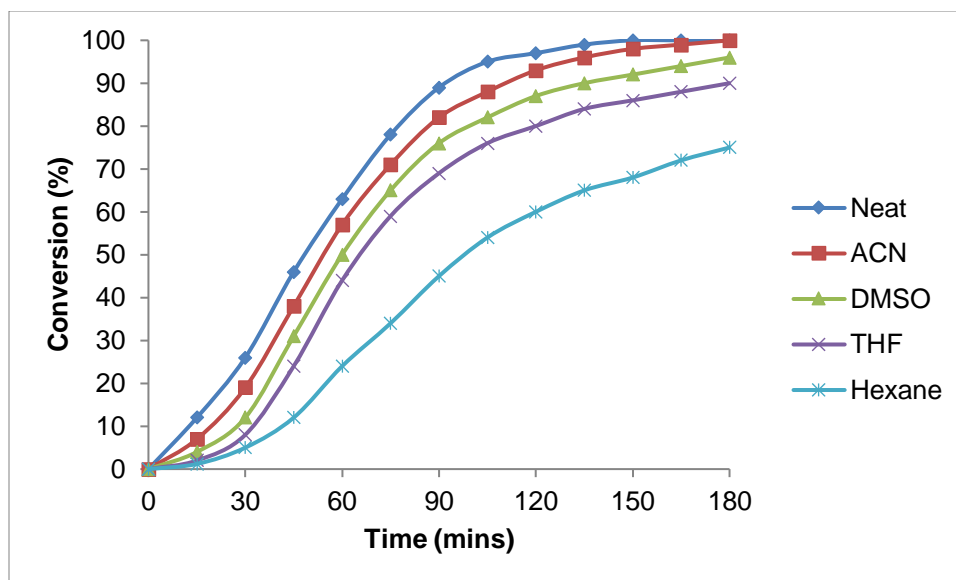


**Figure 5.6: Effect of solvent type on the homogeneous reaction**

Three anion exchange resins and potassium fluoride supported on  $\gamma$ -aluminium oxide were tested for catalytic activity under heterogeneous method at similar reaction conditions. The specific conditions for the reaction were; 2.5 g of catalyst and temperature of 40 °C in 10 mL acetonitrile. The most reactive catalyst was Amberlite® IRN-78 (about 100% after 3 h) with potassium fluoride supported on aluminium oxide as the least (about 66% after 3 h) (Figure 5.7). The slower activity of potassium fluoride supported on aluminium oxide can be attributed to the lower temperature used as literature suggests temperatures higher than 60 °C.<sup>133,135</sup> The weakly basic resin with primary tertiary amine groups (Amberlite® IRA-93) was less effective than the strongly basic resins (Amberlite® IRN-78 and Amberlite® IRA-904). The advantage of the use of resins was that the by-product, tetraethoxysilane could be easily separated from the solid catalyst by simple filtration. It can be noted that the anion exchange resins used in this study have not been previously reported in literature for any disproportionation reactions to the best of our knowledge.

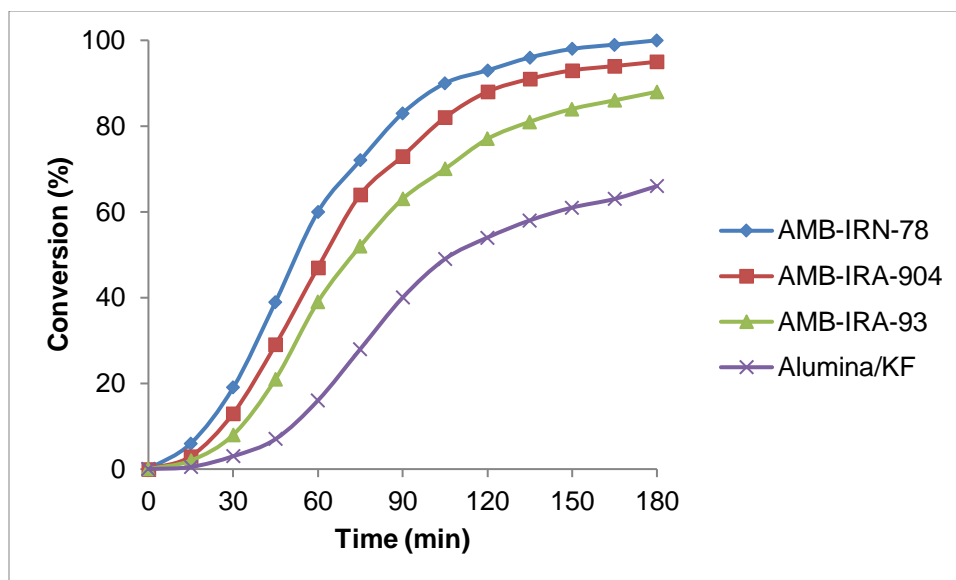


**Figure 5.7: Effect of heterogeneous catalyst type on the reaction**

A plot of relative amount of product with time for the results obtained using AMB-IRN-78 (2.5 g) at 40 °C in 10 mL acetonitrile is shown in Figure 5.8. The reaction produced the target product monosilane (about 25mol% after 3 h) and tetraalkoxysilane (about 75mol% after 3 h) in the reaction of about 1:3 as depicted in the graph. This confirms the absence of side reactions in the process.



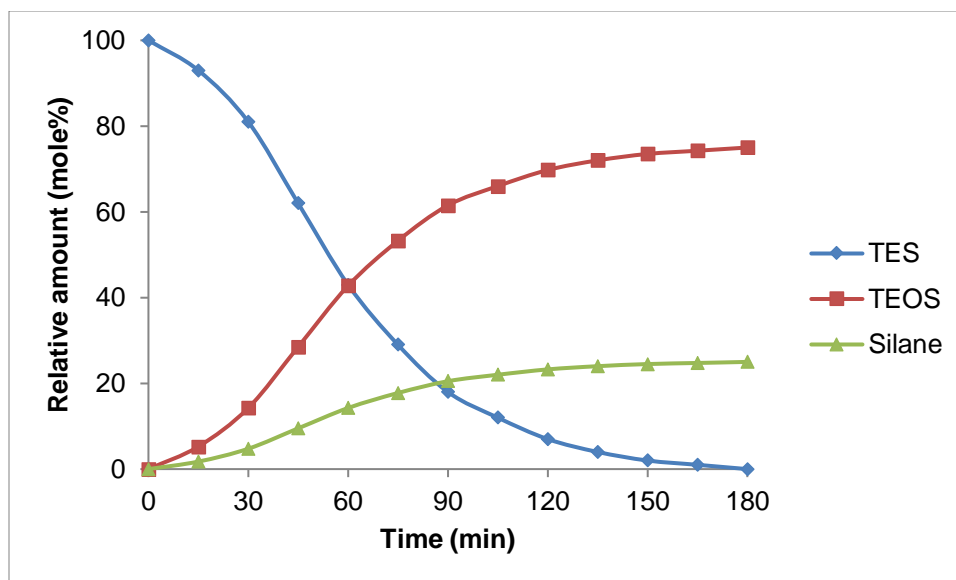


**Figure 5.8: Relative amounts of heterogeneous reaction components with time**

A comparison of triethoxysilane conversion under both heterogeneous (0.25 g of catalyst) and homogeneous catalysis (0.02 eq of catalyst) conditions after 2 h at 40 °C in acetonitrile is shown in Figure 5.9. As can be seen from the graph, heterogeneous catalysts, Amberlite® IRN-78 and Amberlite® IRA-904 showed fairly comparable results (>88%) to homogeneous catalysts (>94%)(Figure 5.9). This observation means that heterogeneous catalyst can be employed for continuous flow production of monosilane.

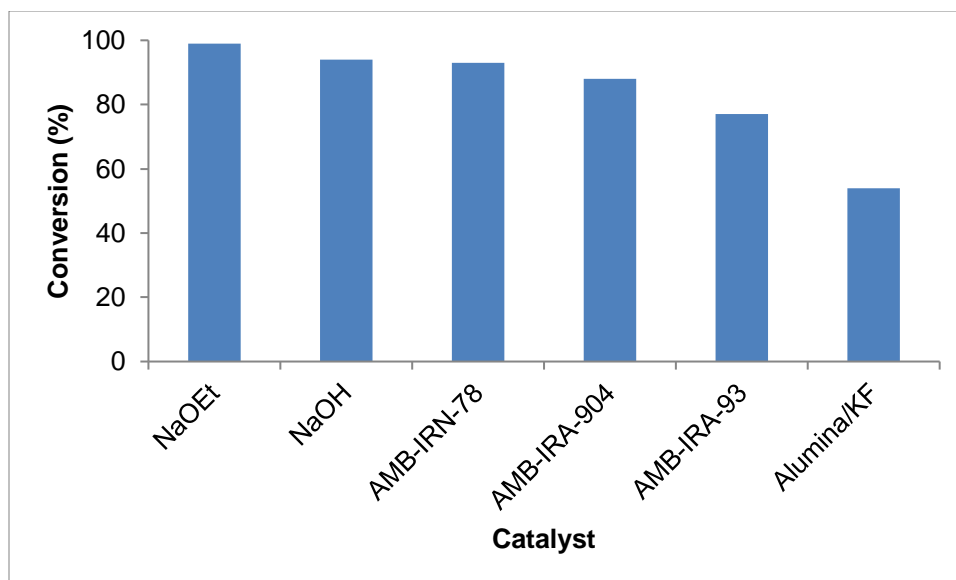


**Figure 5.9: Conversion of triethoxysilane using different catalysts after 2 h**

Figure 5.10 shows comparative yield of monosilane under both homogeneous and heterogeneous catalysis after 2 h at 40 °C from the above experiment. The use of anion exchange resins resulted in yield of greater than 19%, which is fairly comparable to homogeneous catalysts (>23%). It can be noted that the obtained monosilane yield was close to the theoretical one of 25% thus indicating the efficiency of the catalysts used. The use of potassium fluoride supported on  $\gamma$ -aluminium oxide resulted in monosilane yield of about 11.4% and this can be attributed to the same reason as provided previously for low conversion.

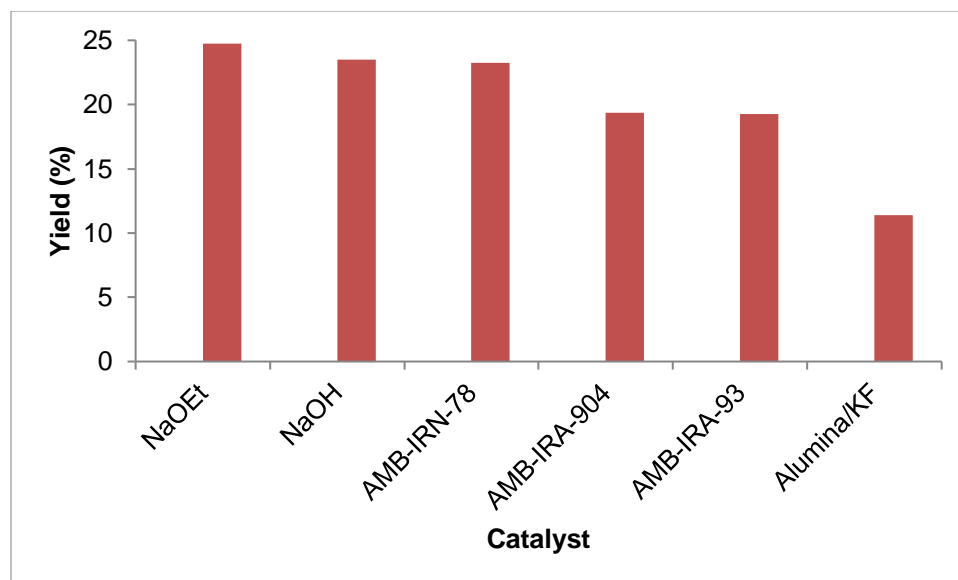


**Figure 5.10: Yield of monosilane using different catalysts after 2 h**

### 5.3 Kinetics studies on the disproportionation reaction

Triethoxysilane undergoes disproportionation upon contact with a base catalyst (Equation 8). In line with the mechanism proposed by previous authors,<sup>131,134,135</sup> we postulate the disproportionation of triethoxysilane to proceed *via* the pentacoordinate silicon intermediates accompanied by the repeated replacement of the ethoxide ion with the hydride ion. Reactions in which the silicon atom is pentacoordinated in intermediate complexes of reaction pathways have since been encountered in many investigations.<sup>172-175</sup> In the present reaction, the pentacoordinate silicon species is formed by the coordination of silicon of a  $(C_2H_5O)_3SiH$  molecule with the basic sites of the anion exchange resin catalyst. This results in the release of a nucleophile,  $C_2H_5O^-$ . The  $C_2H_5O^-$  ion thus formed attacks the silicon atom of another  $(C_2H_5O)_3SiH$  molecule coordinated on the catalyst. This results in the replacement of  $H^-$  with  $C_2H_5O^-$  and  $(C_2H_5O)_4Si$  and  $H^-$  ion are formed. This  $H^-$  ion then attacks the silicon to form a new Si-H bond and a  $C_2H_5O^-$  ion. Repeated replacement  $C_2H_5O^-$  with  $H^-$  results in the formation of monosilane. The reaction occurs gradually at room temperature and rapidly upon mild heating as shown in the above results.

The data obtained on the conversion of triethoxysilane (10.836 mmol) over 2 h at 40 °C using Amberlite® IRN-78 (0.25 g) as a catalyst in acetonitrile is shown in Table 5.1 was used to deduce the kinetic model which best describes the reaction.

**Table 5.1: Triethoxysilane conversion data**

| Time (min) | Triethoxysilane (%) | 1/[A]   | ln [A]  |
|------------|---------------------|---------|---------|
| 0          | 100                 | 0.0100  | 4.6051  |
| 15         | 93                  | 0.0108  | 4.5326  |
| 30         | 81                  | 0.01235 | 4.3944  |
| 45         | 62                  | 0.01613 | 4.1271  |
| 60         | 43                  | 0.02326 | 3.7612  |
| 75         | 29                  | 0.03448 | 3.3673  |
| 90         | 18                  | 0.05556 | 2.8904  |
| 105        | 12                  | 0.08333 | 2.4849  |
| 120        | 7                   | 0.1429  | 1.94591 |

The linearized integrated rate law with time dependence of concentration of triethoxysilane for a first order process after taking natural logarithm is written as;

$$\ln[A] = \ln[A_0] - kt \quad (30)$$

Where; A is triethoxysilane.

A plot of  $\ln[A]$  versus time ( $t$ ) gives a straight line with slope  $-k$  and intercept  $\ln[A]_0$ .

The integrated rate law with time dependence of concentration for the second order kinetic model is as shown in Equation 31 below.

$$\frac{1}{[A]} = kt + \frac{1}{[A_0]} \quad (31)$$

A plot of  $1/[A]$  versus  $t$  is a straight line with slope  $k$  and intercept  $1/[A]_0$ .

The above rate laws together with zero-order kinetic model were fit on the data in Table 5.1 and results are shown in Figures 5.11-5.13. It can be seen from comparison of the correlation coefficients ( $R^2$ ) obtained for the three plots that the first order kinetic model ( $R^2=0.9746$ ) best fits the data for the disproportionation of triethoxysilane. The rate constant,  $k$ , for the first order kinetic model was deduced from the gradient of the graph (Figure 5.12) as  $0.0226 \text{ min}^{-1}$  which translates to  $3.77 \times 10^{-4} \text{ s}^{-1}$ .

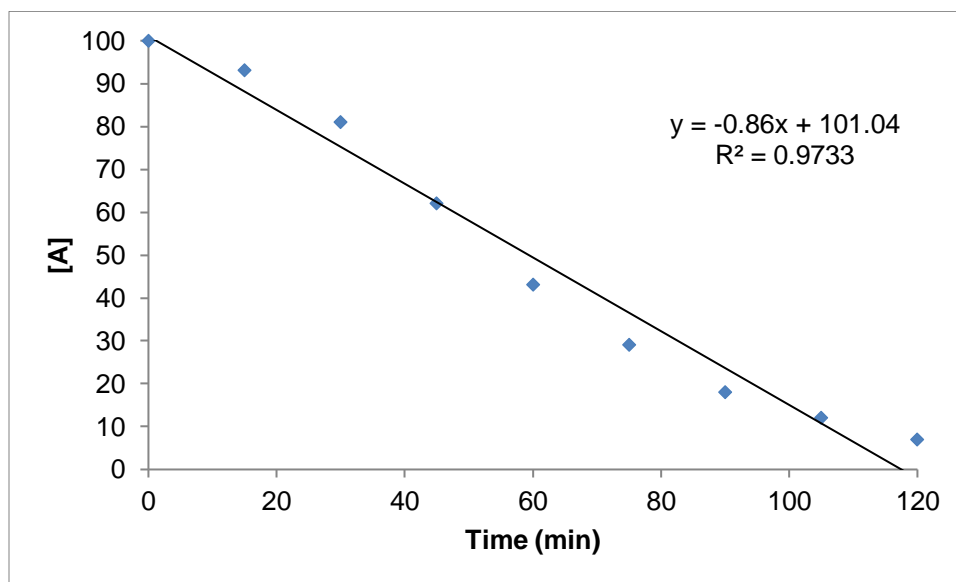


**Figure 5.11: Zero-order kinetics plot**

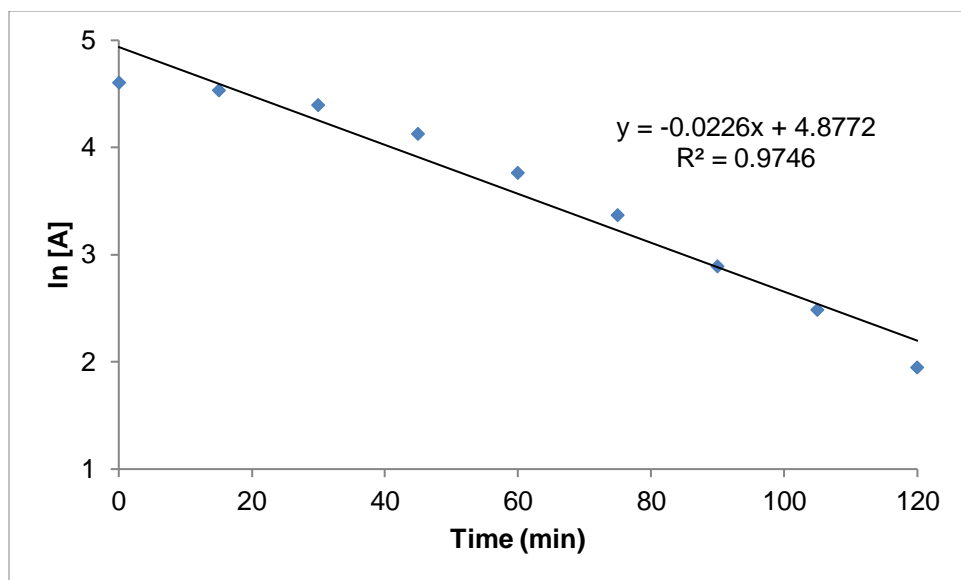


**Figure 5.12: First order kinetics plot**

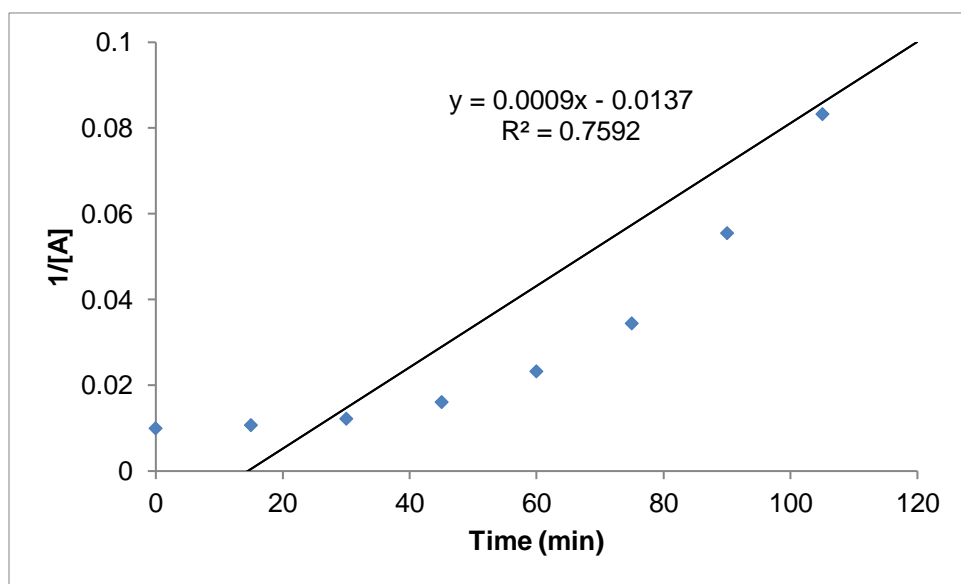


**Figure 5.13: Second order kinetics plot**

The first order kinetics model was also fit to the data obtained from the conversion of triethoxysilane at 30 and 55 °C at a constant reaction time of 120 min using Amberlite® IRN-78 (0.25 g) as acatalyst to estimate the respective rate constants. The deduced rate

constants (Table 5.2) were used to determine the activation energy using the Arrhenius equation.

The half-life ( $t_{1/2}$ ) for the first order kinetic model for triethoxysilane disproportionation was calculated for each of the three different temperatures (Table 5.2) using the following formula;

$$t_{1/2} = \frac{\ln 2}{k} \quad (32)$$

The half-life was found to decrease with an increase in temperature. It decreased by about a factor of two as temperature was increased from 30 to 55 °C.

**Table 5.2: Variation of the rate constant and half-life with temperature**

| Entry | Temperature (K) | 1/T (K <sup>-1</sup> ) | k (min <sup>-1</sup> ) | k (s <sup>-1</sup> )  | ln k    | t <sub>1/2</sub> (s) |
|-------|-----------------|------------------------|------------------------|-----------------------|---------|----------------------|
| 1     | 303.15          | 3.30 x10 <sup>-3</sup> | 0.0174                 | 2.90x10 <sup>-4</sup> | -8.1456 | 2390                 |
| 2     | 313.15          | 3.19x10 <sup>-3</sup>  | 0.0226                 | 3.77x10 <sup>-4</sup> | -7.8833 | 1838                 |
| 3     | 328.15          | 3.05x10 <sup>-3</sup>  | 0.0324                 | 5.40x10 <sup>-4</sup> | -7.5239 | 1284                 |

The linearized Arrhenius equation after taking natural logarithm to both sides is given by;

$$\ln k = \frac{-Ea}{RT} + \ln A \quad (33)$$

Where;  $k$  is the rate constant (s<sup>-1</sup>),  $Ea$  is the activation energy (Jmol<sup>-1</sup>),  $R$  is the ideal-gas constant (8.314 J/Kmol),  $T$  is the temperature (K) and  $A$  is the pre-exponential factor (s<sup>-1</sup>).

A plot of  $\ln k$  versus  $1/T$  for the data in Table 5.2 gave a straight line (Figure 5.14) in accordance to the Arrhenius equation. The activation energy  $Ea$  was deduced to be 20.56 KJmol<sup>-1</sup> from the slope of  $-Ea/R$ .

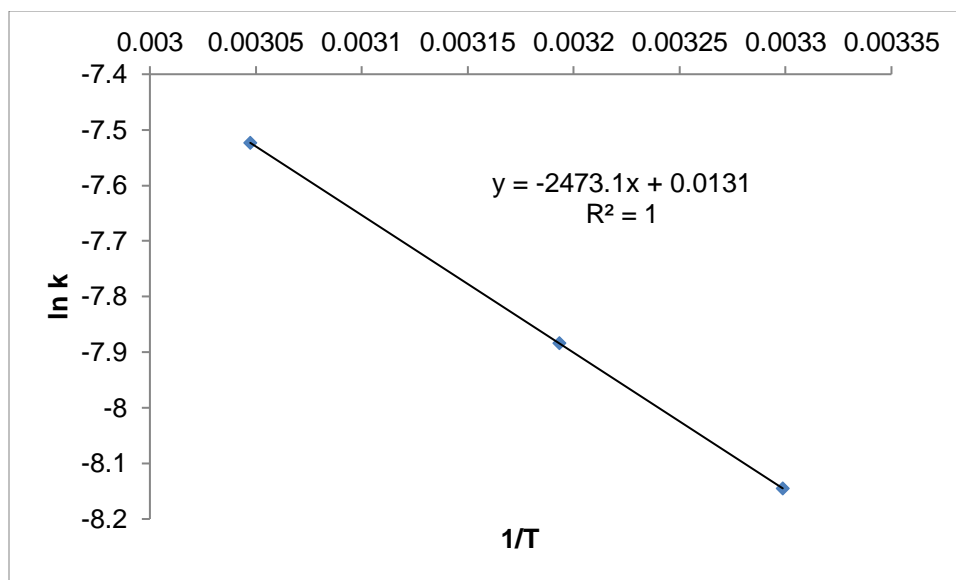


**Figure 5.14: Arrhenius plot of of  $\ln k$  versus  $1/T$**

#### **5.4 Conclusion**

The synthesis of monosilane from the disproportionation of triethoxysilane was successfully carried out under both homogeneous and heterogeneous catalysis. The reaction was best carried out under mild heating conditions (40 to 60 °C) although the fair conversion and yield was obtained at room temperature. The reaction proved more effective under clean conditions as compared to when solvents were used and thus making the process eco-friendly and cost effective. The use of anion exchange resins as catalysts under neat conditions proved to be comparable to the conventional homogeneous method over long reaction times. The resins used have not been previously reported in literature for this reaction to the best of our knowledge. The advantage of this system is that the resins can be easily regenerated for reuse. The kinetic studies on the reaction revealed that the disproportionation of triethoxysilane is best described by the first order kinetic model.

The results obtained show that that anion exchange resins can be easily adapted for solvent free continuous flow synthesis of monosilane in a packed bed flow tubular reactor



at mild heating conditions. This system makes it easier for integrating the alkoxysilane synthesis and its disproportionation to monosilane in a continuous production process.

## CHAPTER 6

### Conclusion and recommendations

#### Conclusion

The work described in this thesis involved the synthesis of organosilicon compounds (trialkoxysilanes and monosilane) which are precursors to the synthesis of solar-grade silicon for application in the photovoltaic industry. The synthesis of trialkoxysilanes was accomplished by the direct reaction of metallic silicon with alcohol in the presence of copper containing compounds as catalysts. Monosilane was synthesized by the subsequent disproportionation of trialkoxysilanes in the presence of various catalysts.

The synthesis of trialkoxysilanes was conducted in a glass batch slurry phase reactor, packed bed flow tubular reactor and also attempted in a slurry phase continuous flow falling film tubular reactor. Key parameters that influence silicon conversion and trialkoxysilane selectivity namely, silicon-catalyst activation temperature and time, catalyst type and loading, alcohol flow rate or residence time and reaction temperature were studied in all types of reactors.

The study was initiated by conducting benchmark studies using the traditional slurry phase batch reactor. Analysis of the silicon-catalyst mixtures after pre-heating was done by SEM-EDS, XRD and XRF and the results confirmed the existence of a  $\text{Cu}_3\text{Si}$  phase which is thought to act as an intermediate for the catalysis of the reaction. Copper (I) chloride and copper (II) hydroxide were the most efficient catalysts at loading (5-10wt%), activation time (5-10 h) and pre-heating temperature of 220-350 °C. Copper (II) hydroxide stability was only limited to shorter reaction cycles (<10 h). The uncatalysed reaction resulted in negligible reaction rates. The selectivity for triethoxysilane and rate of reaction was lower when no pre-heating was done. The effect of flow rate and temperature on the alkoxylation reaction was also investigated using a central composite design and the optimum conditions were found to be flow rate of 0.1mL/min and temperature of 230 °C respectively. The effect of alcohol R-group (C1 to C4) on the reaction revealed that silicon

conversion and selectivity for trialkoxysilane decrease with an increase in carbon chain length. Ethanol showed highest selectivity (>95%) and conversion (about 88%) as compared to all other alcohols studied showing that it could be the most efficient alkoxylation alcohol for this reaction.

After successfully synthesizing alkoxy silanes in batch reactor, the optimised reaction conditions were applied to synthesis the continuous flow falling film tubular reactor. The reaction showed very poor silicon conversion and selectivity to trialkoxysilane. This observation was attributed to poor mass transfer in the reactor.

Focus was then shifted to the synthesis of trialkoxysilanes in a packed bed flow tubular reactor so as to try and improve the reaction in flow mode. The reaction resulted in higher trialkoxysilane selectivity (>97%) than previously got under batch synthesis and the falling film tubular reactor. Silicon conversion was fairly good (64%) when ethanol was used although it was lower than in the batch mode. As similarly observed in the batch synthesis, copper (I) chloride, a soft Lewis acid, was found to be the best catalyst for this reaction and copper (II) hydroxide may be also used over short reaction cycles. When pre-heating temperature was low (220 °C), the rate of reaction was higher compared to other temperatures used. High temperature pre-heating (>500 °C) resulted in the rate of reaction decreasing by almost 50%. It was observed that catalyst loading of 2.5 to 5wt%, activation temperature of 220 °C, activation time of 2.5 to 5 h was adequate for the reaction unlike the batch system which required harsher conditions.

Silicon conversion increased with an increase in reaction temperature up to 240 °C after which it gradually fell. Silicon conversion and triethoxysilane selectivity increased with an increased in alcohol residence time or a decrease in flow rate up to 0.1 mL/min after which it fell slightly at very low flow rates <0.05 mL/min. The optimum temperature and flow rate for the reaction were 240 °C and 0.1 mL/min respectively. In an attempt to improve the conversion of the reaction, the reaction was conducted under pressure at varied flow rates. This resulted in the improvement of conversion but the selectivity to the desired triethoxysilane was significantly lost. When the effect of R-group (C1 to C4) on the

reaction was studied under this method, ethanol gave the highest conversion and selectivity just as in the batch mode. All alcohols showed higher selectivity (>88%) than in the batch mode. Selectivity and conversion generally decreased with an increase in alkyl group carbon chain.

Synthesis of monosilane from triethoxysilane was successfully conducted in batch mode using various homogeneous and heterogeneous catalysts. The reaction was monitored by quantifying the conversion of triethoxysilane over time. The by-product (tetraethoxysilane) was also quantified and the result was used to estimate the amount of monosilane formed. Monosilane was characterized by flame test and silver nitrate solution test. The results obtained from homogeneous catalysis showed that the reaction can be conducted at room temperature (conversion >70%) although mild heating at 30-40 °C improved the conversion to 99%. The heterogeneous catalysis mode was characterised by slow conversion at room temperature but mild heating from 30 to 55 °C greatly improved the reaction. The yield of monosilane was high (19-24% at optimum conditions) under both methods in comparison to the theoretical one of 25%. Sodium hydroxide and sodium ethoxide catalysts were evaluated under the homogeneous protocol and both catalysts were able to disproportionate triethoxysilane to monosilane and although sodium ethoxide was slightly more efficient.

The effect of solvent type on the reaction showed that the order of increasing efficiency was; acetonitrile>dimethylsulfoxide>tetrahydrofuran>hexane in both heterogeneous and homogeneous conditions. Conducting the reaction under neat conditions (without using solvents) was more efficient than when solvents were used in both methods. This makes the reaction more environmentally friendly and cheaper. The influence of heterogeneous catalysts type on the reaction showed the order of increasing efficiency as; Amberlite® IRN-78>Amberlite® IRA-904>Amberlite® IRA-93>potassium fluoride supported on  $\gamma$ -aluminium oxide. The use of reusable heterogeneous catalyst offers the advantage of continuous flow production which can be carried out in a packed bed tubular flow reactor. The disproportionation reaction was best described by the first order kinetic model and the activation energy was estimated to be 20.56 KJmol<sup>-1</sup>.

The packed bed flow tubular reactor displayed superior mass transfer than the falling film tubular reactor. The method does not use heat transfer solvents unlike the batch and the falling film tubular reactor systems and thus purification of products and recovery of alcohol reagent is easy. The packed bed flow tubular reactor in the present study can easily be scale up and integrated with the monosilane step for continuously large manufacturing. The advantage of this method over traditional methods is that the reactions are carried out at lower temperatures and at atmospheric pressure. This lowers cost in terms of heat and pressure resistant materials that would otherwise be required for large scale industrial systems. The method is more environmentally friendly than the traditional methods for solar-grade grade silicon production which use toxic and corrosive hydrochloric acid for the generation of equally corrosive chlorosilane precursors.

## **Recommendations**

The results obtained in this study showed that alkoxy silanes and monosilane can be synthesized and as such future work should focus on the production of solar-grade silicon from these precursors. The mechanism and kinetics for the reactions need to be studied in detail so as to come-up with catalysts which are more environmentally friendly than copper compounds. Recent literature indicates that there is a variety of opinions on the source of catalytic activity and the concept of the silicon-copper intermetallides formation on the surface of silicon during the pre-treatment of the contact mass,<sup>176</sup> hence more studies to create a universal approach need to be conducted. The process for the synthesis of trialkoxy silanes should be integrated with that for monosilane for continuous production in a series of packed bed flow tubular reactors. The advantage of the proposed packed bed flow tubular reactor in the present study is that it is easier to upscale a continuous flow reactor system in comparison to a batch reactor, where heat transfer and mixing is far more difficult to control. The future should also consider the scaling up of this continuous production process for commercial purposes.

## References

1. Liang Y, Sun W, Zhu Y, Christie P. Mechanisms of silicon-mediated alleviation of abiotic stresses in higher plants: A review. *Environ Pollut.* 2007; 147:422-428.
2. Oishi T, Watanabe M, Koyama K, Tanaka M, Saegusa K. Process for solar- grade silicon production by molten salt electrolysis using aluminum-silicon liquid alloy. *J Electrochem Soc.* 2011; 158:E93-E99.
3. Filtvedt WO, Javidi M, Holt A, Melaaen MC, Marstein E, Tathgar H, Ramachandran PA. Development of fluidized bed reactors for silicon production. *Sol Energy Mater Sol Cells.* 2010; 94:1980-1995.
4. Luque A, Hegedus S. *Handbook of photovoltaic science and engineering.* New York: Wiley; 2003.
5. Wang HY, Tan Y, Li JY, Li YQ, Dong W. Removal of silicon carbide from kerf loss slurry by Al-Si alloying process. *Sep Purif Technol.* 2012; 89:91-93.
6. Braga AFB, Moreira SP, Zampieri PR, Bacchin JMG, Mei PR. New processes for the production of solar-grade polycrystalline silicon: A review. *Sol Energy Mater Sol Cells.* 2008; 92:418-424.
7. Pichel WJ, Yang MR. *Solar powered: An emerging growth industry facing severe supply constraints.* New York: Piper Jaffray Equity Research; 2005.
8. Abba IA, Grace JR, Bi, HT, Thompson ML. Spanning the flow regimes: generic fluidized bed reactor model. *AIChE J.* 2003; 49:1838-1848.
9. Safarian J, Tranell G, Tangstad M. Processes for upgrading metallurgical-grade silicon to solar-grade silicon. *Energy Procedia.* 2012; 20:88-89.

10. Degoulange J, Perichaud I, Trassy C, Martinuzzi S. Multicrystalline silicon wafers prepared from upgraded metallurgical feedstock. *Sol Energy Mater Sol Cells*. 2008; 92:1269-1273.
11. Koch W, Endrös AL, Franke D, Haßler C, Kalejs JP, Möller HJ. Bulk crystal growth and wafering for PV. In *Handbook of photovoltaic science and engineering*. Luque A, Hegedus S, Eds. John Wiley & Sons; 2003.
12. Ceccaroli B, Lohne O. Solar-grade silicon feedstock. *Handbook of photovoltaic science and engineering*. Wiley; 2003.
13. O'Mara, Herring RB, Hunt LP. Silicon precursors: Their manufacture and properties. *Handbook of semiconductor silicon technology*. Noyes; 1990.
14. Markvart T. *Solar electricity*. 2<sup>nd</sup> Ed. Chichester: Wiley; 2000.
15. Yamada Y, Harada K. Process for producing trialkoxysilane. US Patent 5,260,471; 1993.
16. Wiles C, Watts P. Continuous flow reactors: a perspective. *Green Chem*. 2012; 14:38-54.
17. Wegner J, Ceylan S, Kirschning A. Flow chemistry-A key enabling for multistep organic synthesis. *Adv Synth Catal*. 2012; 354:17-57.
18. Saga T. Advances in crystalline silicon solar cell technology for industrial mass production. *NPG Asia Mater*. 2010; 2:96-120.
19. Masson G, Latour M, Reking M, Theologitis LT, Papoutsi M. Global market outlook for photovoltaics 2013-2017. European photovoltaic industry Association. Brussels; 2013.

20. Masson G, Latour M, Biancardi B. Global market outlook for photovoltaics until 2016. European photovoltaic industry association. Brussels; 2012.
21. Koch EC. Special materials in pyrotechnics: VI. Silicon - an old fuel with new perspectives. *Propellants Explos Pyrotech.* 2007; 32:205-212.
22. Amendola S. Overview of manufacturing processes for solar-grade silicon. [Cited 17 March 2015]. Available from:  
<https://www.yumpu.com/en/document/view/4616920/overview-of-manufacturing-processes-for-solar-grade-rsi-silicon>
23. Luo D, Liu N, Lu Y, Zhang G, Li T. Removal of boron from metallurgical-grade silicon by electromagnetic induction slag melting. *Trans Nonferrous Met Soc. China.* 2011; 21:1178-1184.
24. Johnston MD, Barati M. Distribution of impurity elements in slag-silicon equilibria for oxidative refining of metallurgical silicon for solar cell applications. *Sol Energy Mater Sol Cells.* 2010; 94:2085-2090.
25. Yuge N, Abe M, Hanazawa K, Baba H, Nakamura N, Kato Y, *et al.* Purification of metallurgical-grade silicon up to solar-grade. *Prog Photovolt Res Appl.* 2001; 9:203-209.
26. Zheng S, Engh TA, Tangstad M, Luo X. Separation of phosphorus from silicon by induction vacuum refining. *Sep Purif Technol.* 2011; 82:128-137.
27. Khattak CP, Joyce DB, Schmid F. Production of solar-grade silicon by refining liquid metallurgical-grade silicon. National Renewable Energy Laboratory. Final Report; Colorado: 2001, April 19.



28. Mei PR, Moreira SP, Cardoso E, Côrtes ADS, Marques FC. Purification of metallurgical silicon by horizontal zone melting. *Sol Energy Mater Sol Cells*. 2012; 98:233-239.
29. Pires KCS, Otubo J, Braga AFB, Mei P.R. The purification of metallurgical-grade silicon by electron beam melting. *J Mater Process Technol*. 2005; 169:16-20.
30. Santos IC, Gonçalves AP, Santos CS, Almeida M, Afonso MH, Cruz MJ. Purification of metallurgical-grade silicon by acid leaching. *Hydrometallurgy*. 1990; 23:237-246.
31. Soiland AK. Silicon for solar cells. Thesis. Norwegian University of Science and Technology, 2004.
32. Yoshikawa T, Arimura K, Morita K. Boron removal in the solidification refining of Si with Si-Al melt. *Metall Mater Trans B*. 2005; 36:842-847.
33. Kvande R. Incorporation of impurities during directional solidification of multicrystalline silicon for solar cells. Thesis. Norwegian University of Science and Technology, Trondheim, 2008.
34. Martorano MA, Neto JBF, Oliveira TS, Tsubaki TO. Refining of metallurgical silicon by directional solidification. *Mater Sci Eng B*. 2011; 176:217-226.
35. Tao M. Impurity segregation in electrochemical processes and its application to electrorefining of ultrapure silicon. *Electrochim Acta*. 2013; 89:688-691.
36. Olsen E. and Rolseth S. Three-layer electrorefining of silicon. *Metall Mater Trans B*. 2010; 41:295-302.

37. Pizzini S. Towards solar-grade silicon: Challenges and benefits for low cost photovoltaics. *Sol Energy Mater Sol Cells*. 2010; 94:1528-1533.
38. Queisser HJ. Detailed balance limit for solar cell efficiency. *Mater Sci Eng B*. 2009; 159-160:322-328.
39. Rogers LC. Polysilicon Preparation. *Handbook of semiconductor silicon technology*. Noyes; 1990.
40. Ma X, Zhang J, Wang T, Li T. Hydrometallurgical purification of metallurgical-grade silicon. *Rare Met*. 2009; 28:221-225.
41. Siffert P, Krimmel E. *Silicon: Evolution and future of a technology*. Springer; 2004.
42. Boer KW. *Survey of semiconductor physics Volume II: Barriers, junctions, surfaces and devices*. Spinger; 1992.
43. Luque A, Hegedus S. *Handbook of photovoltaic science and engineering*. 2<sup>nd</sup> Ed. Wiley; 2011.
44. Strebkov DS, Pinov A, Zadde VV, Lebedev EN, Belov EP, Efimov NK *et al*. Chlorine free technology for solar-grade silicon manufacturing. 14th Workshop on crystalline silicon solar cells and modules; 2004 August 8-11; Winter Park, Colorado, USA.
45. Zadde VV, Pinov AB, Strebkov DS. New method of solar-grade silicon production. 12th Workshop on crystalline silicon solar cell materials and processes; 2002 August 11-14; Breckenridge, Colorado, USA.

46. Tsuo Y, Gee J, Menna P, Strebkov D, Pinov A, Zadde V. Environmentally benign silicon solar cell manufacturing, 2<sup>nd</sup> World Conference and Exhibition on Photovoltaic Solar Energy Conversion, 6-10 July, 1998, Hofburg Kongresszentrum, Vienna, Austria.
47. Lewis KM, Cameron RA, Ritscher JS. Process for the direct synthesis of trialkoxysilane. US Patent 7,429,672; 2008.
48. Nauman EB. Chemical reactor design, optimization, and scale up. Wiley; 2008.
49. Trambouze P, Euzen J. Chemical reactors: From design to operation. OPHRYS; 2004.
50. Coker AK. Modeling of Chemical kinetics and reactor design. Gulf Professional Publishing; 2001.
51. Tominaga H, Tamaki M. Chemical reaction and reactor design. Wiley; 1997.
52. Coulson JM, Richardson JF, Peacock FG. Chemical and biochemical reactors and process control. 3<sup>rd</sup> Ed. Elsevier; 1994.
53. Degaleesan S, Dudukovic M, Pan Y. Experimental study of gas induced liquid-flow structures in bubble columns. AIChE J. 2001; 47:1913-1931.
54. Kantarci N, Borak F, Ulgen AF. Bubble column reactors. Review. Process Biochem. 2005; 40:2263-2283.
55. Ramezani M, Mostoufi N, Mehrnia MR. Improved modelling of bubble column reactors by considering the bubble size distribution. Ind Eng Chem Res. 2012; 51:5705-5714.

56. Jakobsen HA. Chemical reactor modelling: Multiphase reactive flows. 2<sup>nd</sup> Ed. Springer; 2014.
57. Matheswaran M, Moon S II. Influence parameters in the ozonation of phenol wastewater treatment using bubble column reactor under continuous circulation. J Ind Eng Chem. 2009; 15:287-292.
58. Hua T, Min J, Xinkui W, Min HE, Tianxi CAI. Alkylation of naphthalene with propylene catalysed by aluminium chloride immobilized on Al-MCM-4. Chin J Catal. 2010; 31:725-728.
59. Salmi TO, Mikkola J, Warna JP. Chemical reaction engineering and reactor technology. CRC Press; 2011.
60. Thoenes D. Chemical reactor development: From laboratory synthesis to industrial production. Springer; 1994.
61. Cybulski A. Fine chemicals manufacture: Technology and engineering. Amsterdam, Gulf Professional Publishing; 2001.
62. Li M, Niu F, Zuo X, Metelski PD, Busch DH, Subramaniam B. A spray reactor concept for catalytic oxidation of *p*-xylene to produce high-purity terephthalic acid. Chem Eng Sci. 2013; 104:93-102.
63. Turpina A, Couvert A, Laplanchea A, Paillier A. Experimental study of mass transfer and H<sub>2</sub>S removal efficiency in a spray tower. Chem Eng Process. 2008; 47:886-892.
64. Couper JR, Penney WR, Fair JR. Chemical process equipment: selection and design. 2<sup>nd</sup> Ed. Elsevier; 2012.

65. Ranade VV, Chaudhari R, Gunjal PR. Trickle bed reactors: reactor engineering & applications. Elsevier; 2011.
66. Saha B, Sharma MM. Esterification of formic acid, acrylic acid and methacrylic acid with cyclohexene in batch and distillation column reactors: ion-exchange resins as catalysts. *React Funct Polym.* 1996; 28:263-278.
67. Qing Z, Yincheng G, Zhenqi N. Experimental studies on removal capacity of carbon dioxide by a packed reactor and a spray column using aqueous ammonia. *Energy Procedia.* 2011; 4:519-524.
68. Liu Y, Wang L. Biodiesel production from rapeseed deodorizer distillate in a packed column reactor. *Chem Eng Process.* 2009; 40:1152-1156.
69. Jana AK. Chemical process modelling and computer simulation. PHI Learning Pvt. Ltd; 2008.
70. Butt JB. Reaction kinetics and reactor design. 2<sup>nd</sup> Ed. CRC Press; 2000.
71. Smith RM. Chemical process: design and integration. John Wiley & Sons; 2005.
72. Azzopardi B, Zhao D, Yan Y, Morvan H, Mudde RF, Lo S. Hydrodynamics of gas-liquid reactors: Normal operation and upset conditions. Chichester, Wiley; 2011.
73. Chern C. Principles and applications of emulsion polymerization. John Wiley & Sons; 2008.
74. Luo W, Sun J, Ye J, Deng W, Liu Q, Guo C. Continuous gas-liquid aerobic oxidation of toluene catalysed by  $[T(p\text{-Cl})PPFe]_2O$  in a series of three stirred tank reactors. *J Ind Eng Chem.* 2014; 21:3061-3067.

75. Lallemand M, Finiels A, Fajula F, Hulea V. Continuous stirred tank reactor for ethylene oligomerization catalysed by NiMCM-41. *Chem Eng J.* 2011; 172:1078-1082.
76. Ancheyta J. Modeling and simulation of catalytic Reactors for petroleum refining. John Wiley & Sons; 2011.
77. Jess A, Wasserscheid P. Chemical technology: An Integral textbook. John Wiley & Sons; 2013.
78. von Harbou E, Schmitt M, Parada S, Grossmann C, Hasse H. Study of heterogeneously catalysed reactive distillation using the D+R tray-A novel type of laboratory equipment. *Chem Eng Res Des.* 2011; 89:1271-1280.
79. Pineda IS, Lee JW, Jung I, Kang YT. CO<sub>2</sub> absorption enhancement by methanol-based Al<sub>2</sub>O<sub>3</sub> and SiO<sub>2</sub> nanofluids in a tray column absorber. *Int J Refrig.* 2012; 35:1402-1409.
80. Albright L. Albright's chemical engineering handbook. CRC Press; 2008.
81. Zaid TA, Benmaza K, Chitour CE. Sulphonation of linear alkyl benzene in a corrugated wall falling film reactor. *Chem Eng J.* 2000; 76:99-102.
82. Talens FI, Hreczuch W, Bekierz G, Szymanowski J. Ethoxylation of alcohols in falling film reactor. *J Disp Sci Technol.* 1987; 18:423-433.
83. Talens-Alesson FI. The modeling of falling film chemical reactors. *Chem Eng Sci.* 1999; 54:1871-1881.
84. Puma GL, Yue PL. A laminar falling film slurry photocatalytic reactor. Part I-model development. *Chem Eng Sci.* 1998; 53:2993-3006.

85. Puma GL, Yue PL. Modelling and design of a thin-film slurry photocatalytic reactor for water purification. *Chem Eng Sci.* 2003; 58:2269-2281.
86. Agarwal A, Bhaskarwar AN. Comparative simulation of falling-film and parallel-film reactors for photocatalytic production of hydrogen. *Int J Hydrogen Energy.* 2007; 32:2764-2775.
87. Van Dam MHH, Corriou JP, Midoux N, Lamine AS, Roizard C. Modeling and measurement of sulfur dioxide absorption rate in a laminar falling film reactor. *Chem Eng Sci.* 1999; 54:5311-5318.
88. Dabir B, Riazi MR, Davoudirad HR. Modelling of falling film reactors. *Chem Eng Sci.* 1996; 51:2553-2558.
89. Levenspiel O. *Chemical reaction engineering.* 3<sup>rd</sup> Ed. Wiley; 1999.
90. Yates JG. *Fundamentals of fluidized-Bed chemical processes: Butterworths monographs in chemical engineering.* Butterworth-Heinemann; 2013.
91. Gupta CK, Sathiyamoorthy D. *Fluid bed technology in materials processing.* CRC Press; 1998.
92. Kunii D, Levenspiel O. *Fluidization engineering: Butterworth-Heinemann Series in Chemical Engineering.* Butterworth-Heinemann; 1991.
93. Yang W. *Handbook of fluidization and fluid-particle systems: Chemical Industries.* CRC Press; 2003.
94. Odedairo T, Al-Khattaf S. Kinetic analysis of benzene ethylation over ZSM-5 based catalyst in a fluidized-bed reactor. *Chem Eng J.* 2010; 157:204-215.

95. Sanfilippo D. Dehydrogenations in fluidized bed: Catalysis and reactor engineering. *Catal. Today*. 2011; 178:142-150.
96. Poling B, Prausnitz J, O'Connell J. *The Properties of gases and liquids*. McGraw-Hill Companies Inc; 2001.
97. Doraiswamy LK, Uner D. *Chemical reaction engineering; Beyond the fundamentals*. CRC Press; 2013.
98. Kuba MG, Prins R, Pirngruber GD. Gas-phase nitration of toluene with zeolite beta. *Appl Catal. A: General*. 2007; 333:78-89.
99. Ghavipour M, Behbahani R M. Fixed-bed reactor modeling for methanol to dimethyl ether reaction over  $\gamma$ -alumina using a new practical reaction rate model. *J. Ind. Eng. Chem*. 2014; 20:1942-1951.
100. Charney R. *Coupling reactions and separations for improved synthetic processes*. ProQuest; 2008.
101. Gottschalk C, Libra JA, Saupe, A. *Ozonation of water and waste Water: A practical guide to understanding ozone and its applications*. Wiley; 2009.
102. Kassner MK. *Novel sustainable solvents for bioprocessing applications*. ProQuest; 2008.
103. Yoshida J, Nagaki A, Yamada D. Continuous flow synthesis. *Drug Discov Today: Technol*. 2013; 10:e52-e59.
104. Watts P, Wiles C. Recent advances in synthetic micro reaction technology. *Chem Commun*. 2007; 443-467.



105. Hartman RL, Jensen KF. Microchemical systems for continuous-flow synthesis. *Lab Chip*. 2009; 9:2495-2507.
106. Kotzsch HJ, Vahlensieck HJ. Esterification method for trichlorosilane. US Patent 3,985,781; 1976.
107. Muraoka H, Asano M, Ohashi T, Yoshida H. Method of manufacturing alkoxysilanes. US Patent 3,775,457; 1973.
108. Wit NPMD. Process for producing silanes. US Patent 3, 072, 700; 1963.
109. Okamoto M, Yamamoto K, Suzuki E, Ono Y. Selective Synthesis of trialkoxysilanes by the reaction of metallic silicon with alcohols using copper (I) chloride as the catalyst. *J Catal*. 1994; 147:15-23.
110. Lewis KM, Yu H. Activation of copper-silicon slurries for the direct synthesis of trialkoxysilanes. US Patent 5,728,858; 1998.
111. Mendicino FG. Process for producing trialkoxysilanes from the reaction of silicon metal and alcohol. US Patent 4,727,173; 1988.
112. Anderson AR, Meyer JG. Process for the manufacture of alkoxysilanes and alkoxy orthosilicates US Patent 6,680,399; 2004.
113. Kareem SH, ALSaady FA, Hikmat NA. Catalysed direct reaction of methanol with silicon. *J Assoc Arab Univ Basic Appl Sci*. 2012; 12:27-32.
114. Lei Z, Sue H, Chunhui Y, Ji L, Kai Y, Chenfa, H *et al*. Effects of double promoters on direct synthesis of triethoxysilane in gas-solid stirred fluidized bed. *Appl Organometal Chem*. 2011; 25:508-513.

115. Ohta O, Yoshizako M. Process for the production of trialkoxysilanes. US Patent 4,931,578; 1990.
116. Lewis KM, Mereigh AT, O'Young C, Cameron RA. Process for direct synthesis of trialkoxysilane. US Patent 7,652,164; 2010.
117. Mendicino FD, Childress TE, Lewis KM, Magri S, Less HY. Surface-active additives in the direct synthesis of trialkoxysilanes. US Patent 5,783,720; 1998.
118. Brand A, Freudenthaler E, Narbeschuber T. Solvents for trialkoxysilane synthesis. US Patent 20030013902 A1; 2003.
119. Han JS, Cho JH, Lee ME, Yoo BR. Slurry phase reaction of elemental silicon with methanol in the presence of copper: Direct synthesis of trimethoxysilane. Bull Korean Chem Soc. 2009; 30:683-686.
120. Harada K, Yamada Y. Process for producing trialkoxysilanes. US Patent 5,362,897; 1994.
121. Brand A. Freshly precipitated CuO as catalyst for the trialkoxysilane synthesis. US Patent 6,380,414; 2002.
122. Roston WA, Cody RD, Bowman MA. Process for the production of alkoxy silanes. UK Patent 2,456,949; 2009.
123. Wahab B, Ellames G, Passey S, Watts P. Synthesis of substituted indoles using continuous flow micro reactors. Tetrahedron. 2010; 66:3861-3865.
124. Rochow EG. The chemistry of silicon: Pergamon international library of science, technology, engineering and social Studies. Comprehensive inorganic chemistry. Volume 9 of Pergamon texts in inorganic chemistry. Elsevier; 2013.

125. Atkins PW, Shriver D. Inorganic chemistry. 5<sup>th</sup> Ed. W.H. Freeman and Company; 2010.
126. Mueller WM, Blackledge JP, Libowitz GG. Metal hydrides. Elsevier; 2013.
127. Tsuo YM, Belov EP, Gerlivanov VG, Zadde VV, Kleschevinkova SI, Korneev NN *et al.* Process for producing monosilane. US Patent 6,103,942; 2000.
128. Muraoka H, Asano, M, Ohashi T, Shimazaki Y. Methods of manufacturing silanes. US Patent 3,829,555; 1974.
129. Imaki N, Haji A, Misu Y. A Method for producing monosilane and a tetraalkoxysilane. US Patent 4,667,047; 1987.
130. Wada K, Haji J, Yakotake I. Method for producing monosilane and tetraalkoxysilane. US Patent 4,904,460; 1990.
131. Parshina LN, Oparina LA, Khil'ko MY, Trofimov BA. Catalysis of triethoxysilane disproportionation with oligoethylene glycol ethers. J Organomet Chem. 2003; 665:246-249.
132. Inaba S, Nagahama H. Process for manufacturing silane. US Patent 4,959, 200; 1990.
133. Ohno H, Ohi T, Ito H, Makhmutov F. Method for producing monosilane and tetraalkoxysilane. US Patent 8,829,221 B2; 2014.
134. Suzuki E, Nomoto Y, Okamoto M, Ono Y. Diethoxysilane formation by the disproportionation of triethoxysilane over heat-treated calcium hydroxide. Catal Lett 1997; 48:75-78.

135. Suzuki E, Nomoto Y, Okamoto M, Ono Y. Disproportionation of triethoxysilane over KF/Al<sub>2</sub>O<sub>3</sub> and heat-treated hydrotalcite. *Appl Catal; A*. 1998; 167:7-10.
136. Ohno H, Ohi T, Ito H, Makhmutov F. Method for producing monosilane and tetraalkoxysilane. US Patent 023 2486 A1; 2015.
137. Armarego WLF, Chai CLL. Purification of laboratory chemicals. 5<sup>th</sup> Ed. Butterworth Heinemann. UK; 2003.
138. Ohta O, Yoshizako M. Process for the production of trialkoxysilanes. European Patent EP 0280517 B14; 1994.
139. Marciniak B. Hydrosilylation: A Comprehensive review on recent advances in silicon science. Springer Science & Business Media; 2008.
140. Jones RG, Ando W, Chojnowski J. Silicon-containing polymers: The science and technology of their synthesis and applications. Springer Science & Business Media; 2013.
141. Okamoto M, Yamamoto K, Wanatabe N, Ono Y. Selective synthesis of triphenoxysilanes by the reaction of metallic silicon with phenol using copper (I) chloride as the catalyst. *J Organomet Chem*. 1996; 515:51-55.
142. Clark, A. The theory of adsorption and catalysis. Academic Press, New York; 1970.
143. Weber G, Gourgouillon N, Gillot B, Barret P. Study of the reactivity of a single crystal of silicon with molten copper (I) chloride. *React Solid*. 1993; 3:127-128.
144. Okamoto M, Osaka M, Yamamoto K, Suzuki E, Ono Y. Effect of pre-treatment conditions of Si-CuCl mixture on the rate and selectivity in the reaction of silicon and methanol using copper (I) chloride catalyst. *J Catal*. 1993; 143:64-85.

145. Lewis KM, Eng RN, Mereigh AT, O'Young C, Cromer SR. Nanosized copper catalyst for direct synthesis of trialkoxysilanes. European Patent EP 2,319,851 A1; 2001.
146. Centi G, Cavani F, Trifirò, F. Selective oxidation by heterogeneous catalysis. Fundamental and applied catalysis. Springer Science & Business Media; 2012.
147. Hou. TH. Handbook of industrial biocatalysis. CRC Press; 2005.
148. Beenackers A.A.C.M, Van Swaaij W.P.M. Mass transfer in gas-liquid slurry reactors. Chem Eng Sci.1993; 48:3109-3139.
149. Vervloet D, Kapteijn F, Nijenhuis J, van Ommen JR. Process intensification of tubular reactors: considerations on catalyst hold-up of structured packings. Catal Today. 2013; 216:111-116.
150. Froment GF, Bischoff KB, De Wilde J. Chemical reactor analysis and design. Wiley; 1990.
151. Sinnott R.K. Chemical engineering design: Chemical engineering. 4<sup>th</sup> Ed. Butterworth-Heinemann; 2005.
152. Rase FH. Fixed-bed reactor design and diagnostics: Gas-phase reactions. Butterworth-Heinemann; 2013.
153. Deutschmann, O. Modeling and simulation of heterogeneous catalytic reactions: From the molecular process to the technical system. John Wiley & Sons; 2013.

154. Godini, HR. Analysis of individual and integrated packed bed membrane reactors for oxidative coupling of methane. Epubli; 2014.
155. Suzuki, E, Okamoto M, Ono Y. Effect of oxide layers on the reaction of silicon with methanol into trimethoxysilane using copper (I) chloride catalyst. Solid State Ionics. 1991; 47:97-104
156. Okamoto M, Wanatabe N, Suzuki, E, Ono Y. Direct synthesis of ethylmethoxysilanes by the liquid-phase reaction of silicon, methanol and ethylene. J. Organomet. Chem. 1995; 489:C12-C16.
157. Pizzini S. Advanced silicon materials for photovoltaic applications. John Wiley & Sons; 2012.
158. Petrova-Koch, V. High-efficient low-cost photovoltaics: Recent developments. Springer Science & Business Media; 2008.
159. Kasap S, Capper P. Springer handbook of electronic and photonic materials. Springer Science & Business Media; 2007.
160. Litteral CJ. Disproportionation of chlorosilane. US Patent 4,113,847; 1978.
161. Bakay CJ. Process for making silane. US Patent 3,968,199; 1976.
162. Morimoto, S. Process for the disproportionation of chlorosilanes. US Patent 4, 613,489; 1986.
163. Willeke GP, Weber RW. Advances in photovoltaics. Academic Press; 2012.
164. Luque A, Hegedus A. Handbook of photovoltaic science and engineering. 2<sup>nd</sup> Ed. John Wiley & Sons; 2012.

165. Higman C, van der Burgt M. Gasification. Gulf professional publishing; 2011.
166. Patnaik P. A Comprehensive guide to the hazardous properties of chemical substances. John Wiley & Sons; 2007.
167. Panda I. The complete book on electroplating & allied chemicals. Asia Pacific Business Press Inc.; 2013.
168. Wabeke RL. Air contaminants, ventilation, and industrial hygiene economics: The practitioner's toolbox and desktop handbook; CRC Press; 2013.
169. Hance CR, Durham, NC, George H. Disproportionation of alkoxysilanes. US Patent 2,580,356; 1950.
170. Arkles B. Silicon esters. 4<sup>th</sup> Ed. John Wiley & Sons; 1997.
171. Belov E, Gerlivanov V, Zadde V, Kleschevnikova S, Korneev N, Lebedev E *et al* Preparation method for high purity silane. Russian Patent 2,129,984; 1999.
172. Chuit, C, Corriu, RJP, Reye, C, Young, JC. Reactivity of penta-and hexacoordinate silicon compounds and their role as reaction intermediates. Chem Rev. 93:1371-448; 1993.
173. Tacke R, Pulm M, Wagner B. Zwitterionic pentacoordinate silicon compounds. Adv Organometal Chem. 44:221-73; 1999.
174. Holmes RR. Comparison of phosphorus and silicon: Hypervalency, stereochemistry and reactivity. Chem Rev. 96:927-950; 1996.

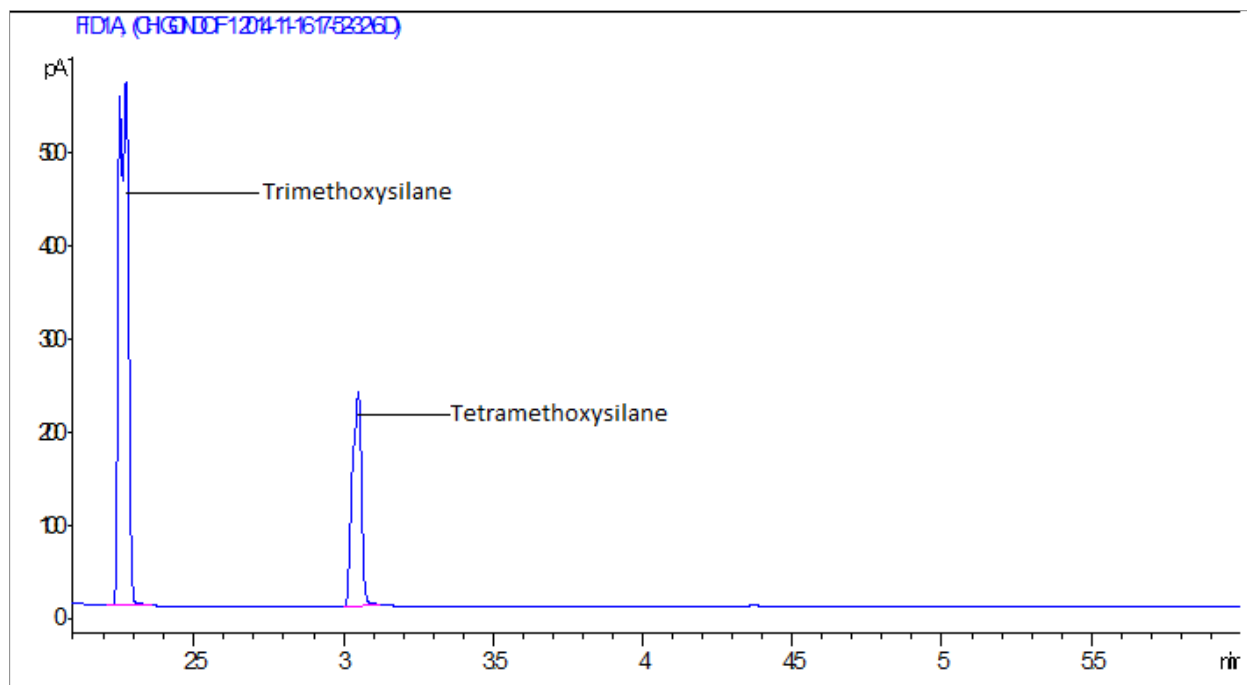
175. Metsänen TT, Gallego D, Szilvási T, Driess M, Oestreich M. Peripheral mechanism of a carbonyl hydrosilylation catalysed by an SiNSi iron pincer complex. *Chem Sci.* 6:7143-7149; 2015.
176. Adonin NY, Prikhod'ko SA, Shabalin AY, Prosvirin IP, Zaikovskii VI, Kochubey DI *et al.* The direct synthesis of trialkoxysilanes: New data for understanding the processes of the copper-containing active sites formation during the activation of the initial silicon based contact mass. *J Catal.* 338:143-153; 2016.



## Appendix

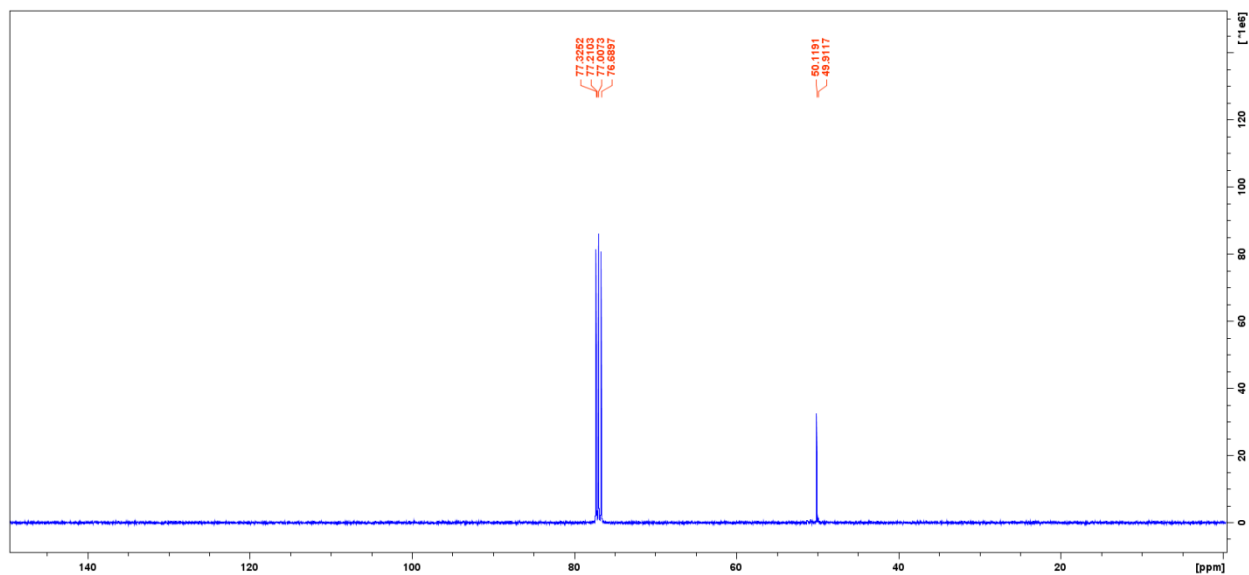
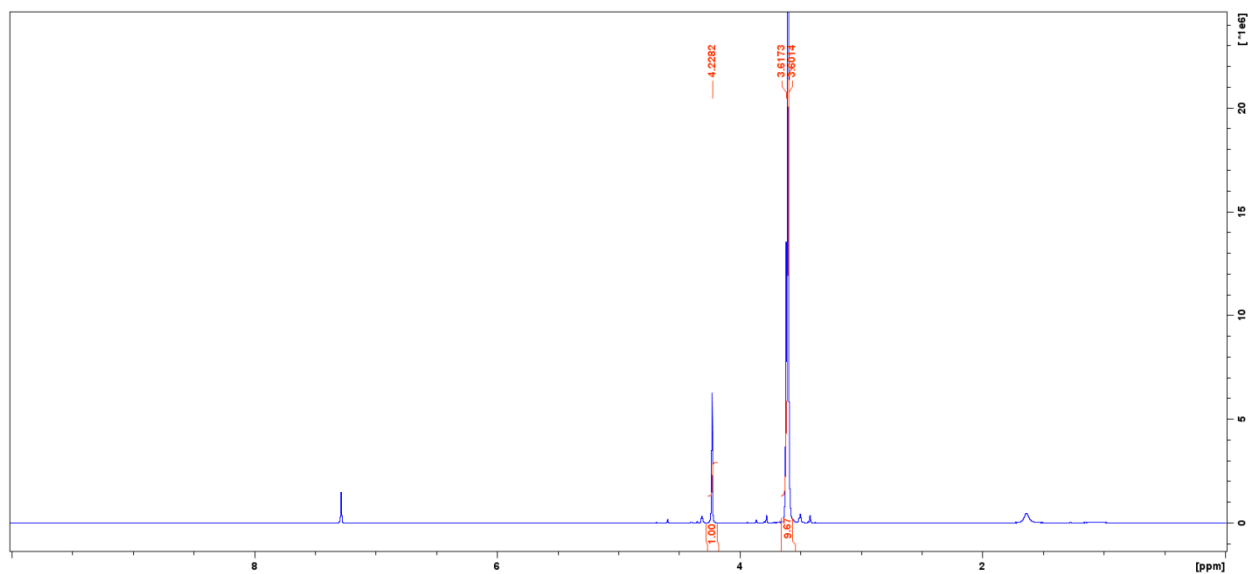
### Appendix A: Characterization data

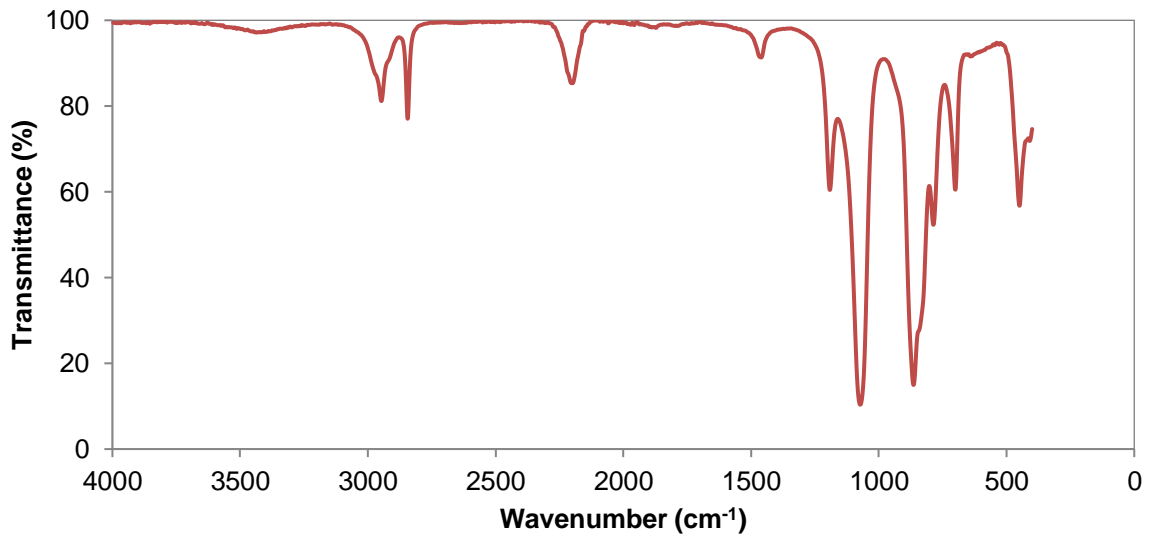
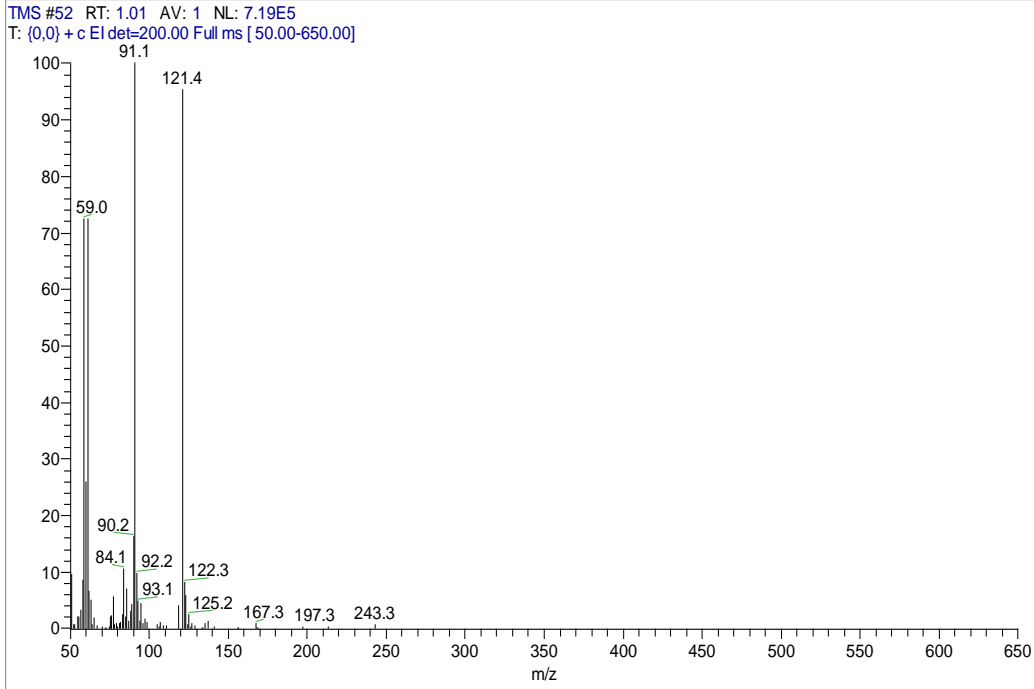
#### Selective synthesis of trimethoxysilane



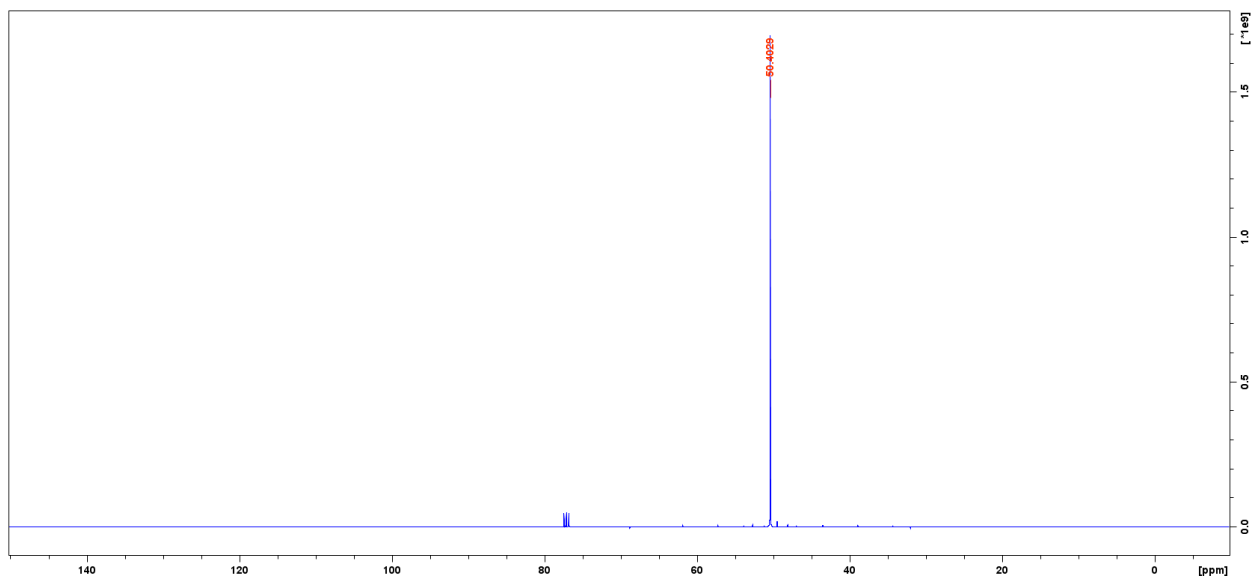
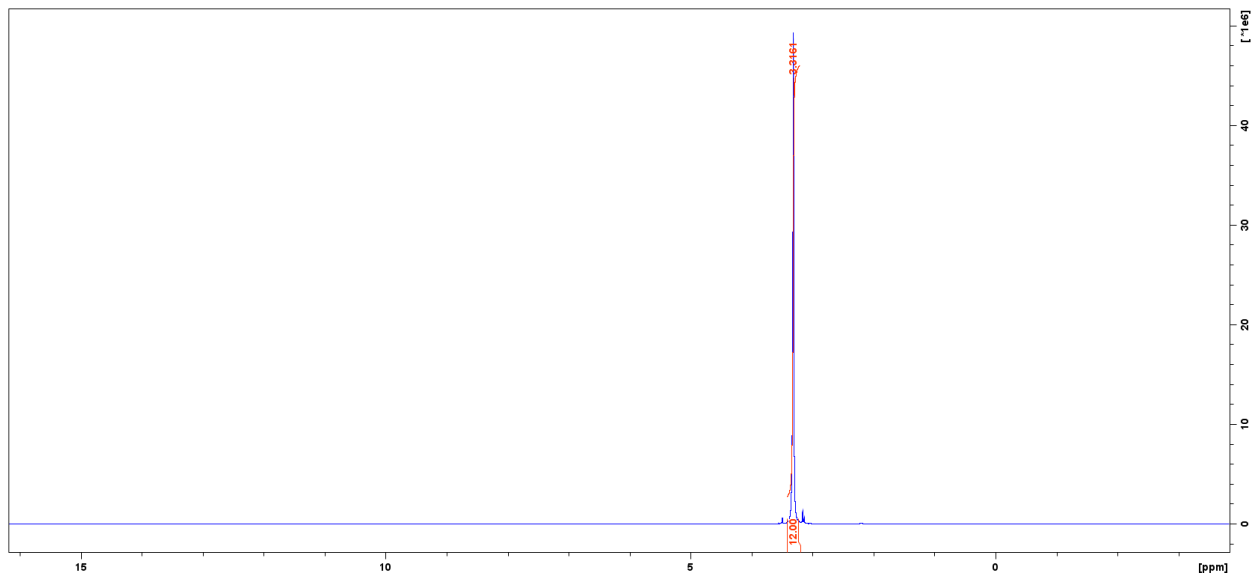
Typical GC chromatogram for the silicon methanol reaction product distillate crude mixture

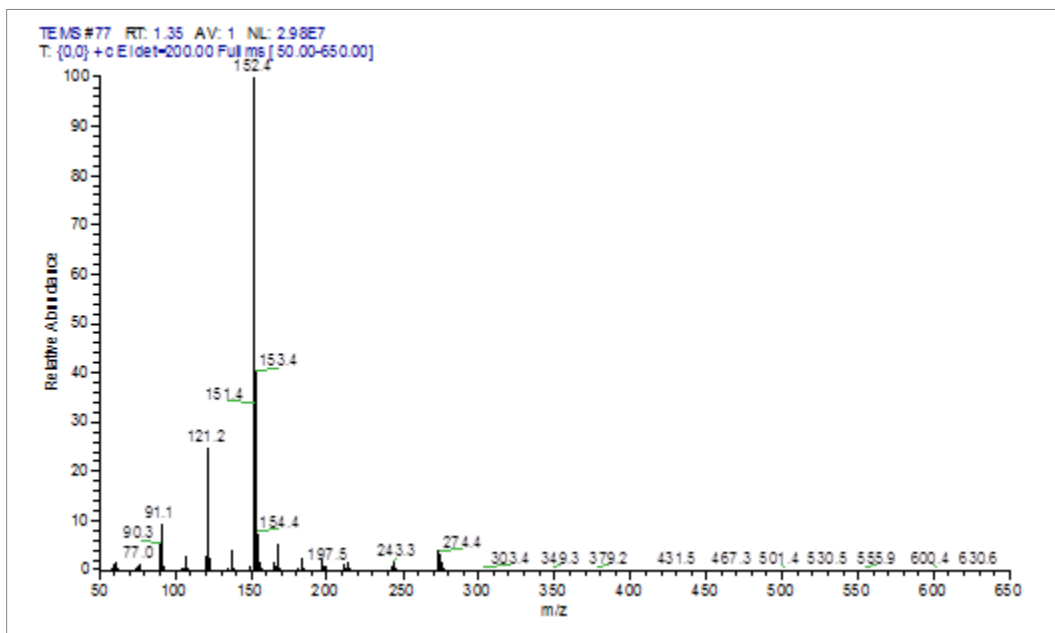
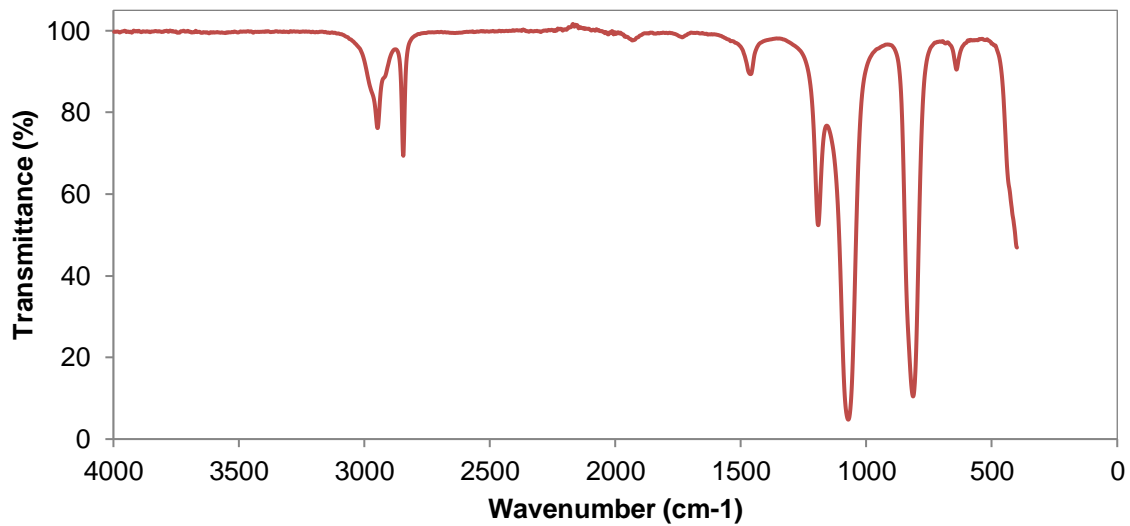
# Trimethoxysilane <sup>1</sup>H NMR, <sup>13</sup>C NMR, IR and GC-MS



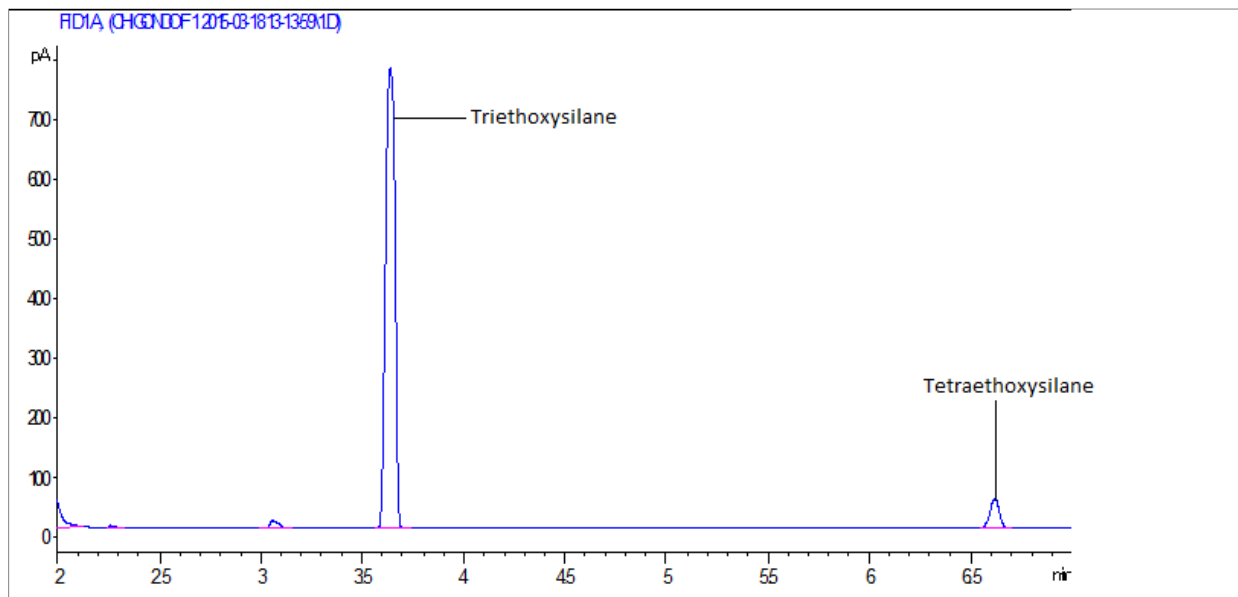


# Tetramethoxysilane $^1\text{H}$ NMR, $^{13}\text{C}$ NMR, IR and GC-MS



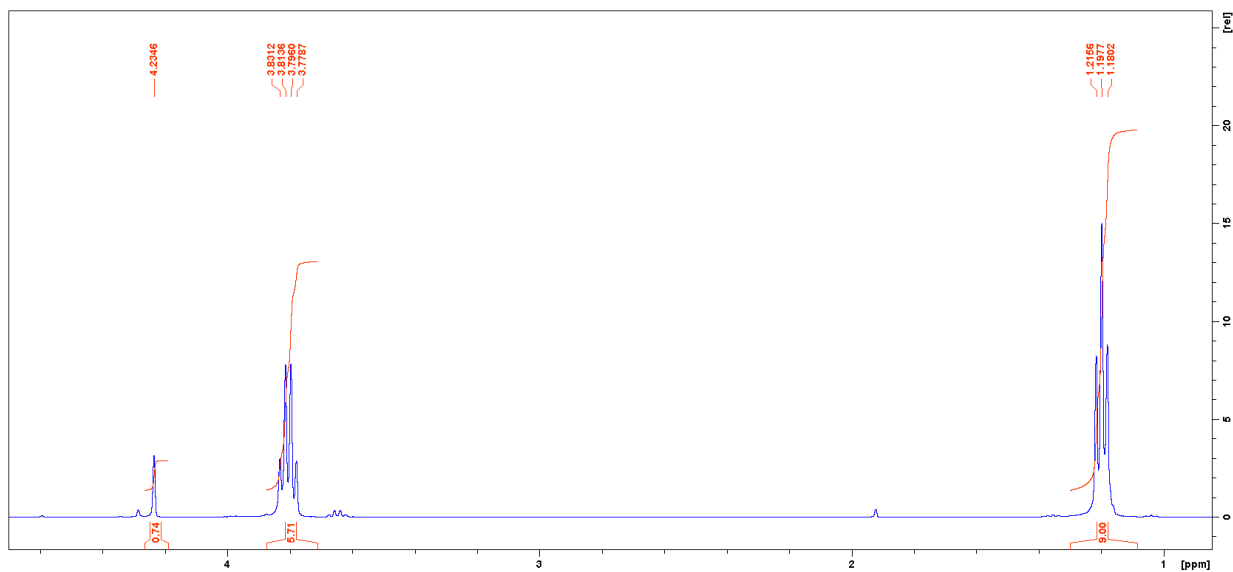


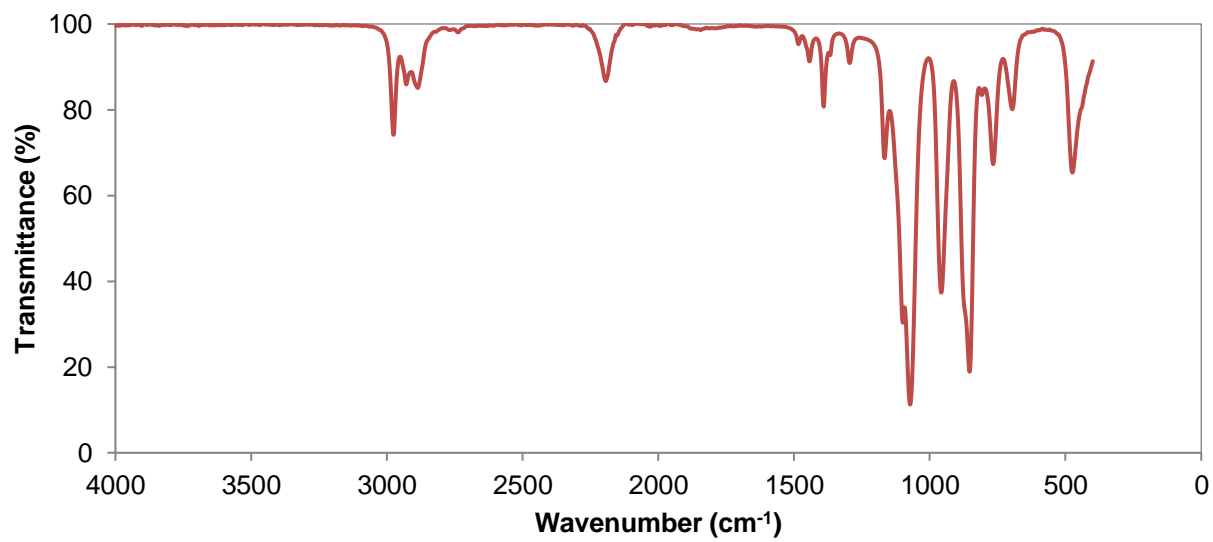
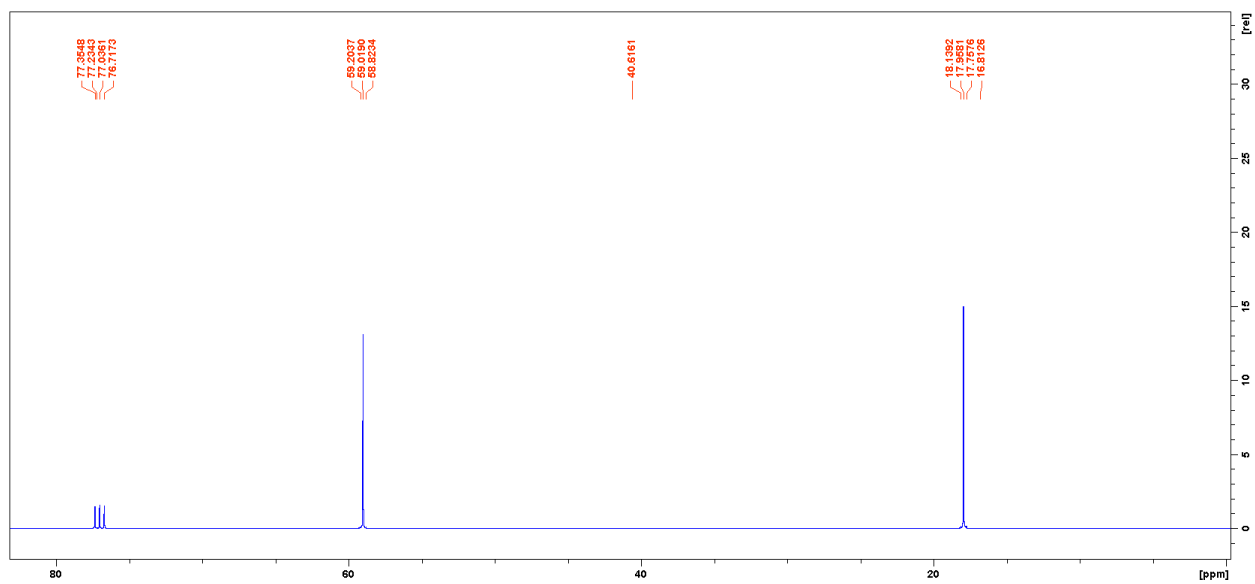
## Selective synthesis of triethoxysilane



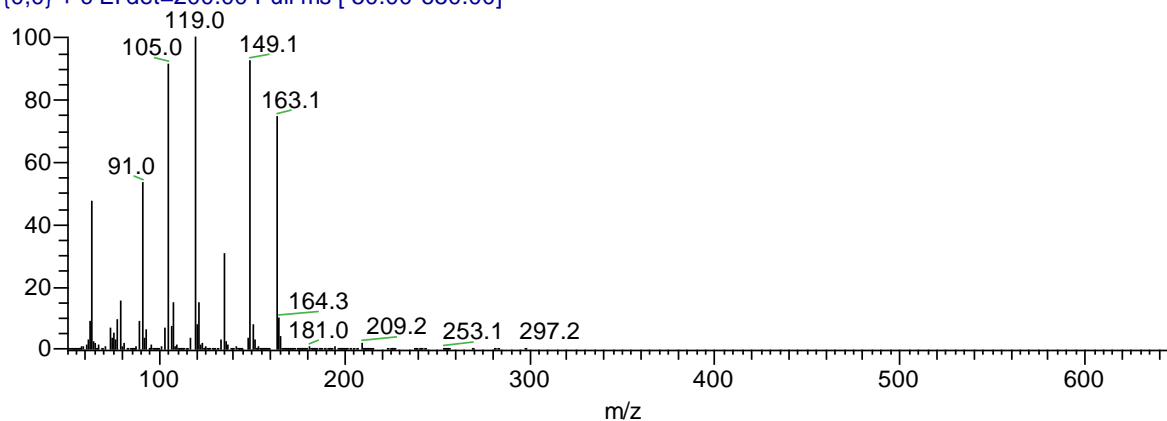
Typical GC chromatogram for the silicon ethanol reaction product distillate crude mixture

## Triethoxysilane $^1\text{H}$ NMR, $^{13}\text{C}$ NMR, IR and GC-MS

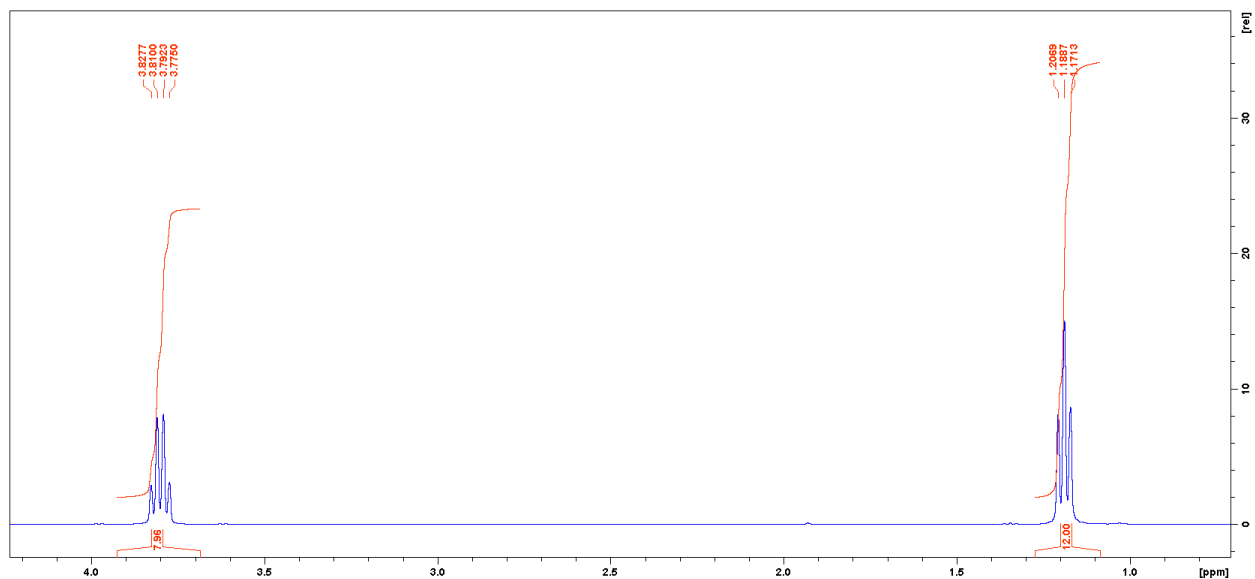




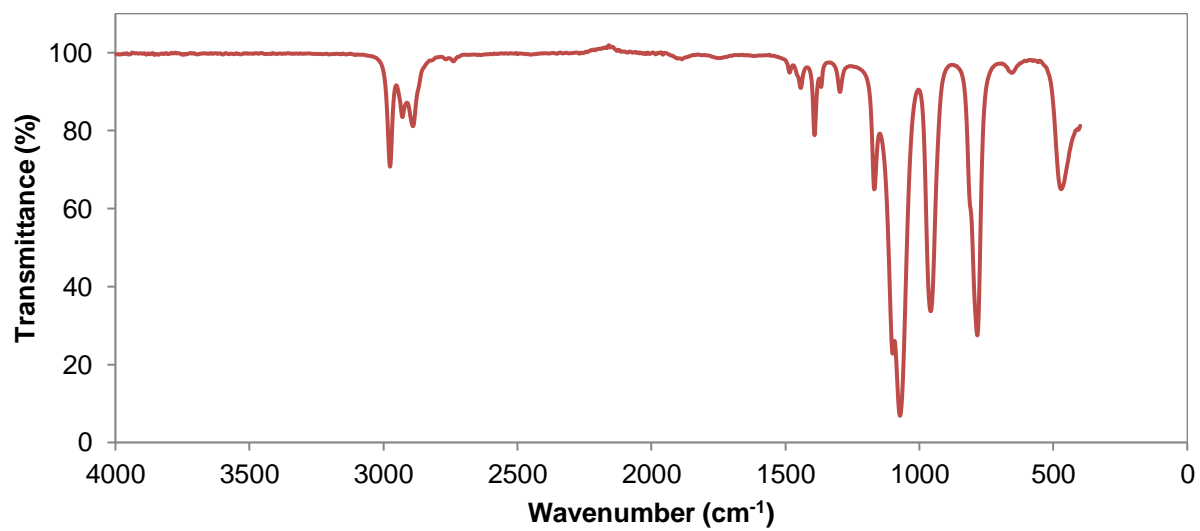
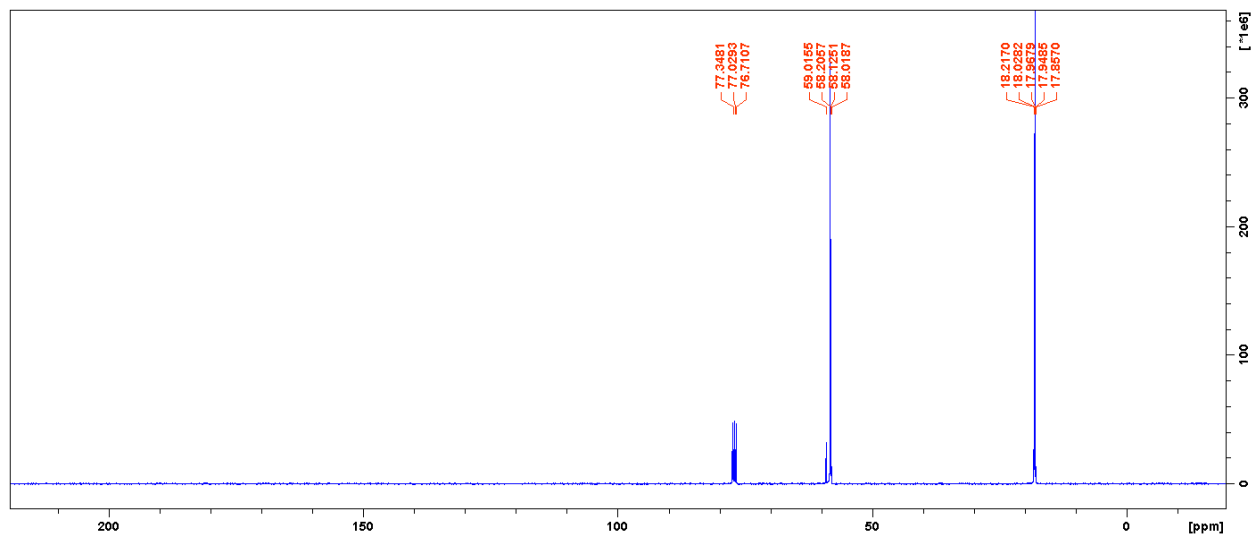
01 #165 RT: 2.81 AV: 1 NL: 4.56E7  
T: {0,0} + c EI det=200.00 Full ms [ 50.00-650.00]

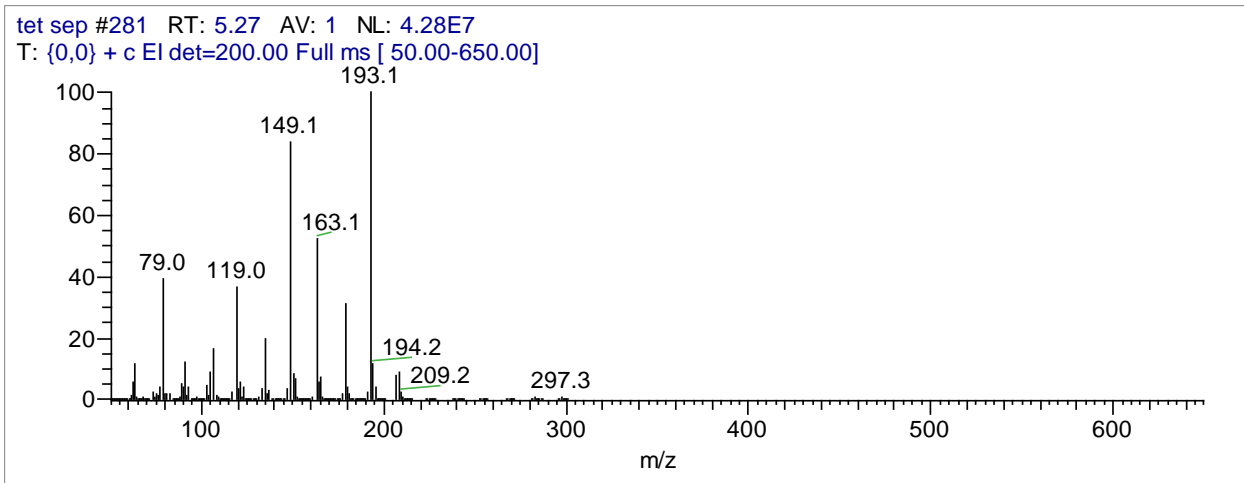


### Tetraethoxysilane $^1\text{H}$ NMR, $^{13}\text{C}$ NMR, IR and GC-MS



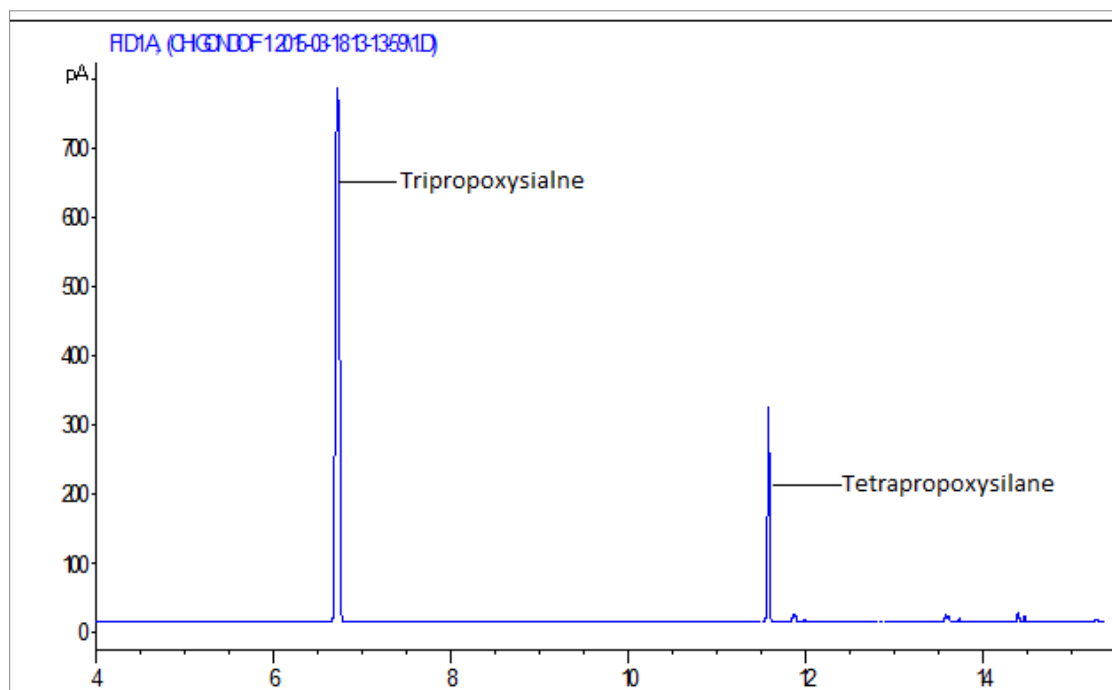




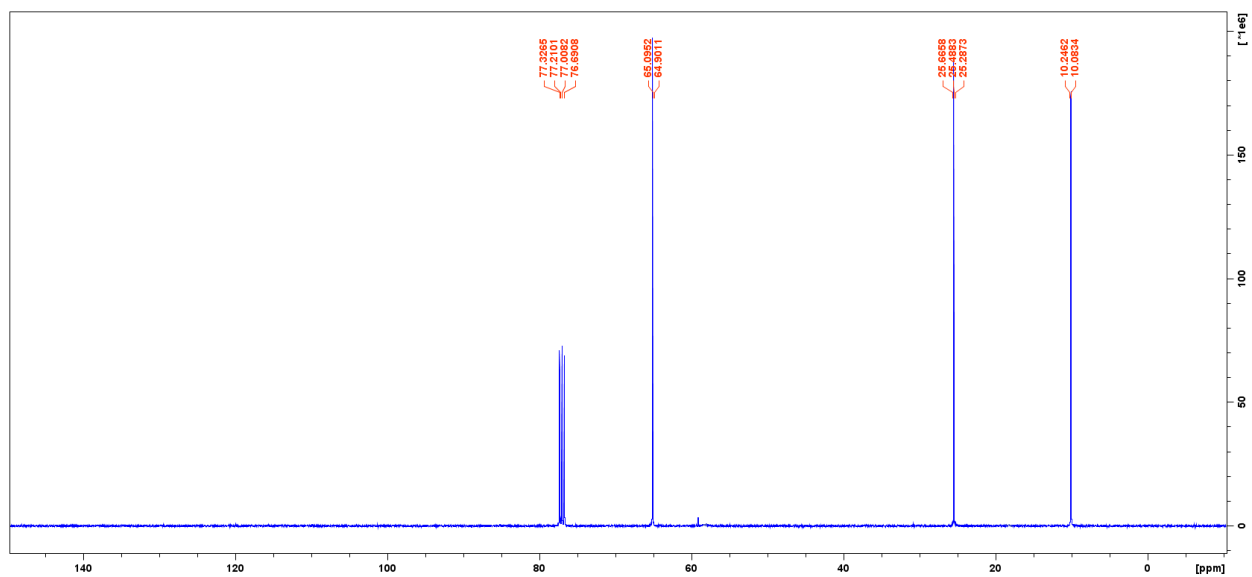
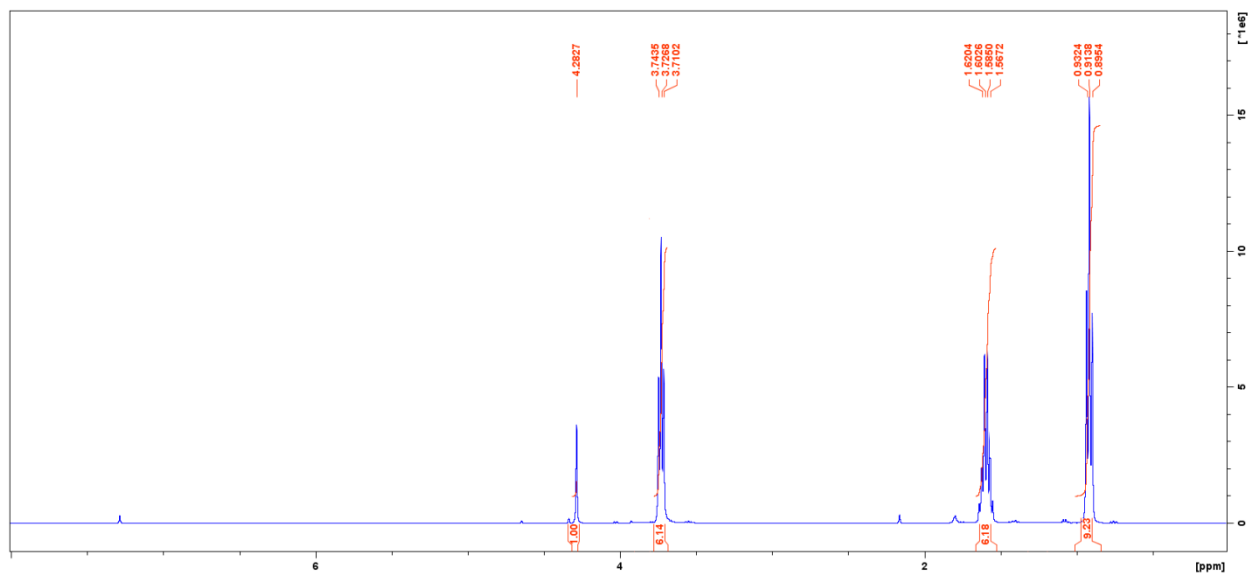


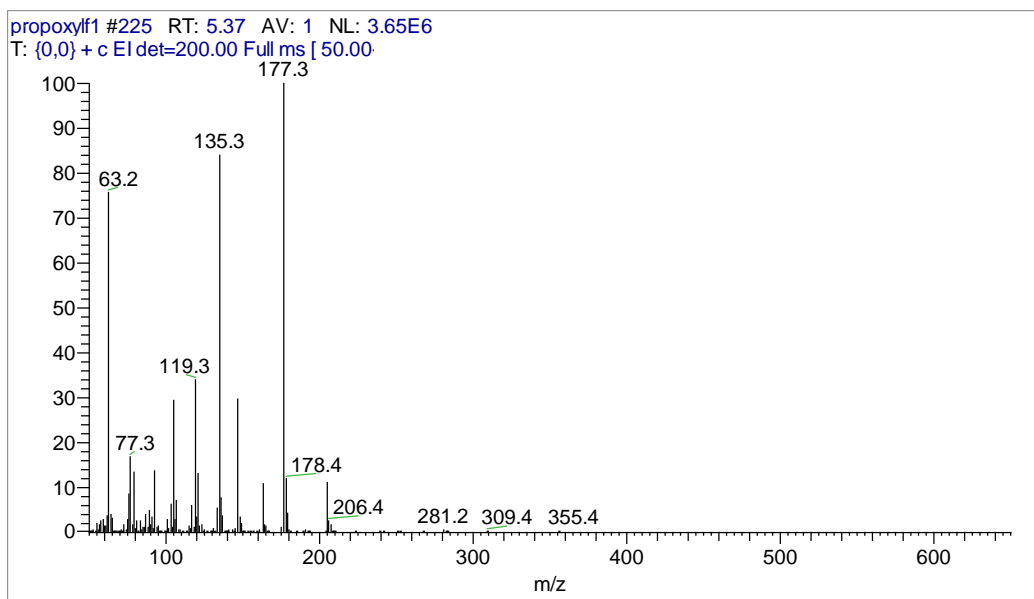
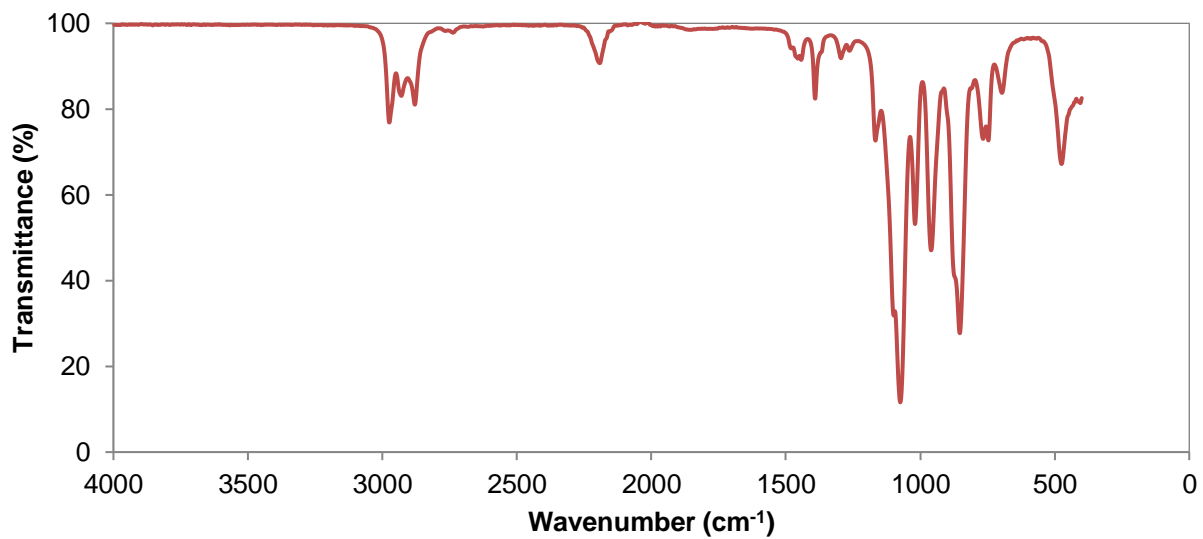
## Selective synthesis of tripropoxysilane

### Tripropoxysilane $^1\text{H}$ NMR, $^{13}\text{C}$ NMR, IR and GC-MS

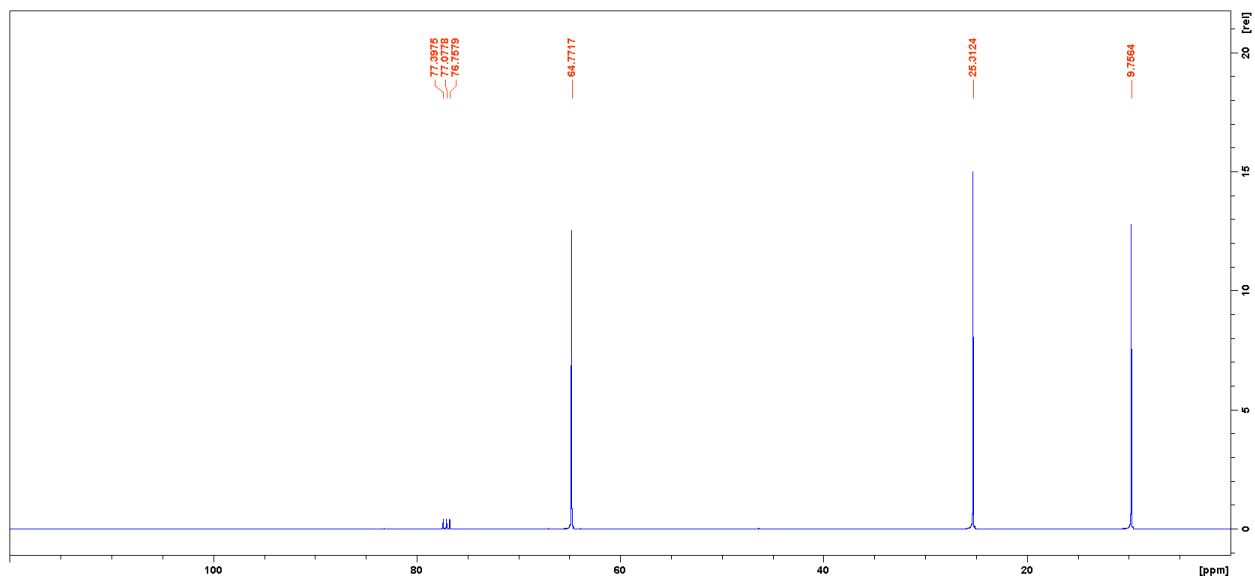
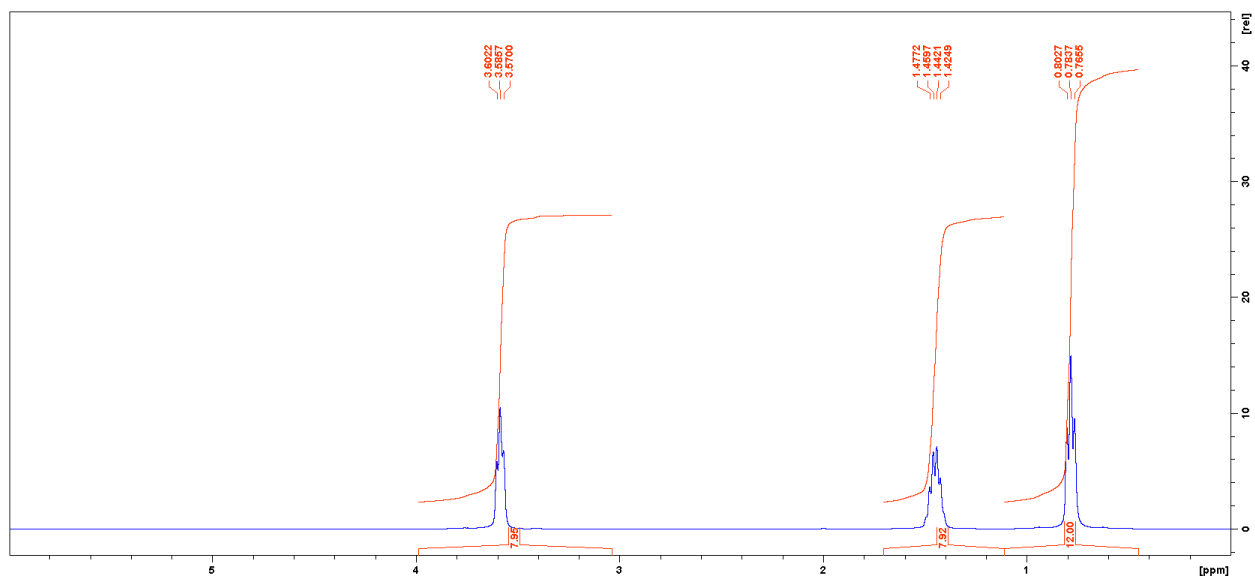


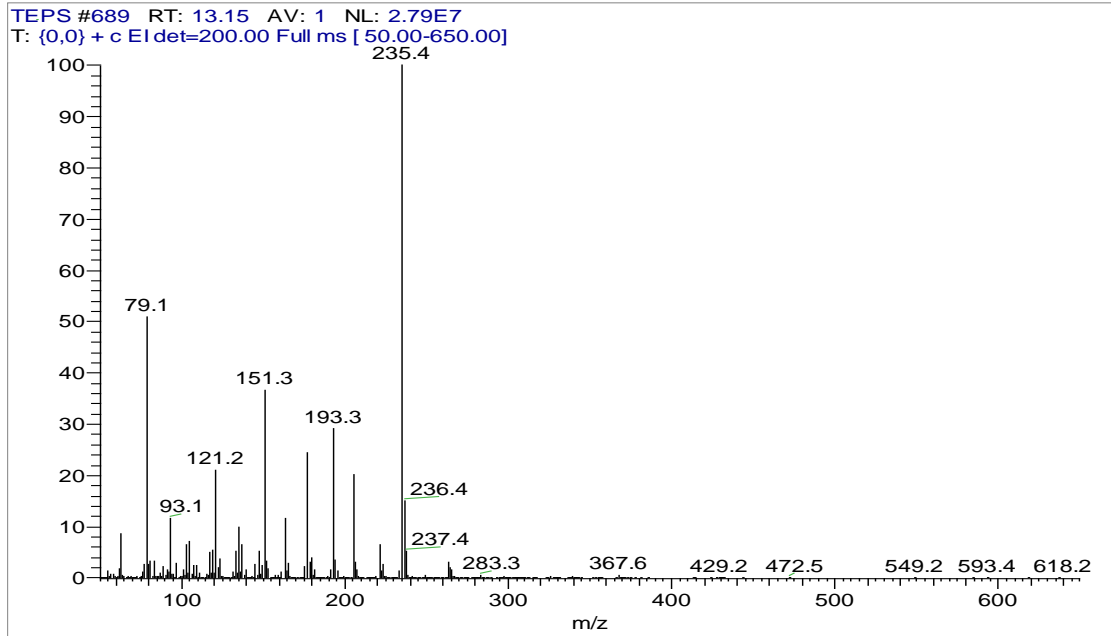
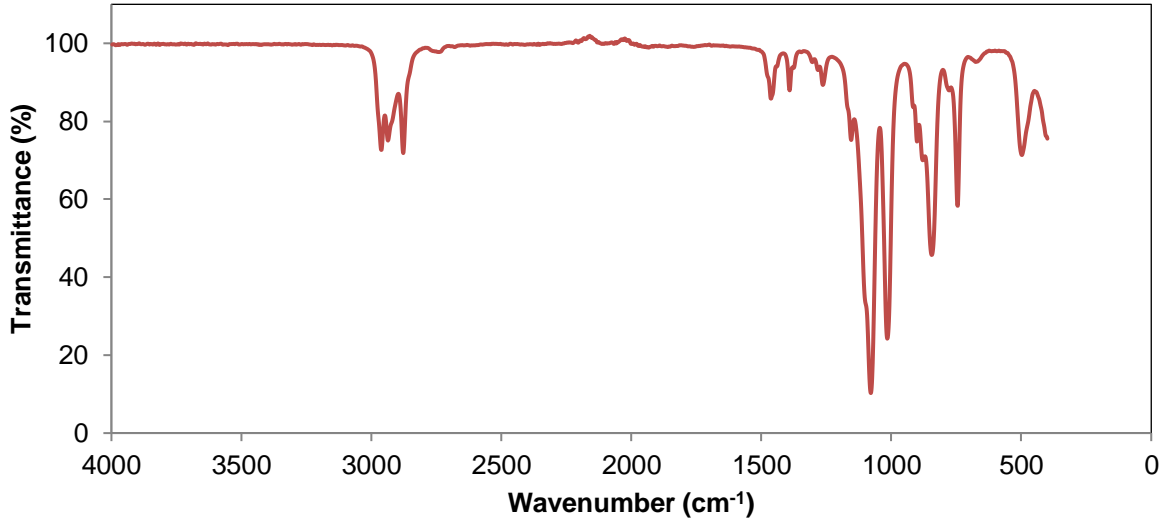
Typical GC chromatogram for the silicon *n*-propanol reaction product distillate crude mixture



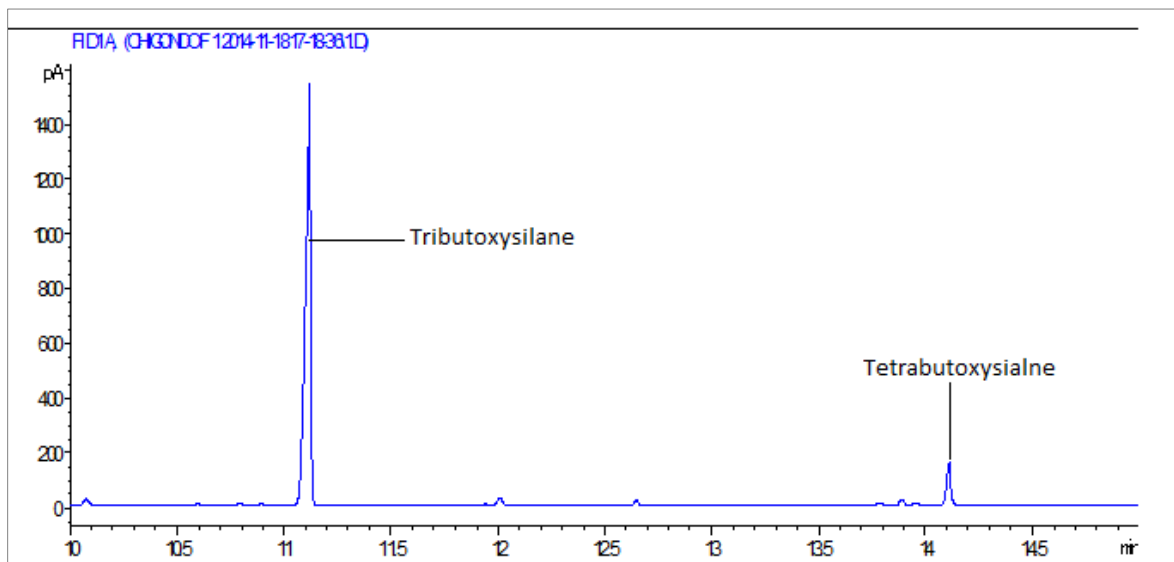


# Tetrapropoxysilane <sup>1</sup>H NMR, <sup>13</sup>C NMR, IR and GC-MS



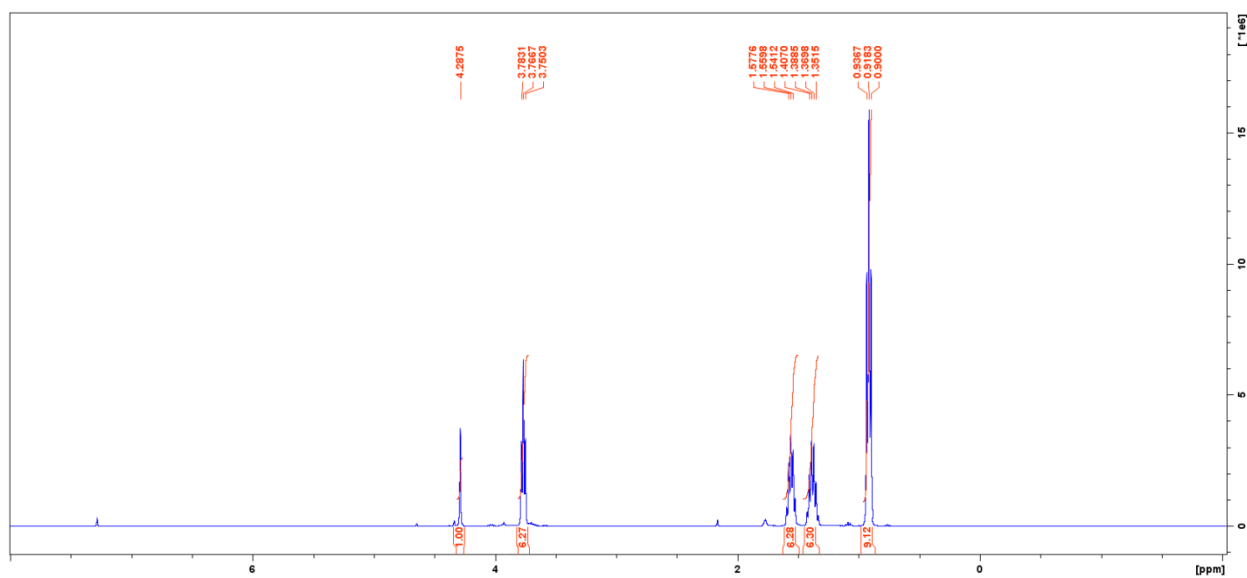


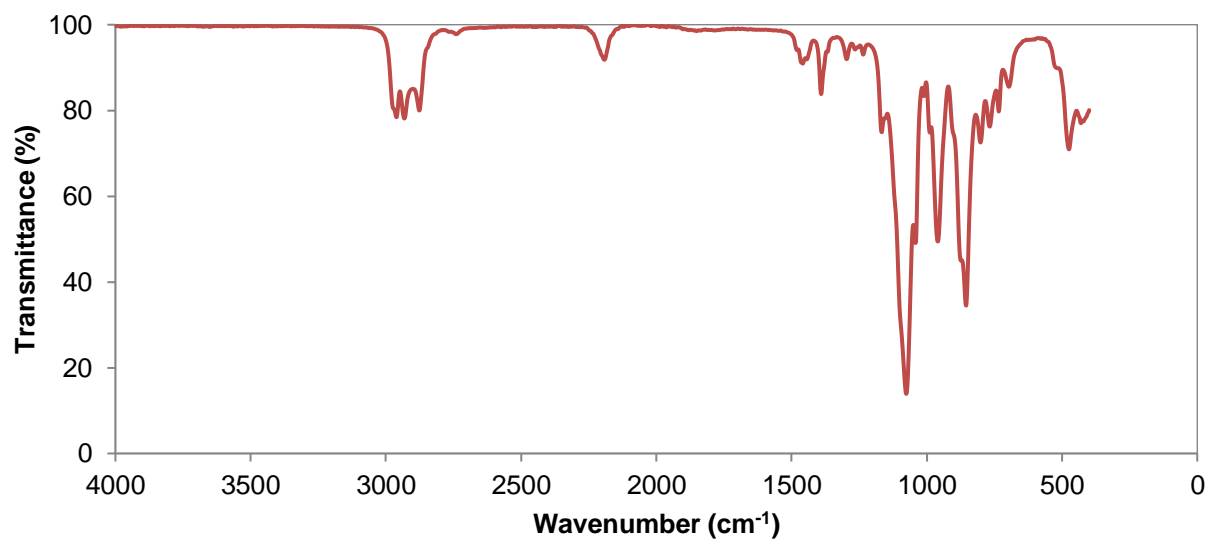
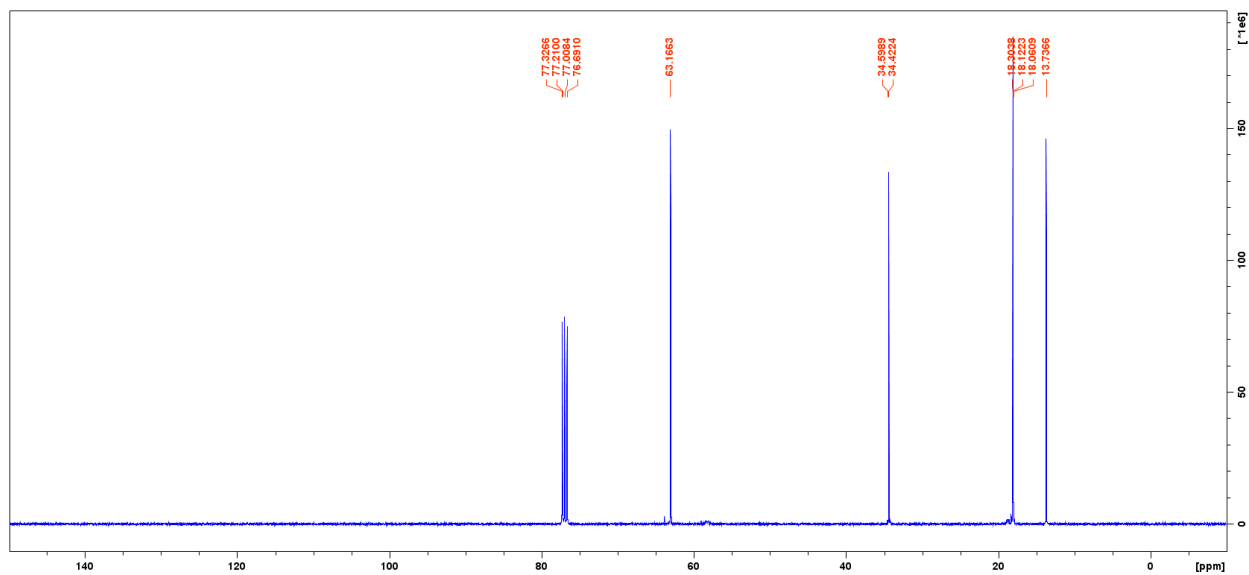
## Selective synthesis of tributoxysilane



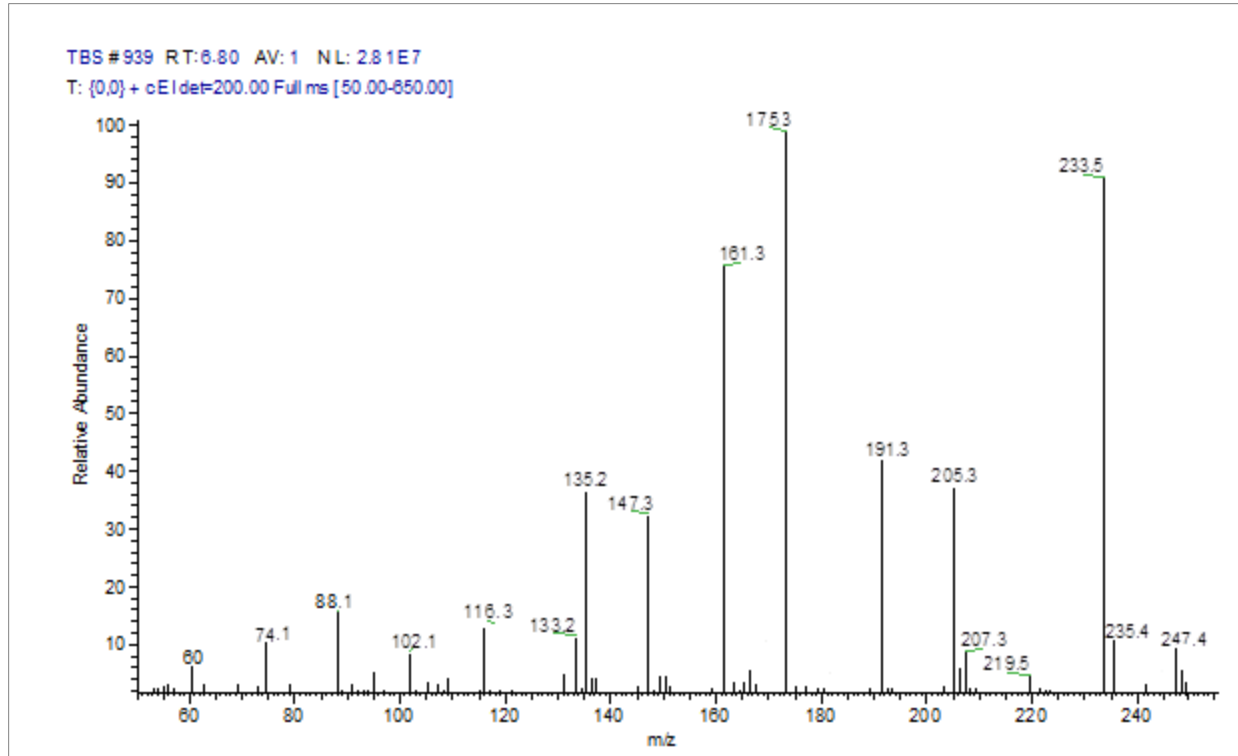
Typical GC chromatogram for the silicon *n*-butanol reaction product distillate crude mixture

## Tributoxysilane <sup>1</sup>H NMR, <sup>13</sup>C NMR, IR and GC-MS

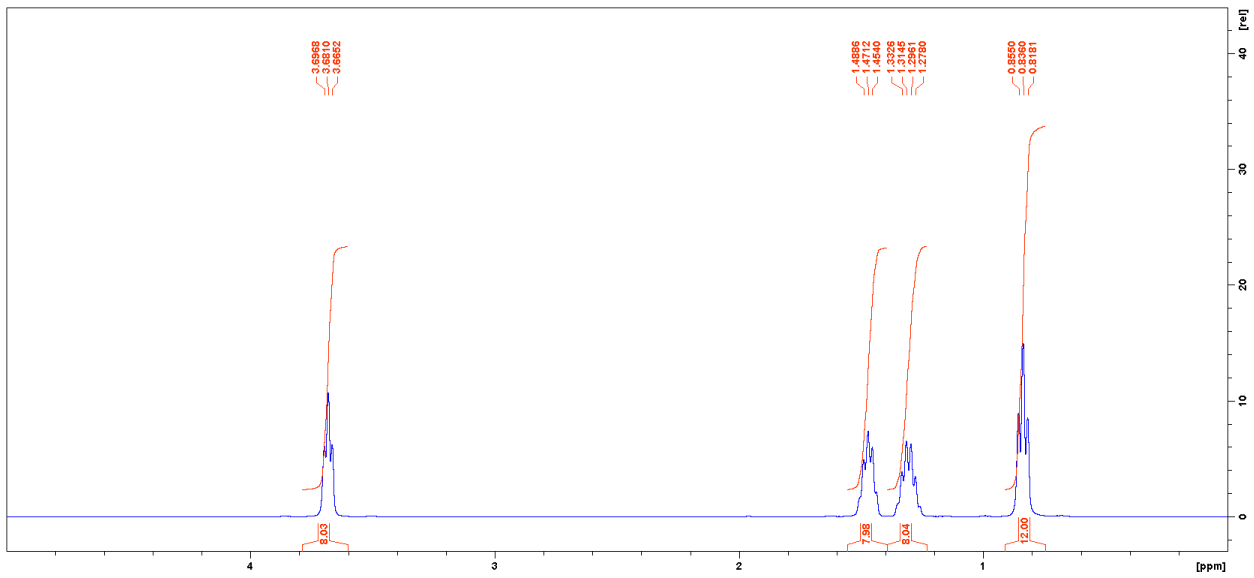


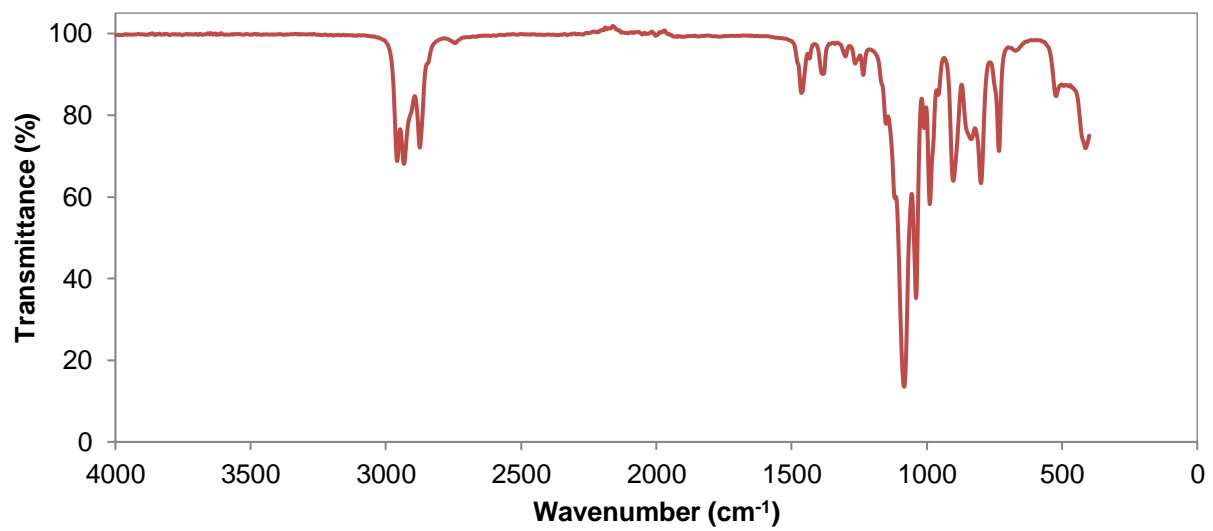
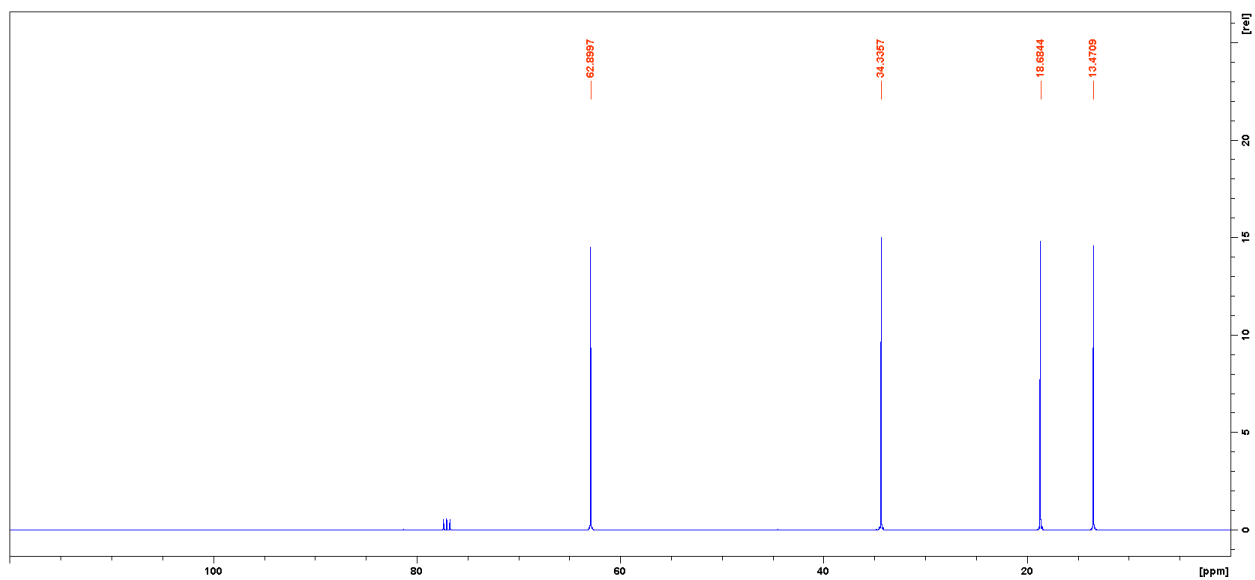


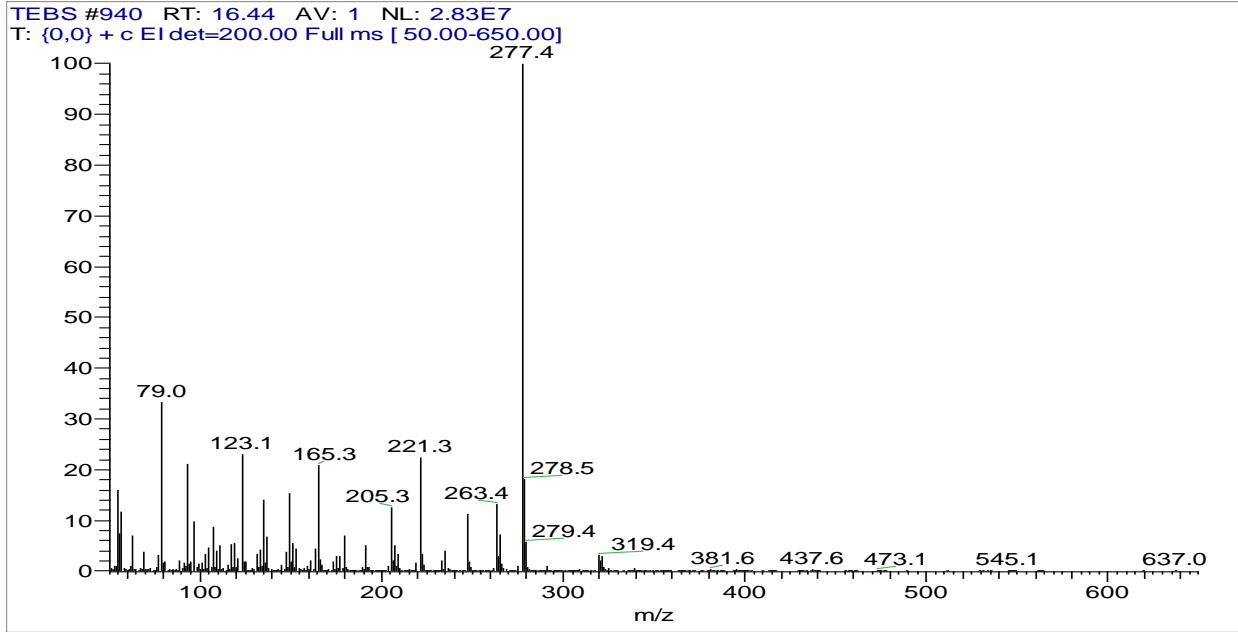




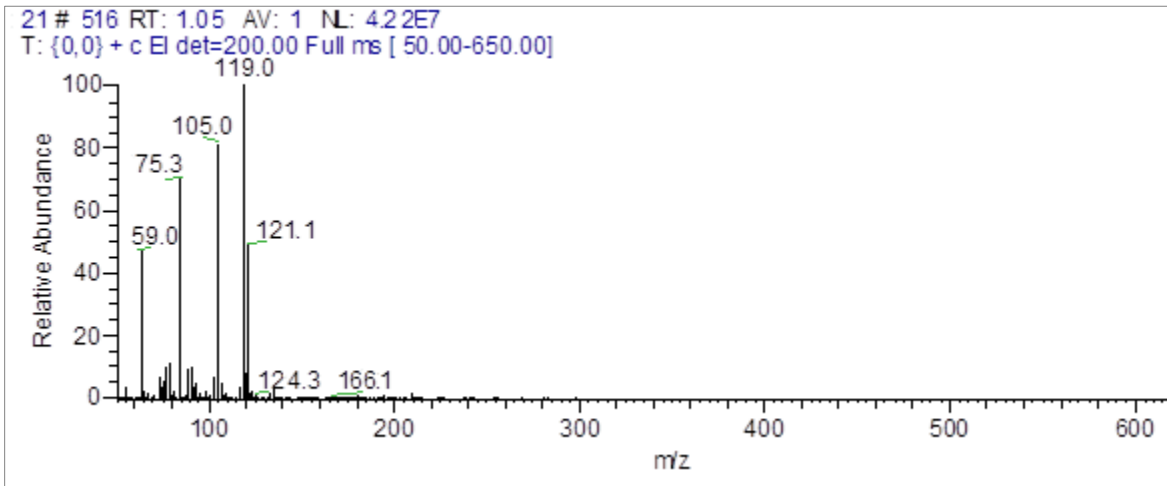
**Tetrabutoxysilane <sup>1</sup>H NMR, <sup>13</sup>C NMR, IR and GC-MS**



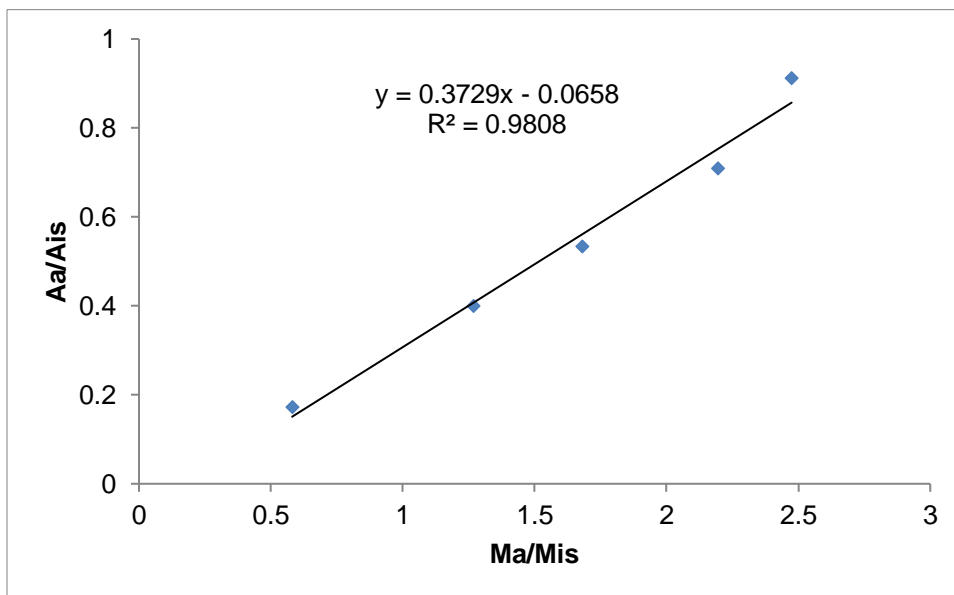




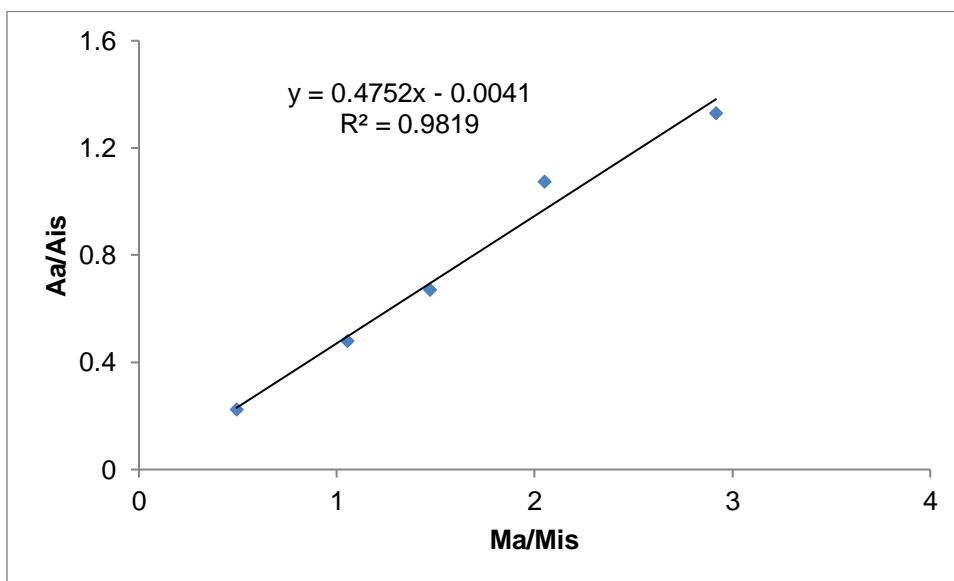
### Diethoxysilane GC-MS



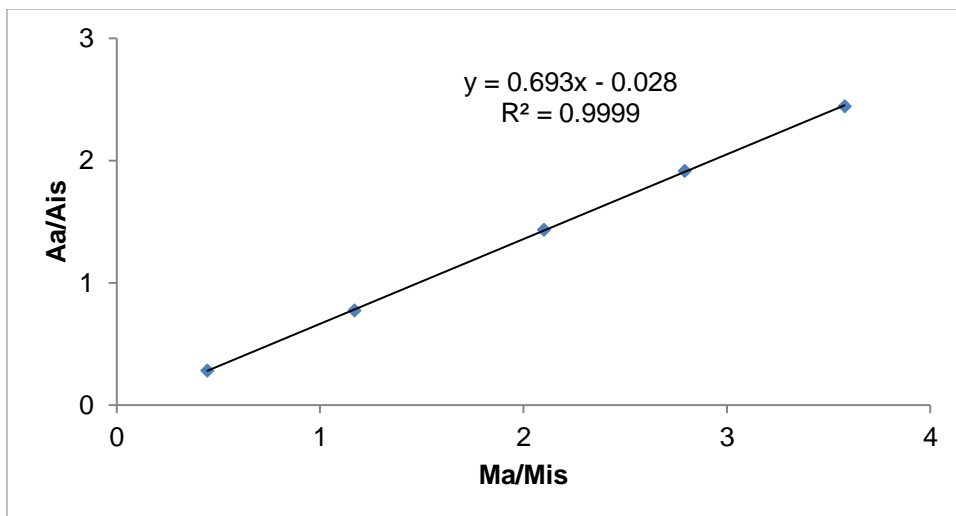
## Appendix B: GC calibration curves for alkoxy silane quantification



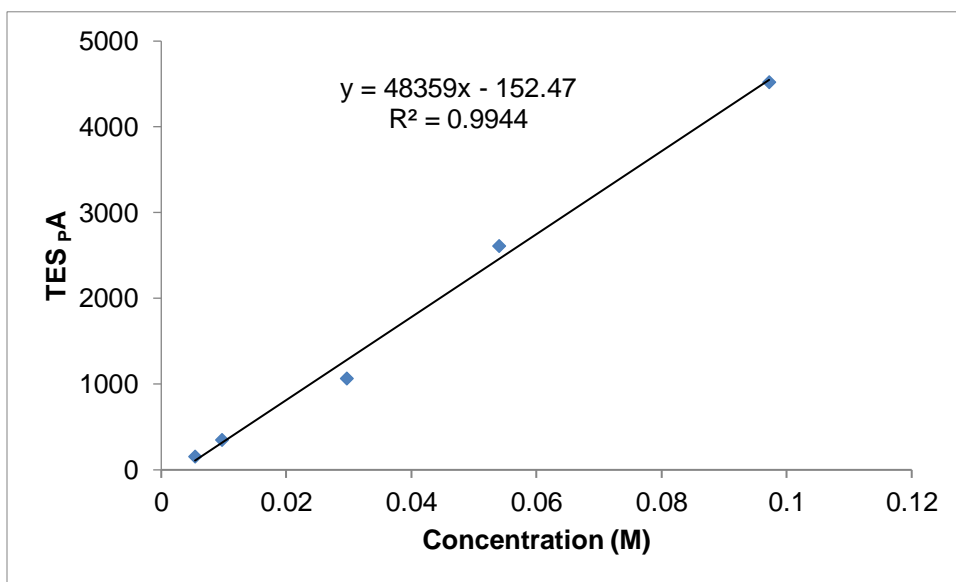
Typical internal standard calibration curve for trimethoxysilane



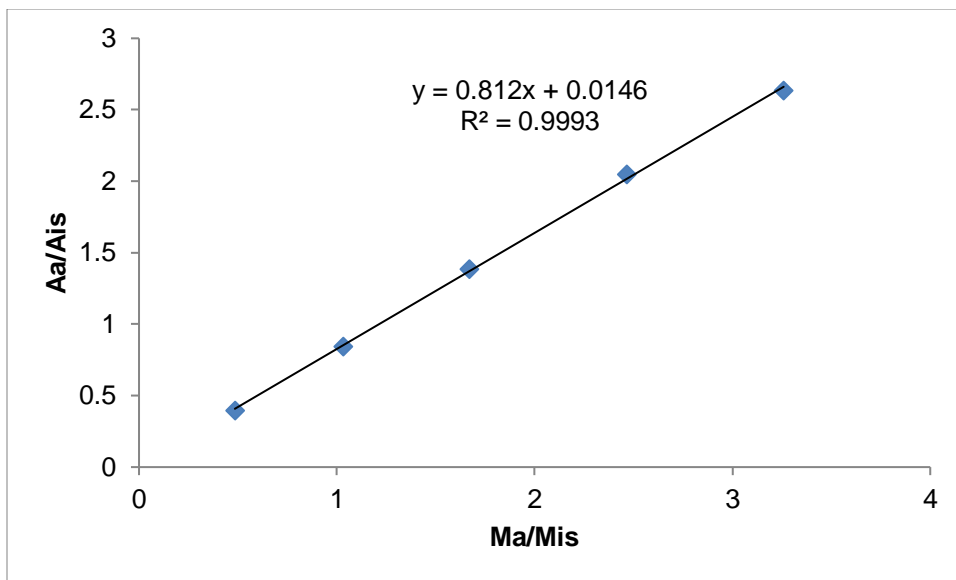
Typical internal standard calibration curve for tetramethoxysilane



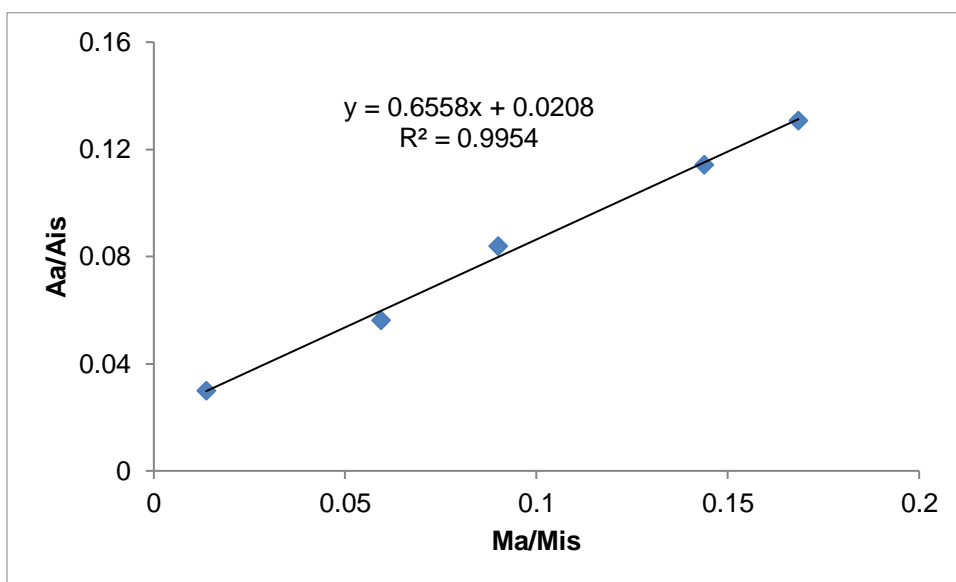
Typical internal standard calibration curve for triethoxysilane



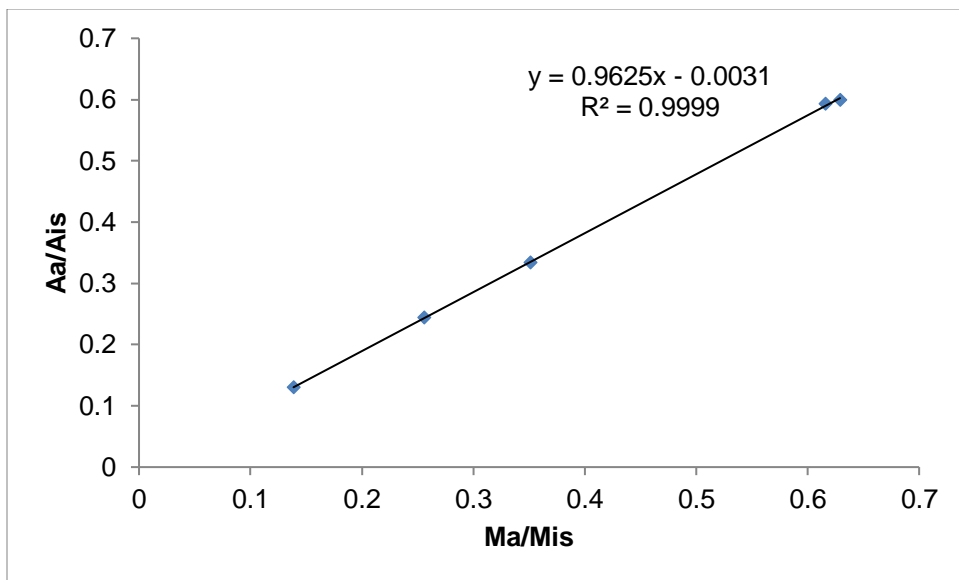
Typical external standard calibration curve for triethoxysilane



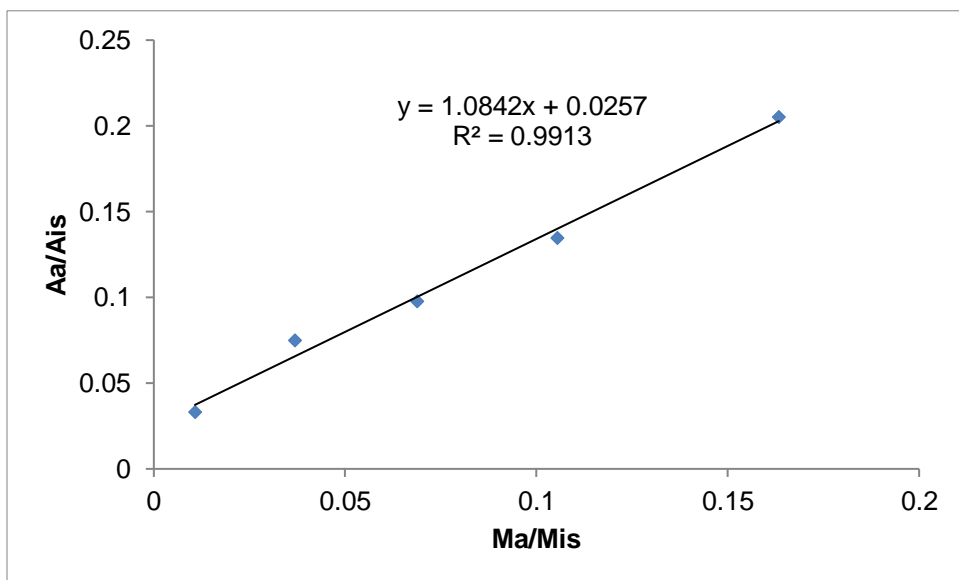
Typical internal standard calibration curve for tetraethoxysilane



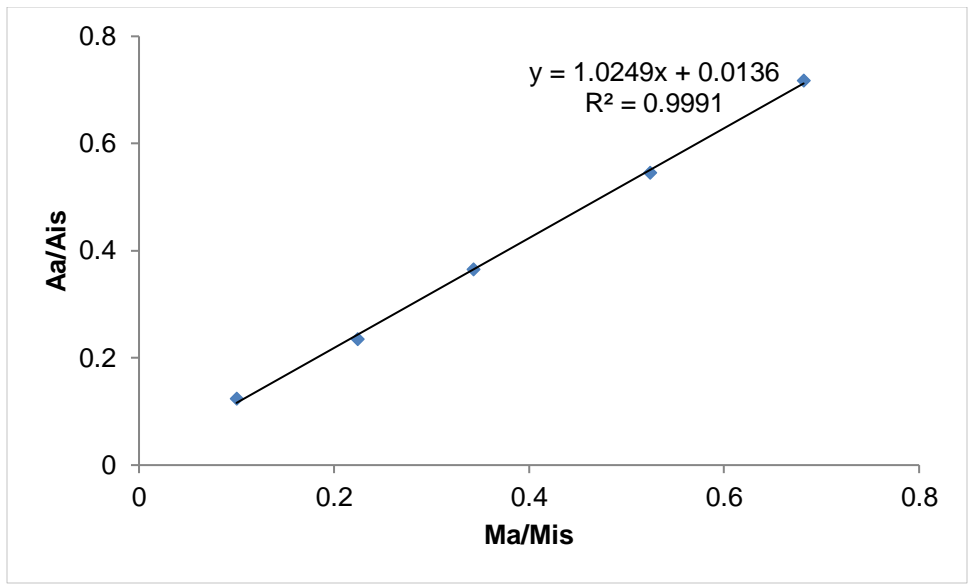
Typical internal standard calibration curve for tripropoxysilane



Typical internal standard calibration curve for tetrapropoxysilane



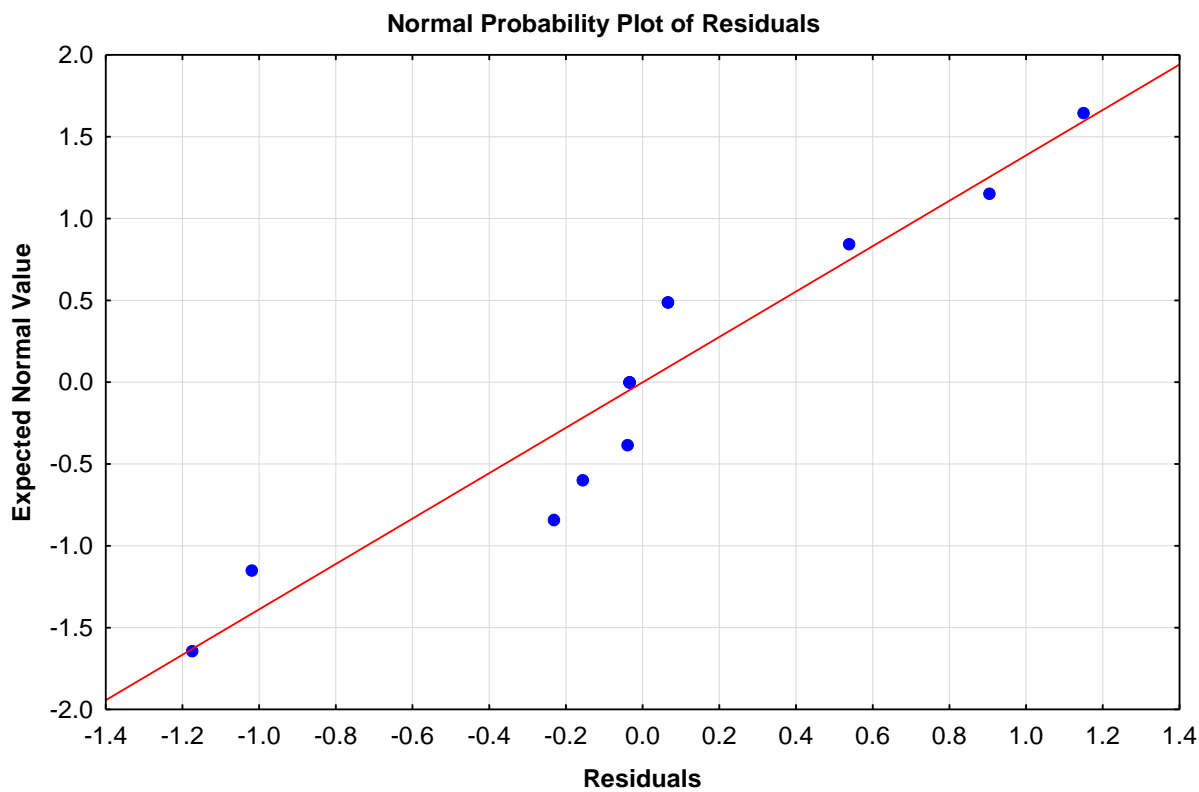
Typical internal standard calibration curve for tributoxysilane



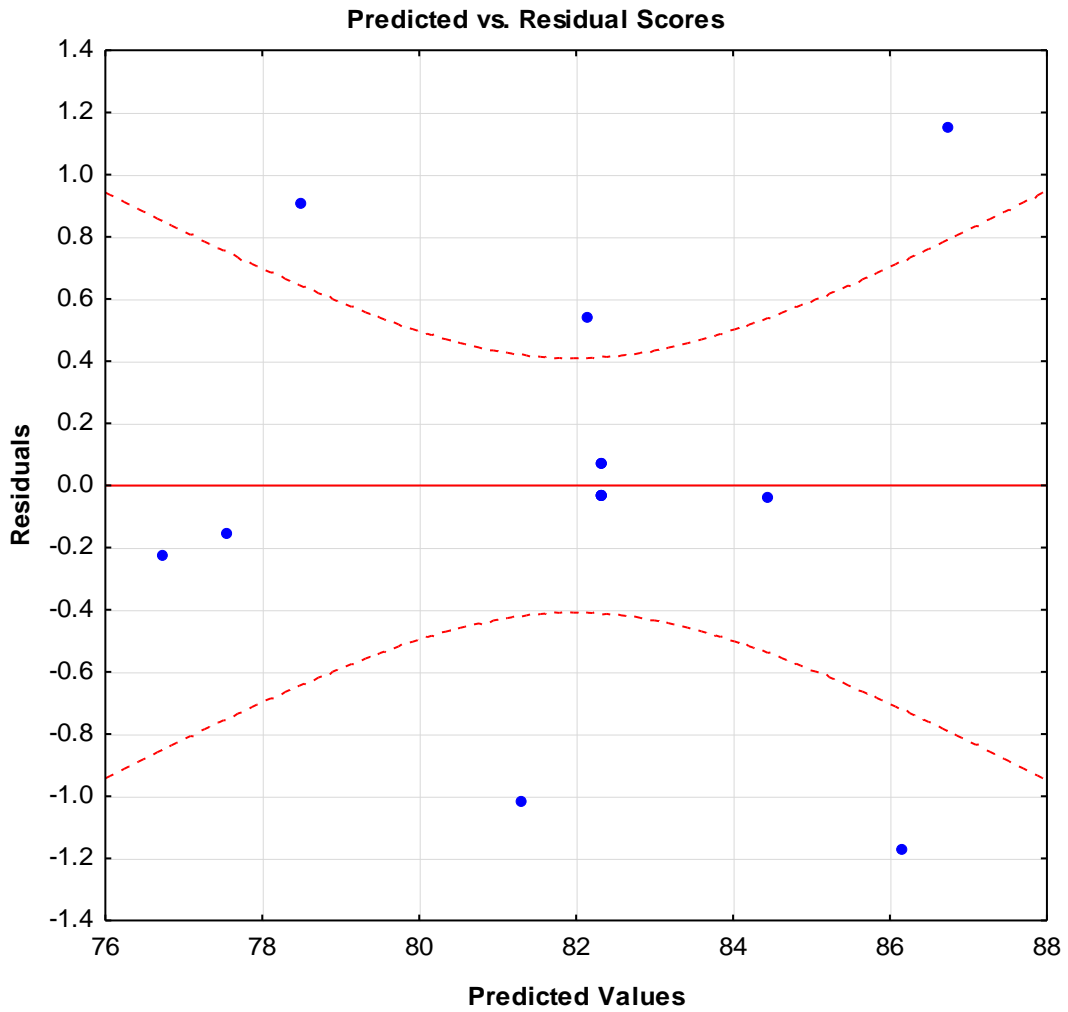
Typical internal standard calibration curve for tetrabutoxysilane



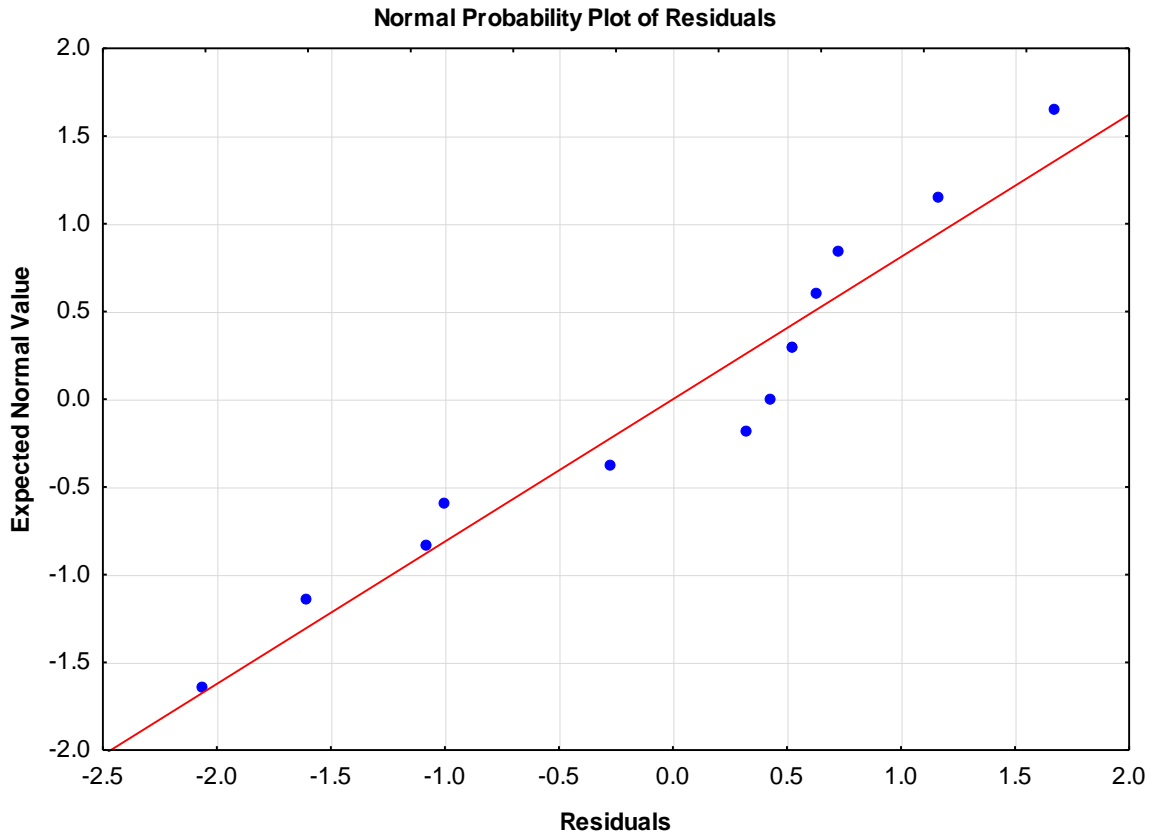
### Appendix C: Response surface model validation graphs



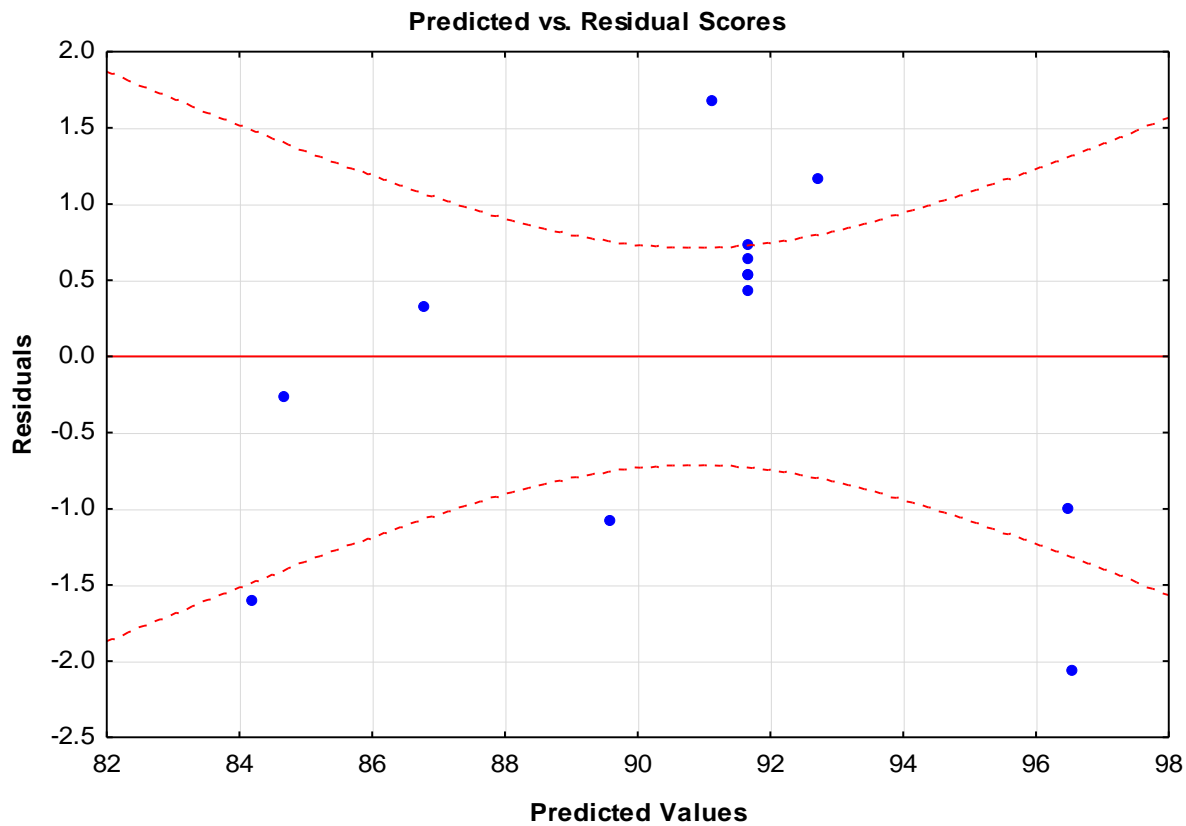
Normal probability plot for residuals for silicon conversion: Batch reactor



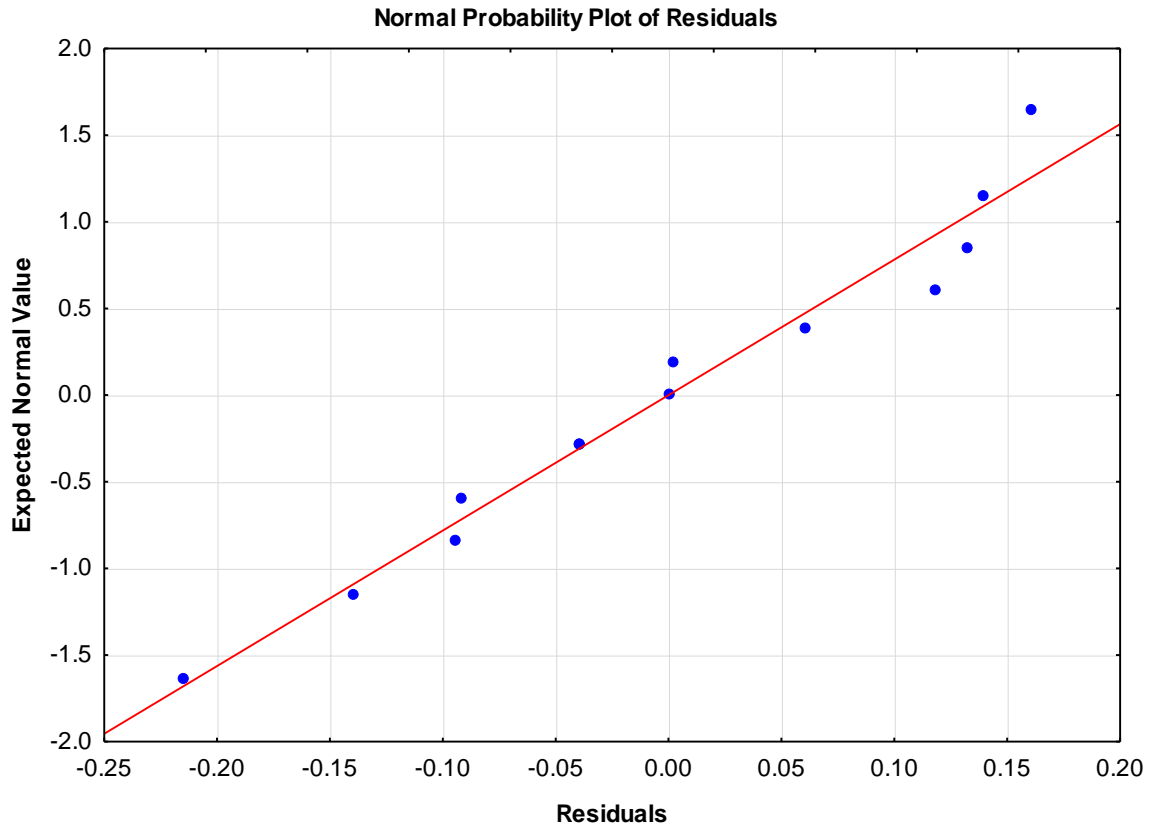
Outlier T plot of residuals for silicon conversion: Batch reactor



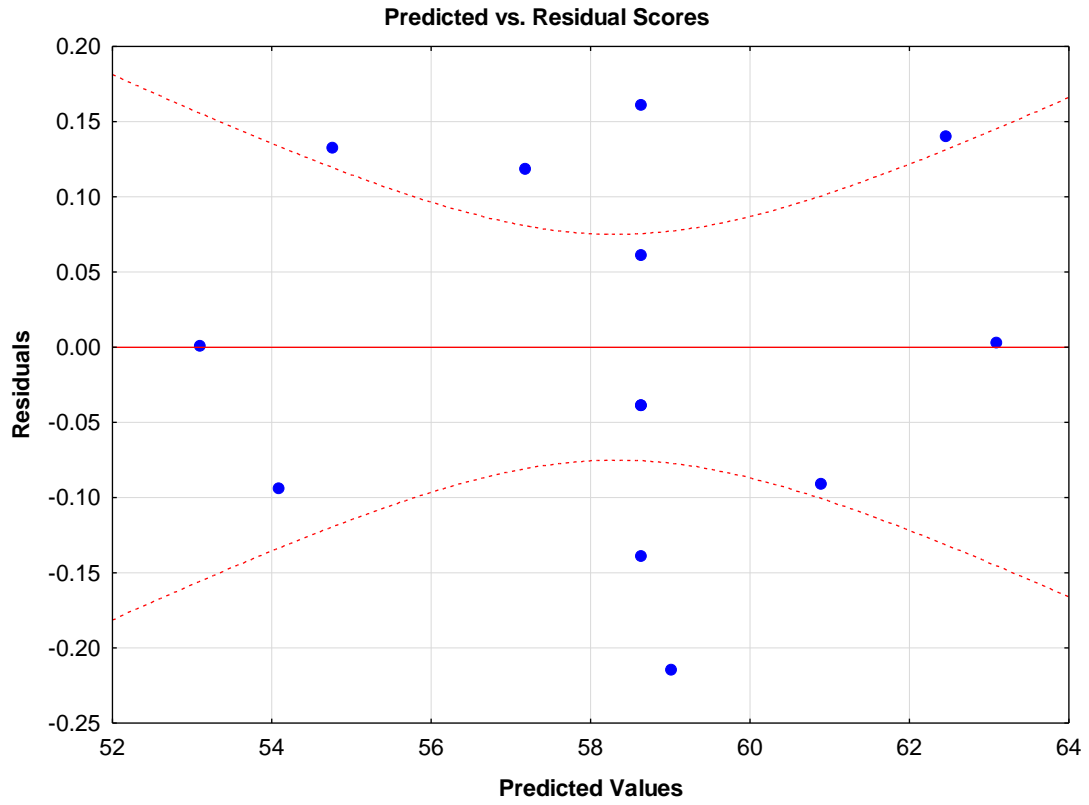
Normal probability plot for residuals for triethoxysilane selectivity: Batch reactor



Outlier T plot of residuals for triethoxysilane selectivity: Batch reactor



Normal probability plot for residuals for silicon conversion: Packed bed flow tubular reactor



Outlier T plot of residuals for silicon conversion: Packed bed flow tubular reactor